PLEASE RETURN
TO
INSTITUTION DATA LIBRARY
McLEAN

Woods Hole Oceanographic Institution
ATLAS - GAZETTEER COLLECTION

464-A
COPY 1
w/drawn

Leslie K. Rosenfeld, Editor

Authors:
Robert C. Beardsley
Carol A. Mills
Leslie K. Rosenfeld
Woods Hole Oceanographic Institution

Alan W. Bratkovich
M. Rustin Erdman
Clinton D. Winant
Scripps Institution of Oceanography

John S. Allen
George R. Halliwell, Jr.
Oregon State University

Wendell S. Brown
James D. Irish
University of New Hampshire

August 1983
Technical Report
Woods Hole Oceanographic Institution
Woods Hole, Massachusetts 02543

Prepared for the National Science Foundation under Grant OCE 80-14941.

Reproduction in whole or in part is permitted for any purpose of the United States Government. This report should be cited as: Woods Hole Oceanog. Inst. Tech. Rept. WHOI-83-23.

Approved for Distribution:

N.P. Fofonoff

N.P. Fofonoff, Chairman
Department of Physical Oceanography

WHOI Technical Report 83-23

COASTAL OCEAN DYNAMICS EXPERIMENT
CODE
1980 NCAR·NOAA·OSU·SIO·UNH·USGS·WHOI 1984

CODE-1: Moored Array and Large-Scale Data Report

CODE Technical Report No. 21

MBL/WHOI
0 0301 0035275 3

83-53

Woods Hole Oceanographic Institution
ATLAS - GAZETTEER COLLECTION

TABLE OF CONTENTS

Woods Hole Oceanographic Institution
ATLAS - GAZETTEER COLLECTION

ABSTRACT

The Coastal Ocean Dynamics Experiment (CODE) was undertaken to identify and study the important dynamical processes which govern the wind-driven motion of coastal water over the continental shelf. The initial effort in this multi-year, multi-institutional research program was to obtain high-quality data sets of all the relevant physical variables needed to construct accurate kinematic and dynamic descriptions of the response of shelf water to strong wind forcing in the 2 to 10 day band. A series of two small-scale, densely-instrumented field experiments of approximately four months duration (called CODE-1 and CODE-2) were designed to explore and to determine the kinematics and momentum and heat balances of the local wind-driven flow over a region of the northern California shelf which is characterized by both relatively simple bottom topography and large wind stress events in both winter and summer. A more lightly instrumented, long-term, large-scale component was designed to help separate the local wind-driven response in the region of the small-scale experiments from motions generated either offshore by the California Current system or in some distant region along the coast, and also to help determine the seasonal cycles of the atmospheric forcing, water structure, and coastal currents over the northern California shelf.

The first small-scale experiment (CODE-1) was conducted between April and August, 1981 as a pilot study in which primary emphasis was placed on characterizing the wind-driven "signal" and the "noise" from which this signal must be extracted. In particular, CODE-1 was designed to identify the key features of the circulation and its variability over the northern California shelf and to determine the important time and length scales of the wind-driven response. This report presents a basic description of the moored array data and some other Eulerian data collected during CODE-1. A brief description of the CODE-1 field program is presented first, followed by a description of the common data analysis procedures used to produce the various data sets presented here. Then basic descriptions of the following data sets are presented: (a) the coastal and moored meteorological measurements, (b) the moored current measurements, (c) the moored temperature and conductivity observations, (d) the bottom pressure measurements, and (e) the wind and adjusted coastal sea level observations obtained as part of the CODE-1 large-scale component.

Woods Hole Oceanographic Institution
ATLAS - GAZETTEER COLLECTION

Woods Hole Oceanographic Institution
ATLAS - GAZETTEER COLLECTION

PLEASE RETURN
TO
INSTITUTION DATA LIBRARY
McLEAN

INTRODUCTION TO THE CODE-1 MOORED ARRAY AND LARGE-SCALE DATA REPORT

By

R. C. Beardsley
L. K. Rosenfeld

Woods Hole Oceanographic Institution
Woods Hole, Massachusetts 02543

A. INTRODUCTION

The Coastal Ocean Dynamics Experiment (CODE) was undertaken to identify and study the important dynamical processes which govern the wind-driven motion of coastal water over the continental shelf. The initial effort in this multi-year, multi-institutional research program was to obtain high-quality data sets of all the relevant physical variables needed to construct accurate kinematic and dynamic descriptions of the response of shelf water to strong wind forcing in the 2 to 10 day band. A series of two small-scale, densely-instrumented field experiments of approximately four months duration (called CODE-1 and CODE-2) were designed to explore and to determine the kinematics and momentum and heat balances of the local wind-driven flow over a region of the northern California shelf which is characterized by both relatively simple bottom topography and large wind stress events in both winter and summer. A more lightly instrumented, long-term, large-scale component was designed to help separate the local wind-driven response in the region of the small-scale experiments from motions generated either offshore by the California Current system or in some distant region along the coast, and also to help determine the seasonal cycles of the atmospheric forcing, water structure, and coastal currents over the northern California shelf.

The first small-scale experiment (CODE-1) was conducted between April and August, 1981 as a pilot study in which primary emphasis was placed on characterizing both the wind-driven "signal" and the "noise" from which this signal must be extracted. In particular, CODE-1 was designed to identify the key features of the circulation and its variability over the northern California shelf and to determine the important time and length scales of the wind-driven response. This report presents a basic description of the moored array data and some other Eulerian data collected during CODE-1. A more complete description of the CODE-1 field program and the motivation behind the experimental design has been given elsewhere by Allen et al. (1982), and other data (e.g., hydrographic, drifter, CODAR, aircraft, etc.) collected in CODE-1 which is not presented here will be presented in separate data reports.

A brief description of the CODE-1 field program will be presented next, followed by a description of the common data analysis procedures used to produce the various data sets presented here.

B. THE CODE-1 FIELD EXPERIMENT

The site selected for CODE-1 is a region of the continental shelf north of San Francisco extending from Point Reyes north to Point Arena (see Figures 1 and 2). Relative to the rest of the California shelf, this location is characterized by both simple bottom topography and large wind stress fluctuations during both winter and summer. The monthly mean wind stresses in the selected region are the largest on the West Coast. More importantly, the fluctuating wind stress exhibits large variability on time scales of several days, superposed on a strong annual cycle which consists of generally southward (upwelling - favorable) winds in the spring and summer and strong variable winds in the winter. The middle and outer shelf in this region has a mud/silty-sand bottom and is generally characterized by an absence of large-scale bedforms (Cacchione et al., 1983), hence relatively well-behaved near-bottom flow was

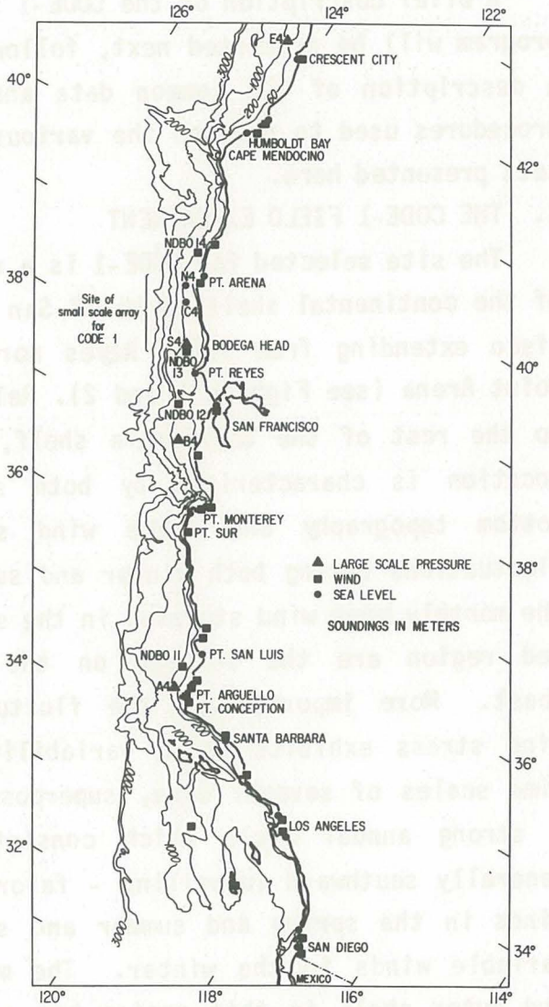

Figure 1. The region of the CODE-1 small-scale experiment shown in relationship to the rest of the California coast and adjacent continental shelf. The locations of the large-scale pressure array and the California wind and sea level stations are also included.

expected and found in CODE-1 (Grant et al., 1983). Finally, the proximity of adequate port and laboratory facilities in San Francisco, Bodega Bay, and Newport (Oregon), combined with the use of a dedicated research vessel, the R/V Wecoma, simplified the logistics in studying this region.

CODE-1 was designed to determine the important time and spatial scales of the most energetic wind-driven response in the different fields of observation and to begin to identify and describe the important kinematic and dynamic features of the response. The major observational elements in CODE-1 were: (a) moored arrays instrumented to measure wind velocity, air temperature, solar radiation, current velocity, water temperature, conductivity, bottom pressure, and to estimate bottom stress, (b) shipboard observations of water temperature, conductivity, and current velocity as a function of depth and (c) aircraft observations of wind velocity, wind stress, sea surface temperature, surface drifter motion, and atmospheric structure. In addition, surface drifters were tracked from shore, and the surface current pattern near the center of the moored array was mapped using a shore-based high frequency radar system called CODAR. Satellite-derived sea surface temperature data and coastal zone color scanner (CZCS) data were collected, and auxiliary measurements of wind, atmospheric pressure, and sea level at appropriate coastal stations and environmental buoys were also obtained. The individual principal investigators responsible for these different observational components are listed in Table 1.

The moored current meter program was designed to examine the vertical and horizontal structure of the current and temperature fields over the shelf and upper slope. Accordingly, a T-shaped array of instrumented moorings was deployed consisting of a five-element cross-shelf transect and a three-element subarray deployed along the 90 m isobath. A plan view of the CODE-1 moored array design is shown in Figure 2, and a schematic side view given in Figure 3. Previous observations suggested that the vertical structure of currents was likely to change most rapidly in a cross-shelf direction and thus the central line located off Stewart's Point near Sea Ranch was most heavily instrumented with moorings deployed in depths of 30 m (C1), 60 m (C2), 90 m

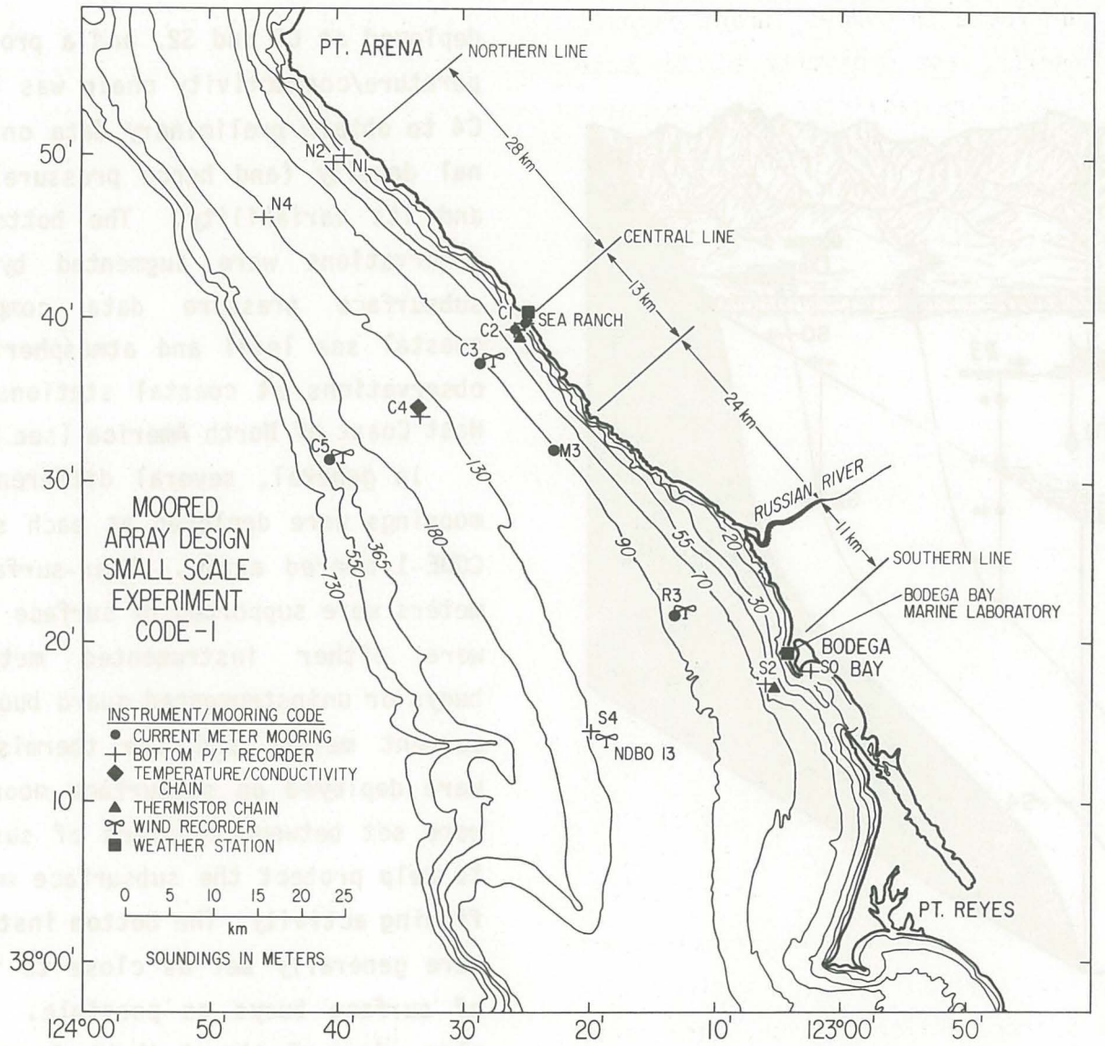

Figure 2. The CODE-1 moored array design, showing the locations of the principal CODE-1 measurement sites along northern (N), central (C), and southern (S) cross-shelf transects. The instrumentation and mooring code indicates the type of measurement made at each site. The meteorological buoy NDBO 14 is not shown since it is located north of Point Arena.

(C3), and 130 m (C4) on the shelf and in 400 m (C5) depth on the adjacent slope. Less heavily instrumented current meter moorings were deployed at M3 and R3 along the 90 m isobath to examine the along-shelf structure. As part of the moored current meter array, meteorological buoys were deployed at C1, C3, and C5 along the central line and at R3 along the 90 m isobath. An electronic failure prior to launch prevented the meteorological instrumentation deployed at C1 from returning any data; thus the C1 meteorological instrumentation is not shown in Figures 2, 3, and 5.)

Coastal sea level measurements were obtained for Arena Cove (near Point Arena) and bottom pressure/temperature instruments were deployed at SO, S2, S4, C1, C2, C4, N1, N2 and N4 (see Figure 2) to (a) measure the along- and cross-shelf structure of the pressure field and (b) allow estimation of the along- and cross-shelf pressure gradients in the region of the CODE-1 small-scale array. Additional bottom pressure/temperature instruments were deployed along the 130 m isobath at A4, B4, and E4 (see Figure 1) as part of the large-scale component. Independent thermistor chains were

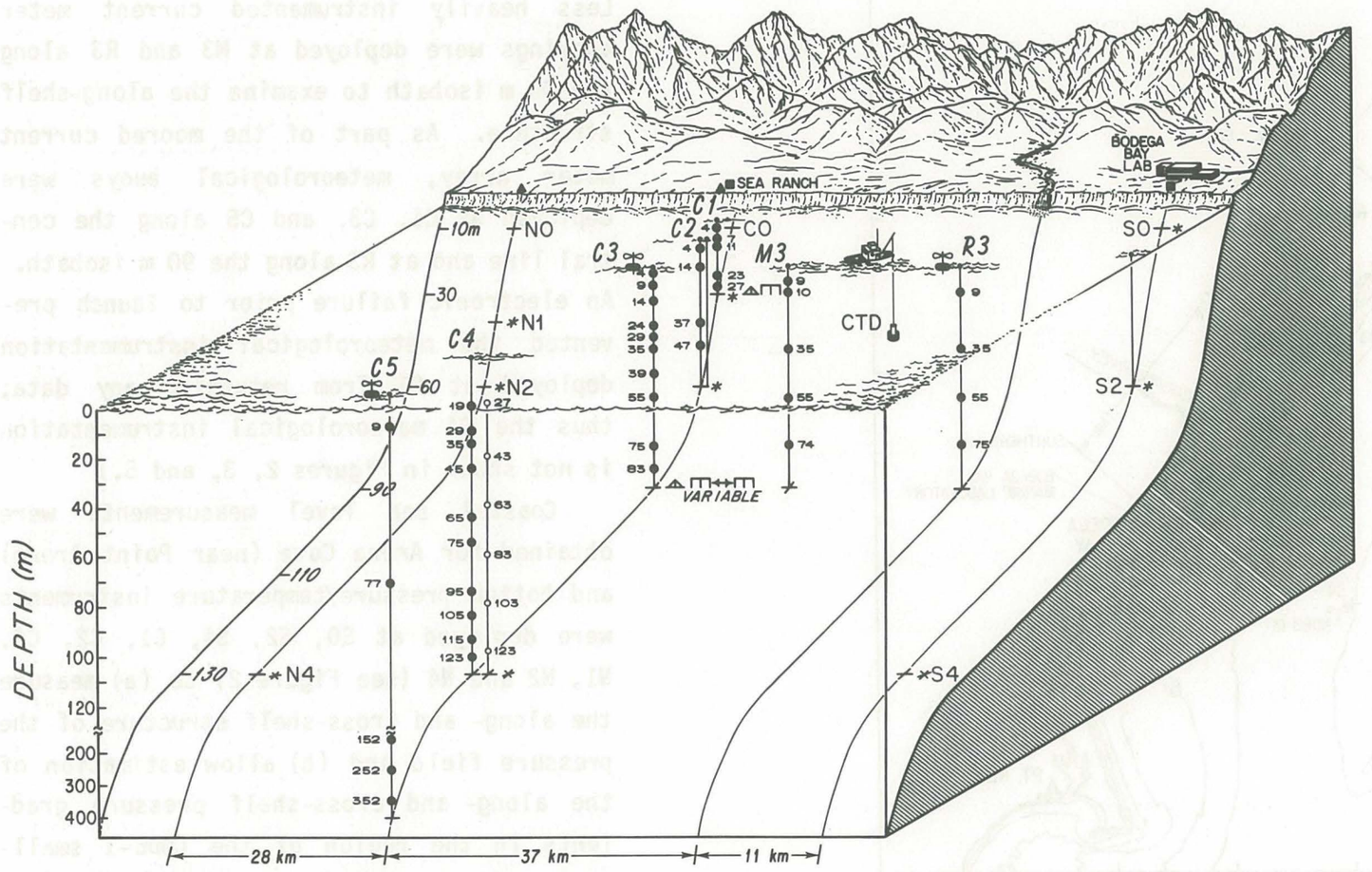

Figure 3. A three-dimensional schematic of the CODE-1 moored array. Current meter locations are identified by (•), meteorological buoys (Ψ), the temperature/conductivity chain (o), the bottom stress instrumentation (⏢, ⊓), bottom pressure/ temperature recorders (*), CODAR shore stations (▲), and coastal meteorological stations (■). Thermistor chains are shown at C2 and S2.

deployed at C2 and S2, and a prototype temperature/conductivity chain was deployed at C4 to obtain preliminary data on the internal density (and hence pressure) structure and its variability. The bottom pressure observations were augmented by synthetic subsurface pressure data computed from coastal sea level and atmospheric pressure observations at coastal stations along the West Coast of North America (see Figure 1).

In general, several different types of moorings were deployed at each site in the CODE-1 moored array. Near-surface current meters were supported by surface buoys which were either instrumented meteorological buoys or uninstrumented guard buoys. Deeper current meters and the thermistor chains were deployed on subsurface moorings which were set between clusters of surface buoys to help protect the subsurface mooring from fishing activity. The bottom instrumentation were generally set as close to the cluster of surface buoys as possible. A detailed plan view of the individual moorings deployed at each site is given in Figure 4. The individual moorings at a site are distinguished by the letter following the site identification. The following scheme was

TABLE 1: CODE Principal Investigators

Investigator (Affiliation)	Research Area
J. Allen (OSU)	Large-scale atmospheric pressure, winds, and coastal sea-level observations.
A. Huyer (OSU)	Hydrography.
R. Davis/C. Winant (SIO)	Small-scale current and temperature measurements, Lagrangian flow measurements, shipboard current measurements, and satellite data.
W. Brown/J. Irish (UNH)	Bottom pressure measurements, density chain and upward Doppler profiler development.
W. Grant/A. Williams III (WHOI) D. Cacchione/D. Drake (USGS)	Bottom stress measurements, swell and wind-wave climate, bottom topography and geology.
R. Beardsley (WHOI)	Long-term current and temperature observations, small-scale buoy wind measurements, overall program coordination.
C. Friehe (NCAR/U.C. Irvine)	Aircraft measurements of wind, wind stress, and planetary boundary layer structure.
M. Janopaul/S. Frisch (NOAA)	CODAR surface-current measurements.

generally used, however, some exceptions were made. Uninstrumented surface buoys supporting sub-surface instrumentation were labelled A, instrumented surface buoys, some of which supported subsurface instrumentation, were labelled B, uninstrumented guard buoys were labelled either G or H, and subsurface current meter and thermistor chain moorings were labelled S. The temperature/conductivity chain deployed at C4 was labelled Q. The relative positions have been determined from a combination of radar ranges and bearings, Loran-C position data, and optical bearings taken during the deployment and recovery cruises and are considered to have an estimated uncertainty of ± 50 m. Coordinates for each mooring are given in Table 2, and relative positions are shown in Figure 4; the coordinates are considered to be less accurate than the positions shown in the figure due to errors in the conversion of Loran-C data into latitude and longitude. A summary of all instrumentation deployed on the different moorings at each site is also listed in Table 2.

The CODE-1 moored array was deployed in stages during a series of cruises conducted

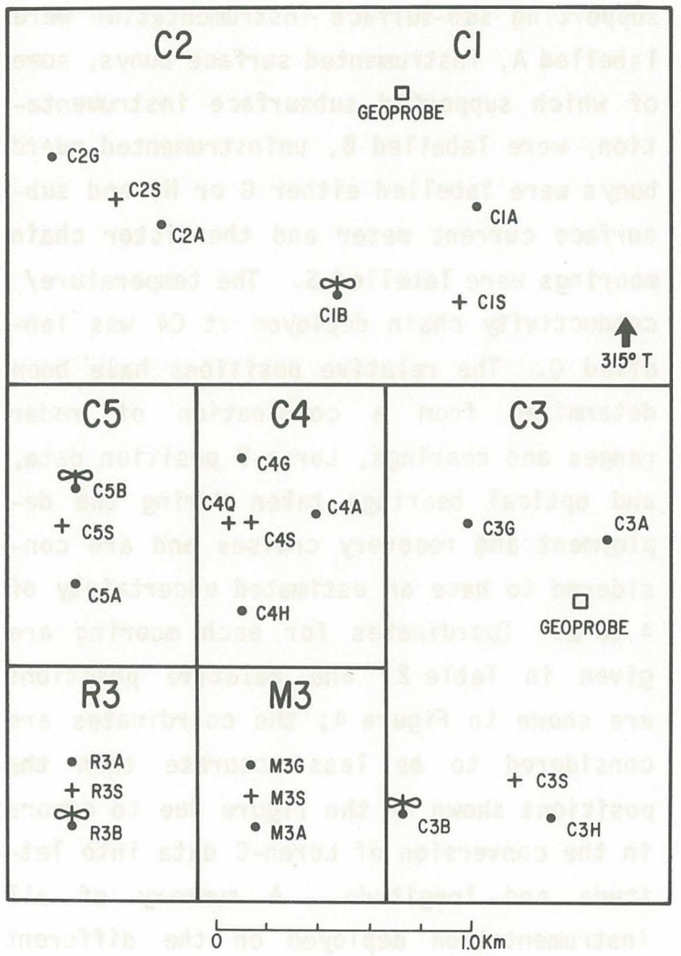

Figure 4. The relative positions of individual moorings at each station are shown in the outlined boxes. The orientation and horizontal scale are common to all boxes.

aboard the research vessels Wecoma, S.P. Lee, E.B. Scripps, and Acania by SIO, UNH, and WHOI between March 23 and April 24. The array was also recovered in stages during a series of cruises aboard the Wecoma, E.B. Scripps, and Acania during the period July 16 to August 8. Consequently, the instruments at different stations had different deployment periods which are shown in Figure 5 along with the times during which other CODE-1 measurements were made. Each individual instrument did not necessarily record good data for all of its variables for the entire period shown. The dates of good data return are included in the separate chapters of this report along with more detailed descriptions of the various moored array data sets.

While the different data sets presented in this report have been processed and edited at different laboratories using the standard procedures and routines used by each group, some common conventions have been used to standardize the basic data sets. For all vector and scalar variables that were sampled at intervals less than one hour, time series of one hour vector or scalar averages, centered on the even hour, have been constructed (e.g., the value assigned to 1200 is an average of data collected between 1130 and 1230). All plots and statistics presented in this report are based on these one-hour averaged time series unless otherwise indicated. Greenwich Mean Time (GMT) is used as the common time reference. Where necessary, time series have been adjusted from Pacific Standard Time (PST) to Greenwich Mean Time by the addition of eight hours (1200 PST corresponds to 2000 GMT).

The vector current and wind data collected in the CODE-1 region have been rotated into a coordinate system aligned with the mean coastline orientation and shelf topography near the central line. The new coordinate system is rotated 43° counterclockwise with respect to true north. Thus the along-shelf component is positive towards 317°T and the cross-shelf component is positive towards 47°T. Vector wind data collected outside of the CODE-1 region as part of the large-scale component have been rotated differently into a local principal axes coordinate system.

The rest of this report is organized in the following way. The coastal and moored

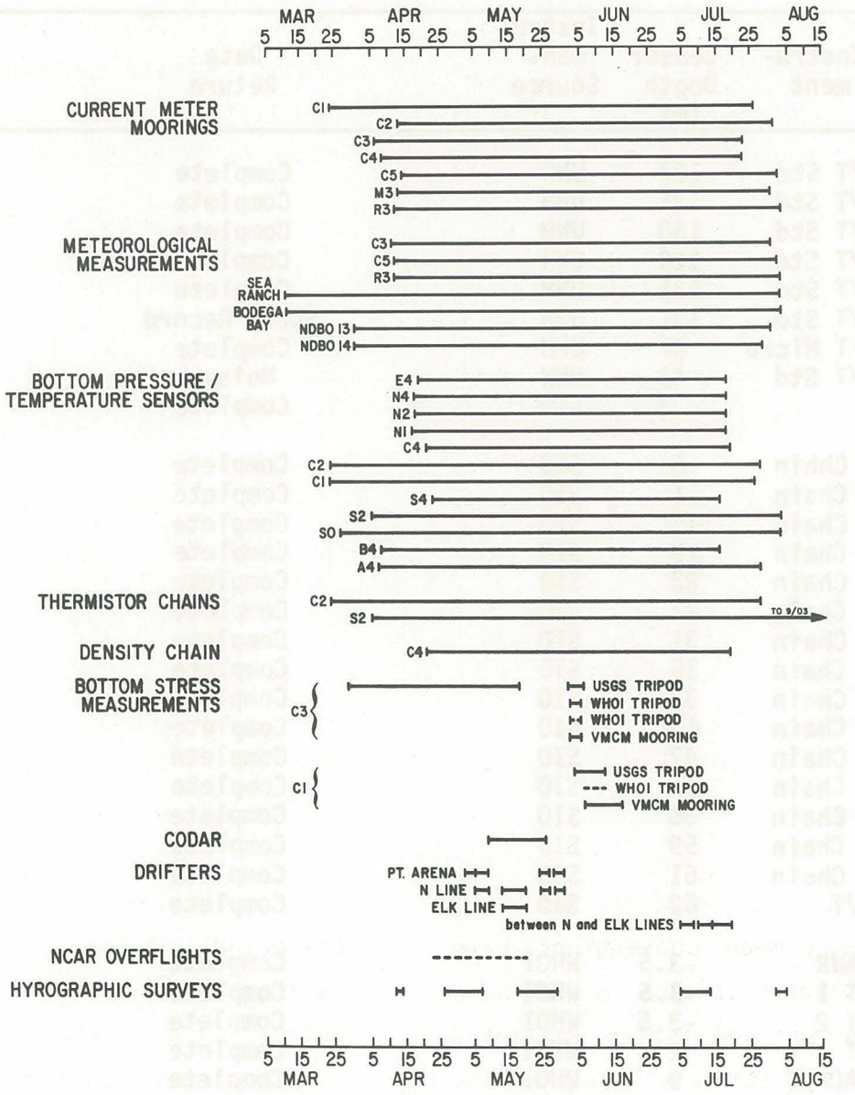

Figure 5. Deployment and recovery schedule for CODE-1 instrumentation.

meteorological and moored current observations made in the CODE-1 small-scale array shown in Figure 2 are presented in Chapters 2 and 3, respectively. All moored temperature and conductivity observations and all bottom pressure observations made in both the CODE-1 small-scale (Figure 2) and CODE-1 large-scale array (Figure 1) are described in Chapters 4 and 5, respectively. The final chapter presents the wind and adjusted coastal sea level observations obtained as part of the CODE-1 large-scale component.

TABLE 2: Moored Instrumentation Deployed in CODE-1

Stn	Mooring	Water Depth (m)	Latitude N	Longitude W	Date Set	Date Recovered	Instrument	Sensor Depth (m)	Instrument Source	Data Return
A4	Bottom	127	34°43.2'	120°50.2'	04/07/81	07/28/81	P/T Std	127	UNH	Complete
B4	Bottom	125	37°17.3'	122°47.0'	04/08/81	07/16/81	P/T Std	125	UNH	Complete
S4	Bottom	130	38°14.2'	123°19.6'	04/23/81	07/16/81	P/T Std	130	UNH	Complete
D4	Bottom	130	39°58.8'	124°10.1'	04/19/81	04/23/81	P/T Std	129	UNH	Complete
E4	Bottom	131	41°53.5'	124°29.5'	04/19/81	07/18/81	P/T Std	131	UNH	Complete
N4	Bottom	131	38°46.2'	123°45.5'	04/18/81	07/18/81	P/T Std	131	UNH	Short Record
N2	Bottom	57	38.49.6'	123°40.0'	04/18/81	07/18/81	P/T Micro	57	UNH	Complete
N1	Bottom	41	38°50.0'	123°39.5'	04/17/81	07/18/81	P/T Std	41	UNH	Noisy
S0	Pier	4	38°18.7'	123°03.1'	03/27/81	08/03/81	P	3	SIO	Complete
S2	S2S	63	38°17.5'	123°05.9'	04/05/81	09/03/81	T Chain	8	SIO	Complete
S2	S2S	63	38°17.5'	123°05.9'	04/05/81	09/03/81	T Chain	11	SIO	Complete
S2	S2S	63	38°17.5'	123°05.9'	04/05/81	09/03/81	T Chain	15	SIO	Complete
S2	S2S	63	38°17.5'	123°05.9'	04/05/81	09/03/81	T Chain	19	SIO	Complete
S2	S2S	63	38°17.5'	123°05.9'	04/05/81	09/03/81	T Chain	23	SIO	Complete
S2	S2S	63	38°17.5'	123°05.9'	04/05/81	09/03/81	T Chain	27	SIO	Complete
S2	S2S	63	38°17.5'	123°05.9'	04/05/81	09/03/81	T Chain	31	SIO	Complete
S2	S2S	63	38°17.5'	123°05.9'	04/05/81	09/03/81	T Chain	35	SIO	Complete
S2	S2S	63	38°17.5'	123°05.9'	04/05/81	09/03/81	T Chain	39	SIO	Complete
S2	S2S	63	38°17.5'	123°05.9'	04/05/81	09/03/81	T Chain	43	SIO	Complete
S2	S2S	63	38°17.5'	123°05.9'	04/05/81	09/03/81	T Chain	47	SIO	Complete
S2	S2S	63	38°17.5'	123°05.9'	04/05/81	09/03/81	T Chain	51	SIO	Complete
S2	S2S	63	38°17.5'	123°05.9'	04/05/81	09/03/81	T Chain	55	SIO	Complete
S2	S2S	63	38°17.5'	123°05.9'	04/05/81	09/03/81	T Chain	59	SIO	Complete
S2	S2S	63	38°17.5'	123°05.9'	04/05/81	09/03/81	T Chain	61	SIO	Complete
S2	S2S	63	38°17.5'	123°05.9'	04/05/81	09/03/81	P/T	62	SIO	Complete
R3	R3B	90	38°21.6'	123°13.0'	04/12/81	08/03/81	VAWR	-3.5	WHOI	Complete
R3	R3B	90	38°21.6'	123°13.0'	04/12/81	08/03/81	AT 1	-3.5	WHOI	Complete
R3	R3B	90	38°21.6'	123°13.0'	04/12/81	08/03/81	AT 2	-3.5	WHOI	Complete
R3	R3B	90	38°21.6'	123°13.0'	04/12/81	08/03/81	T	1	WHOI	Complete
R3	R3B	90	38°21.6'	123°13.0'	04/12/81	08/03/81	VACM/T	9	WHOI	Complete

Mooring designations and instrument abbreviations are defined at the end of this table.

TABLE 2: Moored Instrumentation Deployed in CODE-1 (Continued)

Stn	Mooring	Water Depth (m)	Latitude N	Longitude W	Date Set	Date Recovered	Instru-ment	Sensor Depth (m)	Instru-ment Source	Data Return
R3	R3S	90	38°21.6'	123°13.1'	04/12/81	08/03/81	VACM/T	35	WHOI	Complete
R3	R3S	90	38°21.6'	123°13.1'	04/12/81	08/03/81	VACM/T	55	WHOI	Complete
R3	R3S	90	38°21.6'	123°13.1'	04/12/81	08/03/81	VACM/T	75	WHOI	Complete
M3	M3A	90	38°32.8'	123°22.6'	04/13/81	07/31/81	VACM/T	9	WHOI	Complete
M3	M3A	90	38°32.8'	123°22.6'	04/13/81	07/31/81	VACM/T	10	WHOI	Complete
M3	M3S	90	38°32.9'	123°22.7'	04/13/81	07/31/81	VACM/T	35	WHOI	Complete
M3	M3S	90	38°32.9'	123°22.7'	04/13/81	07/31/81	VACM/T	55	WHOI	Complete
M3	M3S	90	38°32.9'	123°22.7'	04/13/81	07/31/81	VACM/T	74	WHOI	Complete
C1	C1B	40	38°39.5'	123°25.2'	04/11/81	08/01/81	VAWR	-3.5	WHOI	No Data
C1	C1B	40	38°39.5'	123°25.2'	04/11/81	08/01/81	I	-3.5	WHOI	No Data
C1	C1B	40	38°39.5'	123°25.2'	04/11/81	08/01/81	AT 1	-3.5	WHOI	No Data
C1	C1B	40	38°39.5'	123°25.2'	04/11/81	08/01/81	AT 2	-3.5	WHOI	No Data
C1	C1B	40	38°39.5'	123°25.2'	04/11/81	08/01/81	T	1	WHOI	No Data
C1	C1A	30	38°39.8'	123°25.1'	03/24/81	07/26/81	VMCM/T	4	SIO	Complete
C1	C1A	30	38°39.8'	123°25.1'	03/24/81	07/26/81	VMCM/T	7	SIO	Complete
C1	C1A	30	38°39.8'	123°25.1'	03/24/81	07/26/81	VMCM/T	11	SIO	Complete
C1	C1A	30	38°39.8'	123°25.1'	03/24/81	07/26/81	VMCM/T	14	SIO	No Data
C1	C1S	33	38°39.6'	123°24.8'	03/24/81	07/26/81	VMCM/T	23	SIO	Complete
C1	C1S	33	38°39.6'	123°24.8'	03/24/81	07/26/81	VMCM/T	27	SIO	Complete
C1	C1S	33	38°39.6'	123°24.8'	03/24/81	07/26/81	P/T	33	SIO	Complete
C1	Geoprobe	35	38°40.0'	123°25.5'	06/02/81	06/12/81	4 EM,2T, P,TR,N,CA	34	USGS	Complete

Mooring designations and instrument abbreviations are defined at the end of this table.

TABLE 2: Moored Instrumentation Deployed in CODE-1 (Continued)

Stn	Mooring	Water Depth (m)	Latitude N	Longitude W	Date Set	Date Recovered	Instrument	Sensor Depth (m)	Instrument Source	Data Return
C2	C2S	67	38°39.3'	123°25.8'	03/24/81	07/28/81	T Chain	8	SIO	Complete
C2	C2S	67	38°39.3'	123°25.8'	03/24/81	07/28/81	T Chain	11	SIO	Complete
C2	C2S	67	38°39.3'	123°25.8'	03/24/81	07/28/81	T Chain	15	SIO	Complete
C2	C2S	67	38°39.3'	123°25.8'	03/24/81	07/28/81	T Chain	19	SIO	Complete
C2	C2S	67	38°39.3'	123°25.8'	03/24/81	07/28/81	T Chain	23	SIO	Complete
C2	C2S	67	38°39.3'	123°25.8'	03/24/81	07/28/81	T Chain	27	SIO	Complete
C2	C2S	67	38°39.3'	123°25.8'	03/24/81	07/28/81	T Chain	31	SIO	Complete
C2	C2S	67	38°39.3'	123°25.8'	03/24/81	07/28/81	T Chain	35	SIO	Complete
C2	C2S	67	38°39.3'	123°25.8'	03/24/81	07/28/81	T Chain	39	SIO	Complete
C2	C2S	67	38°39.3'	123°25.8'	03/24/81	07/28/81	T Chain	43	SIO	Complete
C2	C2S	67	38°39.3'	123°25.8'	03/24/81	07/28/81	T Chain	47	SIO	Complete
C2	C2S	67	38°39.3'	123°25.8'	03/24/81	07/28/81	T Chain	51	SIO	Complete
C2	C2S	67	38°39.3'	123°25.8'	03/24/81	07/28/81	T Chain	55	SIO	Complete
C2	C2S	67	38°39.3'	123°25.8'	03/24/81	07/28/81	T Chain	59	SIO	Complete
C2	C2S	67	38°39.3'	123°25.8'	03/24/81	07/28/81	T Chain	61	SIO	Complete
C2	C2S	67	38°39.3'	123°25.8'	03/24/81	07/28/81	P/T	66	SIO	Complete
C2	C2A	63	38°39.3'	123°25.6'	04/13/81	08/01/81	VMCM	4	WHOI	Complete
C2	C2A	63	38°39.3'	123°25.6'	04/13/81	08/01/81	VMCM	11	WHOI	No Data
C2	C2A	63	38°39.3'	123°25.6'	04/13/81	08/01/81	VMCM/T	14	SIO	Complete
C2	C2A	63	38°39.3'	123°25.6'	04/13/81	08/01/81	VMCM	37	WHOI	Short Record
C2	C2A	63	38°39.3'	123°25.6'	04/13/81	08/01/81	VMCM	47	WHOI	Short Record
C3	C3B	94	38°36.5'	123°28.1'	04/11/81	07/31/81	VMWR	-3.5	WHOI	Complete
C3	C3B	94	38°36.5'	123°28.1'	04/11/81	07/31/81	VAWR	-3.5	WHOI	Complete
C3	C3B	94	38°36.5'	123°28.1'	04/11/81	07/31/81	AT 1	-3.5	WHOI	Complete
C3	C3B	94	38°36.5'	123°28.1'	04/11/81	07/31/81	AT 2	-3.5	WHOI	Short Record
C3	C3B	94	38°36.5'	123°28.1'	04/11/81	07/31/81	I	-3.5	WHOI	Complete
C3	C3B	94	38°36.5'	123°28.1'	04/11/81	07/31/81	T	1	WHOI	Complete

Mooring designations and instrument abbreviations are defined at the end of this table.

TABLE 2: Moored Instrumentation Deployed in CODE-1 (Continued)

Stn	Mooring	Water Depth (m)	Latitude N	Longitude W	Date Set	Date Recovered	Instrument	Sensor Depth (m)	Instrument Source	Data Return
C3	C3A	90	38°37.2'	123°28.3'	04/06/81	07/23/81	VMCM/T	4	SIO	Complete
C3	C3A	90	38°37.2'	123°28.3'	04/06/81	07/23/81	VMCM/T	9	SIO	Complete
C3	C3A	90	38°37.2'	123°28.3'	04/06/81	07/23/81	VMCM/T	14	SIO	Complete
C3	C3A	90	38°37.2'	123°28.3'	04/06/81	07/23/81	VMCM/T	24	SIO	Short Current Record/T Complete
C3	C3A	90	38°37.2'	123°28.3'	04/06/81	07/23/81	VMCM/T	29	SIO	Complete
C3	C3S	90	38°36.7'	123°28.0'	04/06/81	07/25/81	VMCM/T	35	SIO	Complete
C3	C3S	90	38°36.7'	123°28.0'	04/06/81	07/25/81	VMCM/T	39	SIO	Complete
C3	C3S	90	38°36.7'	123°28.0'	04/06/81	07/25/81	VMCM/T	45	SIO	T Only
C3	C3S	90	38°36.7'	123°28.0'	04/06/81	07/25/81	VMCM/T	55	SIO	Short Current Record/T Complete
C3	C3S	90	38°36.7'	123°28.0'	04/06/81	07/25/81	VMCM/T	65	SIO	T Only
C3	C3S	90	38°36.7'	123°28.0'	04/06/81	07/25/81	VMCM/T	75	SIO	Short Current Record/T Complete
C3	C3S	90	38°36.7'	123°28.0'	04/06/81	07/25/81	VMCM/T	83	SIO	Complete
C3	Geoprobe	94	38°37.0'	123°28.2'	03/29/81	06/11/81	4 EM,2T, P,TR,N,CA	93	USGS	Short Current Record/Rest Complete
C4	C4Q	133	38°34.3'	123°32.7'	04/21/81	07/19/81	T/C Chain	27	UNH	Complete
C4	C4Q	133	38°34.3'	123°32.7'	04/21/81	07/19/81	T/C Chain	43	UNH	Complete
C4	C4Q	133	38°34.3'	123°32.7'	04/21/81	07/19/81	T/C Chain	63	UNH	Complete
C4	C4Q	133	38°34.3'	123°32.7'	04/21/81	07/19/81	T/C Chain	83	UNH	Complete
C4	C4Q	133	38°34.3'	123°32.7'	04/21/81	07/19/81	T/C Chain	103	UNH	Complete
C4	C4Q	133	38°34.3'	123°32.7'	04/21/81	07/19/81	T/C Chain	123	UNH	Complete
C4	C4Q	133	38°34.3'	123°32.7'	04/21/81	07/19/81	P/T	133	UNH	Complete
C4	C4A	133	38.34.5'	123.32.6'	04/08/81	07/23/81	VMCM/T	4	SIO	T Only
C4	C4A	133	38.34.5'	123.32.6'	04/08/81	07/23/81	VMCM/T	9	SIO	No Data
C4	C4A	133	38.34.5'	123.32.6'	04/08/81	07/23/81	VMCM/T	14	SIO	No Data
C4	C4A	133	38.34.5'	123.32.6'	04/08/81	07/23/81	VMCM/T	19	SIO	Complete
C4	C4A	133	38.34.5'	123.32.6'	04/08/81	07/23/81	VMCM/T	24	SIO	T Only - Short Record
C4	C4A	133	38.34.5'	123.32.6'	04/08/81	07/23/81	VMCM/T	29	SIO	Complete

Mooring designations and instrument abbreviations are defined at the end of this table.

TABLE 2: Moored Instrumentation Deployed in CODE-1 (Continued)

Stn	Mooring	Water Depth (m)	Latitude N	Longitude W	Date Set	Date Recovered	Instrument	Sensor Depth (m)	Instrument Source	Data Return
C4	C4S	133	38°34.3'	123°32.7'	04/08/81	07/23/81	VMCM/T	35	SIO	Complete
C4	C4S	133	38°34.3'	123°32.7'	04/08/81	07/23/81	VMCM/T	45	SIO	Complete
C4	C4S	133	38°34.3'	123°32.7'	04/08/81	07/23/81	VMCM/T	55	SIO	T Only - Short Record
C4	C4S	133	38°34.3'	123°32.7'	04/08/81	07/23/81	VMCM/T	65	SIO	Complete
C4	C4S	133	38°34.3'	123°32.7'	04/08/81	07/23/81	VMCM/T	75	SIO	Complete
C4	C4S	133	38°34.3'	123°32.7'	04/08/81	07/23/81	VMCM/T	83	SIO	No Data
C4	C4S	133	38°34.3'	123°32.7'	04/08/81	07/23/81	VMCM/T	95	SIO	Complete
C4	C4S	133	38°34.3'	123°32.7'	04/08/81	07/23/81	VMCM/T	105	SIO	Complete
C4	C4S	133	38°34.3'	123°32.7'	04/08/81	07/23/81	VMCM/T	115	SIO	Complete
C4	C4S	133	38°34.3'	123°32.7'	04/08/81	07/23/81	VMCM/T	123	SIO	Complete
C5	C5B	402	38°31.2'	123°40.5'	04/12/81	08/02/81	VAWR	-3.5	WHOI	Complete
C5	C5B	402	38°31.2'	123°40.5'	04/12/81	08/02/81	AT 1	-3.5	WHOI	Complete
C5	C5B	402	38°31.2'	123°40.5'	04/12/81	08/02/81	AT 2	-3.5	WHOI	Complete
C5	C5B	402	38°31.2'	123°40.5'	04/12/81	08/02/81	I	-3.5	WHOI	Complete
C5	C5B	402	38°31.2'	123°40.5'	04/12/81	08/02/81	T	1	WHOI	Complete
C5	C5B	402	38°31.2'	123°40.5'	04/12/81	08/02/81	VACM/T	9	WHOI	Complete
C5	C5S	402	38°31.1'	123°40.4'	04/14/81	08/02/81	VACM/T	77	WHOI	Complete
C5	C5S	402	38°31.1'	123°40.4'	04/14/81	08/02/81	VACM/T	152	WHOI	Complete
C5	C5S	402	38°31.1'	123°40.4'	04/14/81	08/02/81	VACM/T	252	WHOI	Complete
C5	C5S	402	38°31.1'	123°40.4'	04/14/81	08/02/81	VACM/T	352	WHOI	Complete
Sea Ranch	--	Coastal	38°41.0'	123°25.5'	03/11/81	08/03/81	WR	-10	SIO	Complete
Bodega Bay	--	Coastal	38°19.0'	123°04.0'	03/11/81	08/03/81	WR	-10	SIO	Complete
Bodega Bay	--	Coastal	38°19.0'	123°04.0'	03/11/81	08/03/81	AP	-10	SIO	Complete

Mooring designations and instrument abbreviations are defined at the end of this table.

TABLE 2: Moored Instrumentation Deployed in CODE-1 (Continued)

Mooring Designations:

A - Uninstrumented surface buoy supporting subsurface instrumentation.
B - Surface toroid buoy with meteorological sensors, may have current meters below.
Q - Temperature/conductivity chain on subsurface mooring.
S - Instrumented subsurface mooring, current meter or thermistor chain.

Abbreviations:

I: Insolation
C: Conductivity
N: Nephelometer
P: Bottom Pressure
R: Rotor
T: Water Temperature
AP: Atmospheric Pressure
CA: Camera
EM: Electromagnetic Current Meter
TR: Transmissometer
WR: Wind Recorder
Std: Standard
AT 1: Air Temperature, Thaller Shield
AT 2: Air Temperature, Young Shield
VAWR: Vector Averaging Wind Recorder
VACM: Vector Averaging Current Meter
VMCM: Vector Measuring Current Meter
VMWR: Vector Measuring Wind Recorder

Acknowledgments

The very successful execution of the CODE-1 field program was made possible through the efforts of a great many people, and the CODE principal investigators would like to take this opportunity to express their deep appreciation for the excellent scientific, engineering, and technical support given throughout the program. The skill and cooperation of the research vessels Wecoma (OSU), S.P. Lee (USGS), E.B. Scripps (SIO), and Acania (Naval Postgraduate School) contributed significantly to the success of the seagoing operations, and the officers and crew of the U.S. Coast Guard Base at Yerba Buena Island in San Francisco Bay helped make that facility ideal for staging the field program. The Coastal Ocean Dynamics Experiment has been supported by grants to the individual institutions from the Ocean Sciences Division of the National Science Foundation.

This technical report has been prepared at WHOI under the editorship of L. Rosenfeld. The graphics have been prepared by J. Zwinakis with input on report format from D. Bourne. The text and tables have been typed by A.-M. Michael and C. Mills prepared the layout of the final report. R. Beardsley and R. Limeburner provided editorial assistance. The CODE principal investigators would like to express their appreciation to this group and especially to L. Rosenfeld for her efforts as editor. The final preparation and production of this report has been supported by the Ocean Sciences Division of the National Science Foundation.

References

Allen, J. S., R. C. Beardsley, W. S. Brown, D. A. Cacchione, R. E. Davis, D. E. Drake, C. Friehe, W. D. Grant, A. Huyer, J. D. Irish, M. M. Janopaul, A. J. Williams, and C. D. Winant, 1982. A preliminary description of the CODE-1 Field Program. WHOI Technical Report No. 82-51, CODE Tech. Report No. 9.

Cacchione, D. A., D. E. Drake, W. D. Grant, and A. J. Williams, III, 1983. CODE Geology Report. WHOI Technical Report No. 83- , CODE Tech. Report No. 17.

Grant, W. D., A. J. Williams III, S. M. Glenn, D. A. Cacchione, and D. E. Drake, 1983. High frequency bottom stress variability and its predictions during CODE-1. WHOI Technical Report No. 83-19, CODE Tech. Report No. 15.

CODE-1:
COASTAL AND MOORED
METEOROLOGICAL OBSERVATIONS

By

C. A. Mills
R. C. Beardsley

Woods Hole Oceanographic Institution
Woods Hole, Massachusetts 02543

A. INTRODUCTION

The Coastal Ocean Dynamics Experiment (CODE) is a multi-institutional field observation and data analysis program designed to identify and evaluate the dominant physical processes which govern wind-driven motion of coastal water over the continental shelf. This report presents coastal and moored buoy meteorological observations obtained during the pilot field experiment (CODE-1) conducted off northern California during April through July, 1981. We will describe first the design and motivation of the meteorological sampling array, then describe the various instrumentation systems used and, finally, present the basic meteorological data sets in primarily graphical form. The overall CODE-1 field experiment and the different measurement programs are described in some detail in a separate technical report by The CODE Group (Allen, et al., 1982).

B. METEOROLOGICAL ARRAY DESIGN AND INSTRUMENTATION

B.1 Array Design

Serial meteorological data was collected during CODE-1 over the spatial array shown in Figure 1. Coastal wind measurements were made at Sea Ranch and the Bodega Bay Marine Laboratory using portable self-recording anemometer systems installed and maintained by SIO personnel; self-recording instrumented buoys were deployed by WHOI at C1, C3, C5 and R3 to obtain surface meteorological data. The initial objectives of this moored array were: (a) to obtain, at representative positions within the CODE-1 area, accurate seasonal measurements of the horizontal wind velocity, air and sea surface temperature, and insolation which could be used to construct time series estimates of the surface wind, wind stress, and heat flux, and to examine the cross-shelf and along-shelf structure as well as the coherence of these fields; (b) to obtain engineering information on the different wind and air temperature sensors deployed on the WHOI buoys. The cross-shelf structure information was to be provided by the subarray formed by the coastal station at Sea Ranch, and the C1, C3, and C5 meteorological buoys which spanned the shelf along the CODE-1 central line out to the upper slope. Along-shelf structure information was to be obtained from the minimum subarrays formed by C3 and R3 located along the 90 m isobath

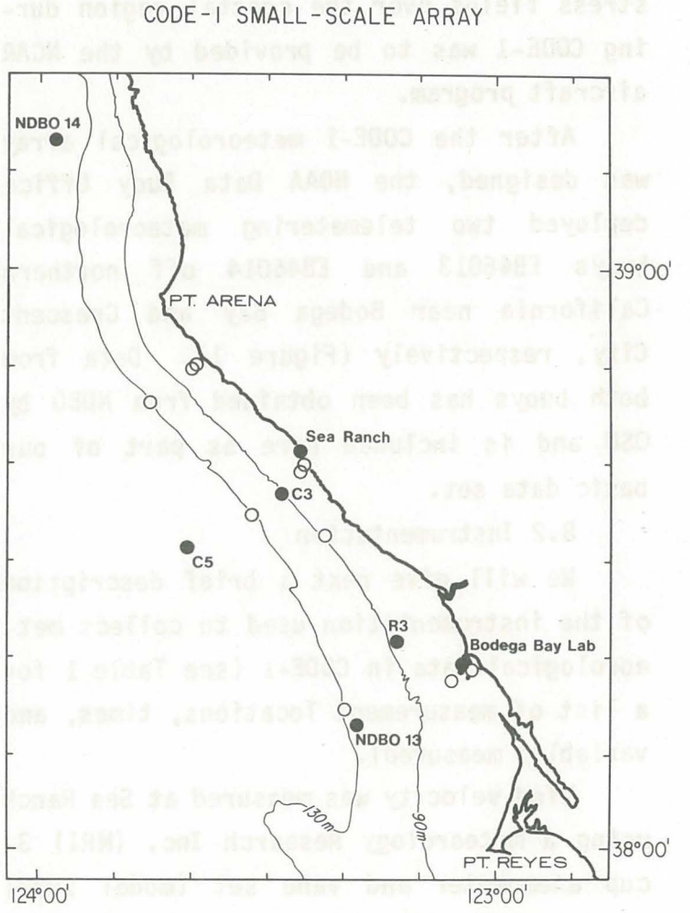

Figure 1. Stations where wind measurements were obtained during CODE-1 are shown as darkened circles.

and the Sea Ranch and Bodega Bay coastal stations. Additional information on the spatial structure of the wind and wind stress fields over the coastal region during CODE-1 was to be provided by the NCAR aircraft program.

After the CODE-1 meteorological array was designed, the NOAA Data Buoy Office deployed two telemetering meteorological buoys EB46013 and EB46014 off northern California near Bodega Bay and Crescent City, respectively (Figure 1). Data from both buoys has been obtained from NDBO by OSU and is included here as part of our basic data set.

B.2 Instrumentation

We will give next a brief description of the instrumentation used to collect meteorological data in CODE-1 (see Table 1 for a list of measurement locations, times, and variables measured).

Wind velocity was measured at Sea Ranch using a Meteorology Research Inc. (MRI) 3-cup anemometer and vane set (model 1022) mounted 10 m above the ground at the northern end of a deserted barn located roughly 100 m inshore of the coastal cliffs. The analog signals were separately averaged for

Table 1: The Coastal and Moored Meteorological Data Obtained in CODE-1.

Name	Location (°N/°W)	Start/Stop (GMT)	Sensor Height (m)	Variables
COASTAL				
Bodega Bay Marine Lab	38°19.0 123°04.0	810311/ 810803	10.0*	Wind Speed, Direction, Atmospheric Pressure
Sea Ranch (Black's Point)	38°41.0 123°25.5	810311/ 810811	10.0*	Wind Speed, Direction
WHOI BUOY				
C1	38°39.5 123°25.2		3.5	System failed prior to launch.
C3	38°36.5 123°28.1	810412/ 810731	3.5	Wind Speed, Direction, (2) Air Temperature, Water Temperature (1 m), Insolation
C5	38°31.2 123°40.5	810412/ 810801	3.5	Wind Speed, Direction, (2) Air Temperature, Water Temperature, (1 m), Insolation
R3	38°21.6 123°13.0	810413/ 810803	3.5	Wind Speed, Direction, (2) Air Temperature, Water Temperature (1 m)
NDBO BUOY				
13	38°13.0 123°18.0	810401/ 810731	10.0	Wind Speed, Direction, Air Temperature, Water Temperature (1 m), Atmospheric Pressure
14	39°13.0 123°58.0	810401/ 810729	10.0	Wind Speed, Direction, Air Temperature, Water Temperature (1 m), Atmospheric Pressure

*Approximate height above ground.

4 minutes, then recorded on tape. A similar sensor set was mounted on a tower approximately 10 m above the ground at the Bodega Bay Marine Laboratory. Atmospheric pressure was also measured at the Bodega Bay Lab using a 45 psia Paroscientific, Inc. digiquartz pressure sensor. The pressure output was averaged for 4 minutes and then recorded with the wind speed and direction data. These two coastal meteorological stations were established and maintained by SIO personnel, who also carried out the preliminary data processing before sending the edited data to WHOI.

The WHOI toroid buoys were instrumented to measure horizontal wind velocity at 3.5 m height with vector-averaging wind recorders (VAWRs) equipped with a utility wind vane and 3-cup anemometer set developed by Professor G. C. Gill of the University of Michigan (see Figure 2). This anemometer has a threshold of < 0.7 m/s and a distance constant of about 3.7 m, while the vane has a threshold of < 0.7 m/s and a damping ratio of 0.37. The Gill utility sensor sets were purchased from the R. M. Young Company (models 6301 and 6101) and modified to supply appropriate digital signals to the vec-

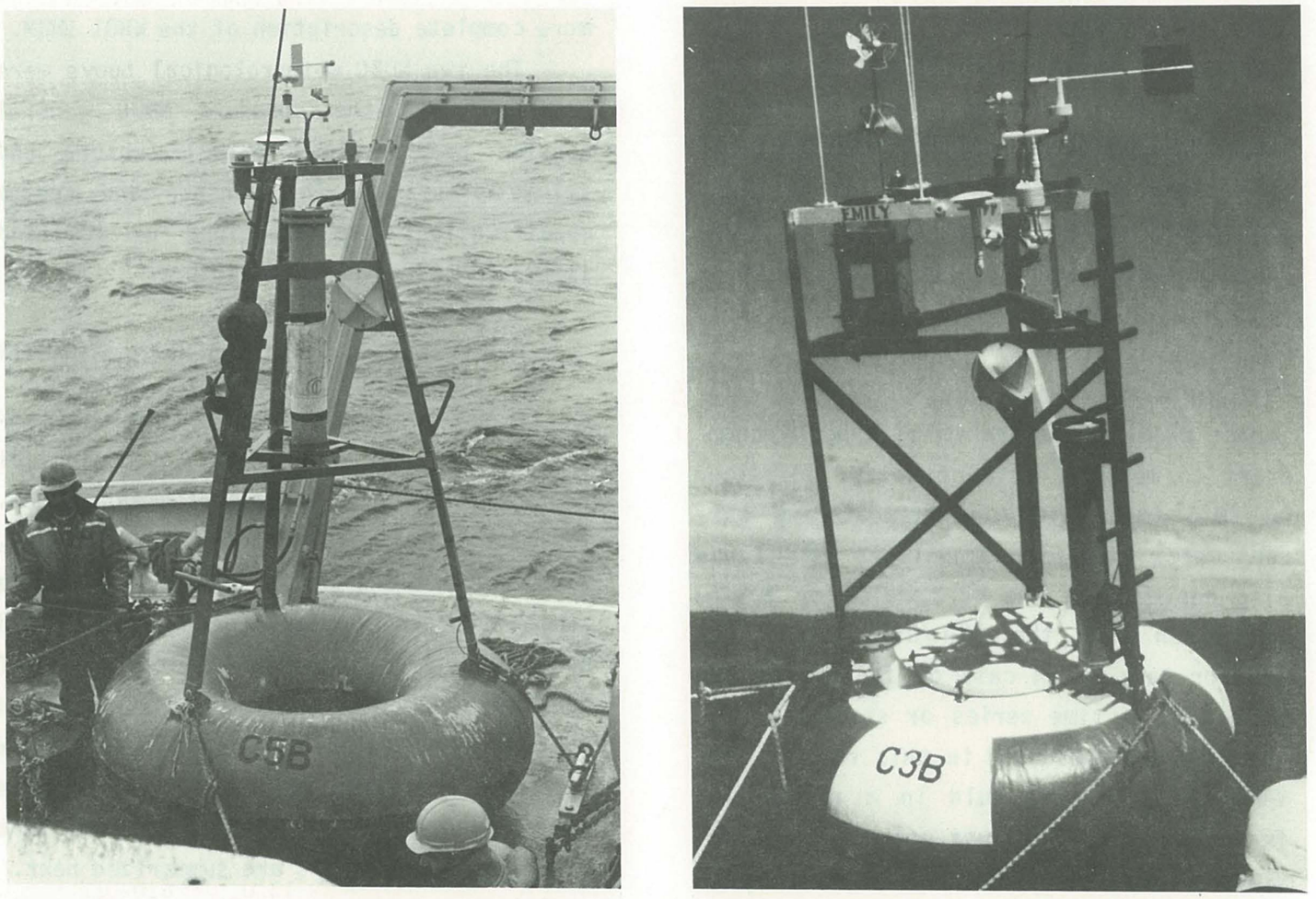

Figure 2. The C5 (above left) and C3 (above right) WHOI toroid buoys prior to launch from the R/V Wecoma. The frame on each buoy supports a VAWR equipped with a Gill cup and vane sensor set and insolation and air temperature sensors. The C3 frame also supported a VMCM equipped with wind propellers for comparison and redundancy. The C3 toroid was oriented into the wind (to provide clear flow to both velocity sensors) by a large steering vane (not shown in this photograph) mounted on the trailing edge of the frame. All toroids were deployed on slack moorings with rigid bridles for stability.

tor computer in the VAWR. For redundancy and also for comparison of shields, two air temperature sensors were installed on each buoy at 3 m. Thermistors were mounted in naturally-ventilated radiation shields based on designs by Professor Gill, one a glass dome modified for use at sea (R. M. Young Company, model 43103C), the other, a modified Thaller shield [model II, Gill (1979)] manufactured at WHOI. The C3, C5, and R3 buoys were also equipped with Epply Company (model 8-48) black and white type pyranometers to measure incident solar radiation. An EG&G (model 630) vector-measuring current meter with wind propellers (VMWR) was also deployed on the C3 toroid for intercomparison with the VAWR/Gill sensor set and for back-up in case of failure of the Gill set. No time series or statistics for the VMWR are presented in this report. The VAWR and VMWR were held in a rectangular frame and the toroid was oriented into the wind by a large steering vane mounted on the trailing side of the frame. Nearly symmetrical triangular frames were used to support the VAWR's on the other toroids. Water temperature was measured on all buoys with a precision thermistor mounted at 1 m depth. See Weller and Davis (1980) for a more complete description of the WHOI VMCM.

The two NDBO meteorological buoys were equipped with the standard NDBO general service buoy payload (GSBP) sensors and telemetry system. The sensors and system specifications are described by Hamilton (1980) and given here in Table 2.

B.3 Field Calibration of VAWR/Gill Systems

A short intercomparison test was conducted with the four WHOI meteorological buoys just prior to their deployment at sea. The four buoys were placed in a line (C5, R3, C1, C3) along the northwest side of the finger dock at the Yerba Buena Coast Guard Base, and data from the period 0000 GMT April 9 to 1400 GMT April 10 was compared to give some checks on sensor and system performance. Winds during this period were generally light (0.5 to 4 m/sec) and from the west. The results are summarized next.

(1) Wind Speed, S: Linear regression of the 7.5 min vector average speeds of one VAWR against another VAWR yielded the following results:

$y = a + bx$	std. error
SR3 = 0.018 + 1.008 SC3,	± .135,
SC5 = 0.012 + 1.028 SR3,	± .078,
SC5 = 0.016 + 1.044 SC3,	± .113.

The manufacturer states ± 0.5% interchangeability of the 3-cup anemometer sensors in wind tunnel tests, but gives no accuracy specifications under natural flow conditions. Without additional field calibration, we interpret the above results to indicate that (a) the maximum differences between anemometers was less than 5%, and (b) the wind speed was uniform within 5% over the spatial array. It seems likely, however, that the anemometer accuracy is much better than 5% and the observed differences were due to real differences in the flow caused by the dock geometry and siting. A proper anemometer intercomparison experiment is planned for CODE-2.

(2) Wind Direction: The orientations of the different buoys were determined optically by sighting over the VAWR cases with a hand-held protractor. These orientations disagreed with the internal compass readings, suggesting that either the optical orientations may be in error or the mag-

netic field was not uniform over the finger dock. The latter was confirmed by subsequent measurement of the magnetic field over the test area on the dock with a portable ship's compass, so we have assumed in our analysis that the optically-determined instrument orientations were correct to within 1°. The wind directions recorded by the two end VAWRs (C3 and C5) agreed to within 3°, indicating that the wind field was also reasonably uniform in direction over the extent of the array. This implies that a consistent 14.7° difference in the wind directions recorded by the R3 VAWR was due to an accumulation of angular offsets in the compass, vane follower, and sensor frame orientation. To correct for this error, we have added a constant 15° clockwise rotation to the R3 VAWR direction data.

(3) Air Temperature, T: Comparison of the air temperature data from this dock test and CODE-1 and other field experiments indicated that the modified Thaller type shield is less sensitive than the glass dome shield to diurnal radiation effects; thus only air temperature data measured with the modified Thaller type shield in CODE-1 is presented here. Comparison of this data for the duration of the dock test yields the following differences:

$$TC5 - TC3 = 0.064 \pm 0.087^{\circ}C,$$
$$TC5 - TR3 = 0.016 \pm 0.129^{\circ}C,$$
$$TC3 - TR3 = 0.080 \pm 0.096^{\circ}C.$$

While these differences are within the ± 0.1°C interchangeability specification given by the thermistor manufacturer, larger errors can be caused by diurnal radiation effects. Gill (1979) reports that the insolation error is < 0.5°C for windspeeds above 4 m/s for a modified Thaller shield (model II) made from several types of plastic materials. The WHOI shield was made from aluminum and painted white, and should exhibit similar insolation error characteristics.

(4) Insolation, I: Linear regression between the two insolation sensors gives in $cal/cm^2/min$

$$IC5 = - 0.003 + 1.056 \times IC3,$$
$$\text{std. error} = \pm 0.18$$

This difference is within the manufacturer's calibration of ± 3%.

B.4 System Accuracy and Performance

The two SIO coastal stations and three WHOI meterological buoys (C3, C5, and R3) returned high quality data for most of the CODE-1 deployment period. The Gill utility wind vane and 3-cup anemometer set proved to be a rugged and reliable, yet responsive, pair of sensors, and these sensors in the present configuration will be used in the second small scale experiment, CODE-2. An unusual electronic failure in the tape recorder caused the C1 VAWR to stop prior to launch so that no useful scientific data were obtained at C1.

A summary of the sensor and system characteristics for the different meteorological instrumentation systems is given in Table 2. The information on the SIO instrumentation was provided by C. Winant. J. Dean and D. Payne provided additional information on the VAWR specifications. The direction accuracy listed for the VAWRs is taken from a field study of VACM direction errors by Bryden (1976). The characteristics of the GSBP measurement and telemetry system used in the NDBO buoys are taken from Hamilton (1980).

Table 2: Meteorological Sensor and System Characteristics

	Parameter	Sensor	Manufacturer (Model)	Range	Sensor Accuracy	Sampling/Recording Scheme	System Accuracy
COASTAL	Wind Speed	3-Cup Anemometer	Meteorological Research, Inc. (1022)	0-60 m/s	±0.5 m/s or 1%	4 min average of each variable recorded every 4 min	± 0.7 m/s or 1%
	Wind Direction	Vane		0-360°	± 5°		± 5°
	Atmos. Pressure	Digiquartz	Paroscientific	0-45 psia	± 0.1 mb		± 0.4 mb
WHOI BUOY	Wind Speed	3-Cup Anemometer	RM Young (6301)*	0-54 m/s	< 5%	Vector-averaged recorded every 7.5 min	< 5%
	Wind Direction	Vane	" " (6101)*				
		Magnetic Compass	EG&G (VACM)	0-360°	± 3.1°		± 3.1°
	Air Temperature	Thermistor	Yellow Springs Instruments (44034)	0-30°	± 0.1°C	1-7/8 min average of each variable recorded every 7.5 minutes.	± 0.3°C
	Water Temperature	Thermistor	Thermometrics, Inc.	0-30°	± 0.005°C		± 0.01°C
	Insolation	Pyranometer	Epply Co. (8-48)	0-2 cal/cm^2 per minute	5%		< 10%
NDBO BUOY	Wind Speed	Propeller	NDBO General Service Buoy Payload	0-80 m/s		8.5 min average of each variable at 1 Hz. Averaged value transmitted every hour.	± 1 m/s or 10%
	Wind Direction	Vane and Flux-gate Compass		0-360°			± 10°
	Air Temperature	Thermistor		-15° to 50°C		One sample per hour transmitted every hour.	± 1°C
	Water Temperature	Thermistor		-15° to 50°C			± 1°C
	Atmos. Pressure	Variable Capacitance		900-1100 mb		8.5 min average of 4 sec samples transmitted once every hour.	± 1 mb

*These parts were modified at WHOI.

C. DATA PROCESSING

Preliminary processing of the SIO coastal wind and pressure data was performed by C. Winant, S. Lentz, and A. Bratkovich at SIO, and a vector-averaged one hour edited version sent to WHOI for further analysis. The Bodega Bay anemometer failed during the period April 23 to May 22, 1981; this gap was filled with data taken from the analog output of a nearby anemometer owned and maintained by the Marine Laboratory. A comparison between the two anemometer records, during a period when both were functioning, indicated good agreement so that the overall quality of the patched Bodega Bay wind time series is good.

Meteorological data recorded on standard magnetic tape (1/8" 4-track cassettes) in the WHOI VAWRs were transcribed onto 9-track computer-compatible tape at WHOI. The data were then converted to scientific units, edited to remove launch and retrieval transients, linearly interpolated across missing or erroneous data cycles, and stored on magnetic tape in Maltais format (Maltais, 1969). A vector-averaged one hour version was then made for each VAWR data set for further analysis. The VAWRs functioned correctly with the exception of the C1 VAWR failure and a mid-deployment failure of one temperature sensor cable on the C3 VAWR.

The NDBO buoy meteorological data was obtained from NDBO by J. Allen and G. Halliwell at OSU and then transmitted to WHOI where missing data gaps were edited and a one-hour version prepared for further analysis.

The basic data set presented here thus consists of edited vector-averaged one hour time series for wind and the other measured variables. All wind time series have been rotated into a standard coordinate system, with the X or East axis pointing onshore towards 47°T and the Y or North axis pointing along-shelf towards 317°T. All wind data are presented in this coordinate system unless otherwise listed. Greenwich Mean Time (GMT) is used throughout this report (GMT = PST + 8 hr).

We also present here wind stress computed from the observed wind data. The computational scheme uses the neutral steady state drag coefficient C_{dn} and iterative method given by Large and Pond (1981) where

$$10^3 C_{dn} = \begin{cases} 1.2 & U_{10} < 11 \text{ m/s}, \\ 0.49 + 0.065\, U_{10} & 11 \text{ m/s} < U_{10} < 25 \text{ m/s}. \end{cases} \quad (1)$$

Neutral stability is assumed and the 10 m wind U_{10} is found through iteration from the observed wind U_o at the observation height h_o (in meters) using

$$U_{10} = \frac{U_o}{1 + \frac{\sqrt{C_{dn}(U_{10})}}{K} \ln \frac{h_o}{10}} . \quad (2)$$

The neutral stress is then given by $\tau_o = \rho \times C_{dn}(U_{10}) \times (U_{10})^2$ where the air density has been assumed to be constant at 1.22×10^{-3} gm/cm^3.

There are three main sources of error in this bulk aerodynamic approach, (a) experimental uncertainty in C_{dn}, (b) the effect of stratification on the observed wind profile and the assumption of neutral stability, and (c) time changes in the wind field and sea state, causing additional (temporal) changes in C_{dn}. Based on their own and other field measurements, Large and Pond (1981) estimate the experi-

mental uncertainty in C_{dn} to be of order 10 to 20%. Large and Pond (1981) also provide a method to compute the influence of stratification on derived wind stress using the observed wind, air and sea temperatures, and the relative humidity and bulk aerodynamic formulaes for the Richardson number and stability parameter Z/L (where Z is the observation height and L the Monin-Obukhov length scale). The formulation is strictly valid for values of Z/L in the range from -1 to 0.2. We plot in Figure 3A and B the difference and percent difference between the wind stress τ, computed for a given wind speed U_3 at 3.5 m height with stratification included, and the neutral wind stress τ_n, computed using Equations (1) and (2). The different curves show the stress difference and percent difference as a function of U_3 and the air-sea temperature difference ($\Delta T = T_{air} - T_{sea}$). The magnitude of the neutral stress is also given as a function of U_3 along the top axis. Relative humidity measurements made aboard ship along the CODE central line during May and July give a mean value of 80 ± 4%. Values of 90% for the relative humidity at 3.5 m and T_{sea} = 10°C were used for the computations shown in Figure 3, although the resultant curves are relatively insensitive to changes in T_{sea} between 5 and 15°C and relative humidity between 75 and 95%. The observed ΔT in CODE-1 varied roughly between -1° and 5°, with means at different buoys varying from + 0.8°C at C5 to 1.4°C at C3 and NDBO-13. The observed buoy wind speeds varied between 0 and 17 m/s, with mean wind speeds varying from a low of 7.2 m/s at R3 to 9.0 m/s at NDBO-13. These mean values of ΔT and wind speed S are plotted for the different buoy records in Figure 3B. While it is clear that the stratification will cause τ_n to over-estimate the actual wind stress, the error will be less than 10% for most of the CODE-1 data. Finally, Large and Pond (1981) suggest that due to the finite time required for the sea state to equilibrate with the wind field, C_{dn} is smaller during rising winds and larger during rapidly decreasing winds or large changes in the wind direction.

The emphasis in CODE is on the response of the shelf to strong wind events, and the neutral stability formulation is a reasonable approximation at the higher winds in excess of ~ 4 m/sec. The influence of stability and time variability on wind stress will be discussed in more detail in a later report.

D. DATA PRESENTATION

The coastal and moored meteorological data collected in CODE-1 are presented here in the form of time series plots of wind and other variables, scatter plots of wind, plots of mean wind and wind stress, and tables of standard statistics for all variables. The statistics were computed over the common time period 0000 GMT April 14, 1981 to 0000 GMT July 31, 1981; the time series and scatter plots are based on the same period. The variable-versus-time and the vector-versus-time plots were generated using the basic one hour time series subsampled every four hours.

The basic along- and cross-shelf wind components time series measured at sensor height are shown in Figures 4 and 5. These figures show that the wind is predominantly southward and southwestward and polarized in the along-shelf direction, i.e., the cross-shelf component is weaker than the along-shelf component at each site. The major along-shelf low-frequency wind fluctuations appear coherent over the

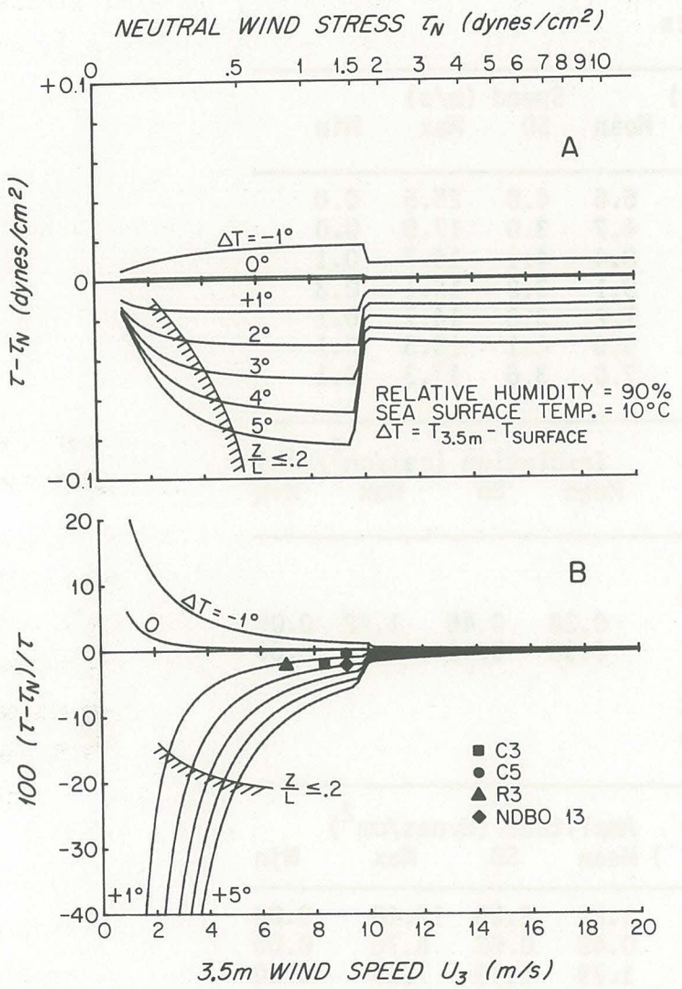

Figure 3. Difference (A) and percent difference (B) between wind stress τ computed with stability included and the neutral wind stress τ_n, plotted as a function of observed 3.5 m wind speed and air-sea temperature difference ΔT. Curve marked $Z/L < 0.2$ indicates boundary of Large and Pond (1981) formulation.

array. The seabreeze, most noticeable at Sea Ranch in late April and early May, has a definite offshore decay since little diurnal variability is clear at C5. The observed air and 1 m seawater temperatures are shown in Figures 6 and 7. Daily insolation (Figure 8) and atmospheric pressure (Figure 9) are also coherent over the array. The basic along- and cross-shelf wind components and vector wind time series are shown in Figures 10 to 16, and standard statistics for these series are given in Table 3. Scatter plots of along- versus cross-shelf components for the individual records (except NDBO-14) are given in Figure 17. These plots clearly illustrate the consistent polarization of the wind fluctuations at each site. The mean observed wind and standard deviations along the principal axes are shown in Figure 18.

Time series plots of the computed neutral wind stress are shown in Figures 19 to 27. The mean wind stress and standard deviations along the principal axes are shown in Figure 28; statistics for the derived stress time series are also given in Table 3.

TABLE 3: Hourly Averaged Statistics For CODE-1 Meteorological Measurements

	Cross-Shelf Wind (m/s)				Along-Shelf Wind (m/s)				Vector Mean (m/s)	Direction (deg.) (Rel to 317°T)	Speed (m/s)			
	Mean	SD	Max	Min	Mean	SD	Max	Min			Mean	SD	Max	Min
Sea Ranch	-0.9	2.6	7.8	-9.3	-5.1	5.9	7.6	-25.2	5.2	189.5	6.6	4.8	25.5	0.0
Bodega Lab	-0.5	1.8	5.0	-6.9	-3.6	3.8	6.1	-16.7	3.7	187.9	4.7	3.0	17.0	0.0
C3B1	0.4	1.2	4.8	-3.2	-7.7	5.1	6.4	-16.5	7.7	177.0	8.4	4.1	16.7	0.1
C5B1	-1.8	1.5	3.8	-5.4	-8.5	4.0	6.2	-14.6	8.7	192.0	9.1	3.2	15.1	0.3
R3B1	1.5	1.3	5.8	-3.5	-6.5	4.6	5.8	-14.3	6.7	167.0	7.2	3.8	14.7	0.1
NDB013	2.0	1.6	8.8	-5.1	-8.4	4.6	6.7	-18.0	8.6	166.6	9.0	4.1	18.5	0.1
NDB014	-1.7	1.6	5.2	-6.4	-6.8	4.3	7.0	-17.2	7.0	194.0	7.6	3.6	17.3	0.1

	Air Temperature (°C)				Surface Temperature (°C)				Atmospheric Pressure (mb)				Insolation (cal/cm^2/min)			
	Mean	SD	Max	Min	Mean	SD	Max	Min	Mean	SD	Max	Min	Mean	SD	Max	Min
Sea Ranch																
Bodega Lab									1012.8	2.9	1021.9	1005.8				
C3B1	10.64	1.36	14.95	8.15	9.25	0.95	13.33	7.75					0.38	0.45	1.42	0.00
C5B1	11.54	0.93	14.88	8.18	10.67	0.99	13.98	8.75					0.38	0.46	1.43	0.00
R3B1	10.73	1.31	14.14	8.11	9.63	1.09	13.53	7.84								
NDB013	10.96	0.97	14.50	7.40	9.54	0.73	12.19	8.05	1015.9	2.6	1024.6	1009.5				
NDB014	11.42	1.06	17.4	8.10	11.41	1.06	17.40	8.10	1015.6	3.1	1025.3	1006.9				

	Cross-Shelf Wind Stress (dynes/cm^2)				Along-Shelf Wind Stress (dynes/cm^2)				Vector Direction		Amplitude (dynes/cm^2)			
	Mean	SD	Max	Min	Mean	SD	Max	Min	Mean	(Rel to 317°)	Mean	SD	Max	Min
Sea Ranch	-0.07	0.52	4.24	-2.31	-1.08	2.26	1.22	-17.28	1.09	183.9	1.21	2.25	17.46	0.00
Bodega Lab	-0.07	0.18	0.61	-1.14	-0.42	0.63	0.64	-5.67	0.43	189.1	0.48	0.62	5.76	0.00
C3B1	0.12	0.29	1.55	-0.51	-1.74	1.53	0.79	-7.24	1.74	176.1	1.79	1.49	7.29	0.00
C5B1	-0.39	0.35	0.51	-1.74	-1.78	1.15	0.68	-5.54	1.83	192.4	1.86	1.15	5.70	0.00
R3B1	-0.37	1.41	0.28	0.27	-1.23	1.11	0.60	-5.04	1.26	167.6	1.30	1.11	5.17	0.00
NDB013	0.35	0.35	1.93	-0.49	-1.53	1.25	0.68	-7.05	1.57	167.1	1.60	1.26	7.27	0.00
NDB014	-0.25	0.25	0.48	-1.28	-1.03	0.94	0.79	-5.98	1.06	193.6	1.10	0.93	6.02	0.00

Number of points for each record is 2593 (108 days) from April 14 to July 31.

Acknowledgments

These data have been collected through the collaboration of many individuals, whose help we want to acknowledge here. C. Winant, A. Bratkovich, S. Lentz, and others at SIO, set up and maintained the Sea Ranch and Bodega Bay stations and supplied us with edited data. J. Allen and G. Halliwell supplied the NDBO buoy data. The VAWR/Gill instruments were developed primarily by J. Dean and J. Poirier at WHOI with input on sensor selection from D. Payne. The WHOI meteorological array was deployed and recovered with great skill by the WHOI Buoy Group. This research was supported by the National Science Foundation.

References

Allen, J. S. et al., 1982. A preliminary description of the CODE-1 Field Program. WHOI Technical Report No. 82-51.

Bryden, H. L., 1976. Horizontal advection of temperature for low frequency motions. Deep-Sea Research, 23: 1165-1174.

Gill, G. C., 1979. Development of a small rugged radiation shield for air temperature measurements on drifting buoys. Technical Report, Department of Atmospheric Sciences, University of Michigan, Ann Arbor, Michigan.

Hamilton, G. D., 1980. NOAA Data Buoy Office Programs. Bulletin Am. Met. Soc., 61(9): 1012-1017.

Maltais, J. A., 1969. A nine-channel digital magnetic tape format for storing oceanographic data. WHOI Technical Report No. 69-55.

Large, W. S. and S. Pond, 1981. Open ocean momentum flux measurements in moderate to strong winds. J. Phys. Oceanog., 11(3): 324-336.

Weller, R. A. and R. E. Davis, 1980. A vector measuring current meter. Deep-Sea Res., 27: 565-582.

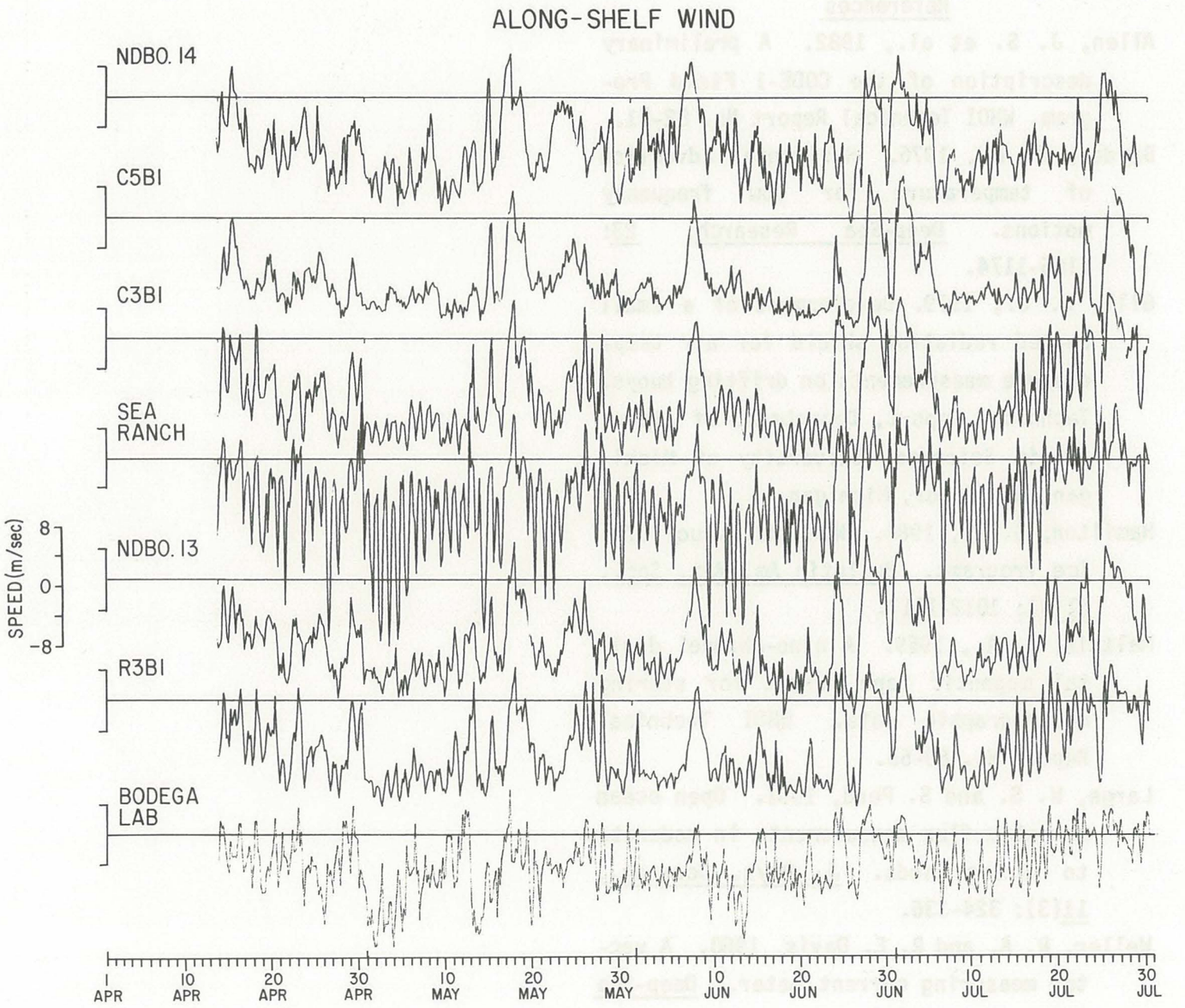
ALONG-SHELF WIND
NDBO. 14
C5BI
C3BI
SEA RANCH
NDBO. 13
R3BI
BODEGA LAB
SPEED (m/sec)
8
0
-8
1 APR
10 APR
20 APR
30 APR
10 MAY
20 MAY
30 MAY
10 JUN
20 JUN
30 JUN
10 JUL
20 JUL
30 JUL

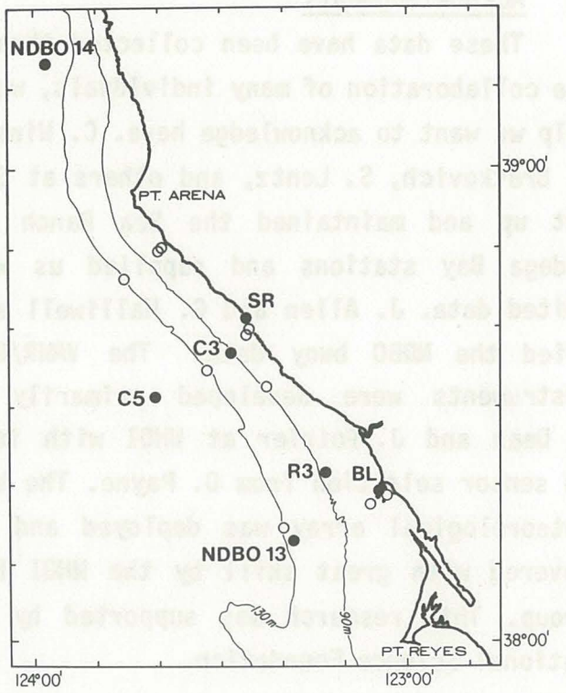
NDBO 14
PT. ARENA
SR
C3
C5
R3
BL
NDBO 13
130m
90m
PT. REYES
39°00'
38°00'
124°00'
123°00'

Figure 4

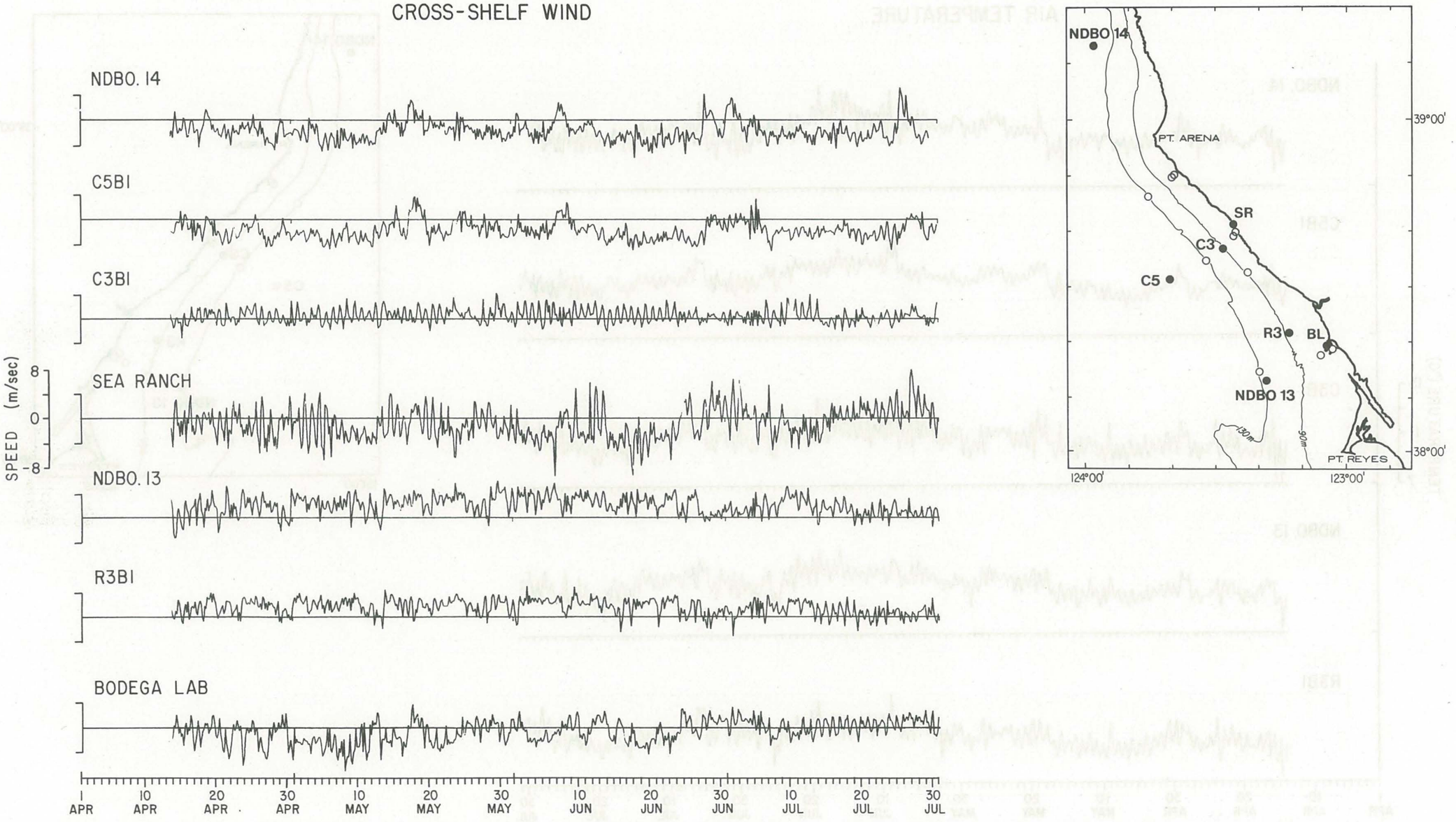
CROSS-SHELF WIND
NDBO. 14
C5BI
C3BI
SEA RANCH
NDBO. 13
R3BI
BODEGA LAB
SPEED (m/sec)
8
0
-8
1 APR
10 APR
20 APR
30 APR
10 MAY
20 MAY
30 MAY
10 JUN
20 JUN
30 JUN
10 JUL
20 JUL
30 JUL
NDBO 14
PT. ARENA
SR
C3
C5
R3
BL
NDBO 13
PT. REYES
39°00'
38°00'
124°00'
123°00'

Figure 5

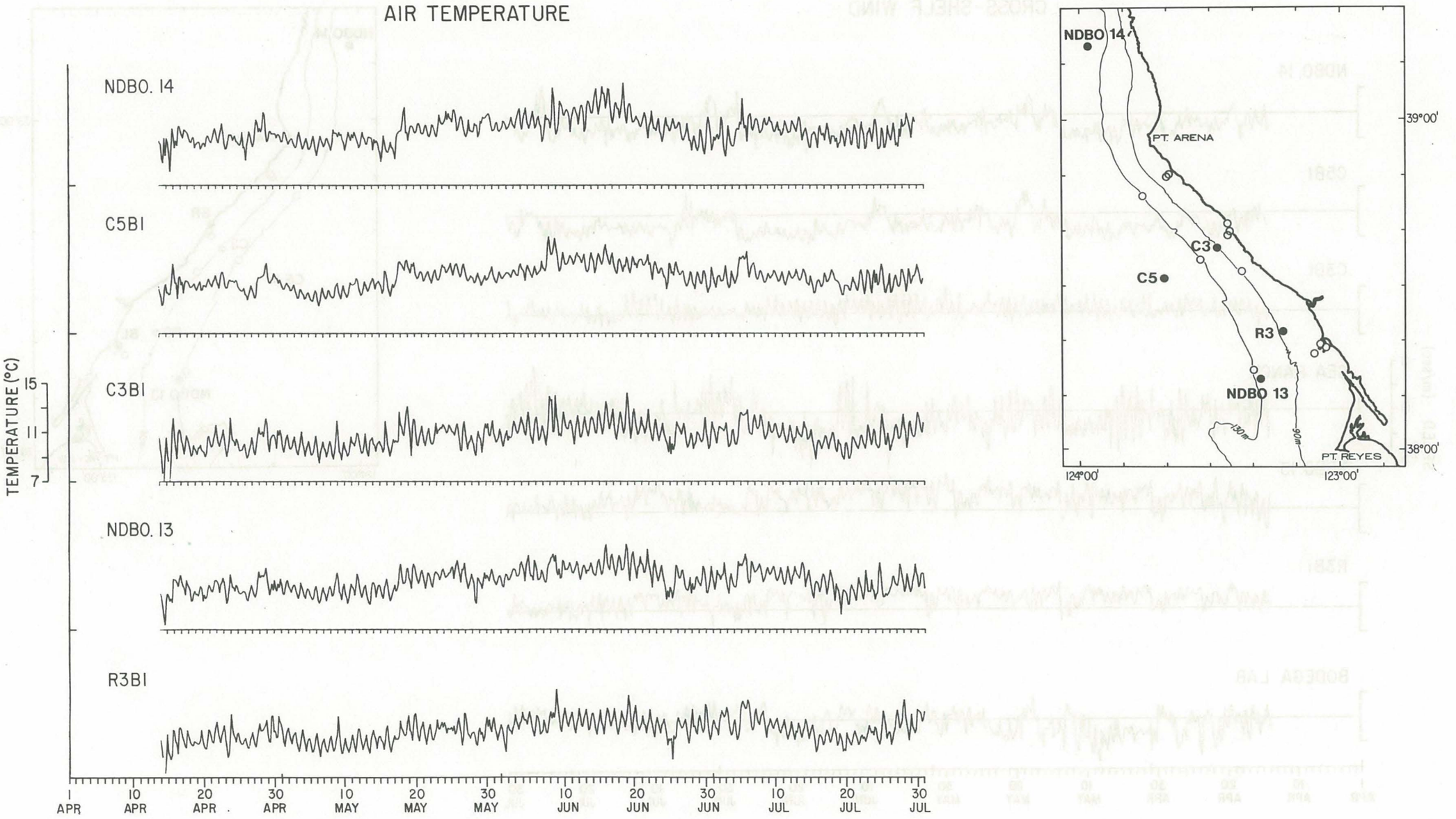
AIR TEMPERATURE
NDBO. 14
C5BI
C3BI
NDBO. 13
R3BI
TEMPERATURE (°C)
15
11
7
1 APR
10 APR
20 APR
30 APR
10 MAY
20 MAY
30 MAY
10 JUN
20 JUN
30 JUN
10 JUL
20 JUL
30 JUL
NDBO 14
PT. ARENA
C3
C5
R3
NDBO 13
PT. REYES
39°00'
38°00'
124°00'
123°00'

Figure 6

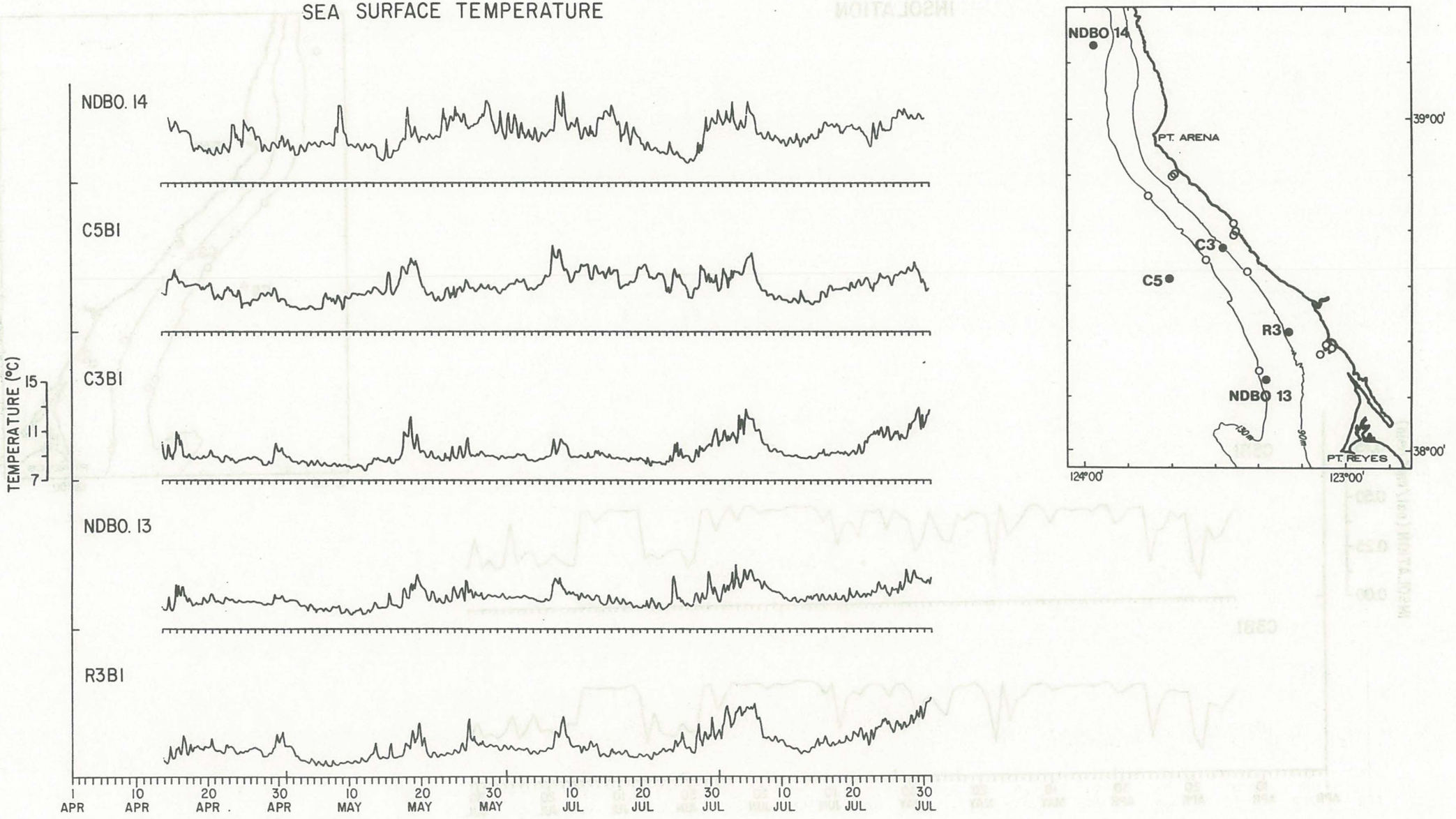
SEA SURFACE TEMPERATURE
NDBO. 14
C5BI
C3BI
NDBO. 13
R3BI
TEMPERATURE (°C)
15
11
7
1 APR
10 APR
20 APR
30 APR
10 MAY
20 MAY
30 MAY
10 JUL
20 JUL
30 JUL
10 JUL
20 JUL
30 JUL
NDBO 14
PT. ARENA
C3
C5
R3
NDBO 13
PT. REYES
39°00'
38°00'
124°00'
123°00'

Figure 7

INSOLATION

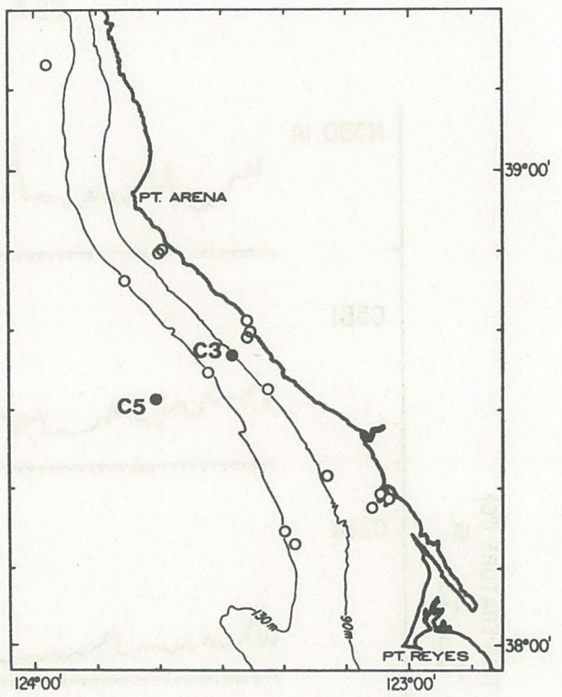

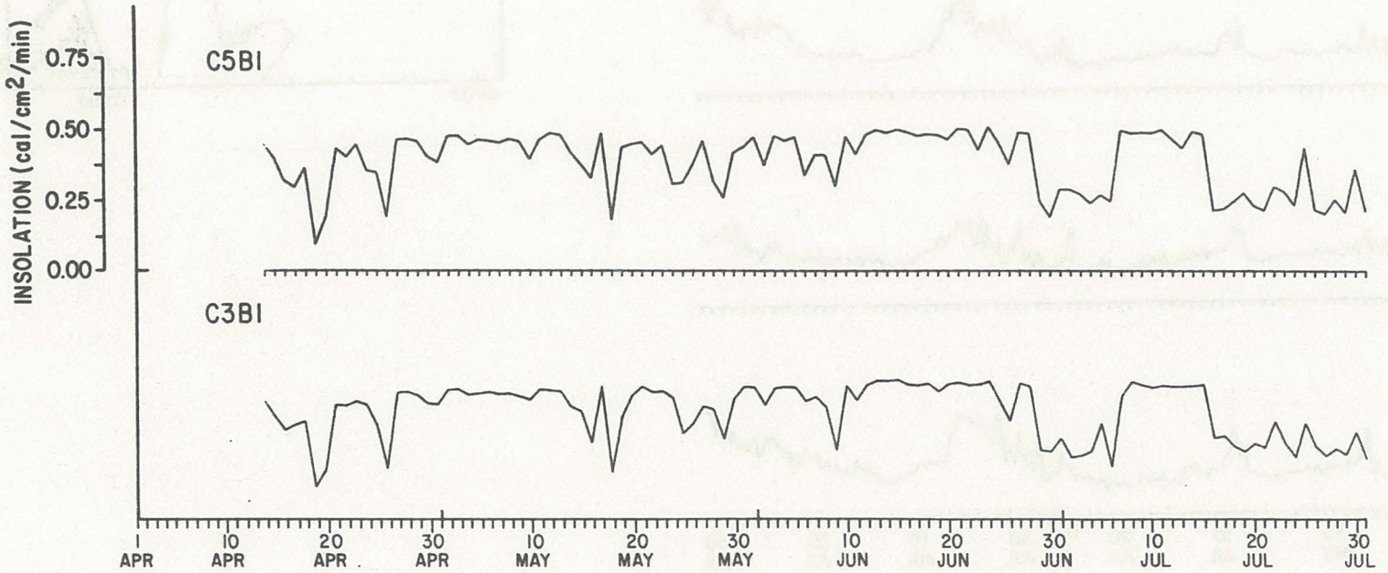

Figure 8

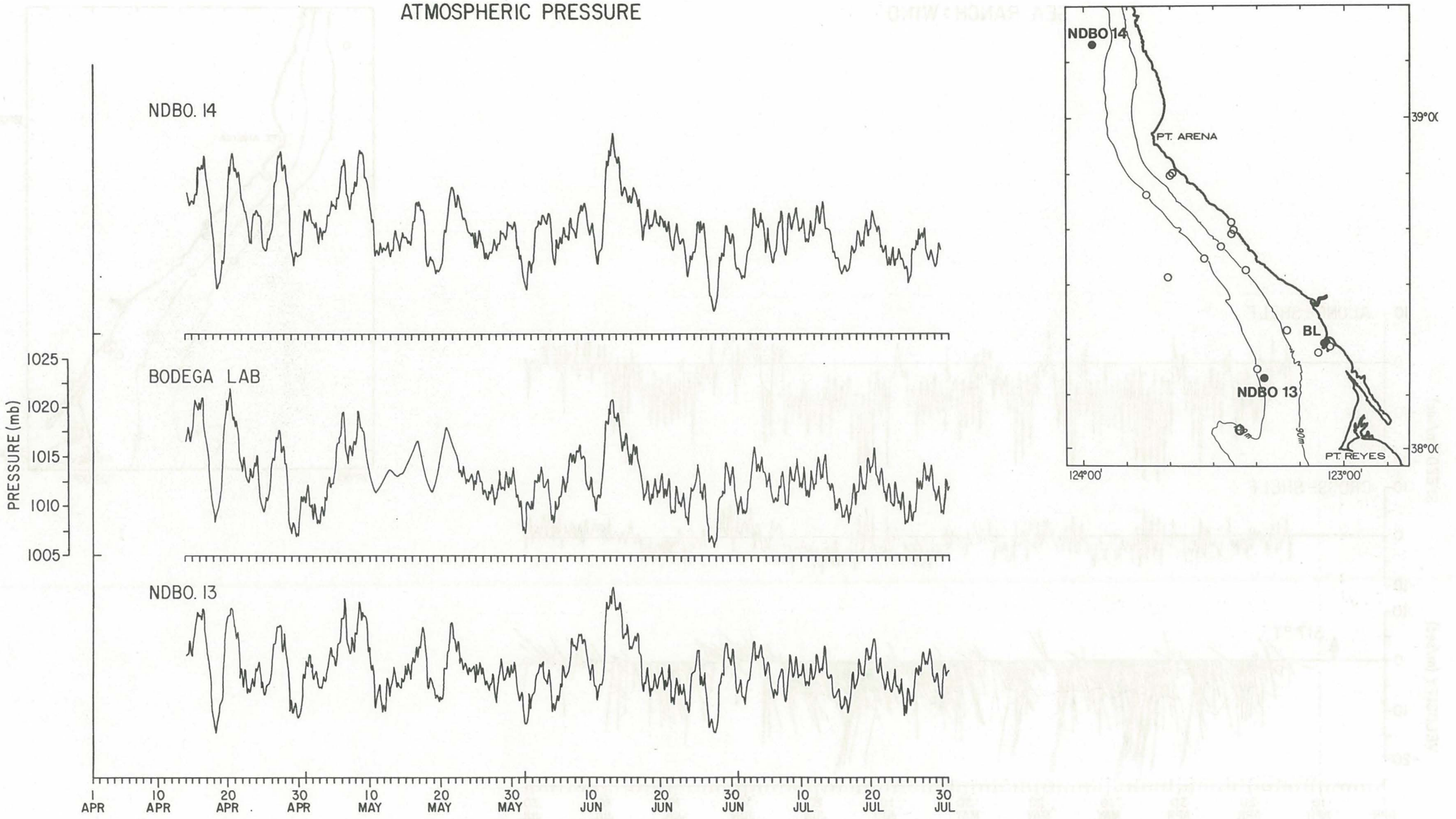
ATMOSPHERIC PRESSURE
NDBO. 14
BODEGA LAB
NDBO. 13
PRESSURE (mb)
1025
1020
1015
1010
1005
1 APR
10 APR
20 APR
30 APR
10 MAY
20 MAY
30 MAY
10 JUN
20 JUN
30 JUN
10 JUL
20 JUL
30 JUL
NDBO 14
PT. ARENA
BL
NDBO 13
PT. REYES
39°0(
38°0(
124°00'
123°00'

Figure 9

SEA RANCH: WIND

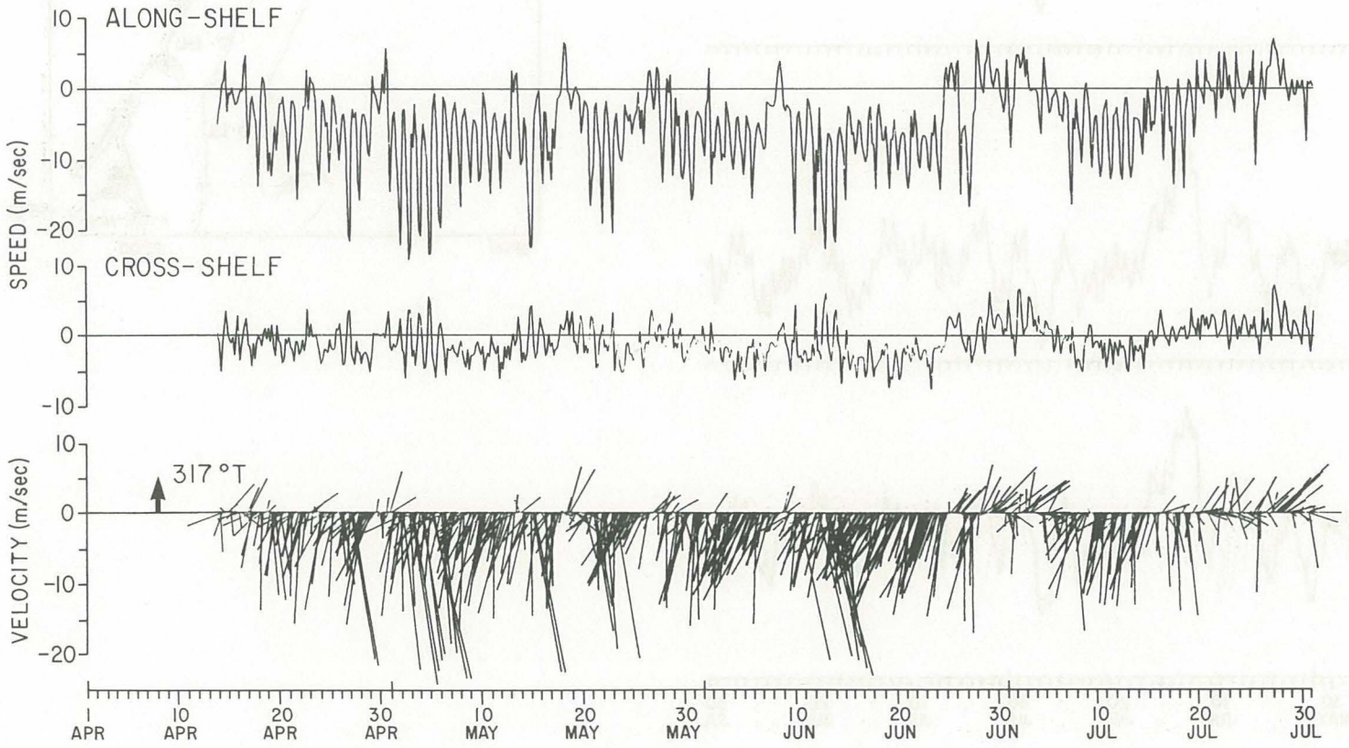

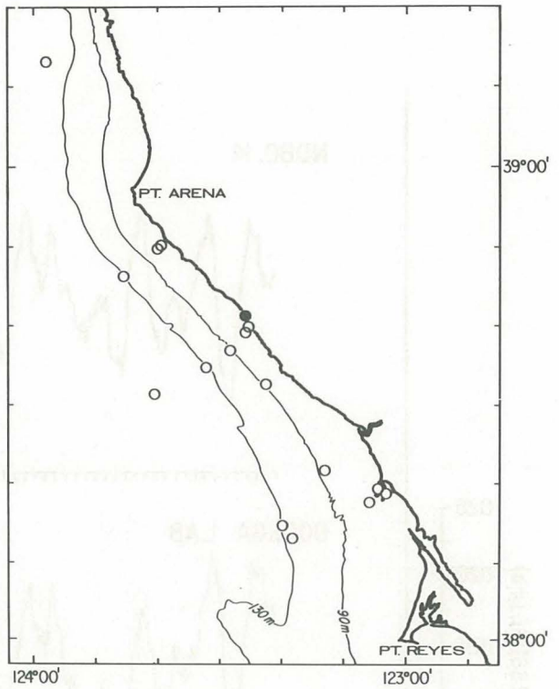

Figure 10

BODEGA LAB:WIND

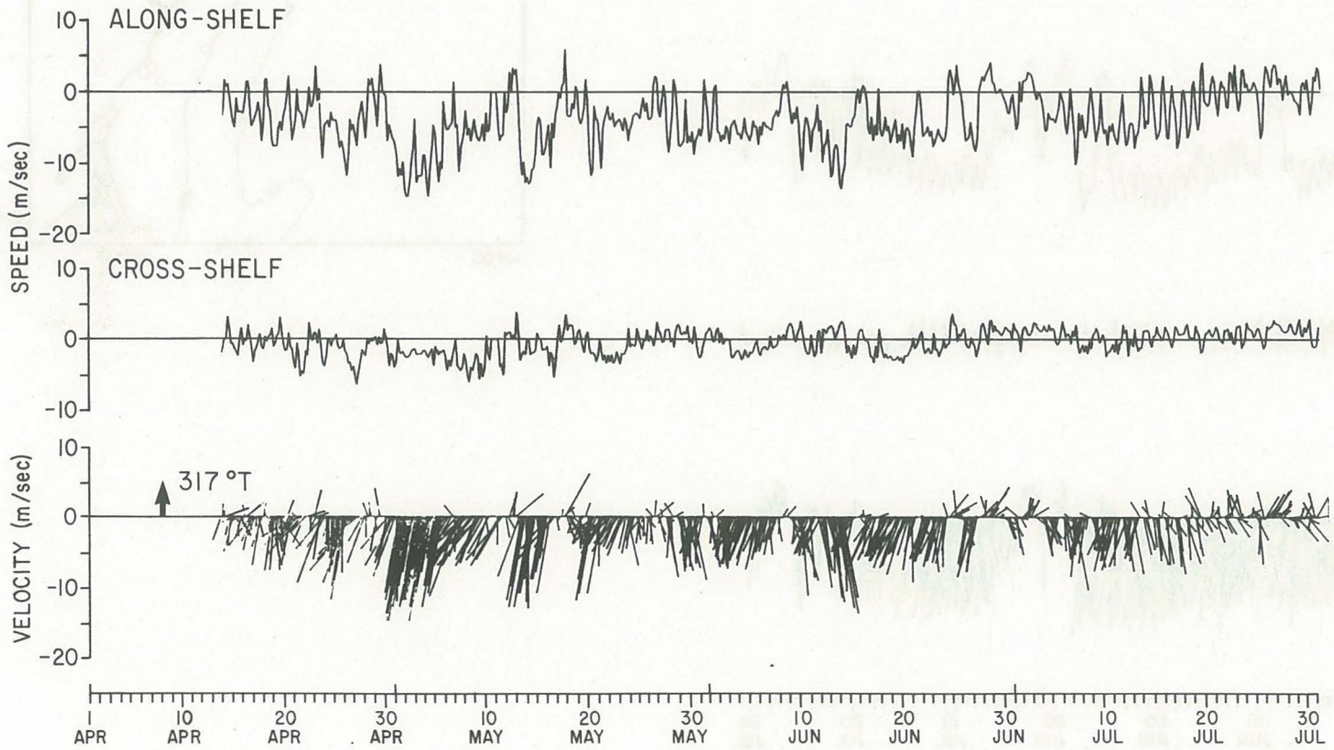

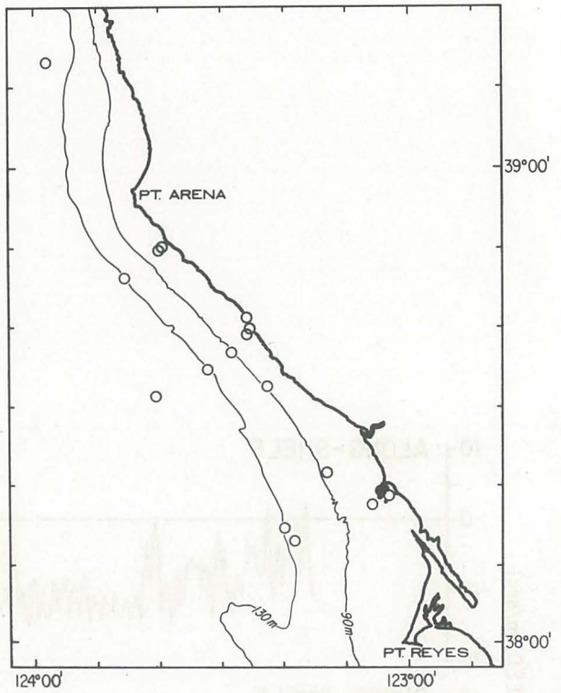

Figure 11

C3B1:WIND

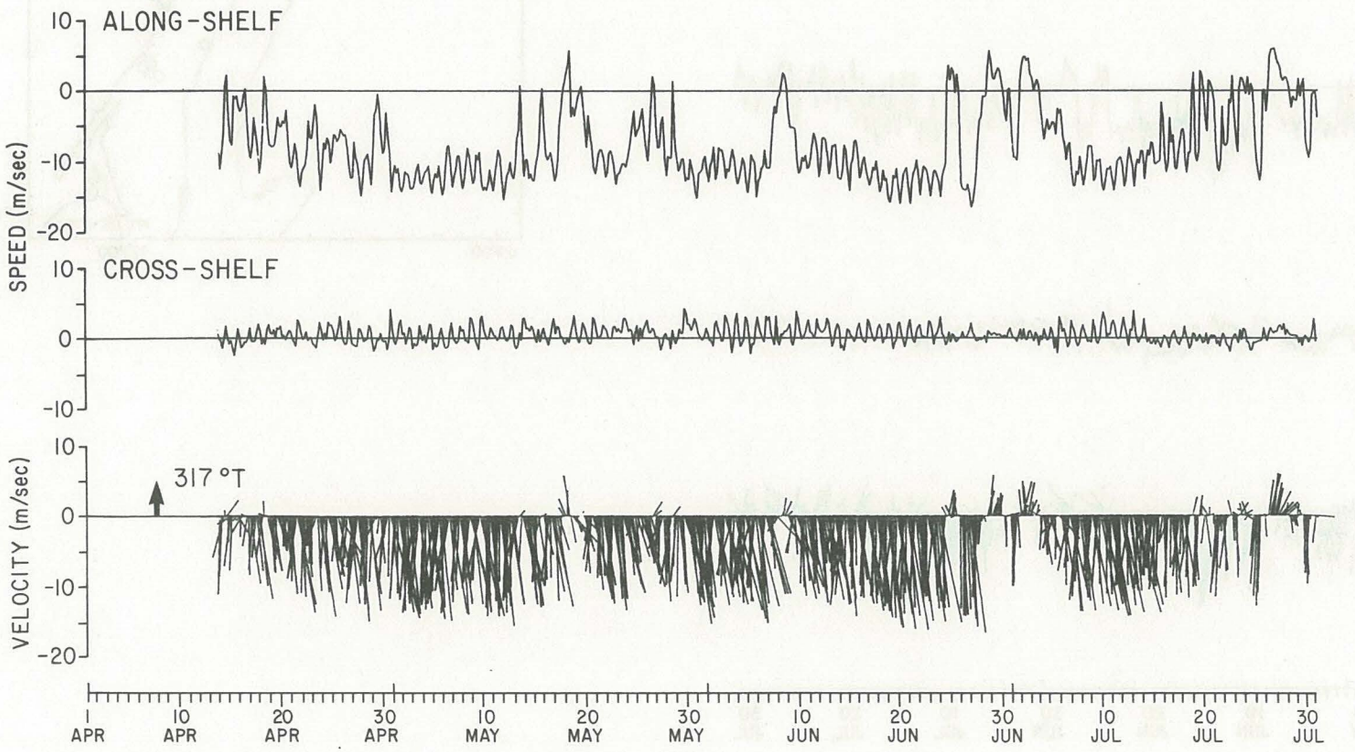

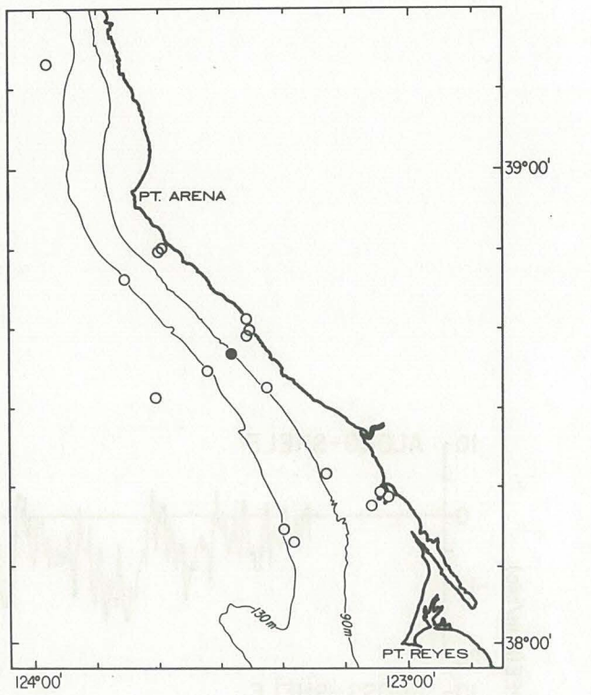

Figure 12

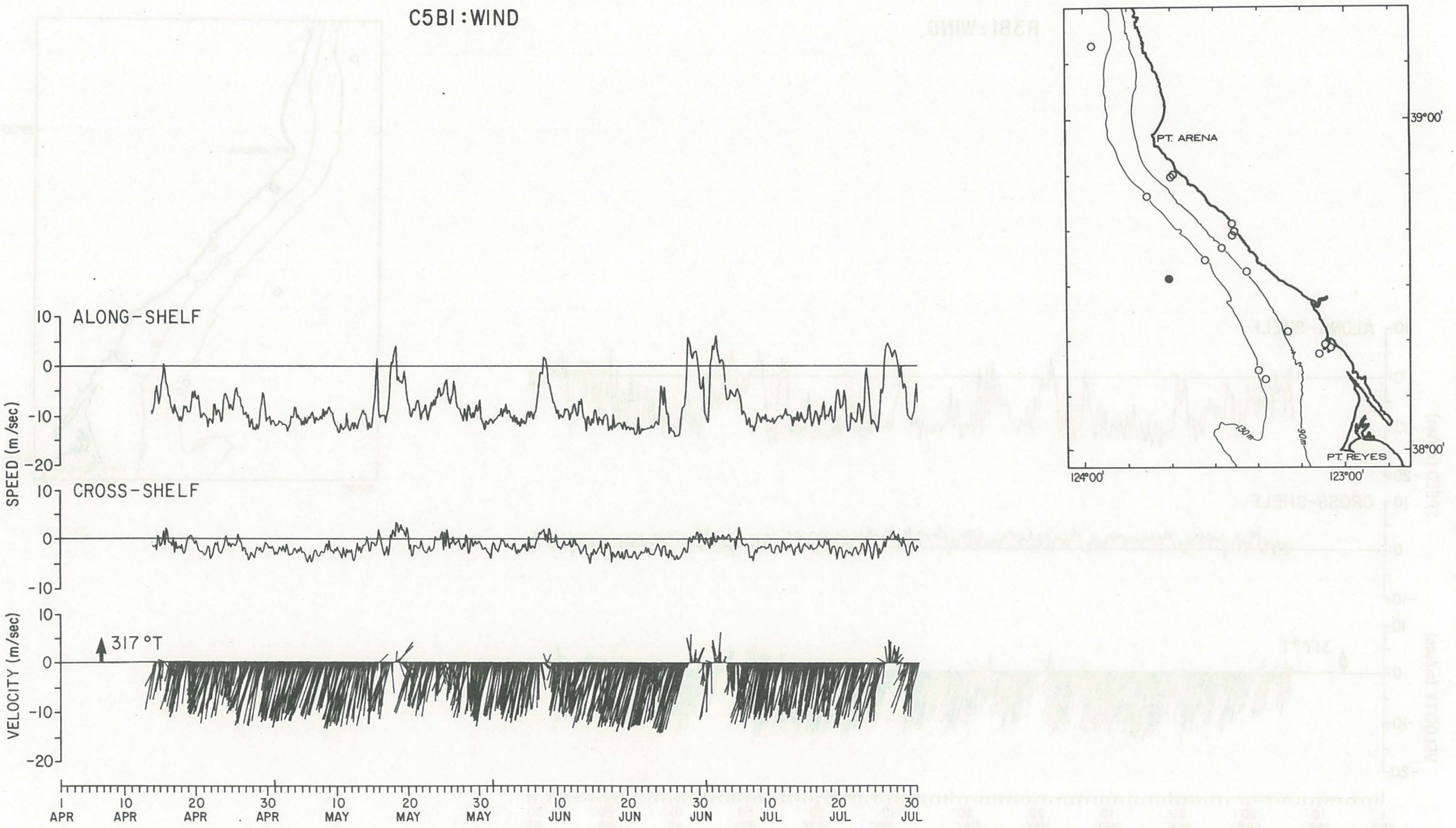
C5BI:WIND
ALONG-SHELF
CROSS-SHELF
SPEED (m/sec)
VELOCITY (m/sec)
10
0
-10
-20
317 °T
1 APR
10 APR
20 APR
30 APR
10 MAY
20 MAY
30 MAY
10 JUN
20 JUN
30 JUN
10 JUL
20 JUL
30 JUL
PT. ARENA
PT. REYES
39°00'
38°00'
124°00'
123°00'
150m
90m

Figure 13

R3BI : WIND

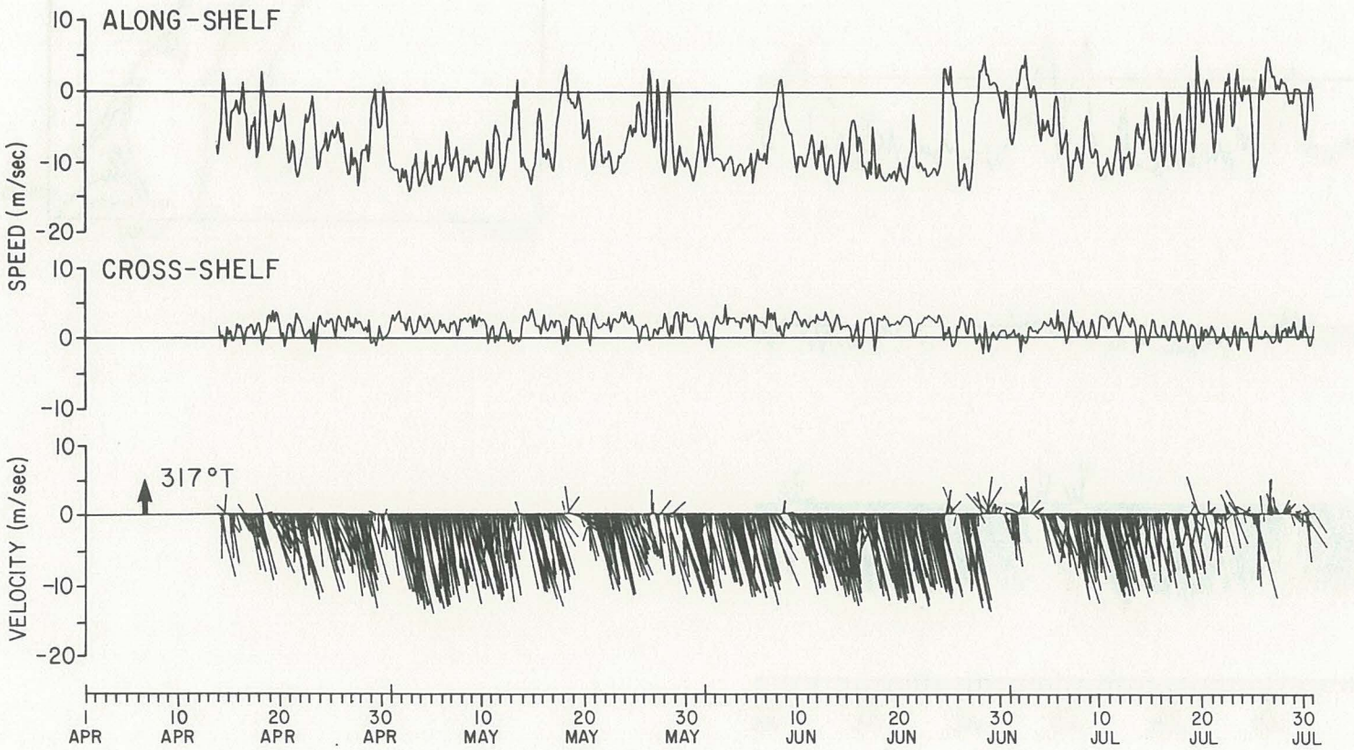

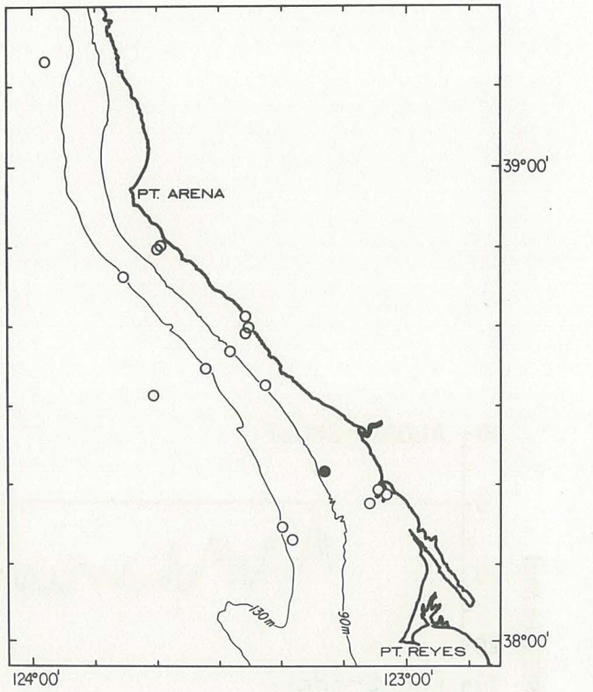

Figure 14

NDBO 13:WIND

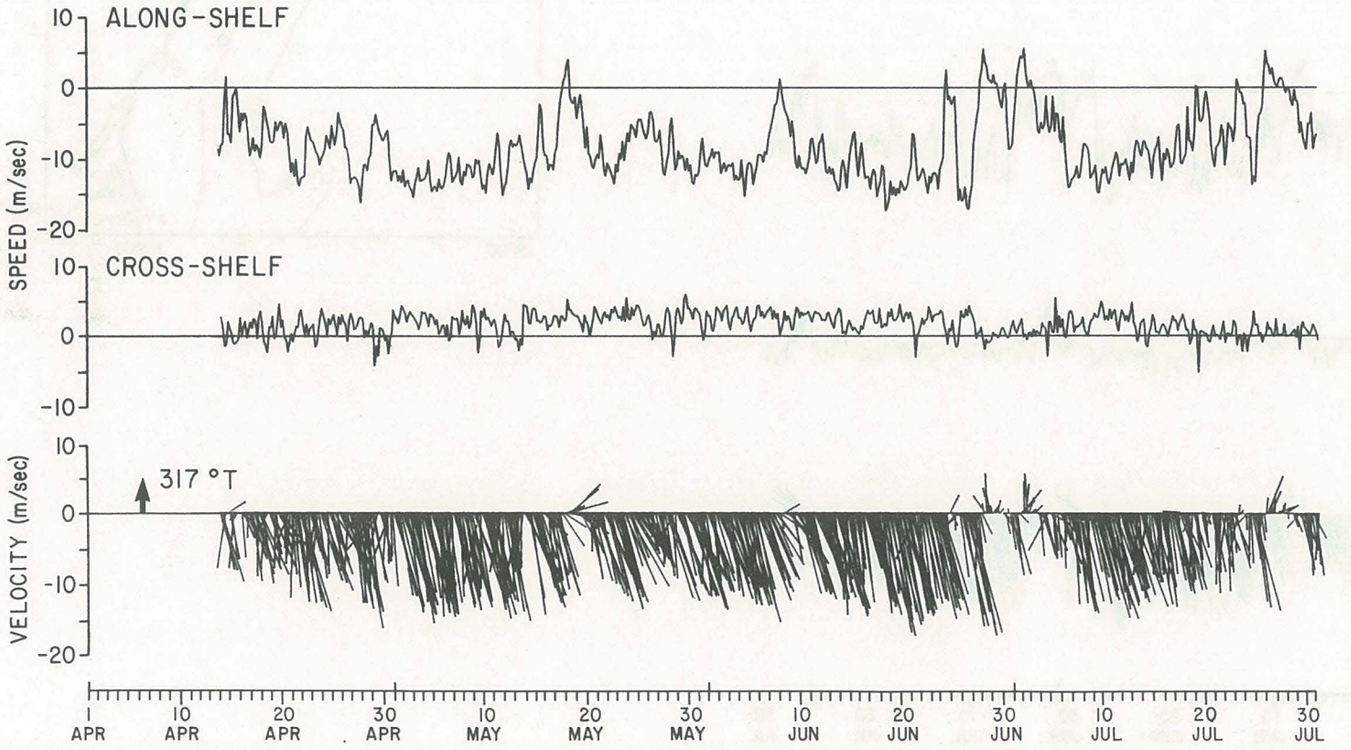

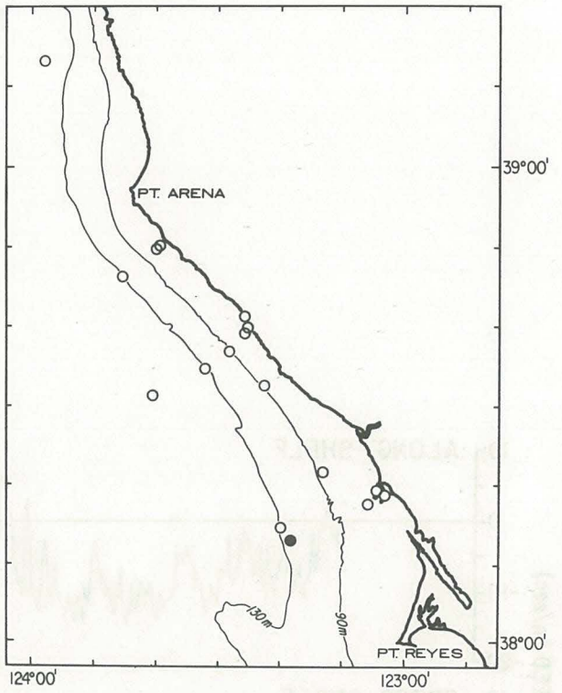

Figure 15

NDBO 14:WIND

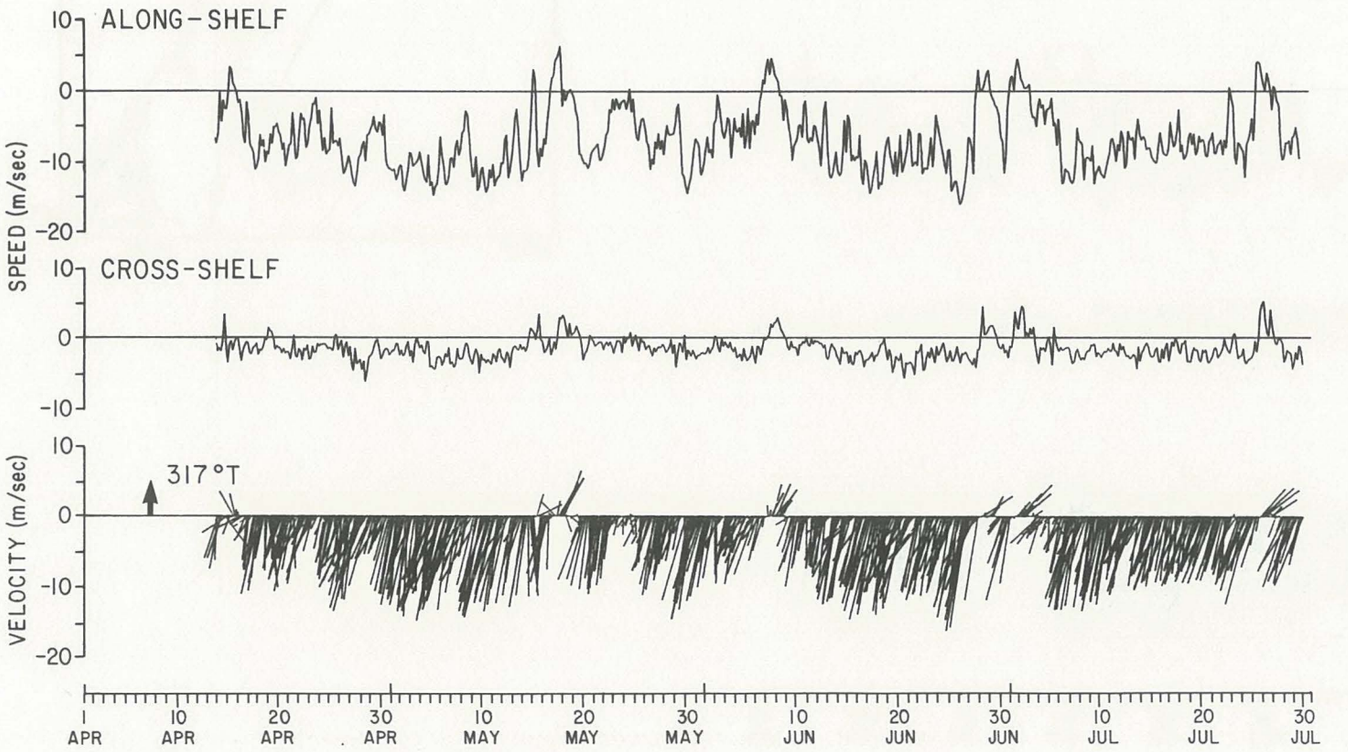

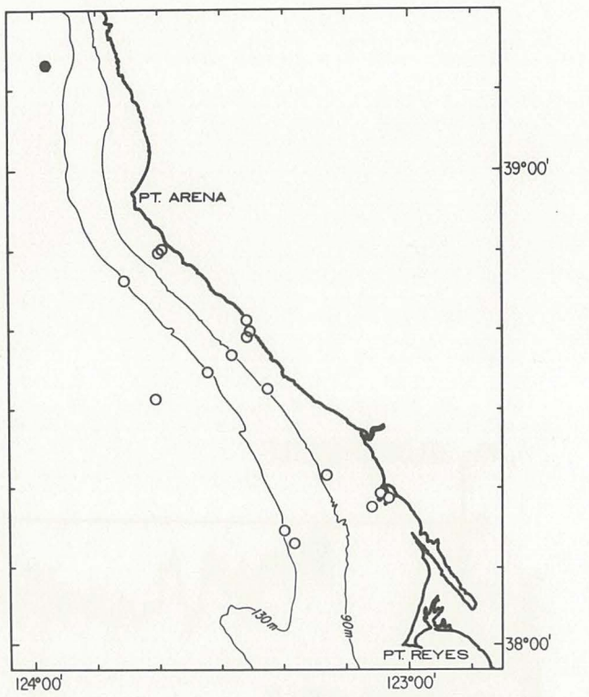

Figure 16

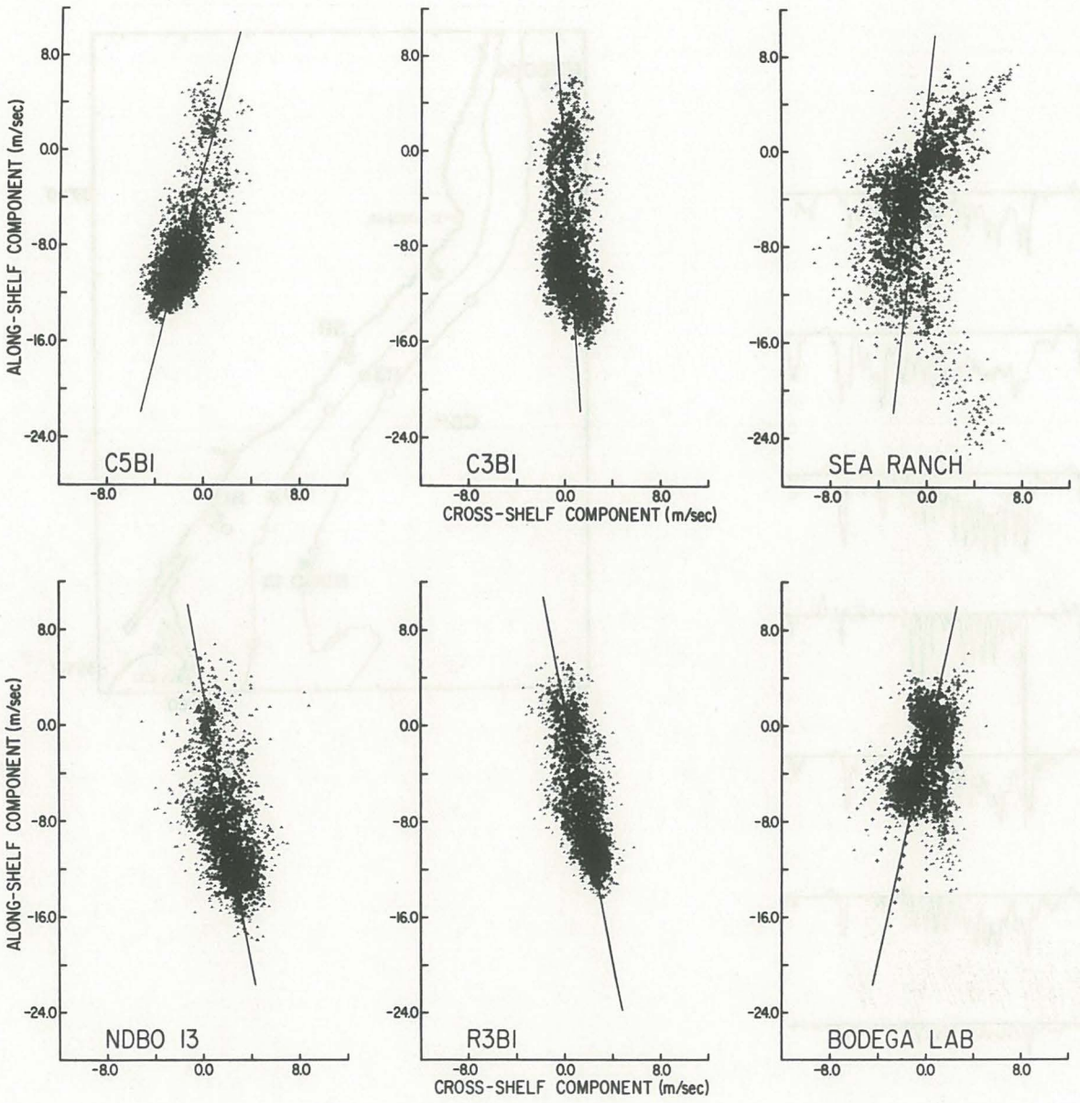

Figure 17. Scatter plots of observed wind time series. Lines show orientation of principal axis for each time series.

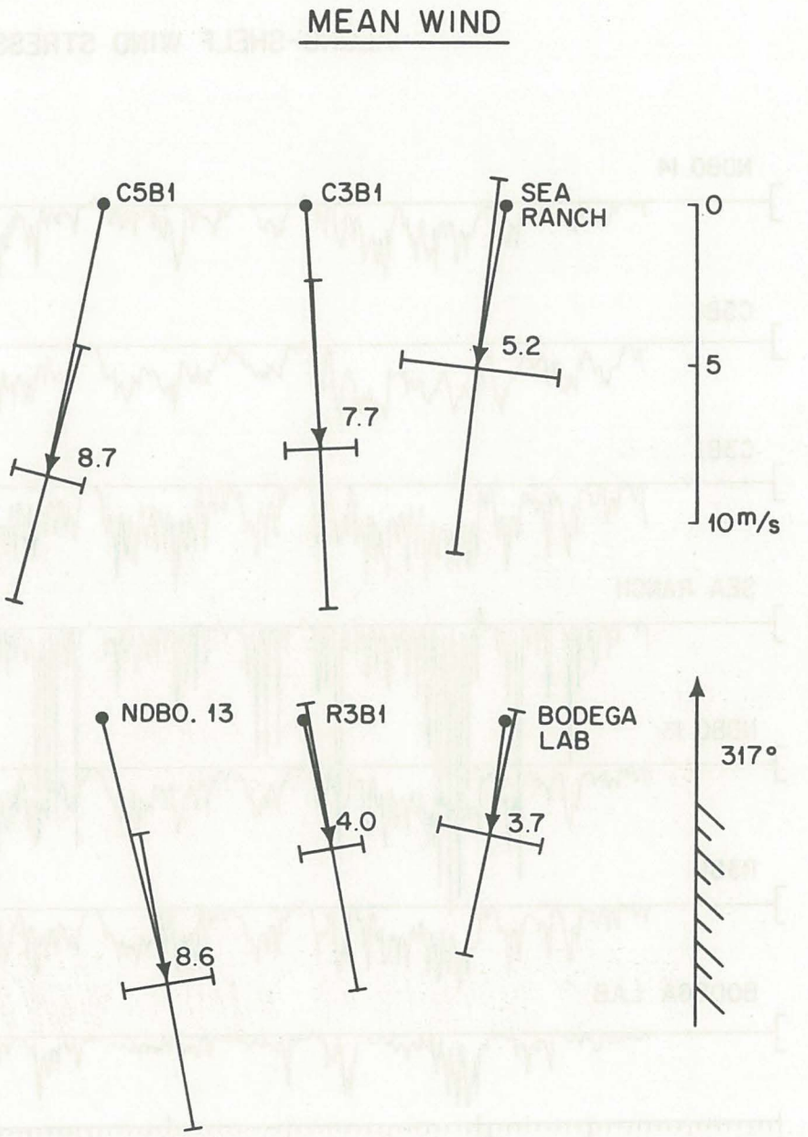

Figure 18. Mean observed wind in m/s. Bracket at tip of mean wind vector shows orientation of principal axes and standard deviations along principal axes.

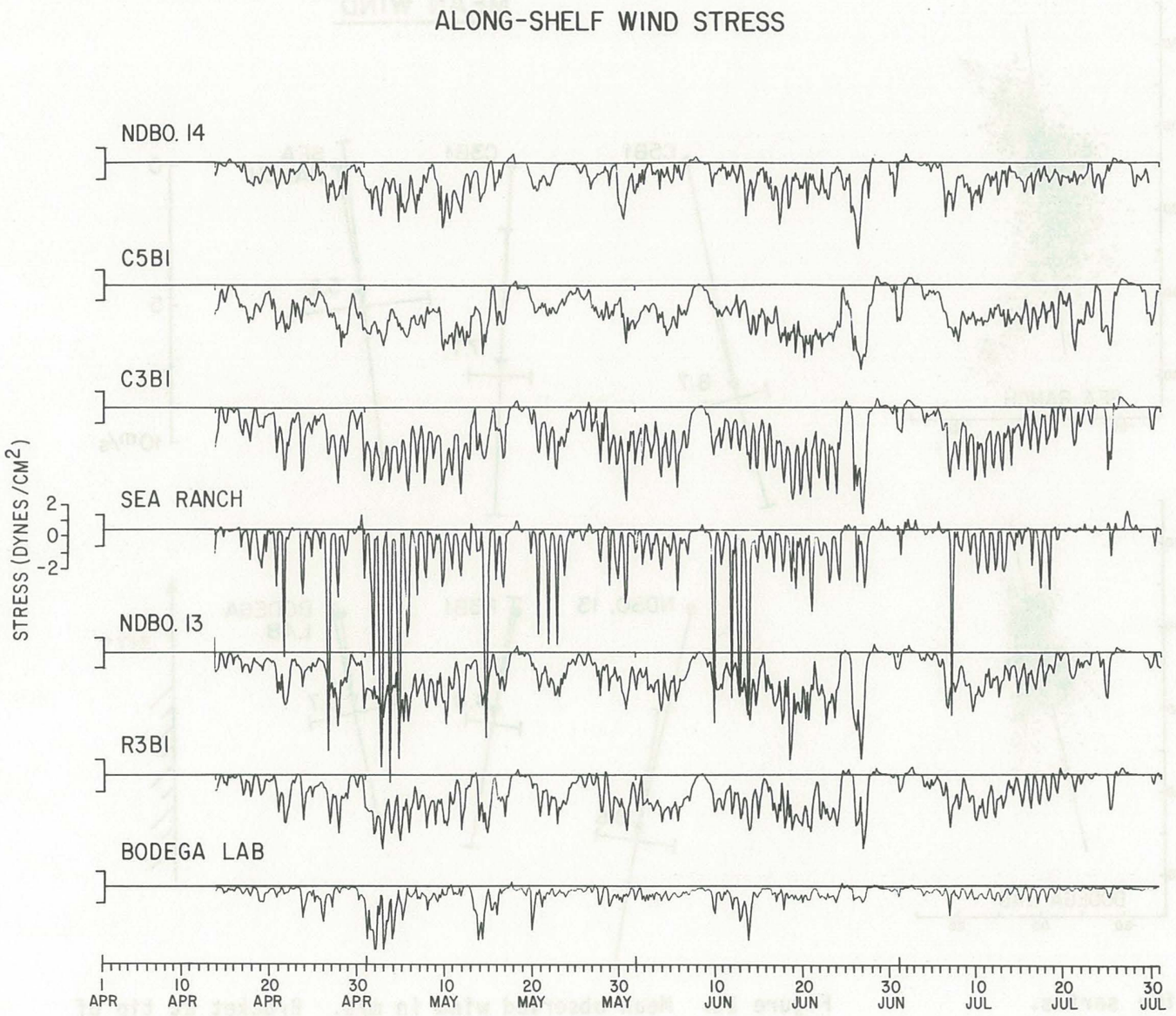
ALONG-SHELF WIND STRESS
NDBO. 14
C5BI
C3BI
SEA RANCH
NDBO. 13
R3BI
BODEGA LAB
STRESS (DYNES/CM2)
2
0
-2
1 APR
10 APR
20 APR
30 APR
10 MAY
20 MAY
30 MAY
10 JUN
20 JUN
30 JUN
10 JUL
20 JUL
30 JUL

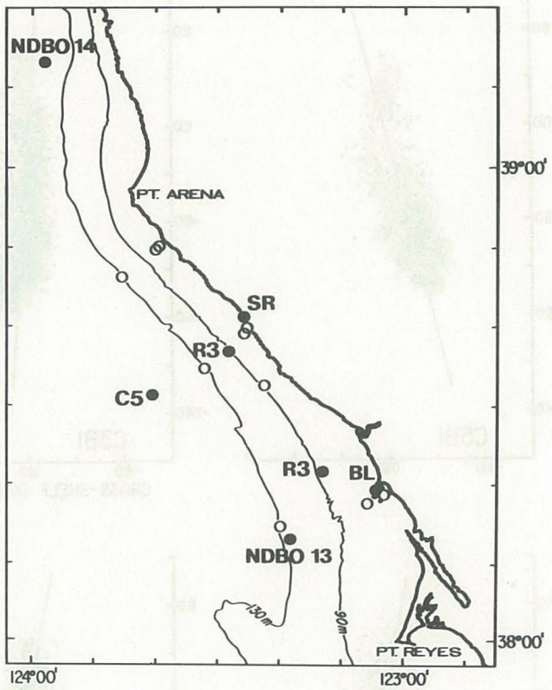
NDBO 14
PT. ARENA
SR
R3
C5
R3
BL
NDBO 13
150m
60m
PT. REYES
39°00'
38°00'
124°00'
123°00'

Figure 19

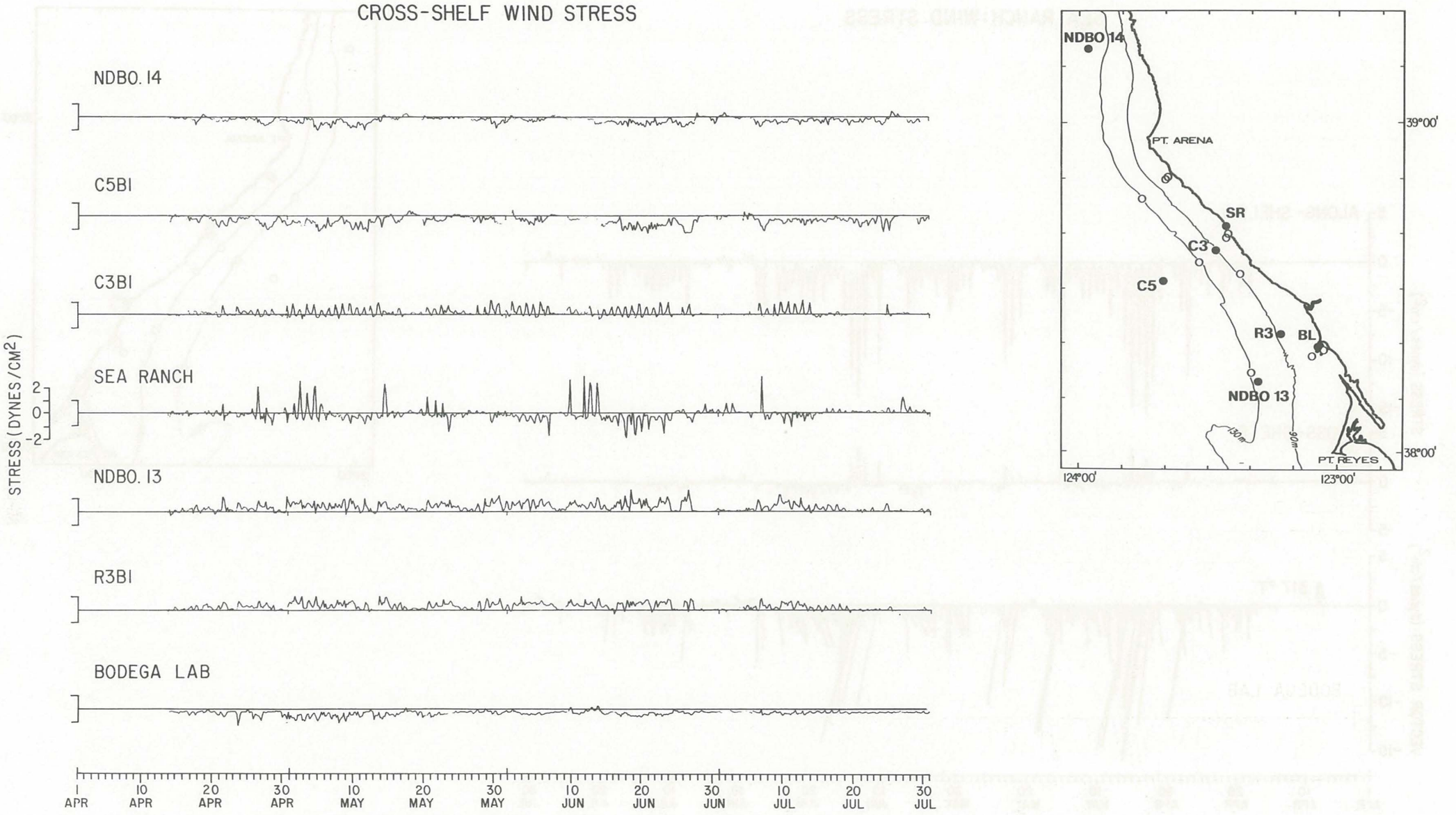
CROSS-SHELF WIND STRESS
NDBO. I4
C5BI
C3BI
SEA RANCH
NDBO. I3
R3BI
BODEGA LAB
STRESS (DYNES/CM2)
2
0
-2
1 APR
10 APR
20 APR
30 APR
10 MAY
20 MAY
30 MAY
10 JUN
20 JUN
30 JUN
10 JUL
20 JUL
30 JUL
NDBO 14
PT. ARENA
SR
C3
C5
R3
BL
NDBO 13
PT. REYES
39°00'
38°00'
124°00'
123°00'

Figure 20

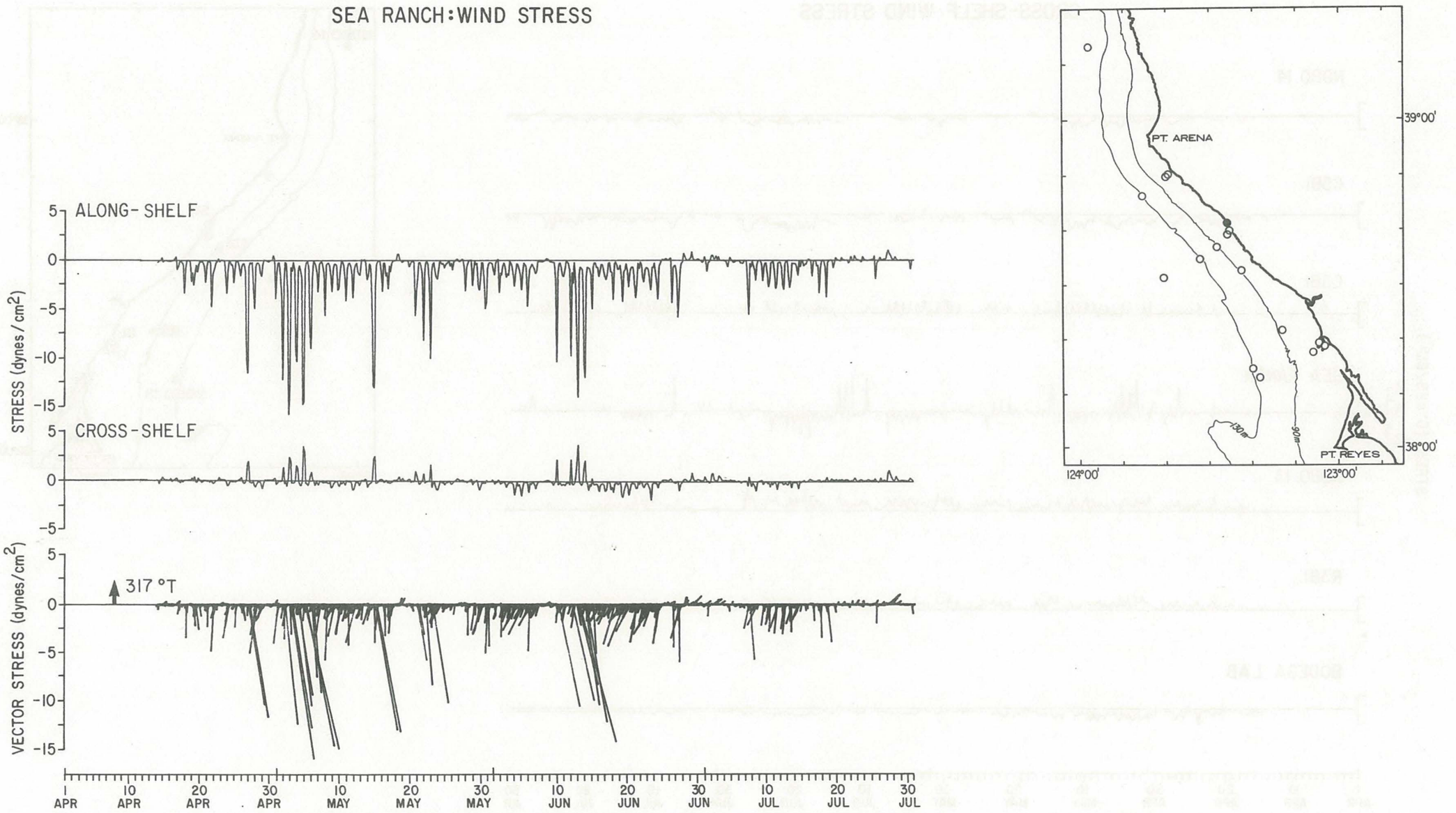
SEA RANCH: WIND STRESS
ALONG-SHELF
CROSS-SHELF
317 °T
STRESS (dynes / cm2)
VECTOR STRESS (dynes/cm2)
5
0
-5
-10
-15
1 APR
10 APR
20 APR
30 APR
10 MAY
20 MAY
30 MAY
10 JUN
20 JUN
30 JUN
10 JUL
20 JUL
30 JUL
PT. ARENA
PT. REYES
39°00'
38°00'
124°00'
123°00'
130m
90m

Figure 21

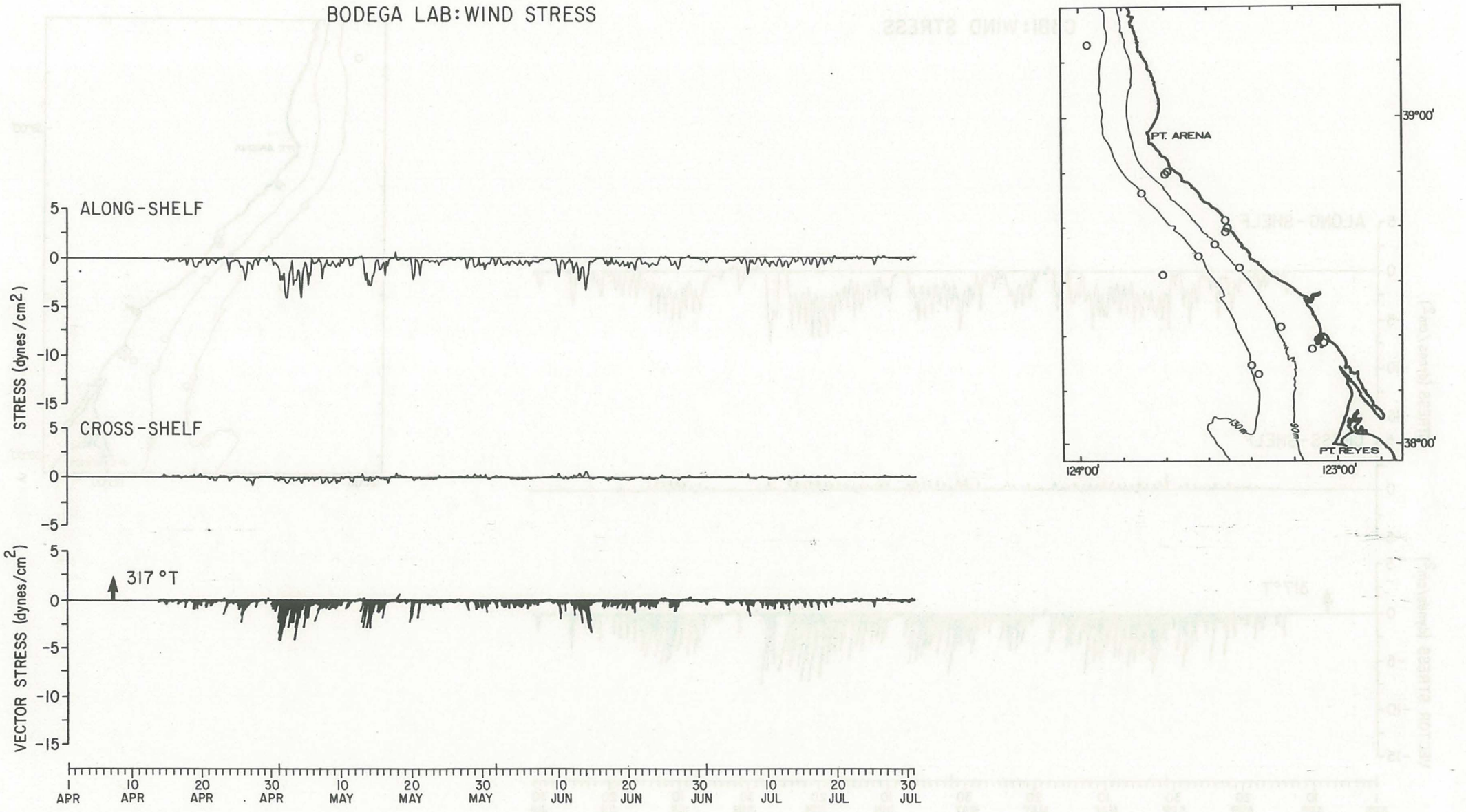
BODEGA LAB: WIND STRESS
ALONG-SHELF
CROSS-SHELF
317 °T
STRESS (dynes/cm2)
VECTOR STRESS (dynes/cm2)
5
0
-5
-10
-15
1 APR
10 APR
20 APR
30 APR
10 MAY
20 MAY
30 MAY
10 JUN
20 JUN
30 JUN
10 JUL
20 JUL
30 JUL
PT. ARENA
PT. REYES
39°00'
38°00'
124°00'
123°00'
130m
90m

Figure 22

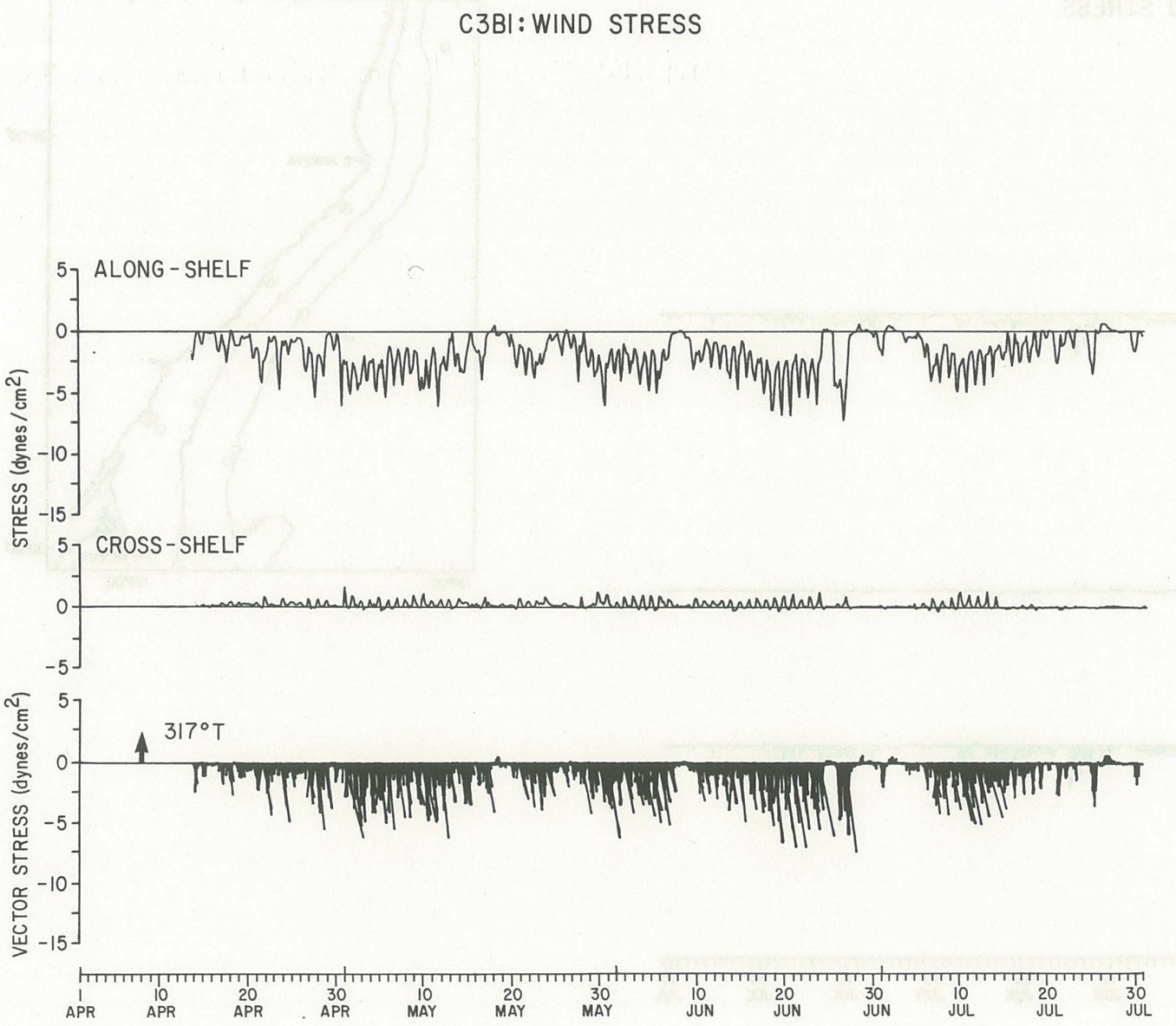
C3BI: WIND STRESS
ALONG-SHELF
CROSS-SHELF
317°T
STRESS (dynes/cm²)
VECTOR STRESS (dynes/cm²)
5
0
-5
-10
-15
1 APR
10 APR
20 APR
30 APR
10 MAY
20 MAY
30 MAY
10 JUN
20 JUN
30 JUN
10 JUL
20 JUL
30 JUL

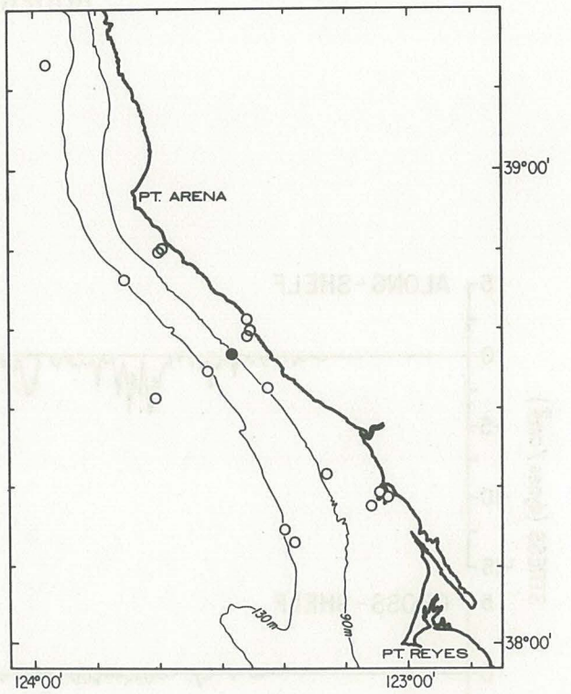
PT. ARENA
PT. REYES
39°00'
38°00'
124°00'
123°00'
130m
90m

Figure 23

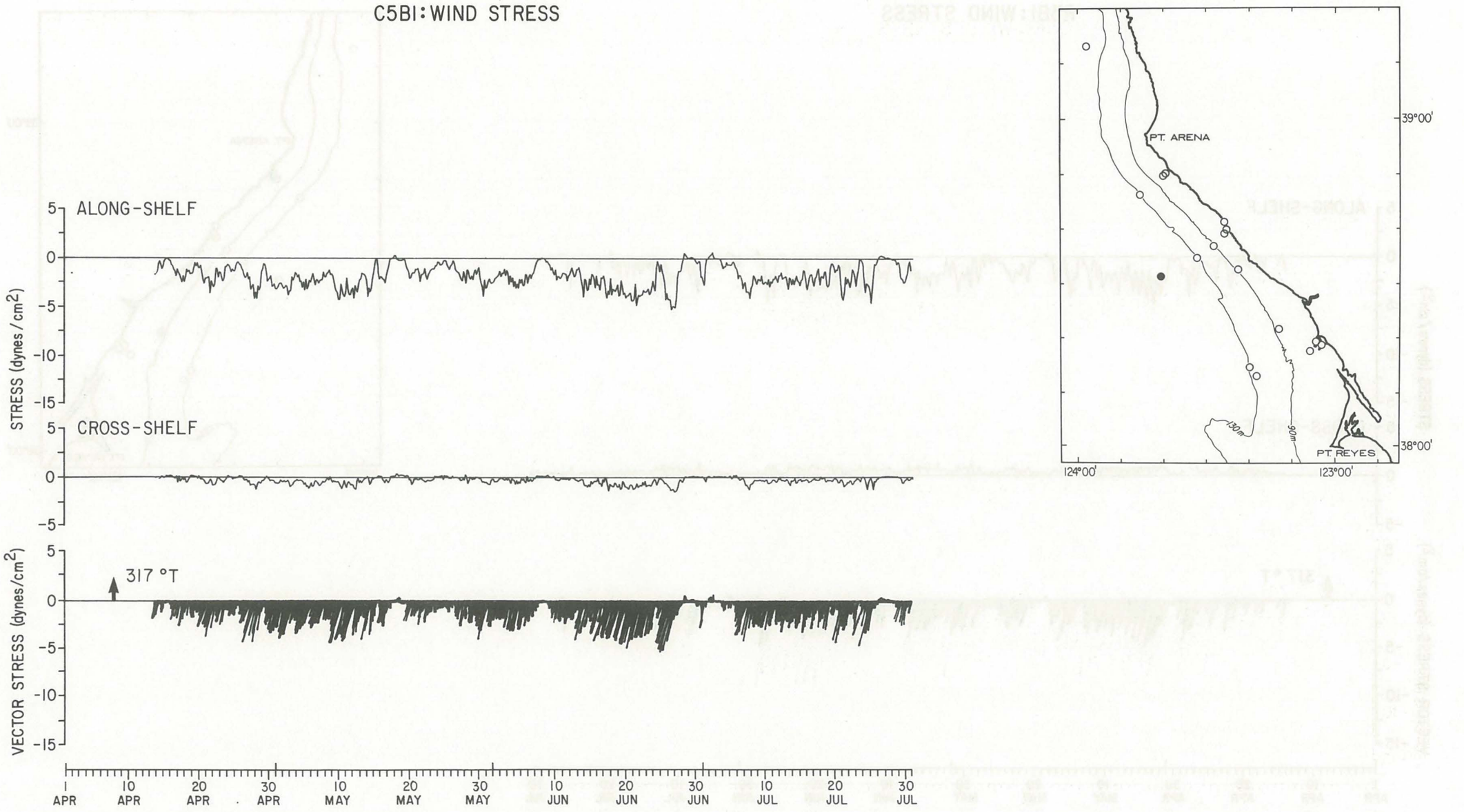
C5BI: WIND STRESS
ALONG-SHELF
CROSS-SHELF
STRESS (dynes/cm2)
VECTOR STRESS (dynes/cm2)
317 °T
5
0
-5
-10
-15
1 APR
10 APR
20 APR
30 APR
10 MAY
20 MAY
30 MAY
10 JUN
20 JUN
30 JUN
10 JUL
20 JUL
30 JUL
PT. ARENA
PT. REYES
130m
90m
39°00'
38°00'
124°00'
123°00'

Figure 24

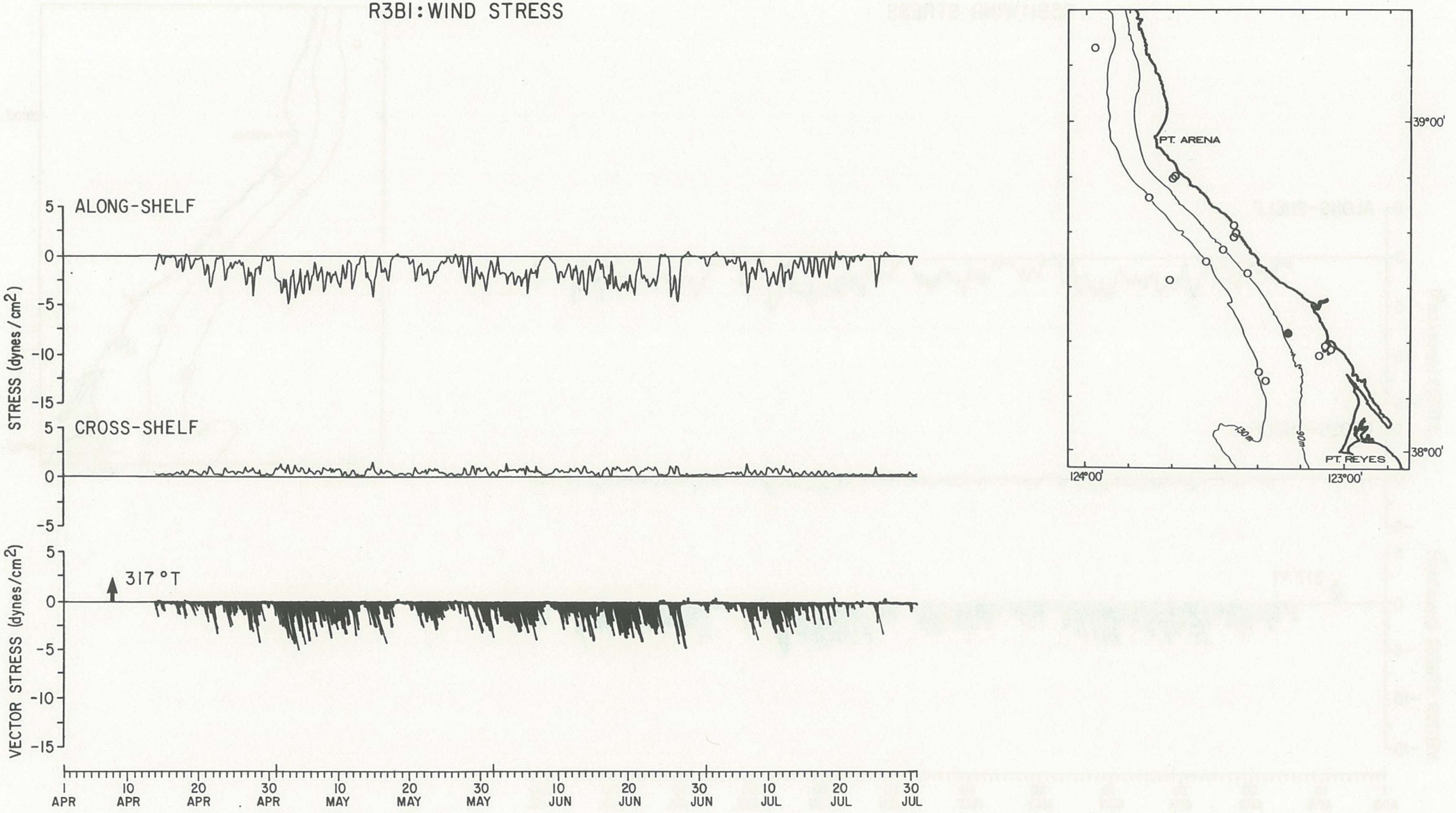
R3BI: WIND STRESS
ALONG-SHELF
CROSS-SHELF
317 °T
STRESS (dynes/cm²)
VECTOR STRESS (dynes/cm²)
5
0
-5
-10
-15
1 APR
10 APR
20 APR
30 APR
10 MAY
20 MAY
30 MAY
10 JUN
20 JUN
30 JUN
10 JUL
20 JUL
30 JUL
PT. ARENA
PT. REYES
39°00'
38°00'
124°00'
123°00'
150m
90m

Figure 25

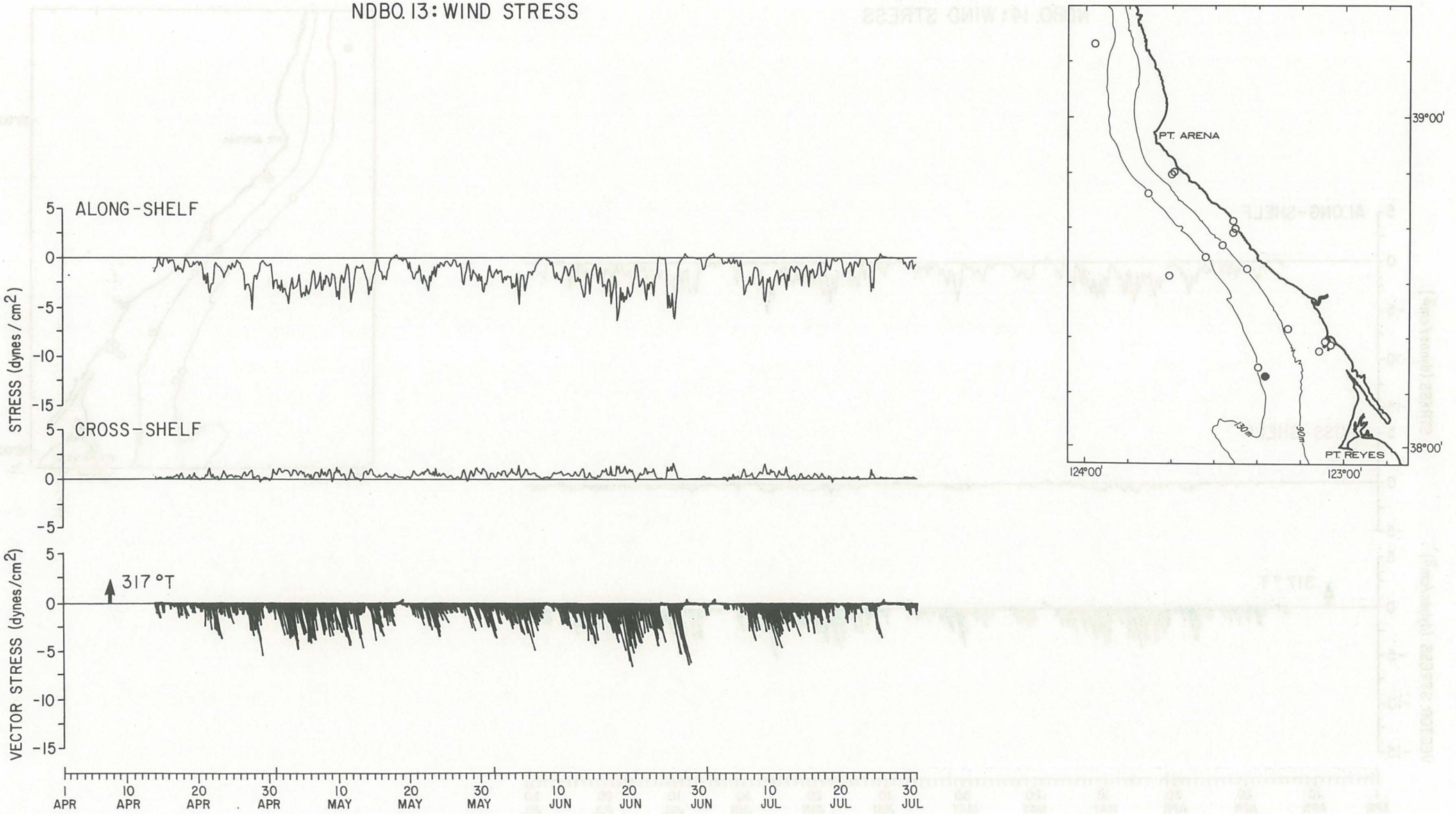
NDBO 13: WIND STRESS
ALONG-SHELF
CROSS-SHELF
STRESS (dynes / cm2)
VECTOR STRESS (dynes/cm2)
317 °T
5
0
-5
-10
-15
1 APR
10 APR
20 APR
30 APR
10 MAY
20 MAY
30 MAY
10 JUN
20 JUN
30 JUN
10 JUL
20 JUL
30 JUL
PT. ARENA
PT. REYES
39°00'
38°00'
124°00'
123°00'
130m
90m

Figure 26

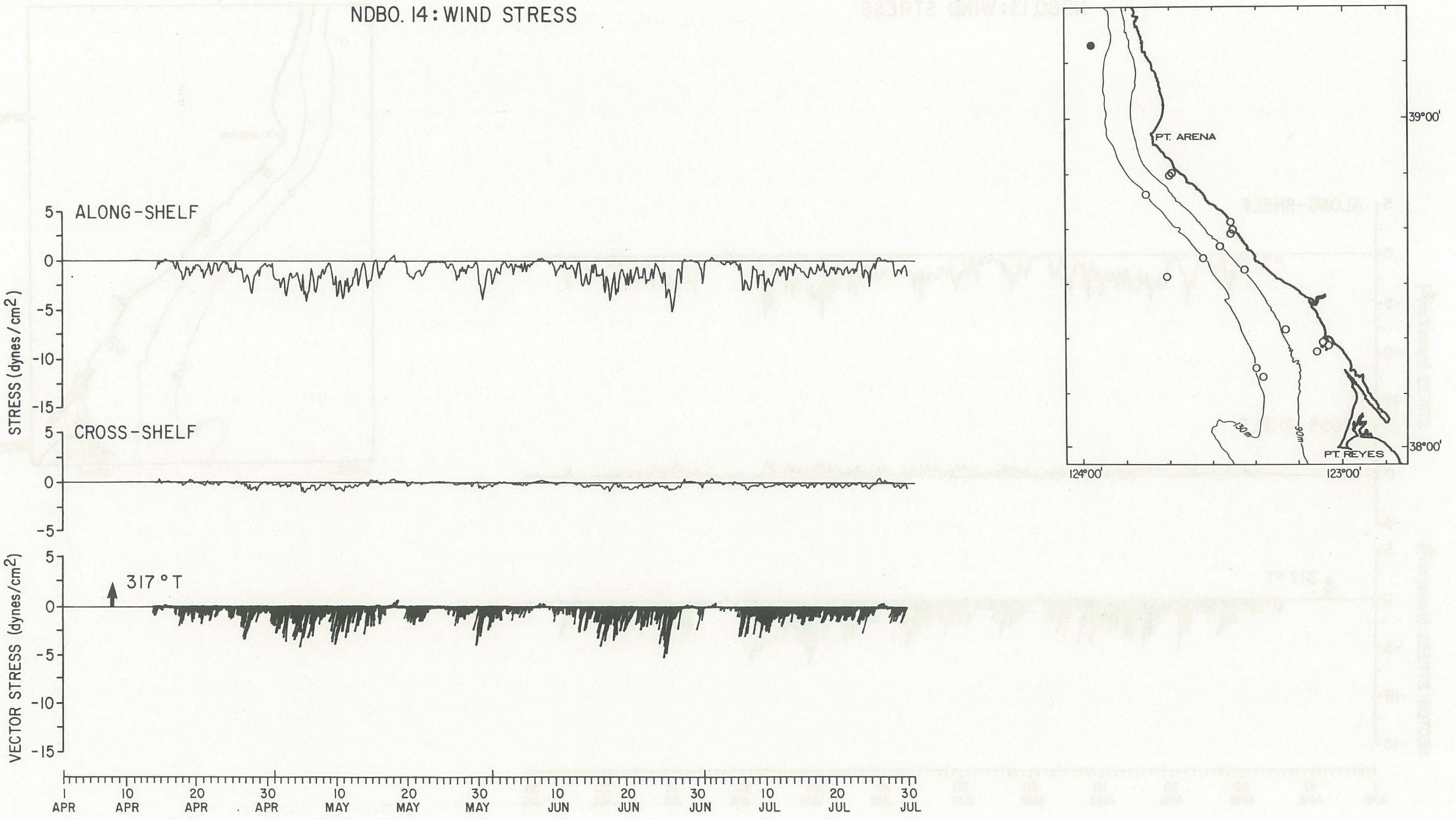
NDBO. 14 : WIND STRESS
ALONG-SHELF
CROSS-SHELF
317 ° T
STRESS (dynes / cm2)
VECTOR STRESS (dynes/cm2)
5
0
-5
-10
-15
1 APR
10 APR
20 APR
30 APR
10 MAY
20 MAY
30 MAY
10 JUN
20 JUN
30 JUN
10 JUL
20 JUL
30 JUL
PT. ARENA
PT. REYES
39°00'
38°00'
124°00'
123°00'
130m
90m

Figure 27

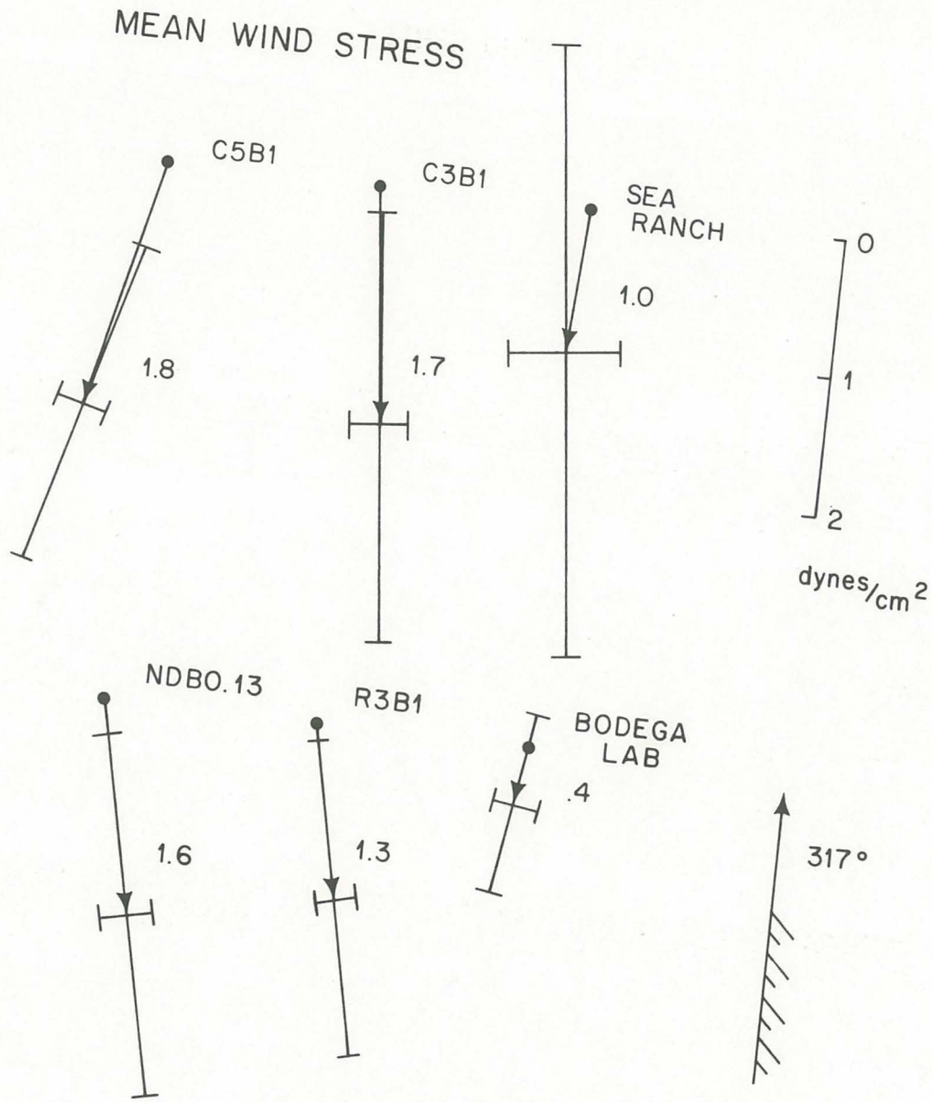

Figure 28. Mean wind stress in dyne/cm^2. Bracket at tip of mean vector shows orientation of principal axes and standard deviations along principal axes.

CODE-1: MOORED CURRENT OBSERVATIONS

By

C. D. Winant
A. W. Bratkovich

Scripps Institution of Oceanography
University of California, San Diego
La Jolla, California 92093

A. INTRODUCTION

The CODE experiment is a multi-institutional field observation and data analysis program designed to evaluate the effect of surface wind stresses upon fluid acceleration in the water column adjacent to a coastal boundary. With this goal in mind, a diverse set of measurements was made that would allow the determination of important terms in the governing equations of motion. This report serves as a guideline to the current observations made during the CODE-1 instrument deployment.

The time frame of interest spans the period 1 April 1981 to 23 July 1981. The experimental site is centered on the northern California continental shelf about 100 km northwest of San Francisco Bay (nominal latitude and longitude is 38°37'N, 123°28'W). A map of the array site and mooring locations is shown in Figure 1. The exact mooring locations are given in Table 2 of the introductory chapter.

Time series of horizontal current components are plotted over the period of interest. Individual data values correspond to hour-long averages (computed using a running mean filter) that are centered on the hour. Horizontal velocity components are referenced to a right-hand coordinate system which has the positive x axis directed towards 47° T (30°M) (approximately normal to local isobaths) and the positive y axis directed towards 317° T (parallel to local isobaths).

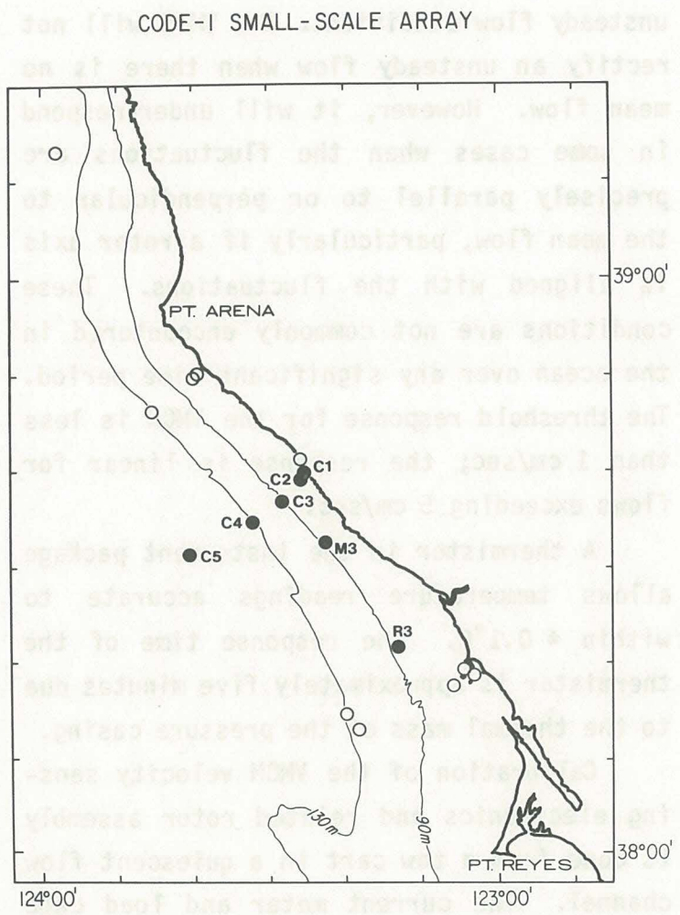

Figure 1. Stations where current measurements were made during CODE-1 are shown as darkened circles.

B. MOORED CURRENT METER OBSERVATIONS

B.1 Moored Array Design

The current meter placement for the CODE-1 experiment was primarily determined by the following considerations. The shelf region south of Point Arena was selected due to the nearly planar bottom topography (on spatial scales of 2-20 km), and the presence of energetic upwelling-favorable winds during spring and early summer. The vertical spacing interval for instruments (O(10 m)) was chosen to insure that adjacent instruments were coherent with each other at subinertial frequencies and that relatively accurate vertically averaged quantities could be inferred at each mooring site. The along-shelf and cross-shelf mooring separations were chosen (based upon past experiments in coastal regions) such that adjacent mooring locations would be coherent at subinertial frequencies and would also

show some of the horizontal spatial structure in the data fields of interest.

B.2 Instrumentation

Two types of current meters were used in the CODE-1 deployment. Vector Measuring Current Meters (VMCM) were used in the SIO moorings (C1, C3, C4). A combination of VMCM's and Vector Averaging Current Meters (VACM) were used in the WHOI moorings (C2, C5, M3, R3).

The VMCM is a Cartesian sampling instrument consisting of two sets of two propellers each, mounted at right angles, as shown in Figure 2.a. The propellers, or rotors, measure two perpendicular components of horizontal velocity. A flux gate compass indicates the orientation of the current meters and allows the processing electronics in the instrument to resolve the measurement into N/S and E/W components. The velocity components measured by each rotor are continuously vector-averaged, and these average values are recorded at a preprogrammed interval (4 minutes) on a cassette within the instrument package.

The VMCM was designed at Scripps Institution to measure small horizontal mean flows in the presence of large vertical and horizontal current fluctuations. It has an accurate cosine response under a variety of unsteady flow conditions. The VMCM will not rectify an unsteady flow when there is no mean flow. However, it will under-respond in some cases when the fluctuations are precisely parallel to or perpendicular to the mean flow, particularly if a rotor axis is aligned with the fluctuations. These conditions are not commonly encountered in the ocean over any significant time period. The threshold response for the VMCM is less than 1 cm/sec; the response is linear for flows exceeding 5 cm/sec.

A thermistor in the instrument package allows temperature readings accurate to within ± 0.1°C. The response time of the thermistor is approximately five minutes due to the thermal mass of the pressure casing.

Calibration of the VMCM velocity sensing electronics and related rotor assembly is done from a tow cart in a quiescent flow channel. The current meter and load cage are rigidly attached to the tow cart and then towed at a steady speed through the water over a fixed distance (usually taken to be 10 meters). Rotor revolutions are counted while the fixed distance interval is traversed for various angles of attack and speed ranges to examine the rotor's cosine response and speed sensitivity. Threshold velocity tests are also conducted by slowly accelerating the tow cart from 0 to 5 cm/s.

Temperature calibrations are performed by replacing the instrument thermistor with a precision decade resistor. A digital code is recorded for a number of resistances in the expected range of variability (each thermistor is calibrated versus temperature at the factory and recalibrated periodically in the laboratory). A least squares fit is then calculated for temperature as a function of instrument count. Finally, a one-point through-instrument calibration point is taken for each instrument before and after each deployment. The final check is made to monitor the overall drift of the temperature sensing electronics and to improve the accuracy of the final temperature estimates (most of the error in the temperature estimation is due to a constant offset from a standard response curve).

For a more detailed description of the VMCM and its response under laboratory and field test conditions, see Weller, 1978.

The VACM is a polar sampling instrument consisting of one speed sensor (Savonius rotor) and one directional sensor (neutrally buoyant vane) as shown in Figure 2.b. Speed and direction measurements are continuously sampled and processed to produce summed Cartesian coordinate velocity vectors. An eddy-current damped magnetic compass and vane follower are used to resolve measurements in N/S and E/W components. Summed velocity component estimates, time and a low-passed temperature value are written to cassette at a predetermined sample interval.

The VACM was designed at Woods Hole Oceanographic Institution to minimize directional averaging errors associated with mismatched vane and rotor response. The threshold response for the VACM is 2.0 cm/s and the instrument's operating range extends to 300 cm/s. A thermistor attached to the inside of the pressure package face plate allows temperature to be measured to an accuracy of ± .01°C. Ocean comparison tests (Halpern et al., 1981) of the VACM and VMCM show that these two types of instruments perform comparably in an upper ocean environment.

Calibration procedures for the VACM are functionally similar to those for the VMCM.

VECTOR MEASURING CURRENT METER (VMCM)

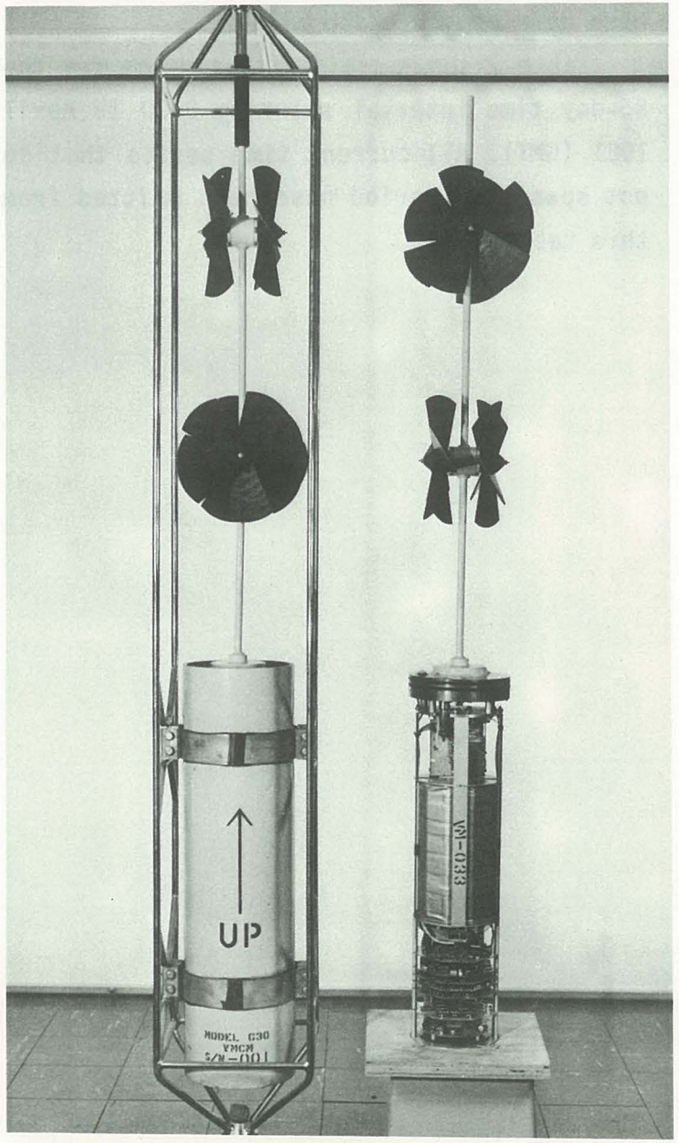

Figure 2a

VECTOR AVERAGING CURRENT METER (VACM)

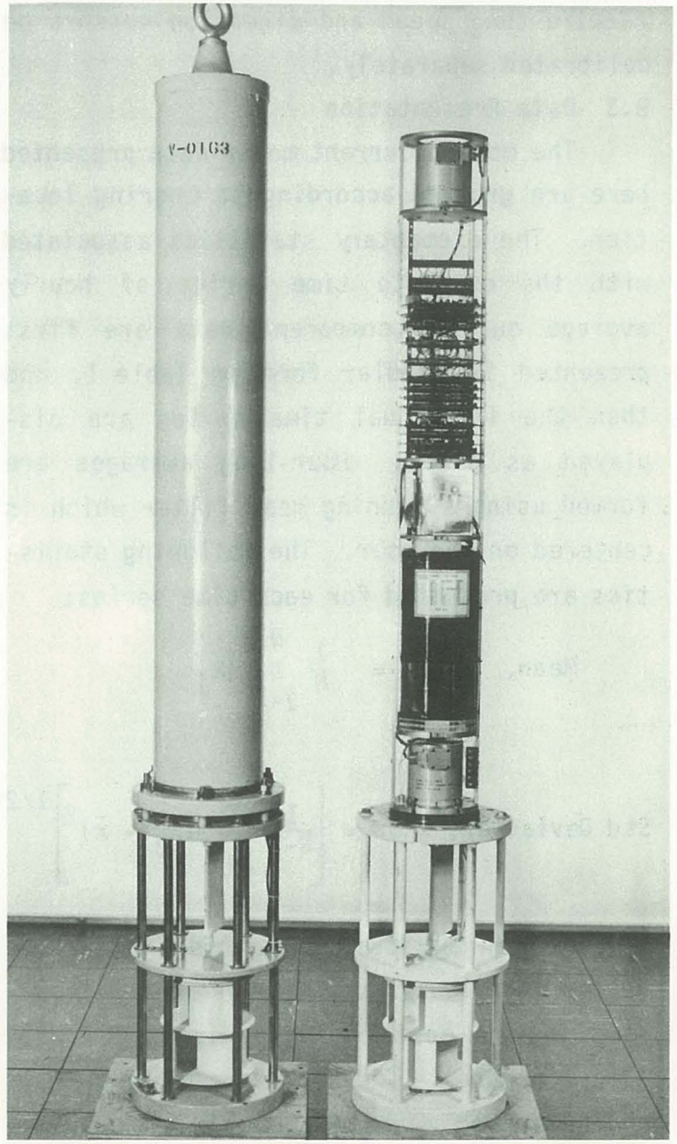

Figure 2b

The rotor and vane assembly on the VACM require that speed and direction sensors be calibrated separately.

B.3 Data Presentation

The moored current meter data presented here are grouped according to mooring location. The elementary statistics associated with the complete time series of hourly average current component data are first presented in tabular form in Table 1, and then the individual time series are displayed as plots. Hour-long averages are formed using a running mean filter which is centered on the hour. The following statistics are presented for each time series:

$$\text{Mean,} \qquad \bar{x} = \frac{1}{N} \sum_{j=1}^{N} x_j$$

$$\text{Std Deviation,} \qquad SD = \left[\frac{1}{N-1} \sum_{j=1}^{N} (x_j - \bar{x})^2 \right]^{1/2}$$

Minimum and maximum values for each time series are also presented. Cross-shelf current (U) is positive when directed toward 47°T (onshore). Along-shelf current (V) is positive when directed toward 317°T. Note that approximate instrument depth is also given in the following tables. All times have been converted to GMT.

Table 2 shows similar statistics for the 85-day time interval starting 0800 15 April 1981 (GMT). All current time series that do not span this period have been omitted from this table.

TABLE 1: Horizontal Current Components (cm/s)

Complete Time Series for All Instruments

Station	Water Depth (m)	Start Time (Mon/Day/Hr)	Stop Time (Mon/Day/Hr)	Duration (Days)	Instrument I.D.	Sensor Depth (m)	Cross-Shelf Mean	Cross-Shelf SD	Cross-Shelf Max	Cross-Shelf Min	Along-Shelf Mean	Along-Shelf SD	Along-Shelf Max	Along-Shelf Min
C1	30	03/25/0800	07/23/1800	120	62 (SIO)	4	-2.67	3.83	16.60	-14.80	-3.18	7.22	25.60	-37.30
		03/25/0800	07/23/1800	120	65 (SIO)	7	0.03	2.46	9.60	-9.20	-0.45	6.53	24.60	-34.40
		03/25/0800	07/23/1800	120	59 (SIO)	11	1.56	2.33	13.40	-11.00	0.81	6.19	18.40	-26.20
		04/01/0800	07/23/1800	113	58 (SIO)	23	1.08	3.24	10.40	-14.80	0.18	5.97	17.60	-24.20
		04/01/0800	07/23/1800	113	56 (SIO)	27	0.49	2.82	9.30	-13.80	0.54	5.04	15.40	-21.70
C2	63	04/14/1300	08/01/1400	109	A1 (WHOI)	4	-3.21	7.07	21.80	-20.40	-0.36	12.44	30.80	-54.30
		04/13/1600	07/13/1800	91	05 (SIO)	14	1.27	3.91	16.00	-15.40	3.33	14.21	40.90	-49.50
		04/14/1300	05/15/1400	31	A4 (WHOI)	37	1.67	2.08	7.80	-6.40	0.52	10.61	28.50	-25.80
		04/14/1300	05/05/1400	21	A5 (WHOI)	47	1.51	3.40	9.80	-8.20	3.31	7.22	22.50	-21.30
C3	90	04/07/0800	07/05/0300	89	64 (SIO)	4	-11.12	8.08	18.80	-49.00	-19.60	23.83	33.60	-84.40
		04/08/2000	07/14/0500	96	04 (SIO)	9	-9.84	8.82	13.90	-45.00	-14.83	24.47	37.20	-78.50
		04/07/0800	07/23/1800	107	50 (SIO)	14	-6.51	9.35	20.10	-45.70	-9.23	21.77	38.80	-66.40
		04/07/0800	04/21/0600	14	53 (SIO)	24	-1.87	7.02	13.20	-29.90	-13.59	22.84	28.50	-54.30
		04/08/2000	07/14/0600	96	02 (SIO)	29	-1.32	6.08	13.30	-21.70	-6.63	20.74	39.60	-62.40
		04/08/2000	07/14/0400	96	03 (SIO)	35	-2.07	6.88	13.40	-28.10	-5.54	19.98	37.30	-60.10
		04/09/0800	07/13/0600	95	61 (SIO)	39	-2.73	9.53	16.70	-37.20	-3.58	18.35	37.70	-52.30
		04/09/0800	04/16/0600	7	69 (SIO)	55	-4.40	3.78	8.10	-13.70	-17.22	10.08	-1.70	-37.10
		04/09/0800	06/11/1300	63	66 (SIO)	75	-2.68	7.06	14.70	-32.10	1.84	13.93	31.40	-38.30
		04/08/2000	07/13/2100	96	15 (SIO)	83	-0.45	4.16	13.70	-16.30	-0.37	13.78	27.00	-37.40
C4	130	04/09/0800	07/13/0000	95	12 (SIO)	19	-6.50	12.09	26.70	-39.50	-23.15	21.14	30.60	-72.80
		04/09/0800	07/14/0700	96	16 (SIO)	29	-5.90	12.38	35.20	-40.00	-20.25	20.46	30.30	-69.80
		04/09/0800	07/23/1800	105	57 (SIO)	35	-3.20	9.86	32.30	-37.50	-11.91	16.44	29.40	-60.50
		04/09/0800	07/14/1100	96	13 (SIO)	45	-3.84	9.39	26.10	-38.40	-13.92	15.86	31.60	-57.80
		04/09/0800	07/13/1700	95	14 (SIO)	65	-1.20	7.24	23.00	-32.90	-8.88	14.21	28.60	-50.30
		04/09/0800	07/23/1800	105	51 (SIO)	75	-0.97	7.20	20.10	-33.10	-5.95	13.20	28.30	-47.10
		04/09/0800	07/23/1800	105	52 (SIO)	95	-0.94	6.97	20.70	-32.50	-3.23	12.49	27.10	-45.50
		04/09/0800	06/21/0800	73	10 (SIO)	105	-1.69	6.75	24.20	-26.80	-3.84	12.33	25.80	-42.30
		04/09/0800	06/27/1700	79	67 (SIO)	115	-1.40	7.11	29.00	-26.80	-2.96	11.62	25.90	-37.20
		04/09/0800	07/14/1000	96	01 (SIO)	123	-1.02	6.18	25.20	-23.80	-0.95	10.51	23.90	-34.40

TABLE 1: Horizontal Current Components (cm/s) (Continued)

Station	Water Depth (m)	Start Time (Mon/Day/Hr)	Stop Time (Mon/Day/Hr)	Duration (Days)	Instrument I.D.	Sensor Depth (m)	Cross-Shelf Mean	Cross-Shelf SD	Cross-Shelf Max	Cross-Shelf Min	Along-Shelf Mean	Along-Shelf SD	Along-Shelf Max	Along-Shelf Min
C5	402	04/12/1300	08/01/1200	111	B2 (WHOI)	9	-11.83	21.32	67.80	-81.00	-19.29	19.25	33.60	-72.50
		04/14/1300	08/02/1200	110	S1 (WHOI)	77	1.26	10.67	35.30	-33.90	-8.30	16.40	38.30	-50.40
		04/14/1300	08/02/1200	110	S2 (WHOI)	152	2.20	7.86	24.60	-27.30	2.02	14.15	40.60	-36.20
		04/14/1300	08/02/1200	110	S3 (WHOI)	252	3.27	6.92	18.90	-23.60	8.98	13.74	37.40	-31.90
		04/14/1300	08/02/1200	110	S4 (WHOI)	352	1.91	4.45	15.50	-18.20	5.93	9.20	25.90	-31.10
M3	90	04/14/1300	07/30/1200	107	A1 (WHOI)	9	-3.11	9.69	28.30	-39.20	0.96	22.18	46.10	-73.50
		04/15/1300	07/31/1200	107	A2 (WHOI)	10	-2.07	7.30	22.00	-33.10	0.39	19.26	41.40	-69.80
		04/14/1300	07/31/1200	108	S1 (WHOI)	35	0.86	6.66	21.10	-29.80	3.03	19.83	44.60	-65.20
		04/14/1300	07/31/1200	108	S2 (WHOI)	55	3.01	6.30	18.10	-27.50	4.98	17.63	41.40	-54.40
		04/14/1300	07/31/1200	108	S3 (WHOI)	74	1.24	4.67	14.90	-15.50	6.16	16.45	44.50	-54.80
R3	90	04/13/1300	08/03/1200	112	B2 (WHOI)	9	-4.20	10.15	28.50	-37.50	-1.96	14.17	35.30	-59.40
		04/13/1300	08/03/1200	112	S1 (WHOI)	35	0.98	7.49	19.10	-27.10	0.23	13.00	27.20	-51.10
		04/13/1300	08/03/1200	112	S2 (WHOI)	55	2.67	4.82	16.20	-13.40	2.17	12.33	27.30	-49.10
		04/13/1300	08/03/1200	112	S3 (WHOI)	75	2.51	4.32	17.00	-14.60	3.03	11.12	28.60	-37.50

Table 2: Horizontal Current Components (cm/s)

Common Time Period

Station	Water Depth (m)	Start Time (Mon/Day/Hr)	Stop Time (Mon/Day/Hr)	Duration (Days)	Instrument I.D.	Sensor Depth (m)	Cross-Shelf Mean	Cross-Shelf SD	Cross-Shelf Max	Cross-Shelf Min	Along-Shelf Mean	Along-Shelf SD	Along-Shelf Max	Along-Shelf Min
C1	30	04/15/0800	07/08/0800	85	62 (SIO)	4	-2.51	3.88	16.60	-12.70	-2.62	7.11	25.60	-34.50
		04/15/0800	07/08/0800	85	65 (SIO)	7	0.12	2.40	9.60	-8.30	0.15	6.21	24.60	-28.70
		04/15/0800	07/08/0800	85	59 (SIO)	11	1.55	2.16	10.50	-5.00	1.19	5.81	18.40	-24.10
		04/15/0800	07/08/0800	85	58 (SIO)	23	1.23	3.15	10.40	-11.40	0.51	5.72	17.60	-24.20
		04/15/0800	07/08/0800	85	56 (SIO)	14	0.68	2.70	9.30	-10.30	0.82	4.84	15.40	-21.70
C2	63	04/15/0800	07/08/0800	85	A1 (WHOI)	4	-4.44	6.84	21.80	-20.40	-1.56	12.63	30.80	-54.30
		04/15/0800	07/08/0800	85	05 (SIO)	14	1.36	3.83	16.00	-10.30	3.64	13.94	40.90	-49.50
C3	90	04/15/0800	07/08/0800	85	04 (SIO)	9	-10.00	8.99	13.90	-45.00	-13.27	24.76	37.20	-78.50
		04/15/0800	07/08/0800	85	50 (SIO)	14	-6.98	9.82	20.10	-45.70	-9.13	22.14	38.80	-65.10
		04/15/0800	07/08/0800	85	02 (SIO)	29	-1.25	6.29	13.30	-21.70	-5.31	21.05	39.60	-62.40
		04/15/0800	07/08/0800	85	03 (SIO)	35	-1.95	7.06	13.40	-28.10	-4.22	20.26	37.30	-60.10
		04/15/0800	07/08/0800	85	61 (SIO)	39	-2.79	9.89	16.70	-37.20	-2.32	18.33	37.70	-52.30
		04/15/0800	07/08/0800	85	15 (SIO)	83	-0.60	4.23	13.70	-16.30	0.40	14.06	27.00	-37.40
C4	130	04/15/0800	07/08/0800	85	12 (SIO)	19	-7.09	11.92	26.70	-39.50	-22.98	21.93	30.60	-72.80
		04/15/0800	07/08/0800	85	16 (SIO)	29	-6.56	12.35	35.20	-40.00	-20.09	21.05	30.30	-69.80
		04/15/0800	07/08/0800	85	57 (SIO)	35	-4.56	9.56	32.30	-37.50	-12.37	17.42	29.40	-60.50
		04/15/0800	07/08/0800	85	13 (SIO)	45	-4.55	9.23	26.10	-38.40	-13.96	16.43	31.60	-57.80
		04/15/0800	07/08/0800	85	14 (SIO)	65	-1.63	7.36	23.00	-32.90	-9.09	14.89	28.60	-50.30
		04/15/0800	07/08/0800	85	51 (SIO)	75	-1.95	7.32	20.10	-33.10	-7.00	14.09	28.30	-47.10
		04/15/0800	07/08/0800	85	52 (SIO)	95	-1.81	7.08	20.70	-32.50	-4.22	13.29	27.10	-45.50
		04/15/0800	07/08/0800	85	01 (SIO)	123	-1.20	6.29	25.20	-23.80	-1.40	10.93	23.90	-34.40
C5	402	04/15/0800	07/08/0800	85	B2 (WHOI)	9	-11.26	21.10	67.80	-81.00	-21.59	17.77	33.60	-72.50
		04/15/0800	07/08/0800	85	S1 (WHOI)	77	2.16	10.81	35.30	-29.00	-11.84	15.12	32.40	-50.40
		04/15/0800	07/08/0800	85	S2 (WHOI)	152	1.84	8.19	24.60	-27.30	-1.05	13.88	40.60	-36.20
		04/15/0800	07/08/0800	85	S3 (WHOI)	252	2.79	7.30	17.20	-23.60	6.84	14.08	34.70	-31.90
		04/15/0800	07/08/0800	85	S4 (WHOI)	352	1.80	4.61	15.50	-18.20	5.49	9.71	25.90	-31.10

Table 2: Horizontal Current Components (cm/s) (Continued)

Station	Water Depth (m)	Start Time (Mon/Day/Hr)	Stop Time (Mon/Day/Hr)	Duration (Days)	Instrument I.D.	Sensor Depth (m)	Cross-Shelf Mean	Cross-Shelf SD	Cross-Shelf Max	Cross-Shelf Min	Along-Shelf Mean	Along-Shelf SD	Along-Shelf Max	Along-Shelf Min
M3	90	04/15/0800	07/08/0800	85	A1 (WHOI)	9	-3.86	9.61	28.30	-39.20	-0.82	23.23	46.10	-73.50
		04/15/0800	07/08/0800	85	S1 (WHOI)	35	0.42	6.79	16.70	-29.50	1.22	20.96	44.60	-65.20
		04/15/0800	07/08/0800	85	S2 (WHOI)	55	2.64	6.60	18.10	-27.50	3.21	18.59	41.40	-54.40
		04/15/0800	07/08/0800	85	S3 (WHOI)	74	1.23	4.77	14.90	-15.50	4.59	17.72	44.50	-54.80
R3	90	04/15/0800	07/08/0800	85	B2 (WHOI)	9	-5.00	10.30	28.50	-37.50	-3.69	14.98	35.30	-59.40
		04/15/0800	07/08/0800	85	S1 (WHOI)	35	0.51	7.88	19.10	-27.10	-1.34	13.85	27.20	-51.10
		04/15/0800	07/08/0800	85	S2 (WHOI)	55	2.97	4.80	16.20	-13.40	0.63	12.89	27.30	-49.10
		04/15/0800	07/08/0800	85	S3 (WHOI)	75	2.95	4.34	17.00	-14.60	1.90	11.75	28.60	-37.50

Acknowledgements

R. C. Beardsley, R. E. Davis and C. D. Winant are the CODE principal investigators responsible for the design and execution of the moored current meters program. The engineering and technical support required was extensive and a number of individuals made substantial contributions to the project. The participation of M. Clifton, J. Dufour, P. Harvey, W. Powell, M. Kirk, S. Lentz, R. Lowe, G. Parks, S. Wald (all from SIO); K. Bradley, A. Ciesluk, P. Clay, J. Dean, R. La Rochelle, R. Limeburner, C. Mills, P. O'Malley, W. Ostrum, J. Poirier, J. Reese, L. Rosenfeld, S. Simkins, D. Simoneau, B. Skelly, and S. Worrilow, (all from WHOI), is greatly appreciated and contributed to the overall success of the field observation program. This work was supported by a grant from the Ocean Sciences Division of the National Science Foundation.

References

Halpern, D., R. A. Weller, M. G. Briscoe, R. E. Davis and J. R. McCullough, 1981. Intercomparison tests of moored current measurements in the upper ocean. J. Geophys. Res., 86: 419-428.

Weller, R. A., 1978. Observations of horizontal velocity in the upper ocean with a new vector averaging current meter. Ph.D. Thesis, University of California, San Diego, CA, 169 pp.

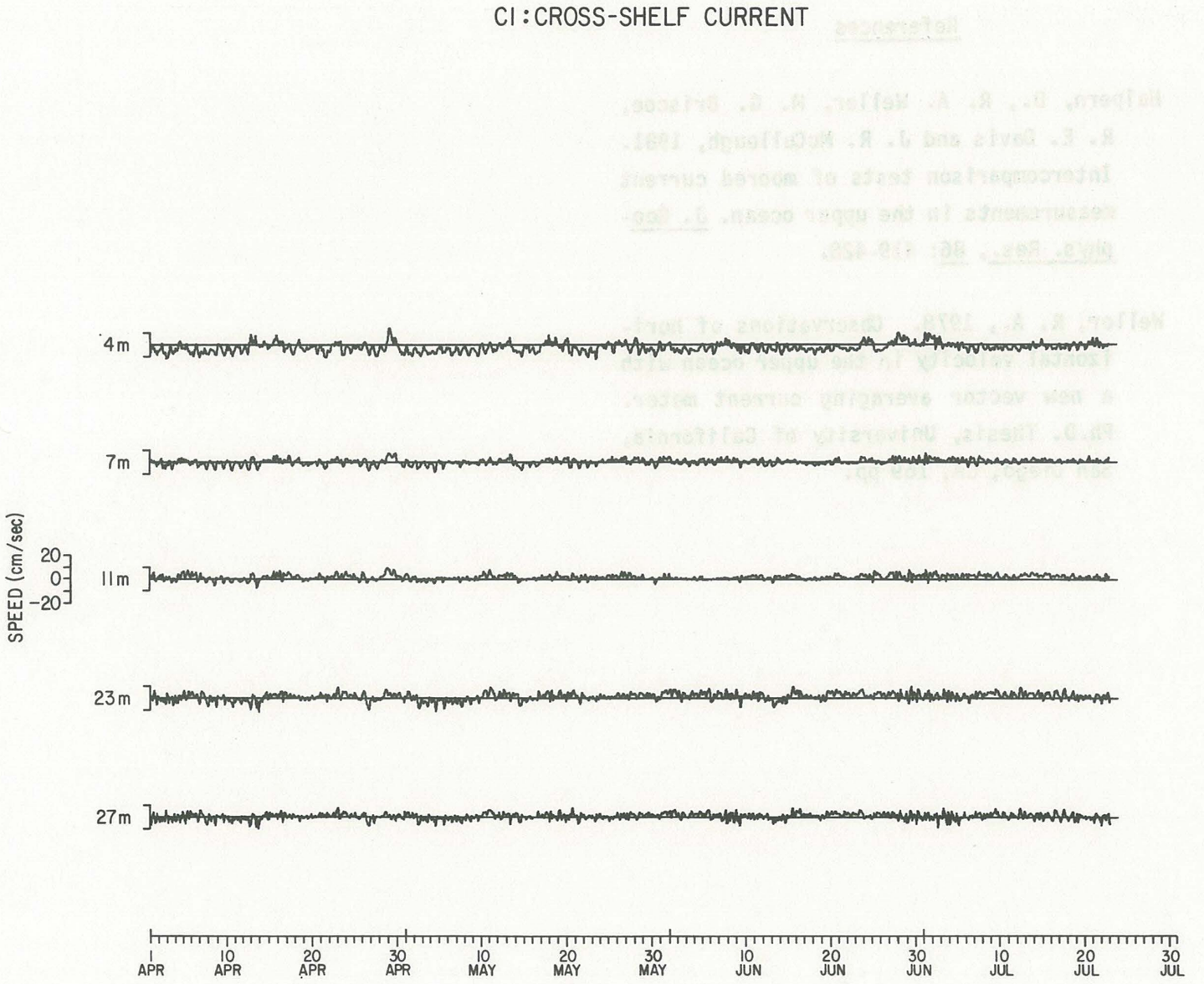
C1 : CROSS-SHELF CURRENT
4m
7m
11m
23m
27m
SPEED (cm/sec)
20
0
-20
1 APR
10 APR
20 APR
30 APR
10 MAY
20 MAY
30 MAY
10 JUN
20 JUN
30 JUN
10 JUL
20 JUL
30 JUL

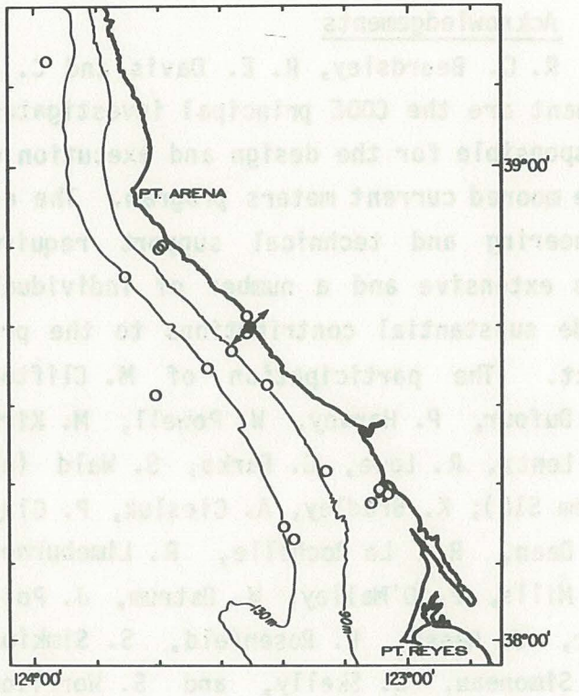
PT. ARENA
PT. REYES
39°00'
38°00'
124°00'
123°00'
100m
200m

Figure 3

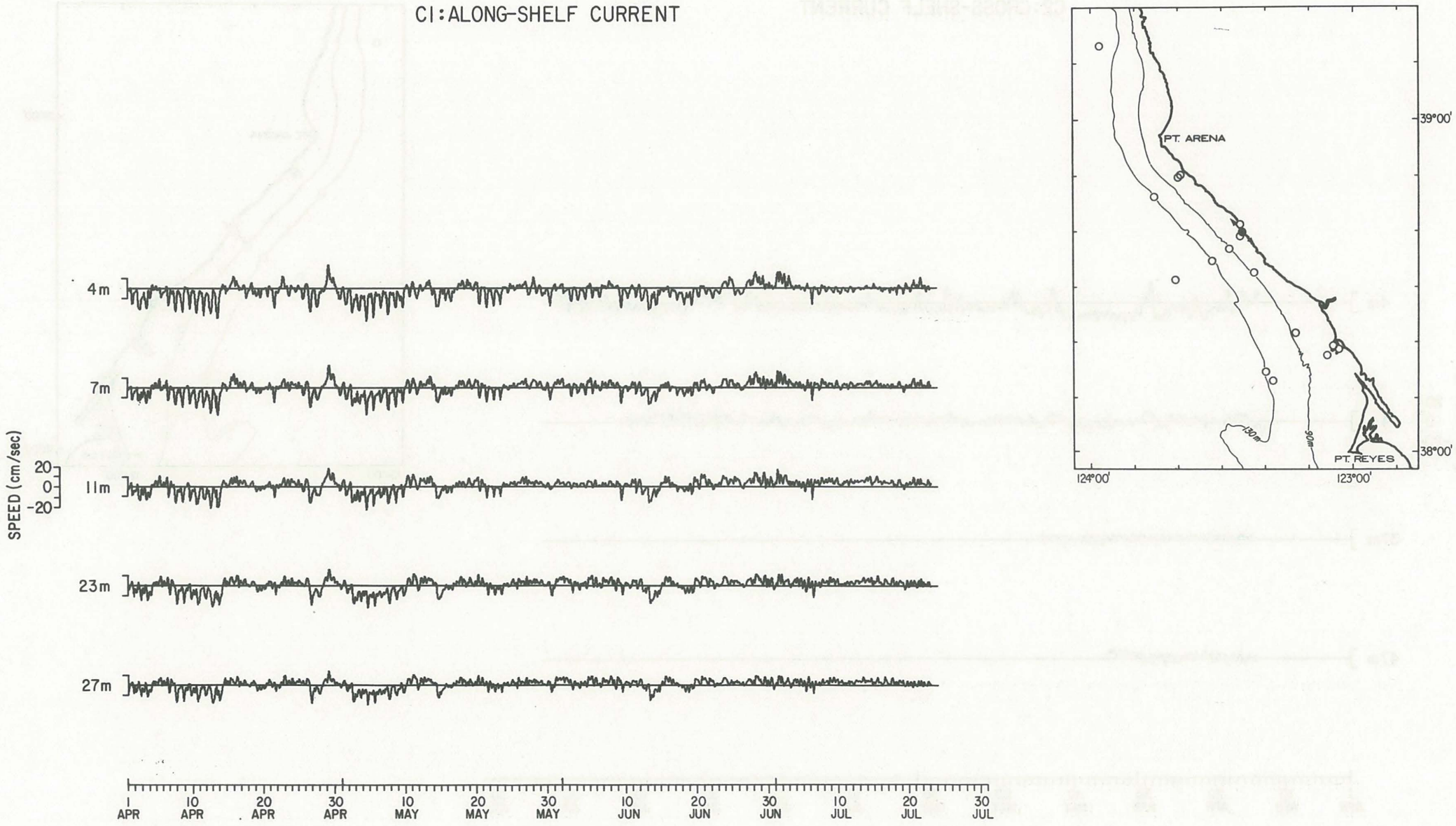
C1:ALONG-SHELF CURRENT
4m
7m
11m
23m
27m
SPEED (cm/sec)
20
0
-20
1 APR
10 APR
20 APR
30 APR
10 MAY
20 MAY
30 MAY
10 JUN
20 JUN
30 JUN
10 JUL
20 JUL
30 JUL
PT. ARENA
PT. REYES
39°00'
38°00'
124°00'
123°00'
130m
90m

Figure 4

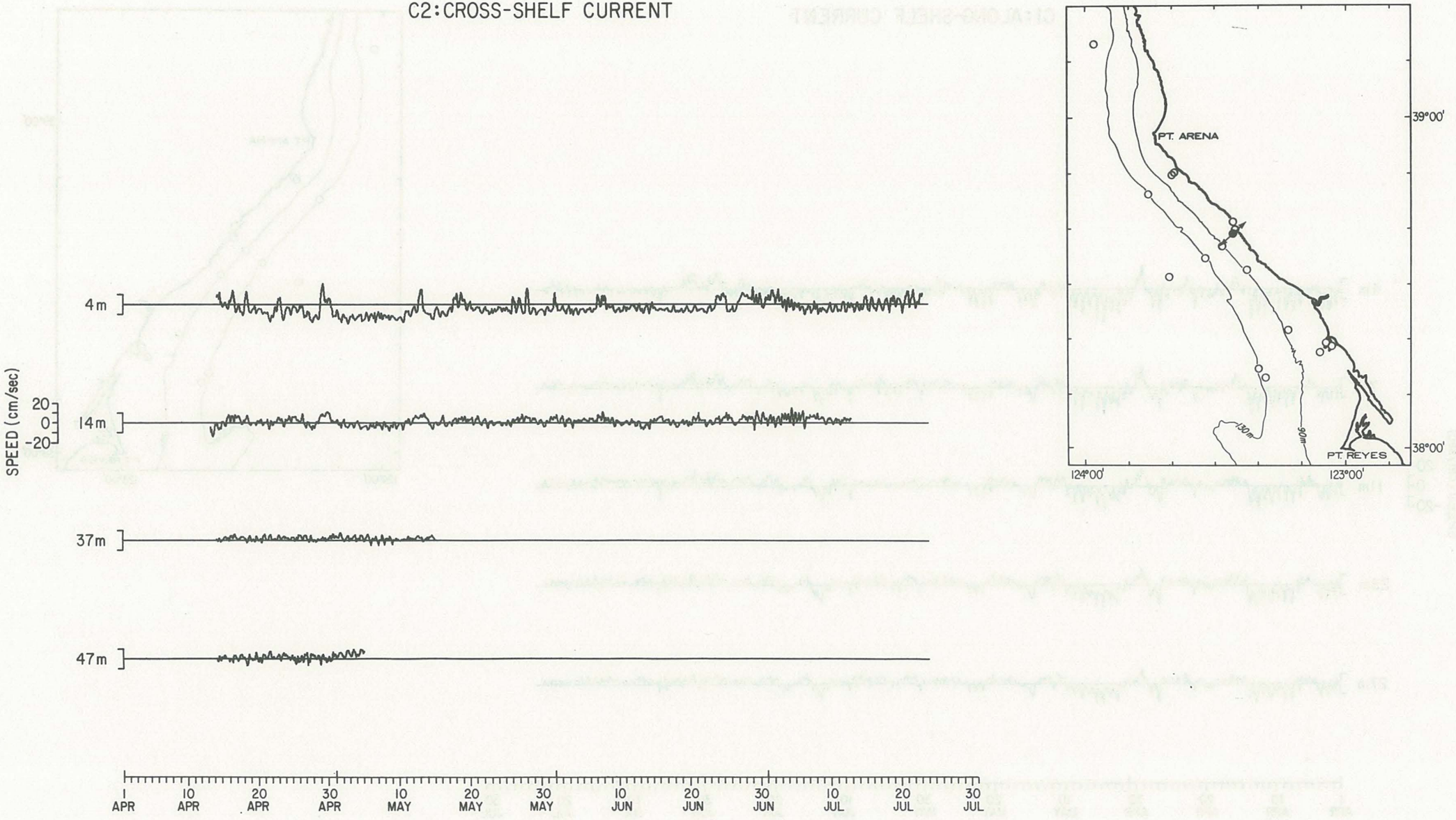
C2:CROSS-SHELF CURRENT
SPEED (cm/sec)
20
0
-20
4m
14m
37m
47m
1 APR
10 APR
20 APR
30 APR
10 MAY
20 MAY
30 MAY
10 JUN
20 JUN
30 JUN
10 JUL
20 JUL
30 JUL
PT. ARENA
PT. REYES
130m
90m
39°00'
38°00'
124°00'
123°00'

Figure 5

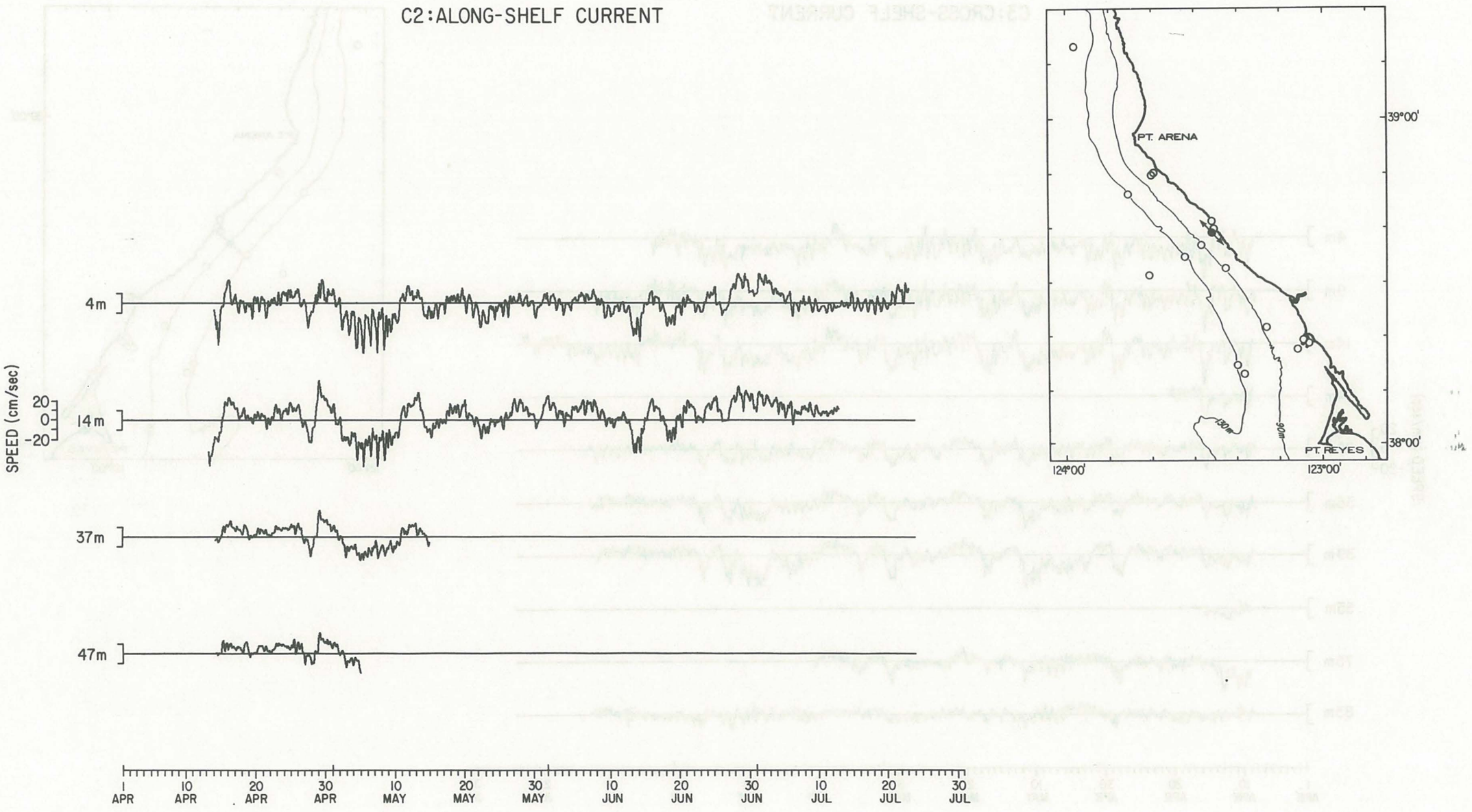
C2:ALONG-SHELF CURRENT
SPEED (cm/sec)
20
0
-20
4m
14m
37m
47m
1 APR
10 APR
20 APR
30 APR
10 MAY
20 MAY
30 MAY
10 JUN
20 JUN
30 JUN
10 JUL
20 JUL
30 JUL
PT. ARENA
PT. REYES
39°00'
38°00'
124°00'
123°00'
100m
200m

Figure 6

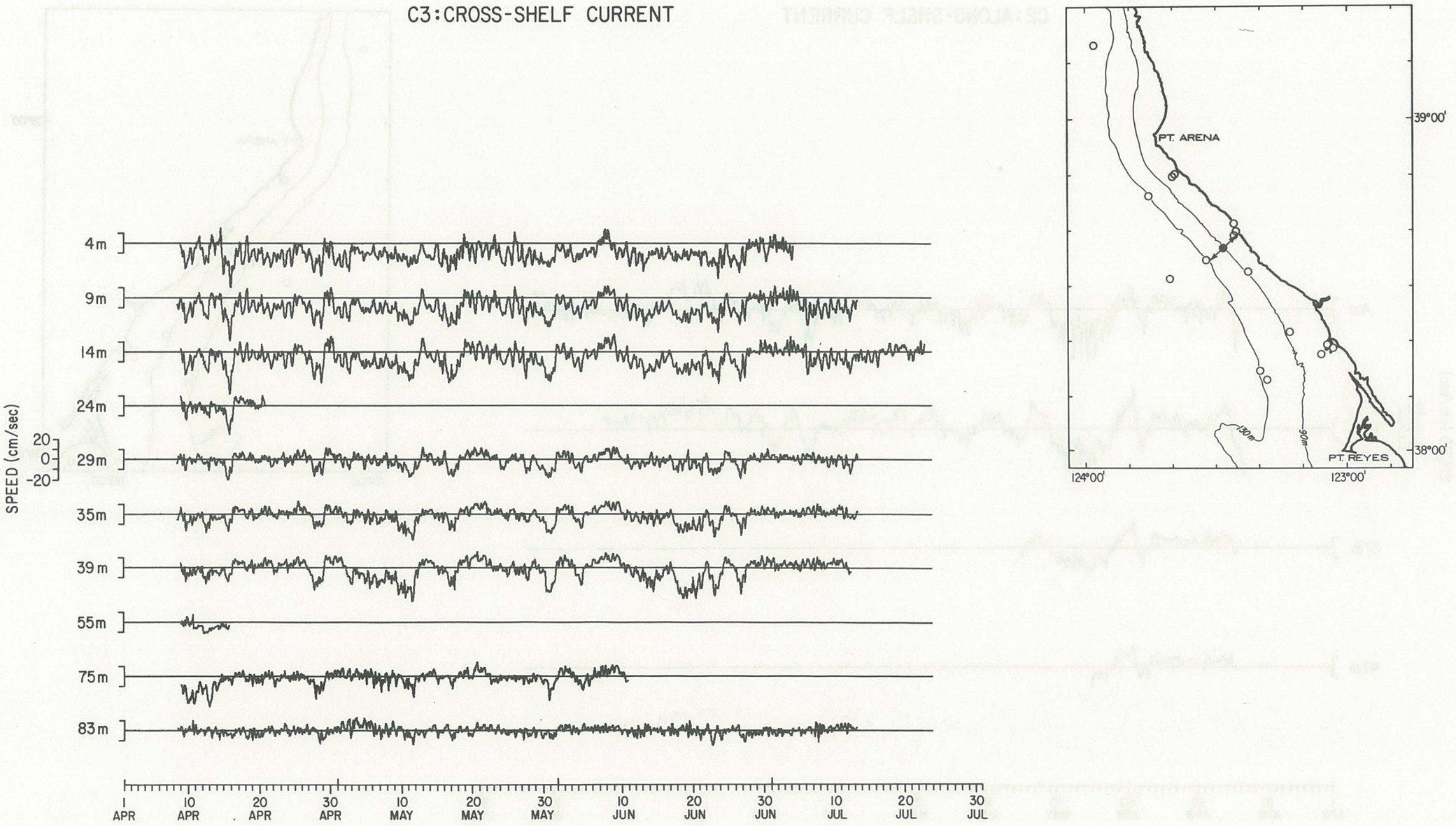
C3:CROSS-SHELF CURRENT
4m
9m
14m
24m
29m
35m
39m
55m
75m
83m
SPEED (cm/sec)
20
0
-20
1 APR
10 APR
20 APR
30 APR
10 MAY
20 MAY
30 MAY
10 JUN
20 JUN
30 JUN
10 JUL
20 JUL
30 JUL
PT. ARENA
PT. REYES
39°00'
38°00'
124°00'
123°00'
130m
90m

Figure 7

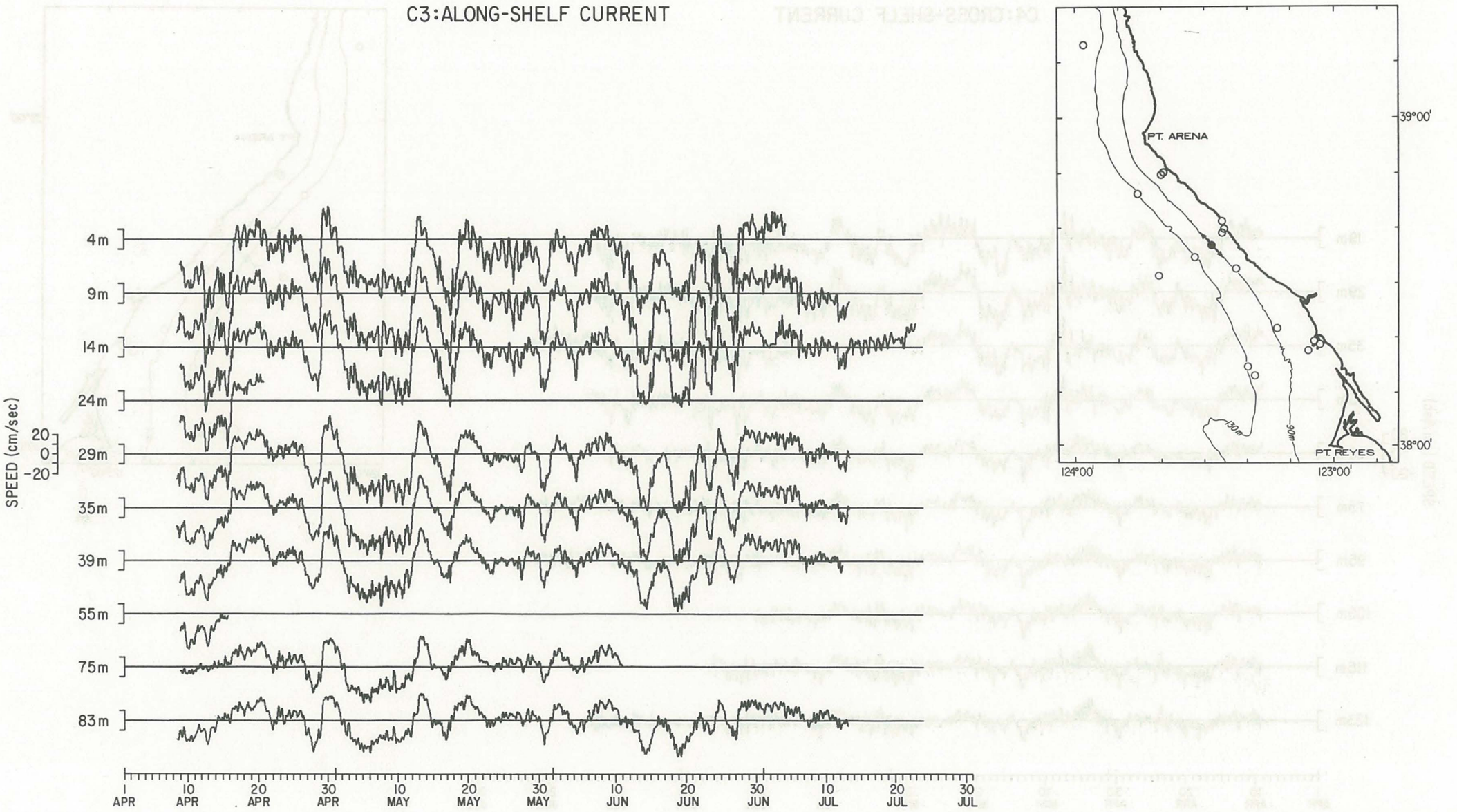
C3:ALONG-SHELF CURRENT
SPEED (cm/sec)
20
0
-20
4m
9m
14m
24m
29m
35m
39m
55m
75m
83m
1 APR
10 APR
20 APR
30 APR
10 MAY
20 MAY
30 MAY
10 JUN
20 JUN
30 JUN
10 JUL
20 JUL
30 JUL
PT. ARENA
PT. REYES
39°00'
38°00'
124°00'
123°00'
130m
90m

Figure 8

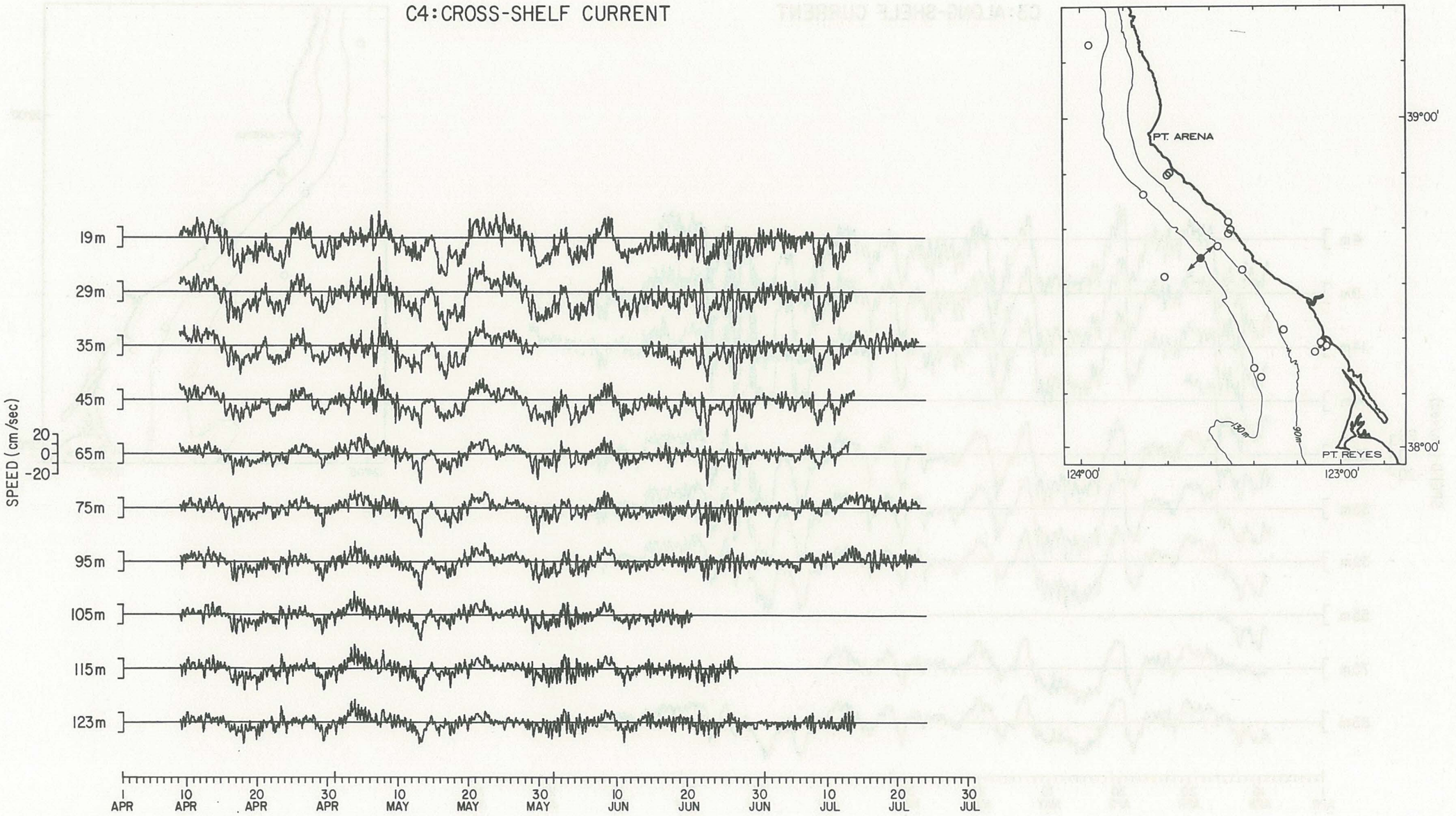
C4:CROSS-SHELF CURRENT
SPEED (cm/sec)
20
0
-20
19m
29m
35m
45m
65m
75m
95m
105m
115m
123m
1 APR
10 APR
20 APR
30 APR
10 MAY
20 MAY
30 MAY
10 JUN
20 JUN
30 JUN
10 JUL
20 JUL
30 JUL
PT. ARENA
PT. REYES
39°00'
38°00'
124°00'
123°00'
130m
90m

Figure 9

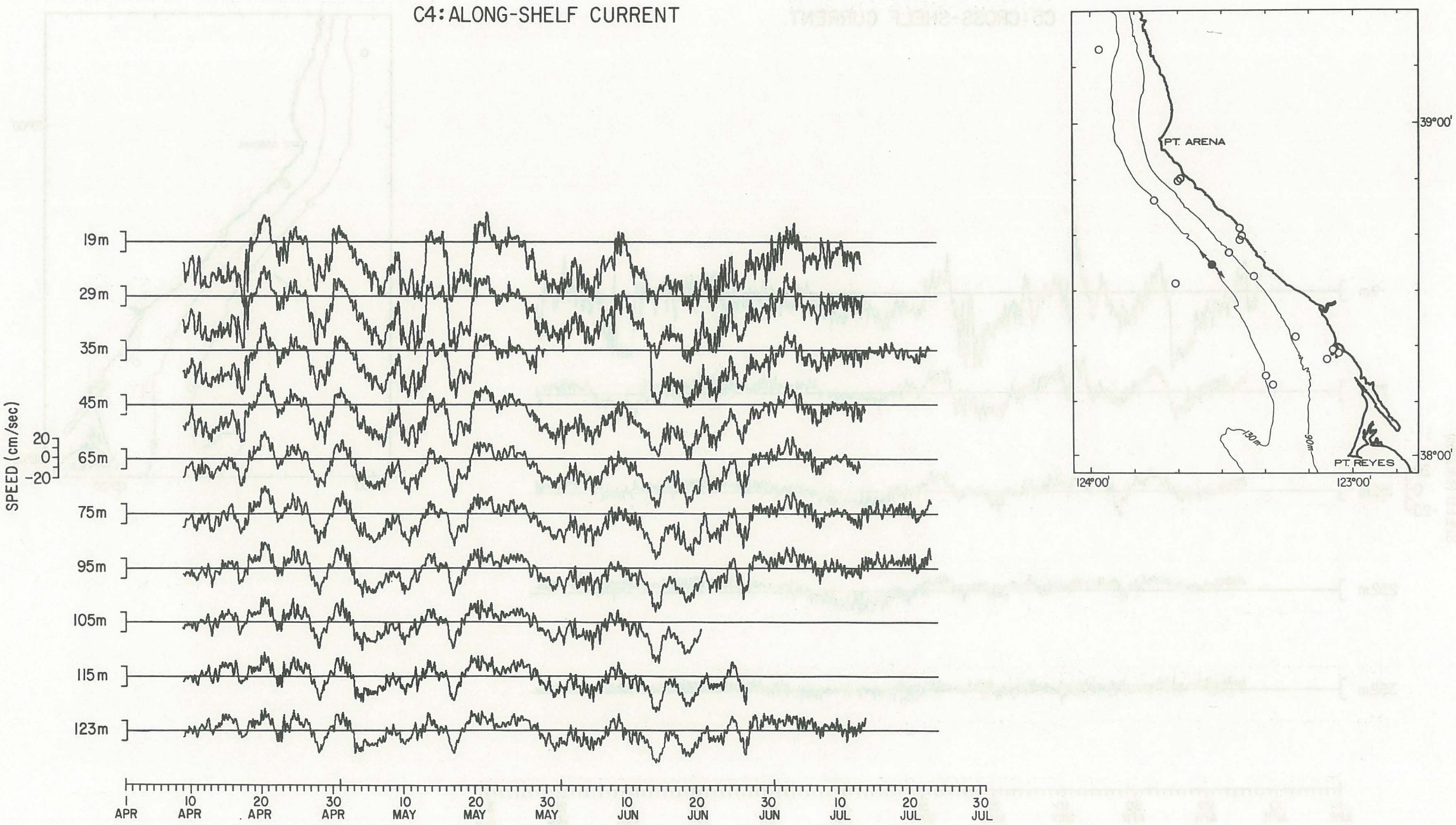
C4: ALONG-SHELF CURRENT
SPEED (cm/sec)
20
0
-20
19m
29m
35m
45m
65m
75m
95m
105m
115m
123m
1 APR
10 APR
20 APR
30 APR
10 MAY
20 MAY
30 MAY
10 JUN
20 JUN
30 JUN
10 JUL
20 JUL
30 JUL
PT. ARENA
PT. REYES
39°00'
38°00'
124°00'
123°00'
130m
90m

Figure 10

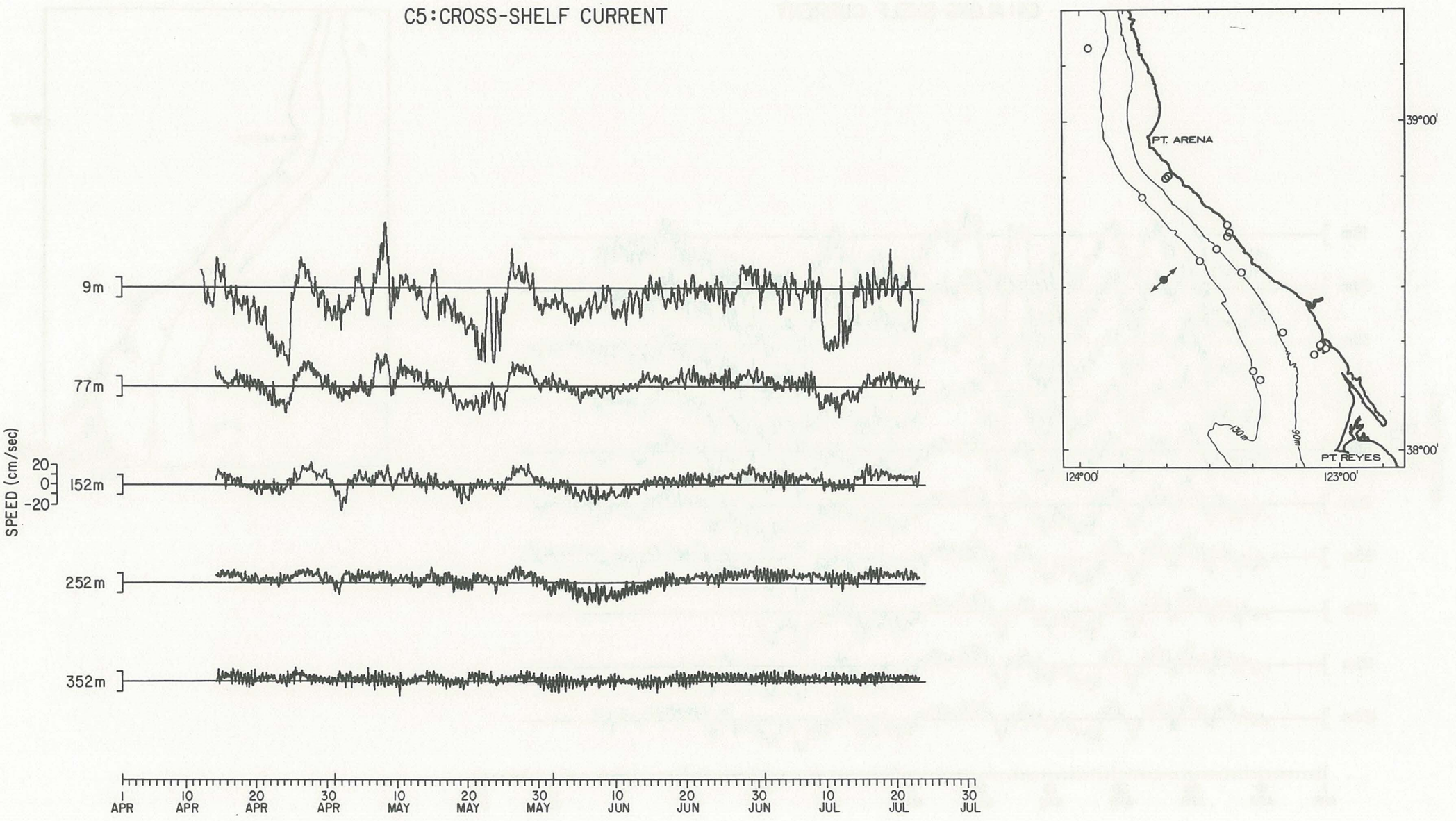
C5:CROSS-SHELF CURRENT
9m
77m
152m
252m
352m
SPEED (cm/sec)
20
0
-20
1 APR
10 APR
20 APR
30 APR
10 MAY
20 MAY
30 MAY
10 JUN
20 JUN
30 JUN
10 JUL
20 JUL
30 JUL
PT. ARENA
PT. REYES
39°00'
38°00'
124°00'
123°00'
150m
90m

Figure 11

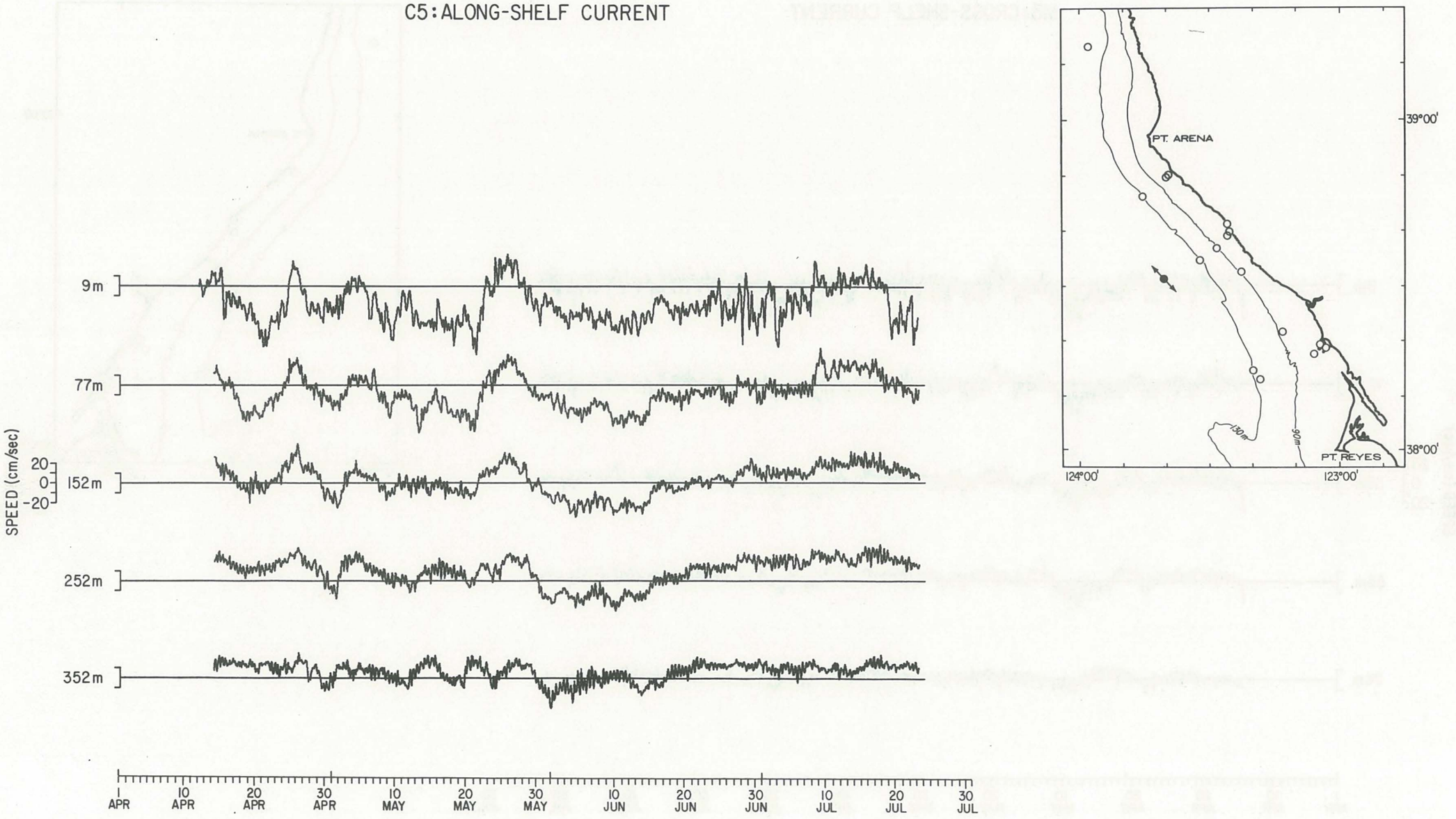
C5:ALONG-SHELF CURRENT
9m
77m
152m
252m
352m
SPEED (cm/sec)
20
0
-20
1 APR
10 APR
20 APR
30 APR
10 MAY
20 MAY
30 MAY
10 JUN
20 JUN
30 JUN
10 JUL
20 JUL
30 JUL
PT. ARENA
PT. REYES
39°00'
38°00'
124°00'
123°00'
130m
90m

Figure 12

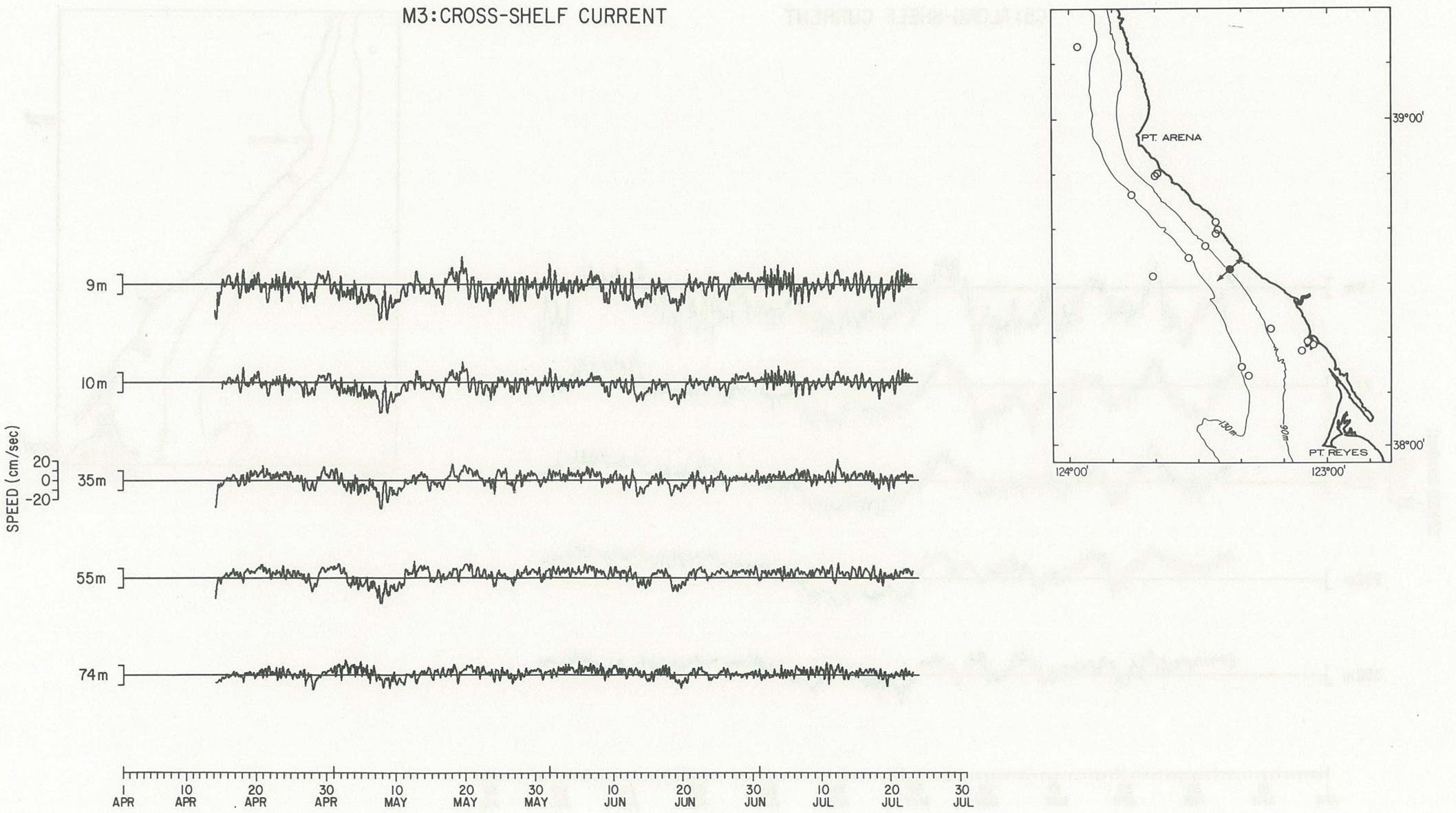
M3:CROSS-SHELF CURRENT
9m
10m
35m
55m
74m
SPEED (cm/sec)
20
0
-20
1 APR
10 APR
20 APR
30 APR
10 MAY
20 MAY
30 MAY
10 JUN
20 JUN
30 JUN
10 JUL
20 JUL
30 JUL
PT. ARENA
PT. REYES
39°00'
38°00'
124°00'
123°00'
90m
130m

Figure 13

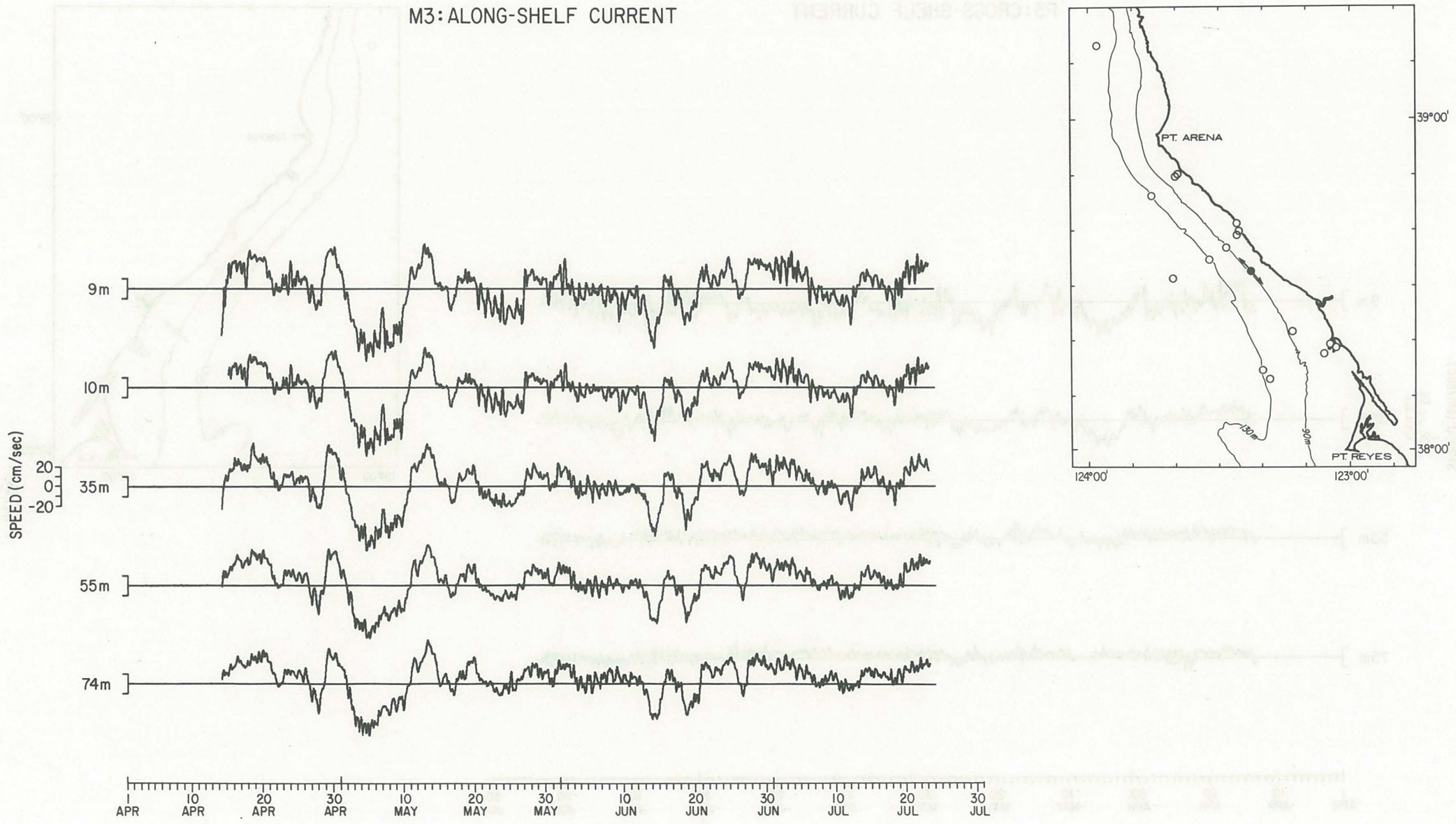
M3: ALONG-SHELF CURRENT
9m
10m
35m
55m
74m
SPEED (cm/sec)
20
0
-20
1 APR
10 APR
20 APR
30 APR
10 MAY
20 MAY
30 MAY
10 JUN
20 JUN
30 JUN
10 JUL
20 JUL
30 JUL
PT. ARENA
PT. REYES
39°00'
38°00'
124°00'
123°00'
130m
90m

Figure 14

R3: CROSS-SHELF CURRENT

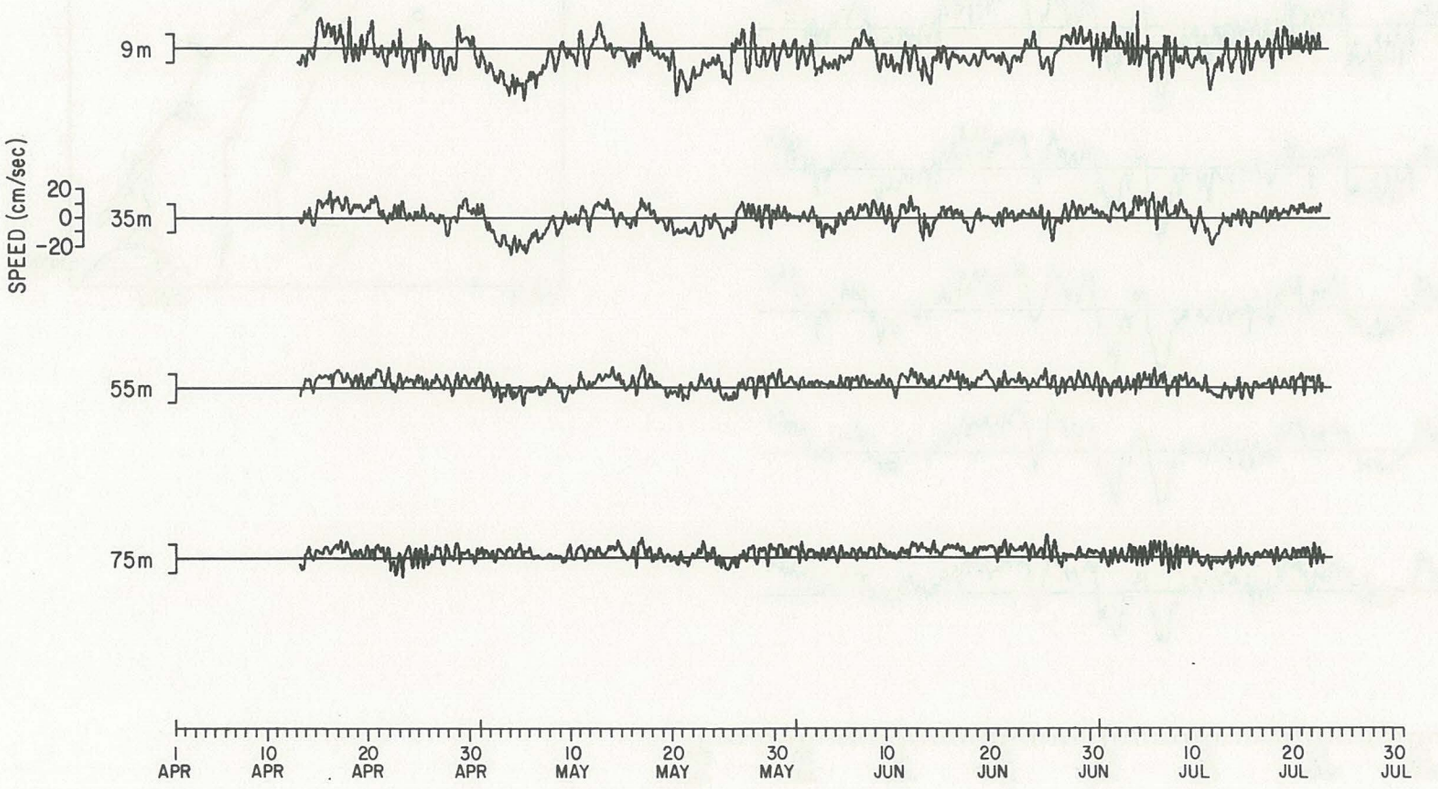

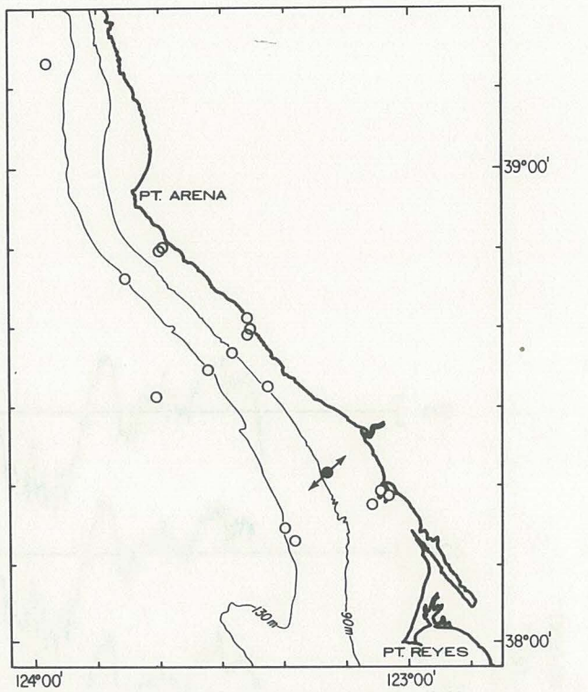

Figure 15

R3: ALONG-SHELF CURRENT

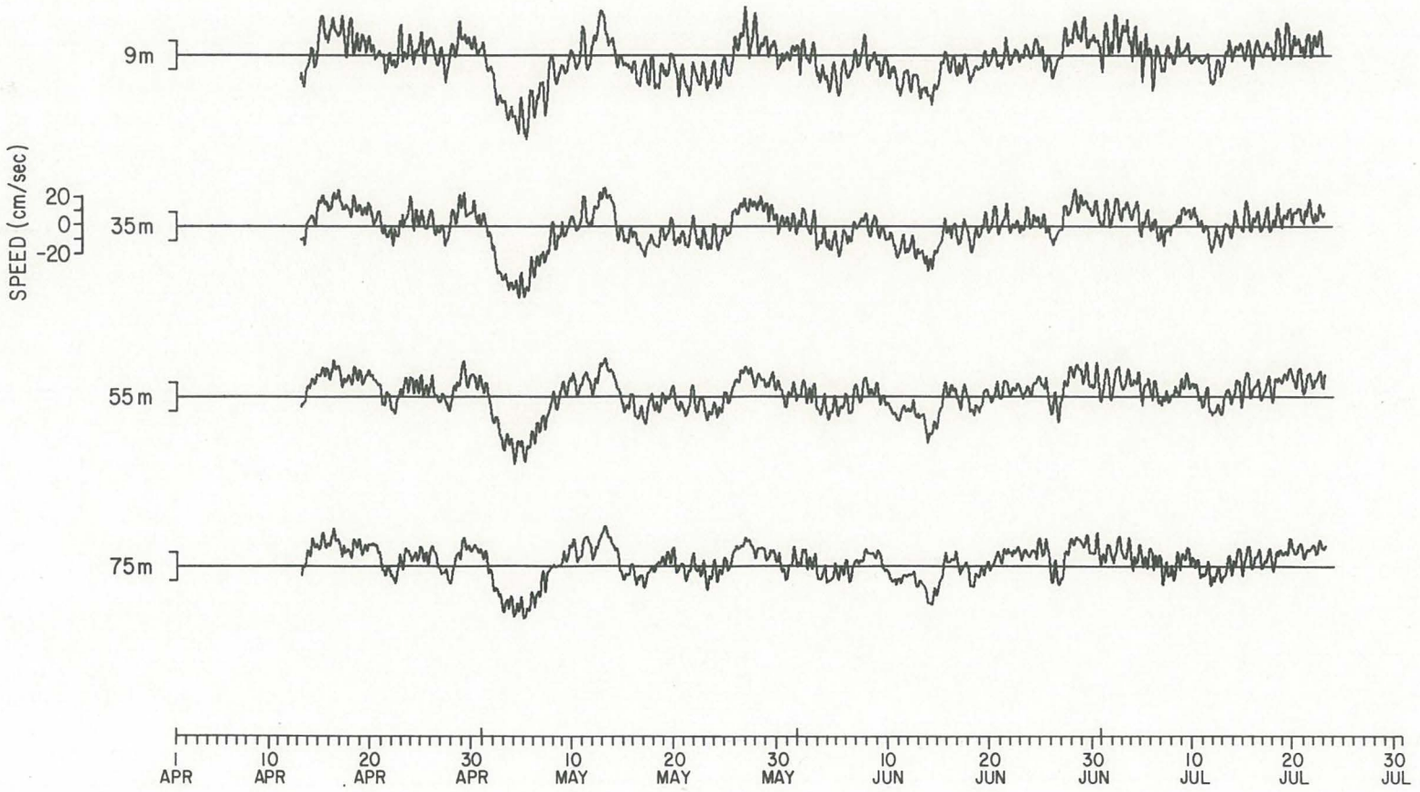

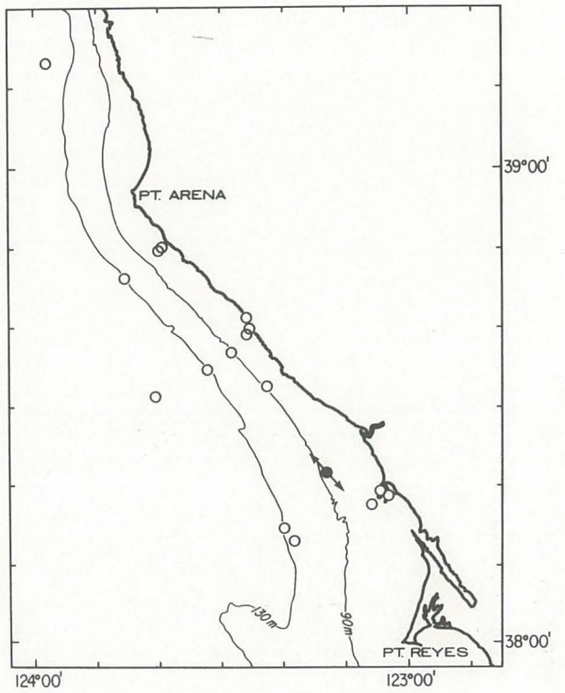

Figure 16

CODE-1:
MOORED TEMPERATURE AND CONDUCTIVITY OBSERVATIONS

by

W. S. Brown
J. D. Irish

Department of Earth Sciences
University of New Hampshire
Durham, New Hampshire 03824

and

A. W. Bratkovich

Scripps Institution of Oceanography
University of California, San Diego
La Jolla, California 92093

A. INTRODUCTION

This report describes the moored temperature and conductivity observations obtained during the first major field phase of the Coastal Ocean Dynamics Experiment (CODE-1), which took place along the northern California coast (shown in Figures 1 and 2) during the months of April through July, 1981. Descriptions of the moored current, pressure and meteorological (primarily wind) observations appear in other chapters of this report. In Section B we describe the array and the instrumentation used in the experiment. The temperature results are presented in Section C, which is followed by a description of the results from the single moored vertical temperature/conductivity array in Section D.

B. MOORED TEMPERATURE AND CONDUCTIVITY ARRAY

The CODE-1 moored temperature array consisted of temperatures measured on each current meter deployed by C. Winant and R. Davis (SIO) and R. Beardsley (WHOI) and bottom pressure/temperature chain instruments deployed by C. Winant (SIO) and W. Brown/J. Irish (UNH) at the stations indicated in Table 2 and shown in Figures 1

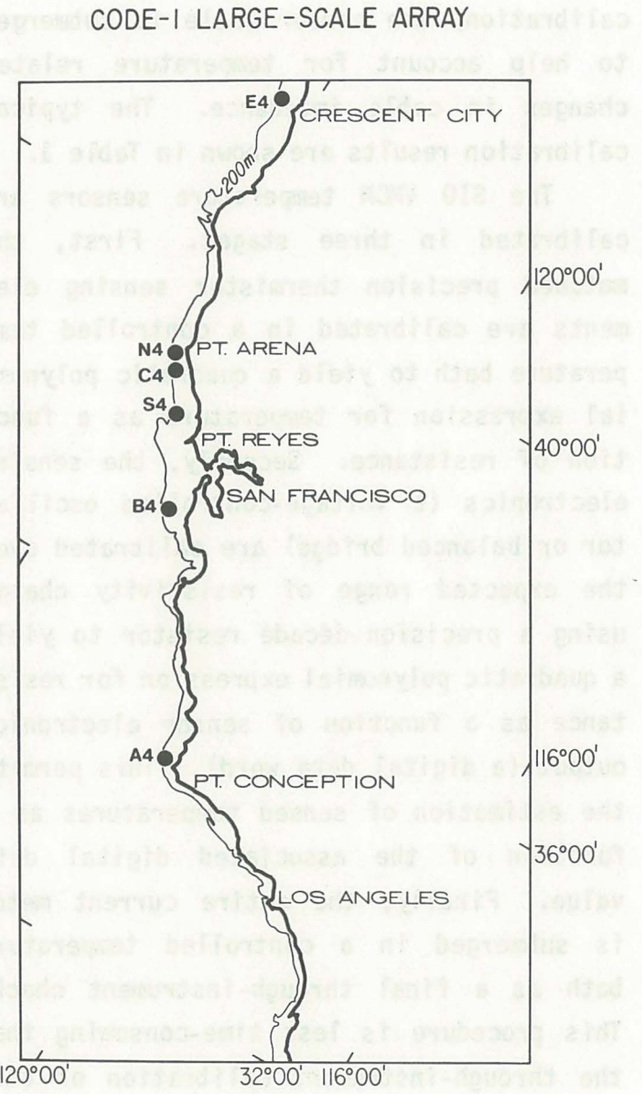

Figure 1. The elements of the large-scale temperature array are shown as darkened circles. N4, C4, and S4 are also part of the small-scale array shown in Figure 2.

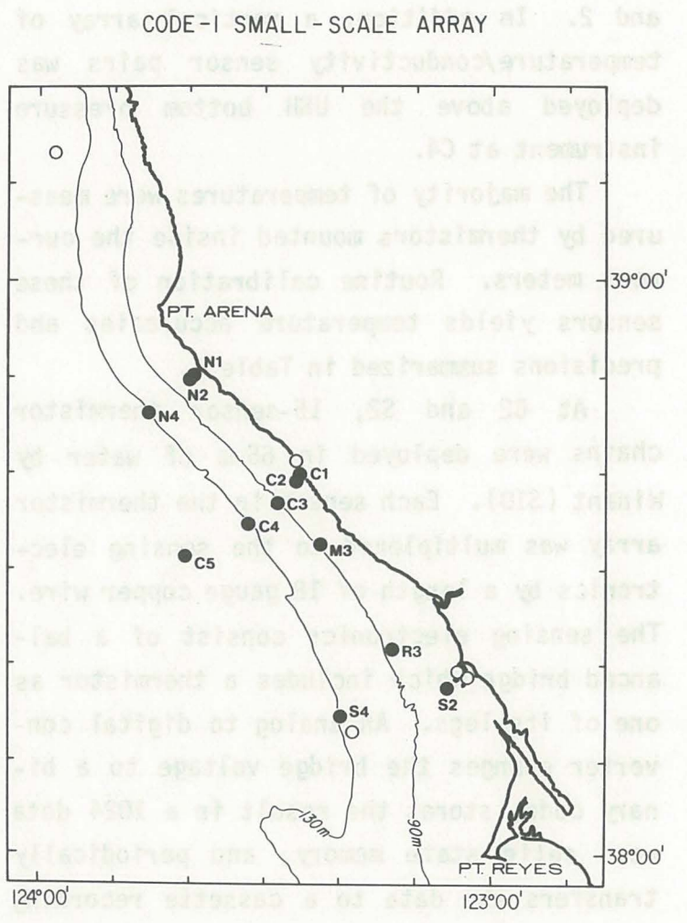

Figure 2. Stations where temperature measurements were made during CODE-1 are shown as darkened circles.

and 2. In addition, a vertical array of temperature/conductivity sensor pairs was deployed above the UNH bottom pressure instrument at C4.

The majority of temperatures were measured by thermistors mounted inside the current meters. Routine calibration of these sensors yields temperature accuracies and precisions summarized in Table 1.

At C2 and S2, 15-sensor thermistor chains were deployed in 65 m of water by Winant (SIO). Each sensor in the thermistor array was multiplexed to the sensing electronics by a length of 18 gauge copper wire. The sensing electronics consist of a balanced bridge which includes a thermistor as one of its legs. An analog to digital converter changes the bridge voltage to a binary code, stores the result in a 1024 data word solid state memory, and periodically transfers the data to a cassette recording device. Each thermistor in the 15-element chain is sampled instantaneously every four minutes along with a precision reference resistor within the instrument package itself. A thermal mass associated with each thermistor produces a sensor time response constant of about five minutes. During calibration, the sensor cable is submerged to help account for temperature related changes in cable impedance. The typical calibration results are shown in Table 1.

The SIO VMCM temperature sensors are calibrated in three stages. First, the matched precision thermistor sensing elements are calibrated in a controlled temperature bath to yield a quadratic polynomial expression for temperature as a function of resistance. Secondly, the sensing electronics (a voltage-controlled oscillator or balanced bridge) are calibrated over the expected range of resistivity change using a precision decade resistor to yield a quadratic polynomial expression for resistance as a function of sensor electronics output (a digital data word). This permits the estimation of sensed temperatures as a function of the associated digital data value. Finally, the entire current meter is submerged in a controlled temperature bath as a final through-instrument check. This procedure is less time-consuming than the through-instrument calibration of each VMCM, but leads to an acceptable measurement accuracy (see Table 1).

TABLE 1:

Uncertainty specifications for the different temperatures measured in CODE-1

	Accuracy	Precision
SIO VMCM (Winant)	± 0.1	± 0.004
SIO VMCM (Davis)	± 0.1	± 0.03
WHOI VMCM	± 0.2	± 0.002
WHOI VACM	± 0.005	± 0.00015
SIO T-CHAIN	± 0.05	± 0.004
UNH T-CHAIN	± 0.01	± 0.0001

The WHOI VACM and VMCM temperature sensors are calibrated in much the same way as the comparable SIO instrumentation with a couple of exceptions. The temperature vs. resistivity fit for the thermistor calibration is to a third order logarithmic expression and the through-instrument calibration point is not performed for the WHOI instruments. The accuracy (see Table 1) of the WHOI temperature sensing instrumentation is improved by keeping extensive time histories of thermistor characteristics and by increasing the precision of the measurement through an extended averaging interval of the sensor electronics output.

At C4, a temperature/conductivity chain was deployed in 130 m of water by W. Brown and J. Irish (UNH) for purposes of obtaining measurements from which we could make estimates of the spatial and temporal variability in the internal pressure. The temperature and conductivity sensors, which were manufactured by Sea Bird Electronics, were deployed in pairs at six elevations. These sensors use a Wein-bridge oscillator to change the variable resistance of a thermistor or a three-electrode conductivity cell into an FM signal. Temperature sensors of this type have been in use for over ten years and typically exhibit long-term drift rates of 5 millidegrees C per year. Recalibrated sensors compare within 2 millidegrees C over several-month periods and can easily resolve a fraction of a millidegree fluctuation.

The conductivity measurement is more difficult. Our previous experience with this type of sensor on the New England continental shelf and the deep mid-Pacific indicated long-term drift rates on the order of 0.001 s/m (0.01 mmhos/cm) over a four-month period. During CODE-1, the in-situ intercomparisons with the CTD showed typical drifts of about 0.01 s/m (0.1 mmhos/cm) for the three-month deployment. There was a tendency for lower sensors to drift more, with the deepest sensors (123 m) drifting three times the typical rate. The larger drifts observed during CODE-1 were probably caused by a fouling of the electrodes by biological growth, fine sediments, etc. A comparison of pre- and post-cruise calibrations indicates less drift than that found in the comparison with CTD observations. We suspect this discrepancy resulted because some of the contamination washed off during shipment from the West Coast. Further discussion of these points appears in Section D.

The sampling rate of the SIO current meter thermistors and thermistor chain was four minutes while the routine sampling rate of the WHOI and UNH sensors was 3.75 minutes and 15 minutes, respectively. The UNH instrument, which has a microprocessor-controlled data logger, had the added advantage of sampling all sensors at 15-second intervals during periods of "interesting" events. This sampling feature will be discussed in more detail in Section D.

C. TEMPERATURE OBSERVATIONS

Hourly values of the temperatures on the central line moorings C1, C2, C3, C4, C4-T/C and C5 are shown in Figures 3 through 8. All time series are plotted relative to the series mean value denoted by the tick mark on the vertical axis. With the exception of C5, each mooring has resolved the local vertical temperature field reasonably well, and the cross-shelf array between C1 and C4 exhibits a variety of structures which may or may not be correlated from mooring to mooring. Upper level temperatures on mooring C5 show some of the major

TABLE 2: Temperature (°C)

Station	Water Depth (m)	Start Time (Mon/Day/Hr)	Stop Time (Mon/Day/Hr)	Duration (Days)	Instrument I.D.	Sensor Depth (m)	Mean	Standard Deviation	Maximum	Minimum
C1	30	03/25/0800	07/23/1800	120	62	4	8.73	0.947	12.59	7.21
		03/25/0800	07/23/1800	120	65	7	8.57	0.915	12.55	7.05
		03/25/0800	07/23/1800	120	59	11	8.49	0.849	12.52	7.03
		04/01/0800	07/23/1800	113	58	23	8.36	0.686	11.82	6.99
		04/01/0800	07/23/1800	113	56	27	8.39	0.668	11.44	6.93
		04/01/0900	07/24/0600	114	Bottom	33	8.39	0.674	11.26	6.96
C3	90	04/12/1300	07/31/1200	110	B1	1	9.25	0.966	13.03	7.74
		04/07/0800	07/05/0300	89	64	4	8.66	0.566	11.84	7.56
		04/08/2000	07/14/0500	96	04	9	8.65	0.544	11.68	7.48
		04/07/0800	07/23/1800	108	50	14	8.60	0.437	10.90	7.57
		04/07/0800	07/23/1800	108	53	24	8.46	0.345	9.94	7.57
		04/08/2000	07/14/0600	96	02	29	8.37	0.318	9.68	7.46
		04/08/2000	07/14/0400	96	03	35	8.30	0.288	9.51	7.48
		04/09/0800	07/13/0600	95	61	39	8.24	0.257	9.27	7.54
		04/08/2000	07/13/1400	96	11	45	8.20	0.271	9.13	7.43
		04/09/0800	07/23/1800	106	69	55	8.13	0.277	8.96	7.32
		04/08/2000	07/01/0200	83	06	65	7.96	0.253	8.54	6.92
		04/09/0800	07/23/1800	106	66	75	8.00	0.325	8.23	6.95
		04/08/2000	07/13/2100	96	15	83	7.92	0.336	8.79	6.90
R3	90	04/13/1300	08/03/1200	112	B1	1	9.68	1.128	13.52	7.84
		04/13/1300	08/03/1200	112	B2	9	9.30	0.769	12.28	7.85
		04/13/1300	08/03/1200	112	S1	35	8.77	0.386	9.91	7.82
		04/13/1300	08/03/1200	112	S2	55	8.44	0.353	9.34	7.67
		04/13/1300	08/03/1200	112	S3	75	8.29	0.375	9.32	7.55
M3	90	04/14/1300	07/31/1200	108	A1	9	9.08	0.709	11.68	7.65
		04/14/1300	07/31/1200	108	S1	35	8.62	0.428	10.52	7.49
		04/14/1300	07/31/1200	108	S2	55	8.32	0.366	9.33	7.24
		04/14/1300	07/31/1200	108	S3	74	8.18	0.384	9.36	7.02

TABLE 2: Temperature (°C) - (Continued)

Station	Water Depth (m)	Start Time (Mon/Day/Hr)	Stop Time (Mon/Day/Hr)	Duration (Days)	Instrument I.D.	Sensor Depth (m)	Mean	Standard Deviation	Maximum	Minimum
C4	133	04/09/0800	07/23/1000	105	68	4	9.25	0.680	12.17	8.12
		04/09/0800	07/14/0000	95	12	19	9.08	0.473	11.28	8.16
		04/09/0800	05/19/0600	39	54	24	8.81	0.383	10.21	8.10
		04/09/0800	07/14/0700	96	16	29	8.95	0.397	10.99	7.98
		04/09/0800	07/23/1800	106	57	35	8.87	0.368	10.77	7.88
		04/09/0800	07/14/1100	96	13	45	8.70	0.346	10.55	7.72
		04/09/0800	04/15/0600	6	55	55	8.39	0.389	9.00	7.85
		04/09/0800	07/13/1700	95	14	65	8.38	0.318	9.60	7.53
		04/09/0800	07/23/1800	106	51	75	8.20	0.282	9.09	7.41
		04/09/0800	07/23/1800	106	52	95	7.97	0.255	8.65	7.27
		04/09/0800	06/21/0800	73	10	105	7.87	0.264	8.51	7.08
		04/09/0800	06/28/0600	80	67	115	7.86	0.265	8.47	6.98
		04/09/0800	07/14/1000	96	01	123	7.86	0.311	8.50	6.89
		04/21/2200	07/19/1800	89	GERDA	133	7.81	0.273	8.27	7.16
C5	400	04/18/0900	08/02/1200	106	B1	1	10.66	0.989	13.90	8.74
		04/12/1300	08/01/1200	111	B2	9	10.50	0.848	13.02	8.75
		04/14/1300	08/02/1200	110	S1	77	9.04	0.337	9.99	8.05
		04/14/1300	08/02/1200	110	S2	152	8.20	0.267	9.03	7.50
		04/14/1300	08/02/1200	110	S3	252	7.52	0.303	8.23	6.69
		04/14/1300	08/02/1200	110	S4	352	6.95	0.273	7.77	6.16
A4	127	04/07/1600	07/28/1600	112	PICKET	127	5.70	0.257	6.55	4.78
B4	125	04/08/2000	07/16/1600	98	KELVIN	125	8.51	0.314	9.40	7.71
S4	130	04/23/2000	07/16/2000	84	KIWI	130	8.05	0.188	8.39	7.53
N4	131	04/18/2200	06/03/2300	46	MICHAEL	131	7.67	0.319	8.44	6.89
N2	57	04/18/2000	07/18/1900	90	MANNING	57	7.99	0.404	9.97	7.16
N1	41	04/18/2000	07/18/1800	90	SHELDRAKE	41	8.53	0.331	10.46	7.79
E4	131	04/19/2200	07/18/0000	89	VOGEL	131	7.14	0.359	7.94	5.98

TABLE 2: Temperature (°C) - (Continued)

Station	Water Depth (m)	Start Time (Mon/Day/Hr)	Stop Time (Mon/Day/Hr)	Duration (Days)	Instrument I.D.	Sensor Depth (m)	Mean	Standard Deviation	Maximum	Minimum
C2/TC	67	03/24/2000	07/26/1200	124	STC*	8	9.00	0.950	12.73	7.52
		03/24/2000	07/26/1200	124	STC	11	8.90	0.913	12.68	7.46
		03/24/2000	07/26/1200	124	STC	15	8.78	0.861	12.53	7.36
		03/24/2000	07/26/1200	124	STC	19	8.69	0.838	12.66	7.29
		03/24/2000	07/26/1200	124	STC	23	8.58	0.793	12.47	7.18
		03/24/2000	07/26/1200	124	STC	27	8.50	0.763	12.35	7.08
		03/24/2000	07/26/1200	124	STC	31	8.44	0.749	12.32	7.04
		03/24/2000	07/26/1200	124	STC	35	8.40	0.717	11.90	6.94
		03/24/2000	07/26/1200	124	STC	39	8.36	0.698	11.82	6.91
		03/24/2000	07/26/1200	124	STC	43	8.32	0.683	11.77	6.88
		03/24/2000	07/26/1200	124	STC	47	8.30	0.671	11.71	6.88
		03/24/2000	07/26/1200	124	STC	51	8.26	0.656	11.59	6.88
		03/24/2000	07/26/1200	124	STC	55	8.25	0.643	11.34	6.89
		03/24/2000	07/26/1200	124	STC	59	8.25	0.629	11.11	6.89
		03/24/2000	07/26/1200	124	STC	61	8.24	0.622	10.98	6.89
		04/01/0800	07/24/0100	114	Bottom	66	8.05	0.453	9.27	6.91
		04/13/2300	07/15/2000	91	05	14	8.63	0.597	11.28	7.62
S2/TC	63	04/05/2000	07/31/0000	116	STC	8	9.46	1.006	12.64	7.74
		04/05/2000	07/31/0000	116	STC	11	9.37	0.933	12.63	7.76
		04/05/2000	07/31/0000	116	STC	15	9.18	0.814	12.07	7.70
		04/05/2000	07/31/0000	116	STC	19	9.05	0.726	11.42	7.72
		04/05/2000	07/31/0000	116	STC	23	8.92	0.660	11.02	7.70
		04/05/2000	07/31/0000	116	STC	27	8.80	0.610	10.85	7.57
		04/05/2000	07/31/0000	116	STC	31	8.71	0.559	10.62	7.55
		04/05/2000	07/31/0000	116	STC	35	8.63	0.532	10.41	7.54
		04/05/2000	07/31/0000	116	STC	39	8.58	0.515	10.24	7.53
		04/05/2000	07/31/0000	116	STC	43	8.52	0.505	10.14	7.51
		04/05/2000	07/31/0000	116	STC	47	8.50	0.502	9.98	7.52
		04/05/2000	07/31/0000	116	STC	51	8.48	0.498	9.92	7.46
		04/05/2000	07/31/0000	116	STC	55	8.47	0.487	9.87	7.48
		04/05/2000	07/31/0000	116	STC	59	8.47	0.518	9.94	7.42
		04/05/2000	07/31/0000	116	STC	61	8.43	0.489	9.79	7.45
		04/05/2200	08/05/1000	121	Bottom	62	8.47	0.511	9.91	7.47

*SIO Thermistor Chain

TABLE 2: Temperature (°C) - (Continued)

Station	Water Depth (m)	Start Time (Mon/Day/Hr)	Stop Time (Mon/Day/Hr)	Duration (Days)	Instrument I.D.	Sensor Depth (m)	Mean	Standard Deviation	Maximum	Minimum
C4/TEMP	133	04/22/0000	07/05/1500	75	GERDA	27	9.28	0.448	10.87	8.29
		04/22/0000	07/04/1900	74	GERDA	43	8.81	0.331	10.01	7.81
		04/22/0000	07/19/1800	88	GERDA	63	8.55	0.316	9.81	7.60
		04/22/0000	07/19/1800	88	GERDA	83	8.32	0.285	9.34	7.41
		04/22/0000	07/19/1800	88	GERDA	103	8.12	0.243	8.86	7.38
		04/22/0000	07/19/1800	88	GERDA	123	7.95	0.260	8.49	7.31
		04/22/0000	07/19/1800	88	GERDA	133	7.81	0.273	8.27	7.16

"events" seen at the inshore central line moorings but, generally, temperature at C5 seems to be uncorrelated with the shallower CODE-area array. Figures 9, 10, and 11 provide some information on the along-shelf variability in the temperature field along the 90 m and 60 m isobaths, respectively. Clearly, there is less similarity among these temperatures in comparison to the central line temperatures. Finally, Figures 12 and 13 provide a look at the bottom temperatures at the UNH bottom pressure sites in the CODE-1 area and along the 130 m isobath, respectively. With the exception of the N1 and N2 temperatures which are only 1.7 km apart, there is very little similarity among the bottom temperature results. As seen in Figure 13, the CODE-1 130 m moorings exhibit significantly less tidal frequency temperature variability relative to other more distant moorings up and down the coast. The statistics for all the temperatures shown in the previous figures are presented in Table 2.

D. TEMPERATURE AND CONDUCTIVITY ARRAY EVALUATION AND RESULTS

An array of temperature and conductivity sensors was deployed at C4 in order to make the measurements required to compute time series of density. Sea Bird, Inc. sensors were used because they have been shown to have the required sensitivity, precision and stability for this task. In part, their performance standard is related to the fact that their output is independent of cable impedance. Ironically, the sensors deployed during CODE-1 incorporated an "improved" circuit design which made them sensitive to cable impedance (a problem which has been corrected for the CODE-2 deployment). The problem of impedance sensitivity became apparent after comparing pre- and post-deployment calibrations. The pre-cruise calibrations, which were performed by the Northwest Regional Calibration Center (NRCC) of NOAA located in Bellevue, Washington, employed a frequency counter which did not load the sensor output. The post-cruise calibrations, which were performed at the UNH calibration facility as described in Appendix A, employed a modified form of our microprocessor-controlled recorder, which did load the sensor output and affected the results. To further complicate the situation, the post-cruise calibrations were not performed with the array cabling used at sea. The overall effect of these difficulties was to produce constant offsets in the different calibrations. Our task was to determine these offsets.

Thus, for CODE-1, we used the CTD observations to perform an in-situ "adjustment" to the pre-cruise calibrations. At the time of deployment and recovery, we made a special effort to gather CTD data for purposes of intercomparison with these moored sensors. In addition, the OSU hydrographic survey (A. Huyer) provided additional CTD data obtained within a 1 km radius of the C4 mooring. An example of this comparison is presented in Figure 14 which shows the difference between CTD results and "observed temperature" at 83 m depth (the depth of the largest vertical temperature gradient). The instantaneous differences, which are as large as ± 0.33°C probably result from spatial variability and make in-situ calibrations difficult. Nevertheless, the comparisons were made and the results for the temperature sensors suggested no statistically significant drift. A constant temperature adjustment was made to each "observed temperature" (as tabulated in Table 3), and produced agreement between moored and CTD

temperatures to within ± .01°C. Low-passed versions of these temperatures presented in Figure 15 show that when sensors were in the surface or bottom mixed layers, they showed the same values without inversions. (Hourly and 15-second data do show inversion for a short period of time, however.) Thus, the adjustment process is probably adequate for subtidal frequency CODE analysis.

The conductivity observations were treated like the temperature observations but in this case a statistically significant drift, which we believe is due to in-situ fouling of the electrodes, was found. The observation of drift toward lower conductivity is consistent with our hypothesis of biological fouling of the electrodes. These drifts were determined from a linear fit to the ARRAY-CTD difference series. The 27 m conductivity sensor was further corrected by subtracting the exponential drift. The details of these corrections are tabulated in Table 3.

Using these corrected temperature and conductivity series, the salinity and density were calculated from the algorithms presented in Appendix B. Conductivity, salinity and density statistics are presen-

TABLE 3: A summary of corrections applied to the mooring C4 (GERDA) temperature/conductivity array observations in order to minimize differences with CTD temperature and conductivity observations. Time, t, is hours after deployment.

Array Location	Serial Number	Depth (dbar)	Applied Correction
T1	500	27	-0.267°C
C1	73		$-0.232 + 2.4\times10^{-5}t + 3.4\times10^{-2}\, e^{-.0028\, t}$ s/m
T2	485	43	-0.050°C
C2	80		+0.0076 s/m
T3	489	63	-0.050°C
C3	79		$-0.0010 + 7.4 \times 10^{-6}t$ s/m
T4	501	83	0.025°C
C4	78		$0.007 + 6.0 \times 10^{-6}t$ s/m
T5	492	103	-0.040°C
C5	59		$-0.0021 + 1.04 \times 10^{-5}t$ s/m
T6	490	123	-0.020°C
C6	76		$-0.0025 + 2.04 \times 10^{-5}$ t s/m
SDT		133	+ 0.130°C

ted in Table 4. The low-passed salinity and sigma-t series are plotted on the absolute scales in the upper panels of Figure 15. Clearly some problems (and uncertainties) remain as density inversions can be seen in a few places.

In summary, the temperature/conductivity array results agree with the CTD observations to within ± 0.01°C, ± 0.02°/₀₀ (after correction) and ± 0.02 sigma-t units. The precision or relative accuracy for a particular time series is more than an order of magnitude better than the absolute uncertainties.

The hourly corrected series is the data base for further analysis and is plotted in Figure 7. In addition to the array temperatures, there is an internal Sea Data thermistor (SDT) sensor in the bottom instrument pressure case. This temperature was also adjusted to fit the CTD series as tabulated in Table 3. The statistics for the normalized corrected density array series are given in Tables 2 and 4.

In addition to recording 15-minute average values from all temperature and conductivity (and pressure) sensors during the entire experiment, GERDA recorded 15-second average values of all sensors on the condition that an "interesting" event was occurring. More specifically, incoming 15-second data from each sensor was converted by means of an in-situ processing scheme into the energy in the frequency band between 2 cph and 120 cph . When this energy for any sensor exceeded a "critical level" the 15-second data from the previous hour for all sensors was recorded. In order to insure the recording of some "interesting" observations during this initial test, the "critical level" was defined as the mean plus two standard deviations of the energy in the previously observed data. With these criteria, 500 records were written for about 100 separate events. Figure 16 shows one such event of about 4 hours duration. One degree C spikes of 15 minute duration are observed. Coherent signals are seen between several different levels. These kinds of results can be used to produce a time varying $T\text{-}\sigma_t$ relationship at a particular site. An example of four hours of 15-second $T\text{-}\sigma_t$ results is shown in Figure 17.

TABLE 4: Conductivity, Salinity, Sigma-t

CONDUCTIVITY (siemans/meter)

Station	Water Depth (m)	Start Time (Mon/Day/Hr)	Stop Time (Mon/Day/Hr)	Duration (Days)	Instrument I.D.	Sensor Depth (m)	Mean	Standard Deviation	Maximum	Minimum
C4	133	04/22/0000	07/05/1500	75	GERDA	27	3.63	0.0397	3.76	3.54
		04/22/0000	07/04/1900	74	GERDA	43	3.59	0.0236	3.67	3.51
		04/22/0000	07/19/1800	88	GERDA	63	3.57	0.0261	3.69	3.49
		04/22/0000	07/19/1800	88	GERDA	83	3.56	0.0227	3.64	3.48
		04/22/0000	07/19/1800	88	GERDA	103	3.55	0.0210	3.61	3.48
		04/22/0000	07/19/1800	88	GERDA	123	3.53	0.0199	3.58	3.48

SALINITY (parts per thousand)

Station	Water Depth (m)	Start Time (Mon/Day/Hr)	Stop Time (Mon/Day/Hr)	Duration (Days)	Instrument I.D.	Sensor Depth (m)	Mean	Standard Deviation	Maximum	Minimum
C4	133	04/22/0000	07/05/1500	75	GERDA	27	33.871	0.0860	34.124	33.284
		04/22/0000	07/04/1900	74	GERDA	43	33.861	0.1093	34.187	33.491
		04/22/0000	07/19/1800	88	GERDA	63	33.943	0.0720	34.115	33.703
		04/22/0000	07/19/1800	88	GERDA	83	33.981	0.0640	34.172	33.729
		04/22/0000	07/19/1800	88	GERDA	103	34.031	0.0615	34.417	33.600
		04/22/0000	07/19/1800	88	GERDA	123	34.054	0.0476	34.167	33.924

SIGMA-T

Station	Water Depth (m)	Start Time (Mon/Day/Hr)	Stop Time (Mon/Day/Hr)	Duration (Days)	Instrument I.D.	Sensor Depth (m)	Mean	Standard Deviation	Maximum	Minimum
C4	133	04/22/0000	07/05/1500	75	GERDA	27	26.209	0.1110	26.505	25.611
		04/22/0000	07/04/1900	74	GERDA	43	26.276	0.1284	26.611	25.830
		04/22/0000	07/19/1800	88	GERDA	63	26.382	0.0903	26.584	26.146
		04/22/0000	07/19/1800	88	GERDA	83	26.447	0.0835	26.663	26.183
		04/22/0000	07/19/1800	88	GERDA	103	26.516	0.0685	26.833	26.094
		04/22/0000	07/19/1800	88	GERDA	123	26.559	0.0629	26.729	26.403

C1: TEMPERATURE

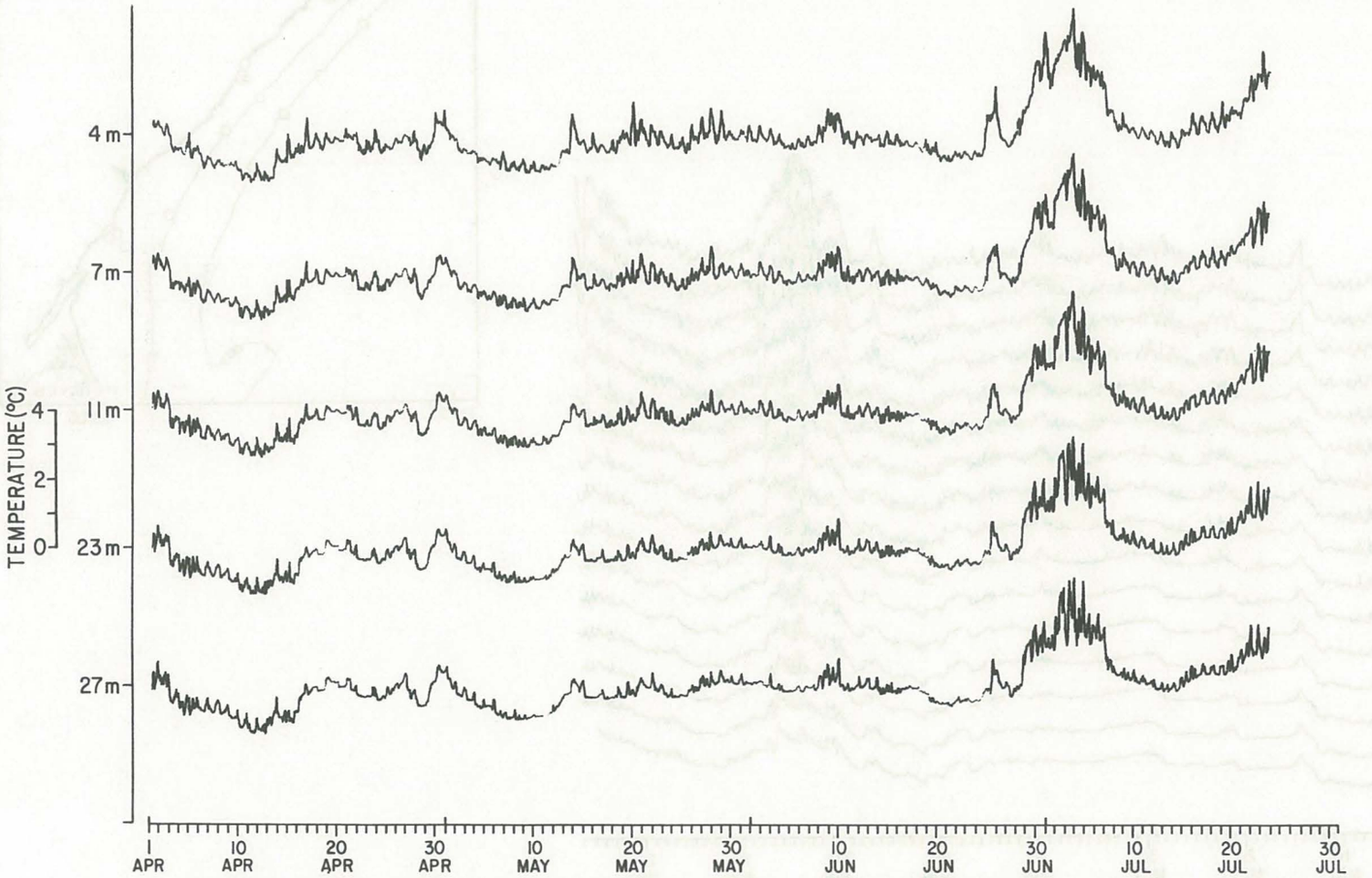

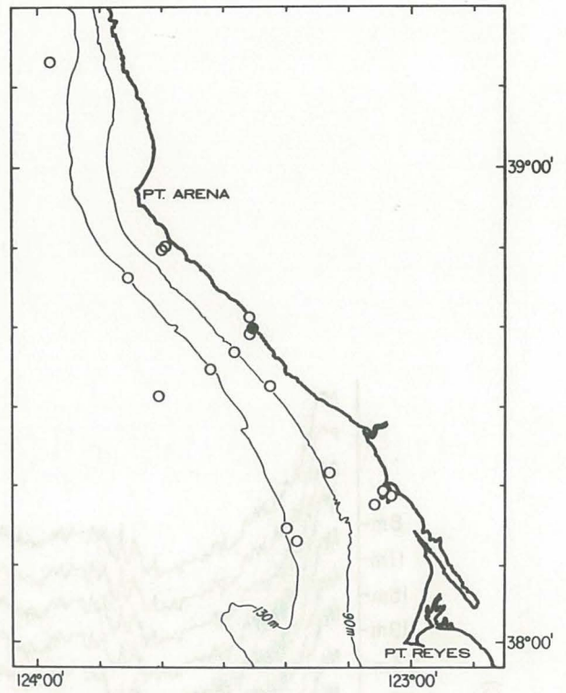

Figure 3. Each series is plotted relative to its mean value (as given in Table 2) which is denoted by the tick mark on the vertical axis.

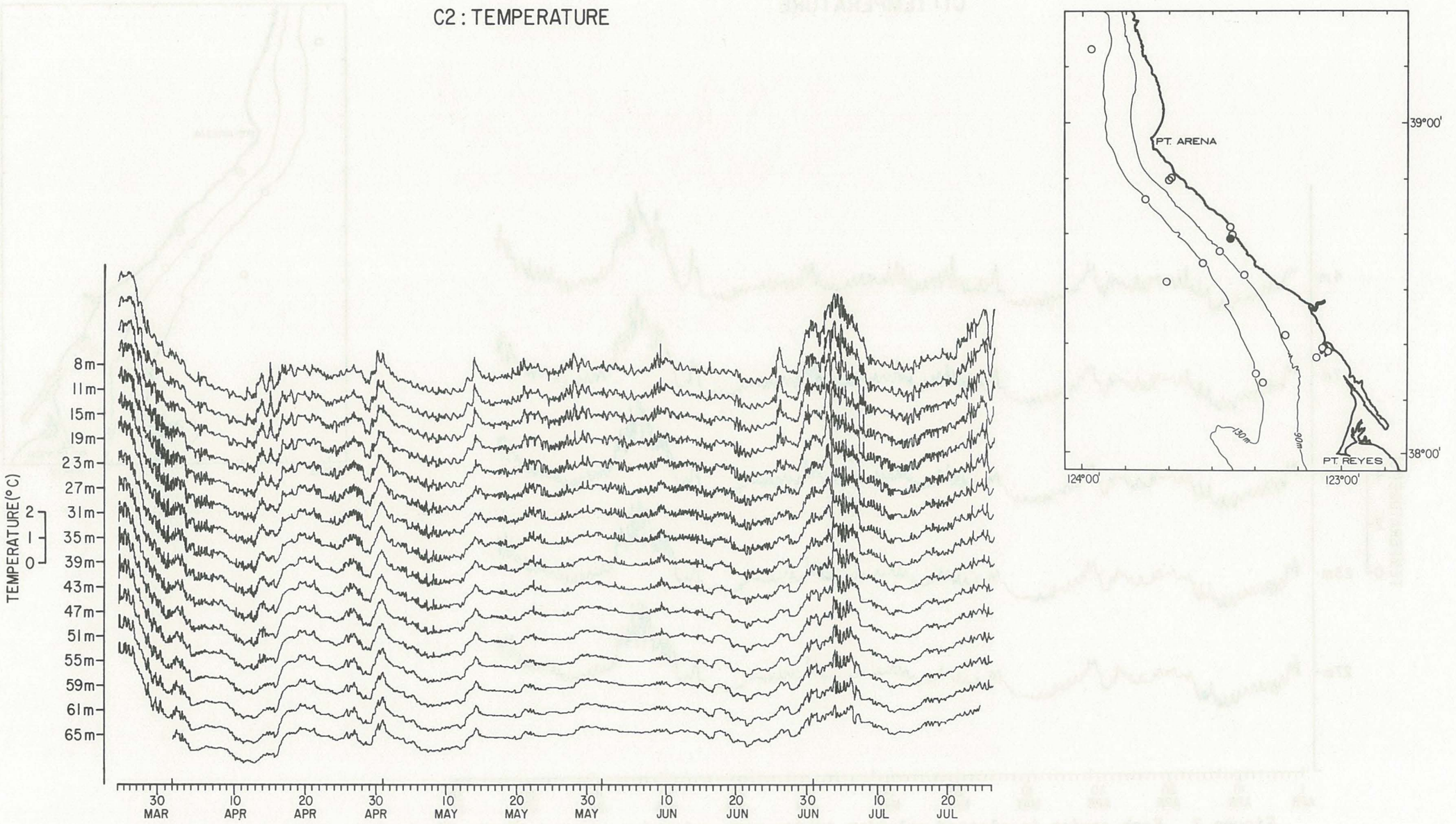

Figure 4. Each series is plotted relative to its mean value (as given in Table 2) which is denoted by the tick mark on the vertical axis.

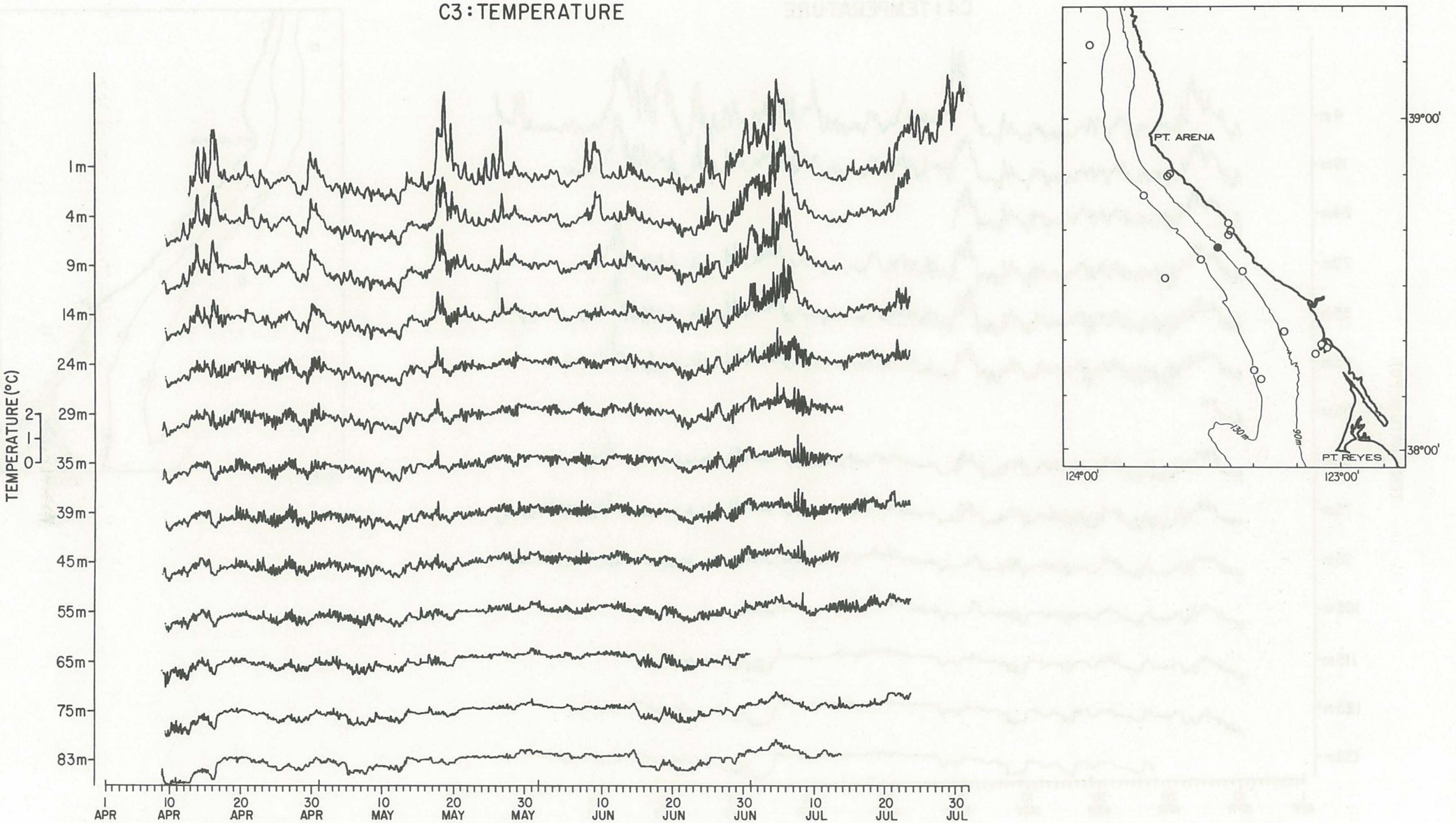

Figure 5. Each series is plotted relative to its mean value (as given in Table 2) which is denoted by the tick mark on the vertical axis.

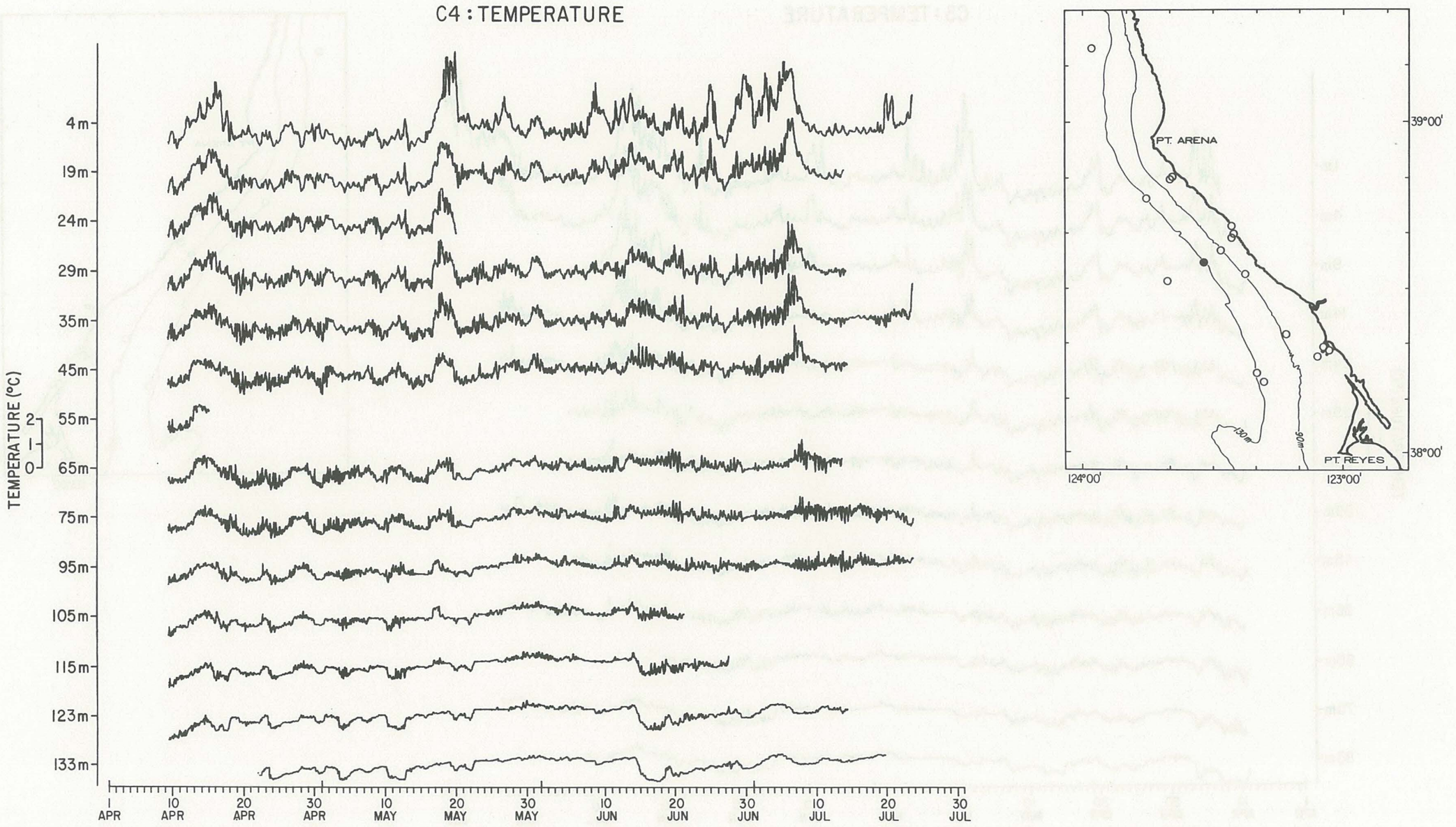

Figure 6. Each series is plotted relative to its mean value (as given in Table 2) which is denoted by the tick mark on the vertical axis.

C4 : TEMPERATURE / CONDUCTIVITY CHAIN

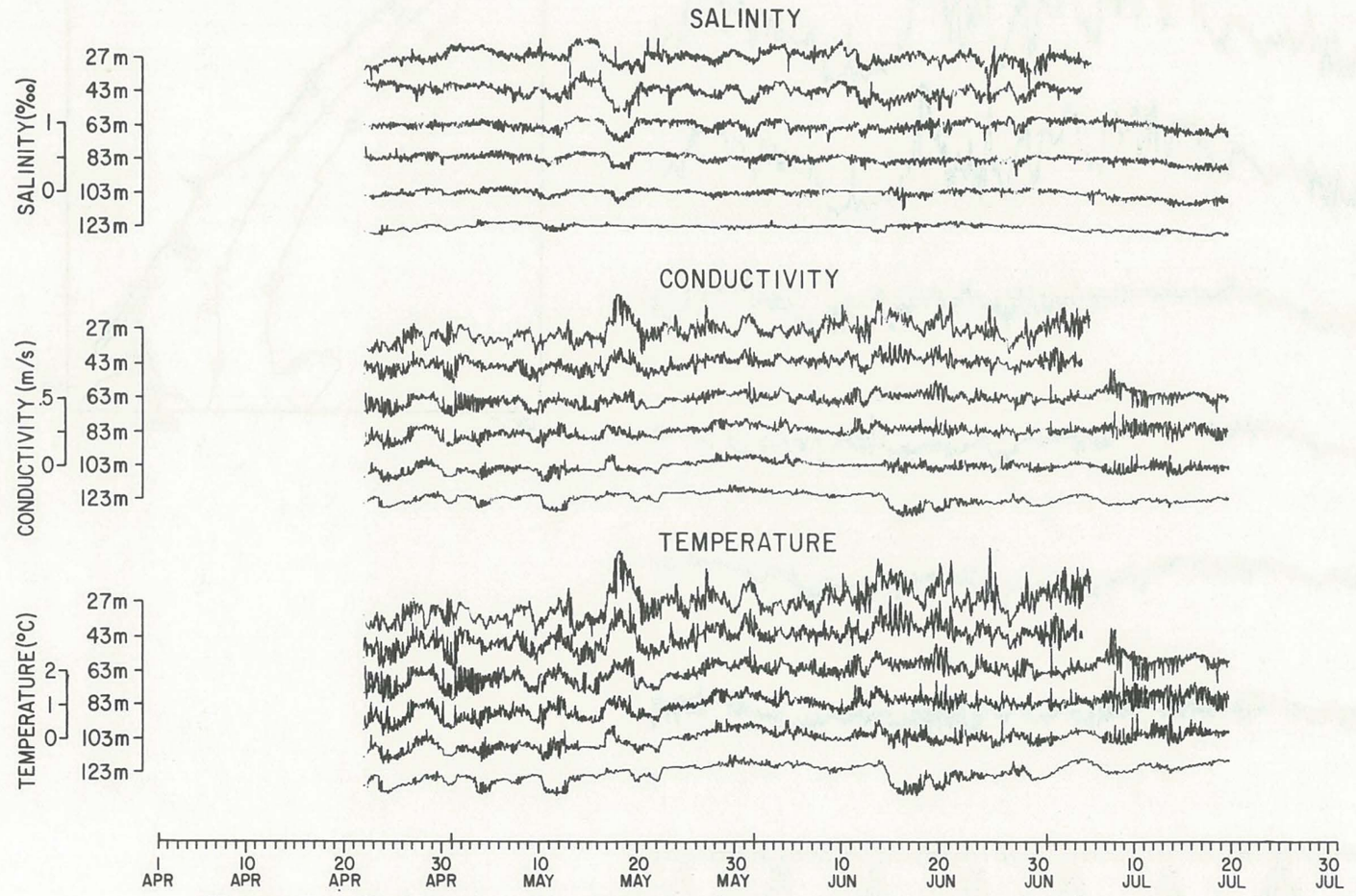

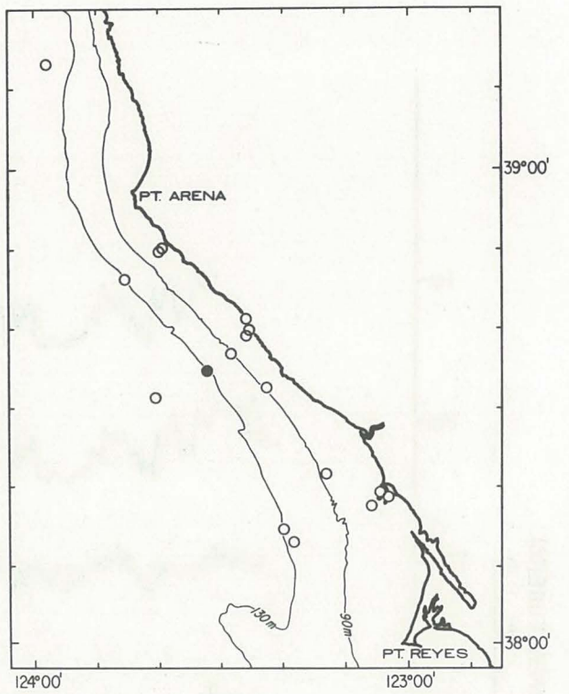

Figure 7. Each series is plotted relative to its mean value (as given in Table 2 for temperature, Table 4 for salinity and conductivity) which is denoted by the tick mark on the vertical axis.

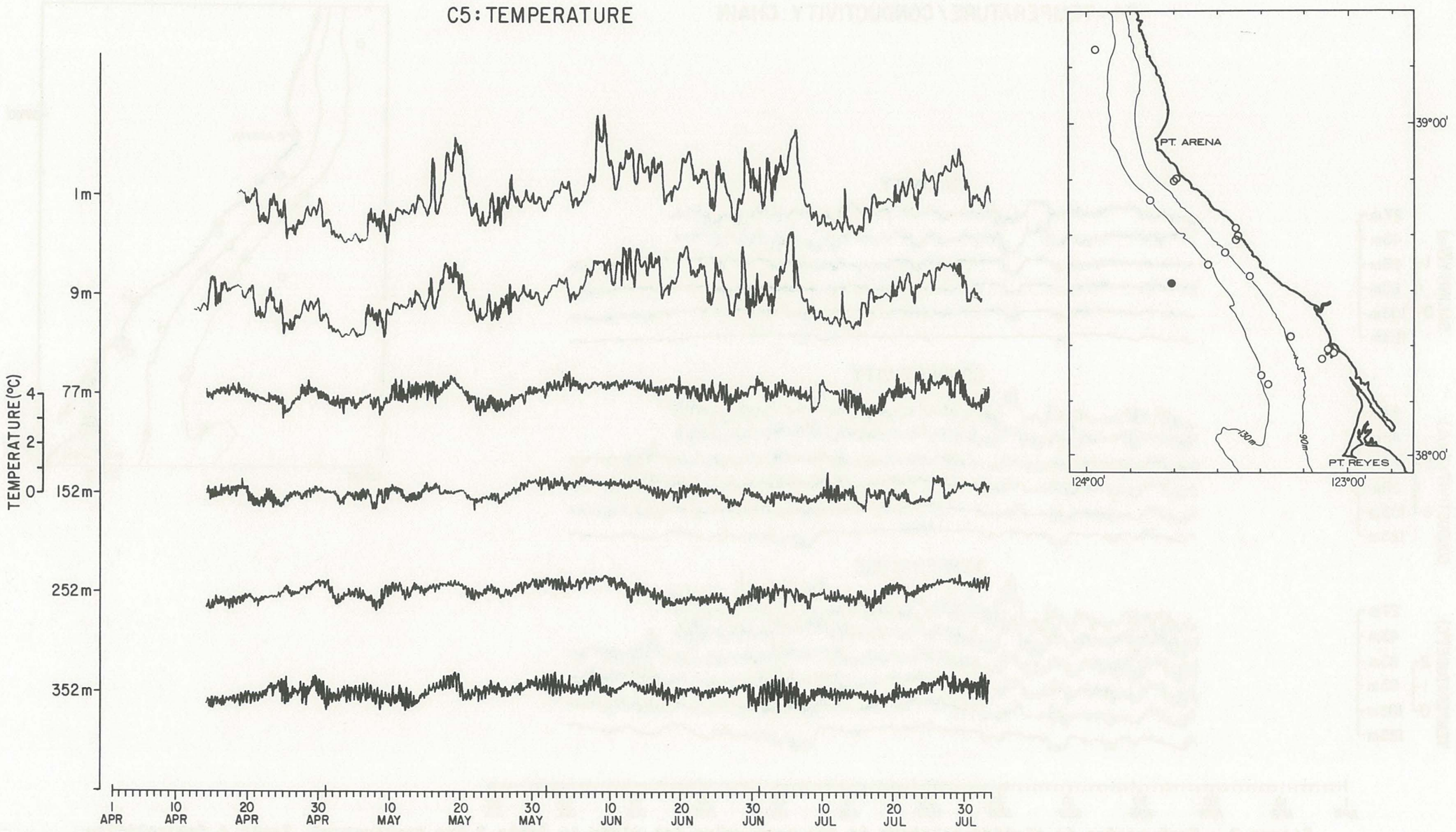

Figure 8. Each series is plotted relative to its mean value (as given in Table 2) which is denoted by the tick mark on the vertical axis.

M3: TEMPERATURE

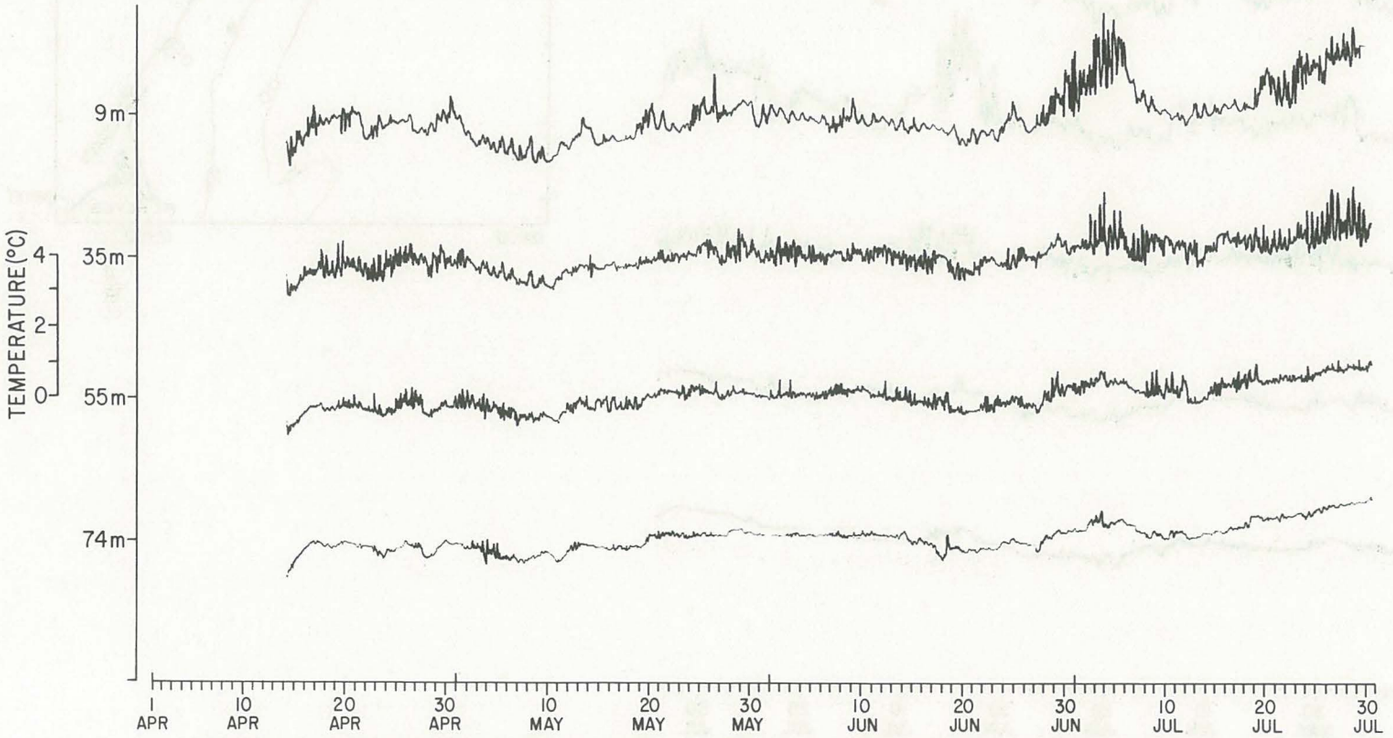

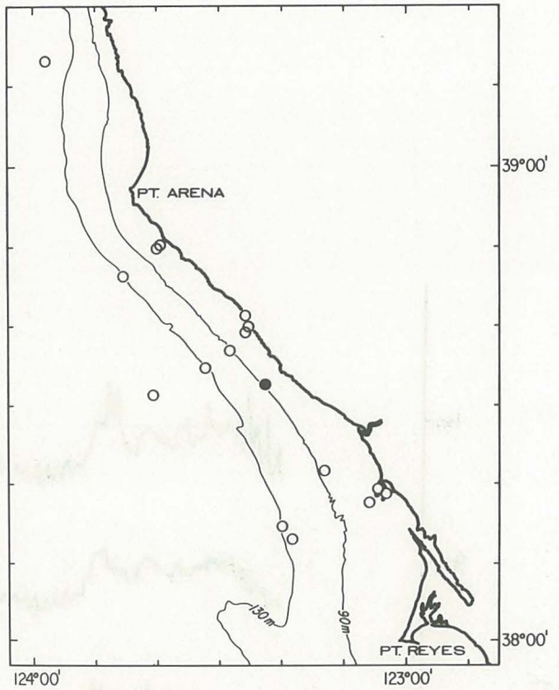

Figure 9. Each series is plotted relative to its mean value (as given in Table 2) which is denoted by the tick mark on the vertical axis.

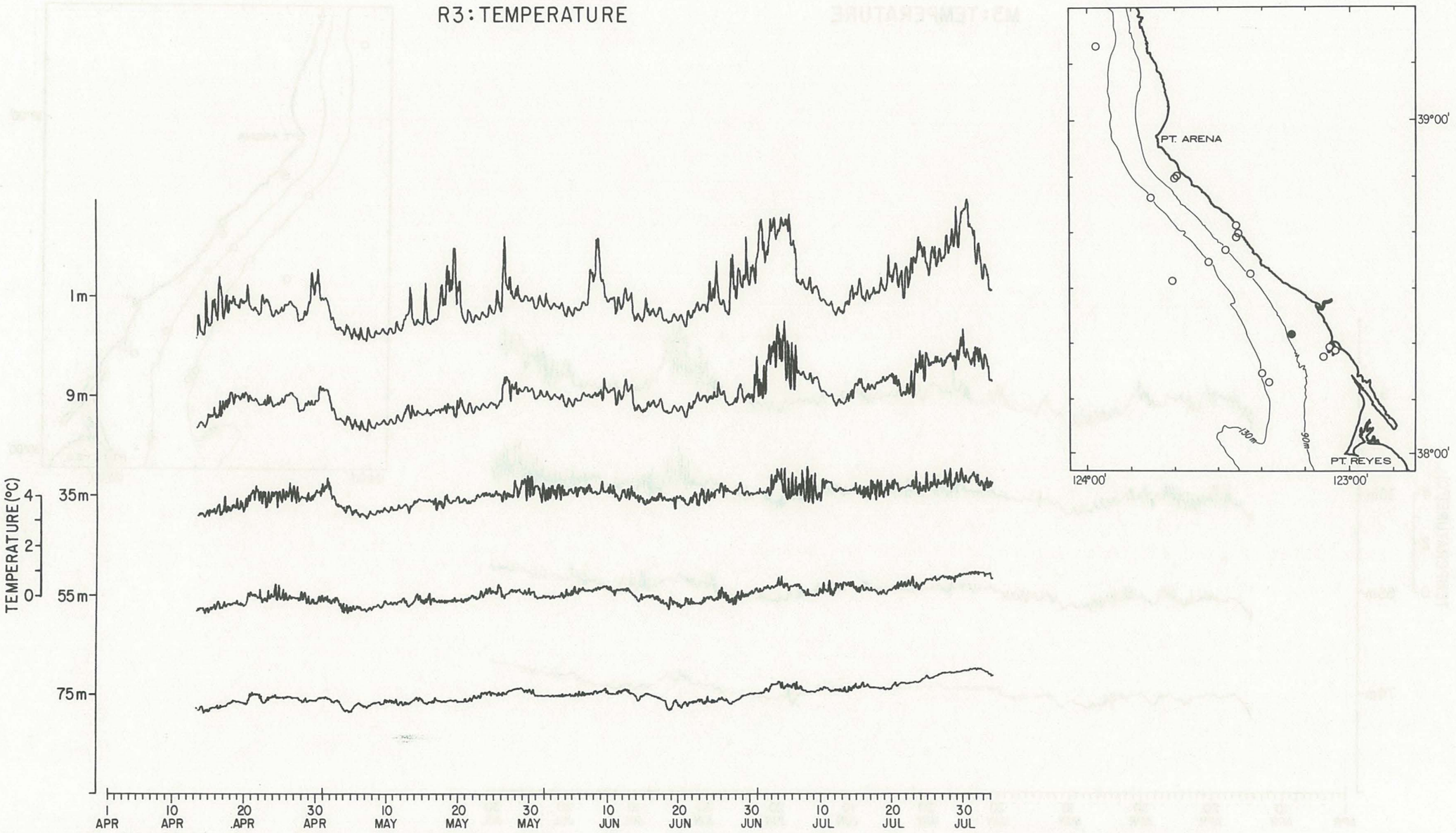

Figure 10. Each series is plotted relative to its mean value (as given in Table 2) which is denoted by the tick mark on the vertical axis.

S2: TEMPERATURE

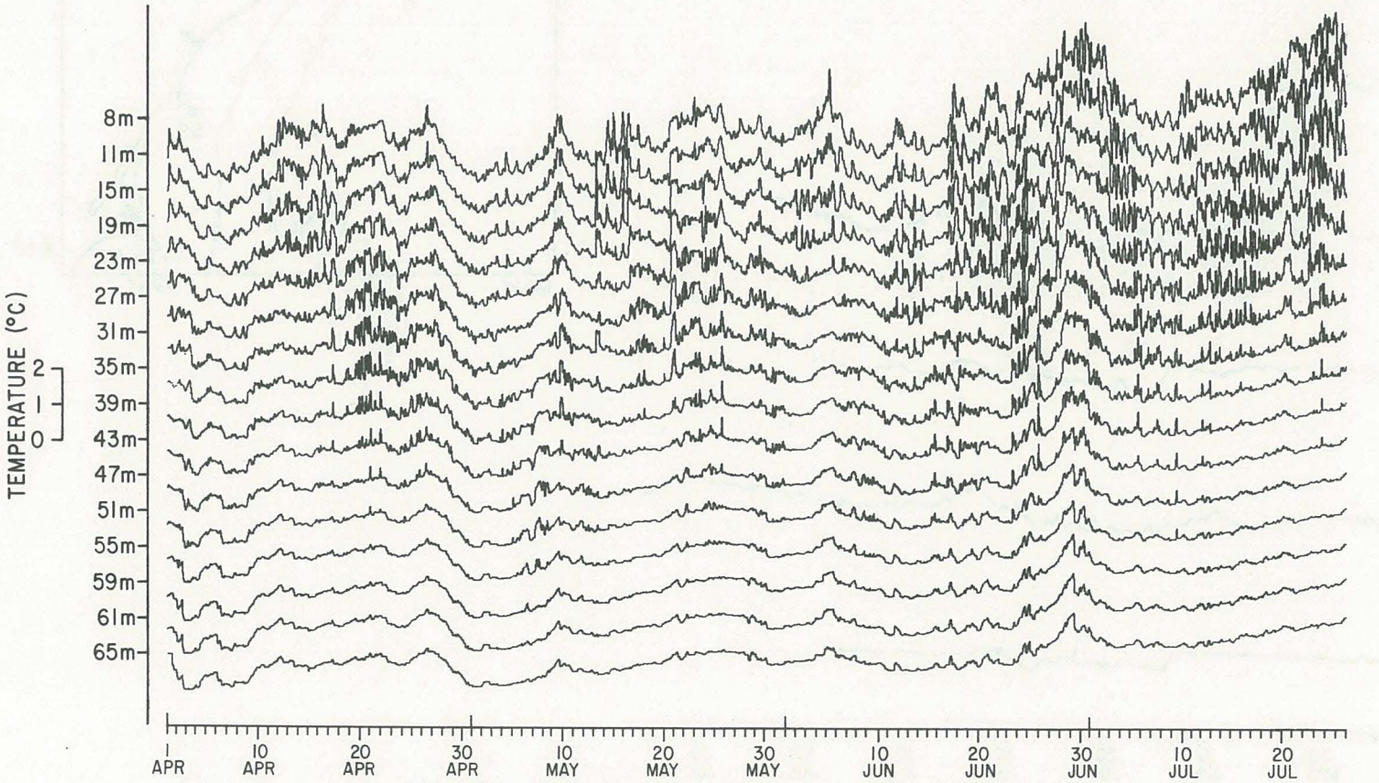

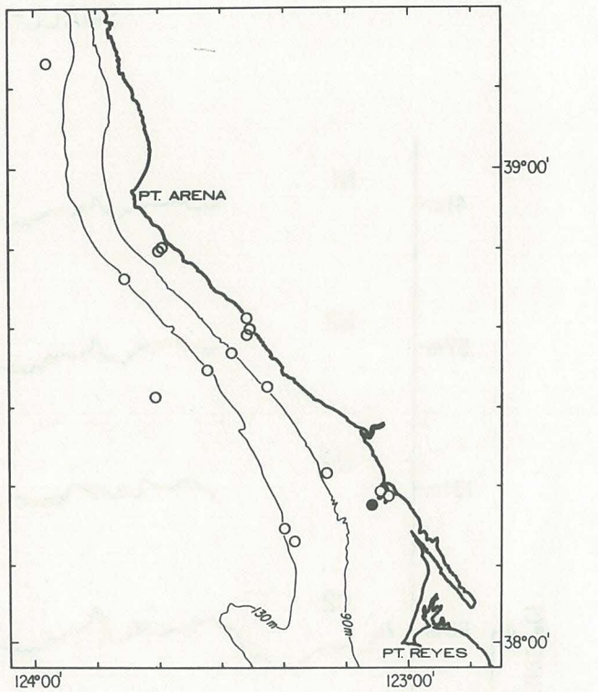

Figure 11. Each series is plotted relative to its mean value (as given in Table 2) which is denoted by the tick mark on the vertical axis.

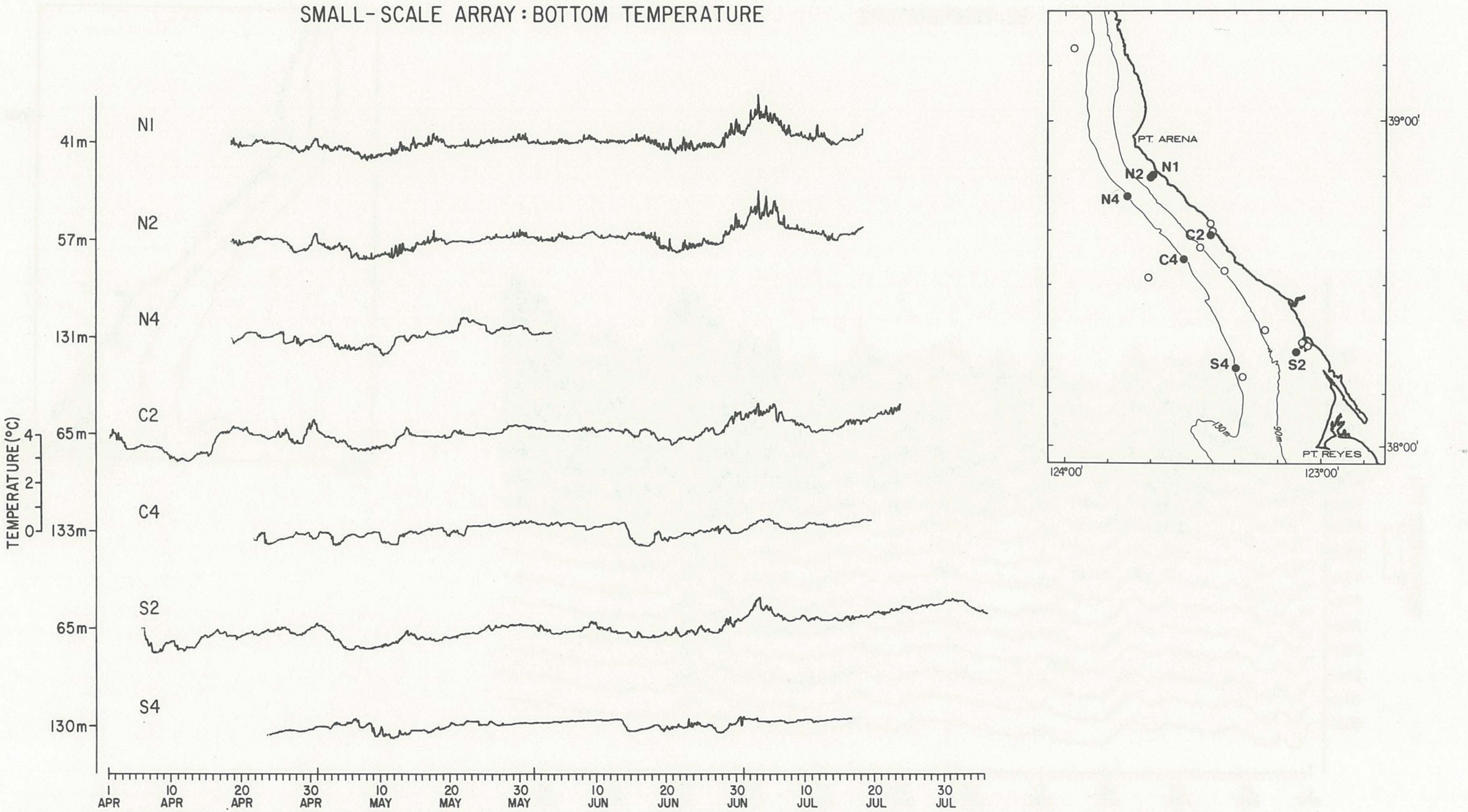

Figure 12. Each series is plotted relative to its mean value (as given in Table 2) which is denoted by the tick mark on the vertical axis.

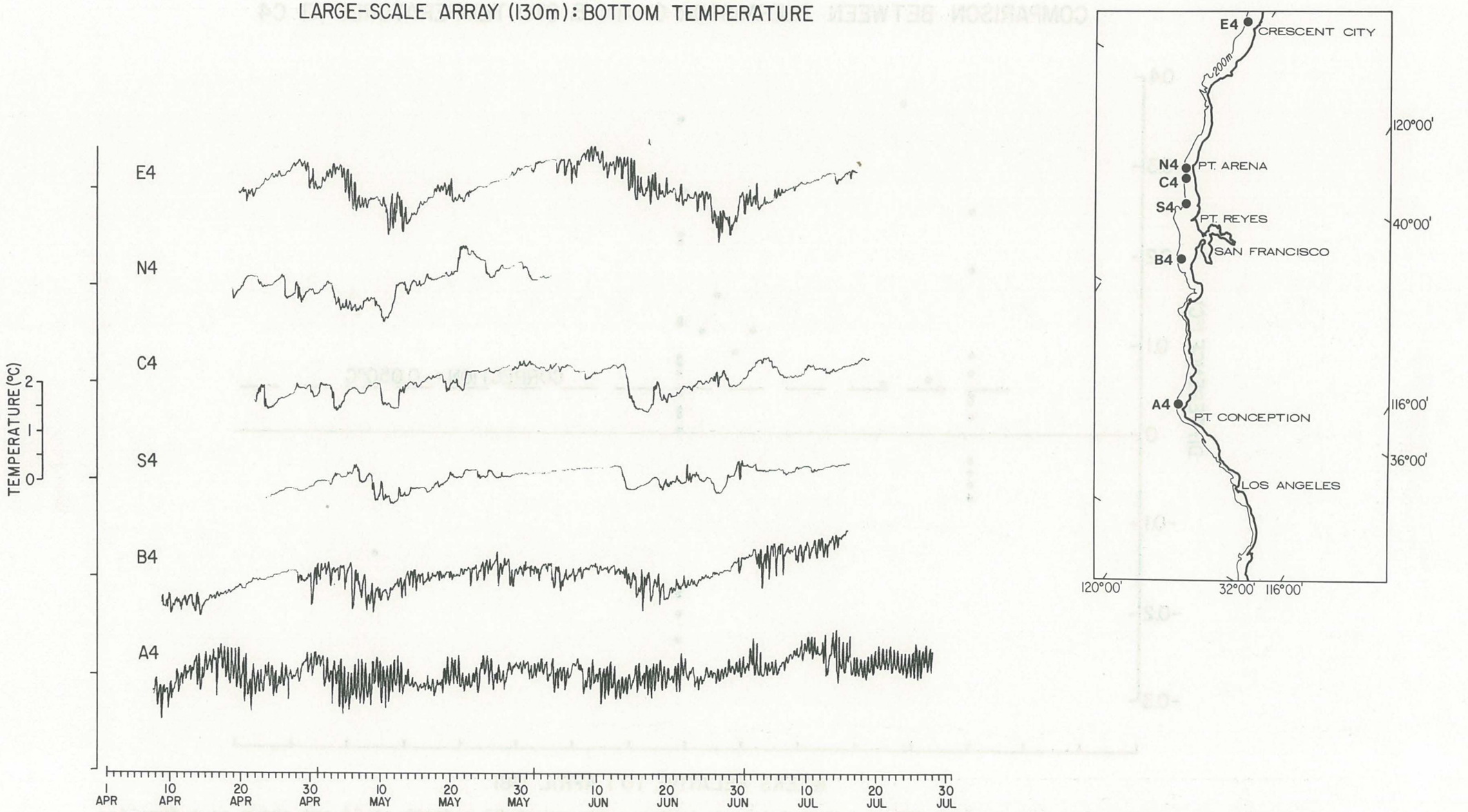

Figure 13. Each series is plotted relative to its mean value (as given in Table 2) which is denoted by the tick mark on the vertical axis.

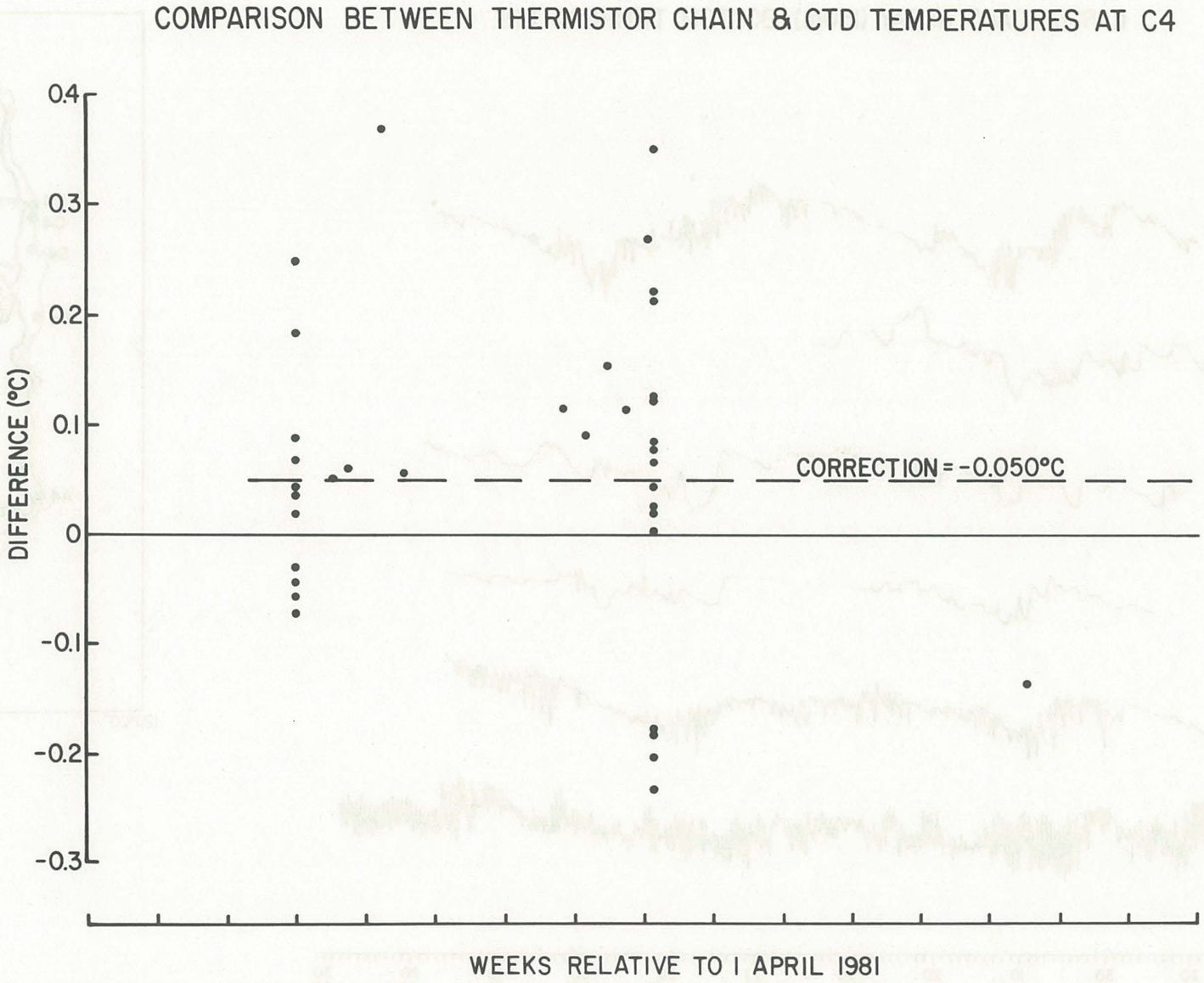

Figure 14. Differences between the CTD and thermistor chain temperatures at 83 m depth at C4 are shown as a function of time. Although some dots may appear to be aligned in the vertical, the observations were actually separated in time.

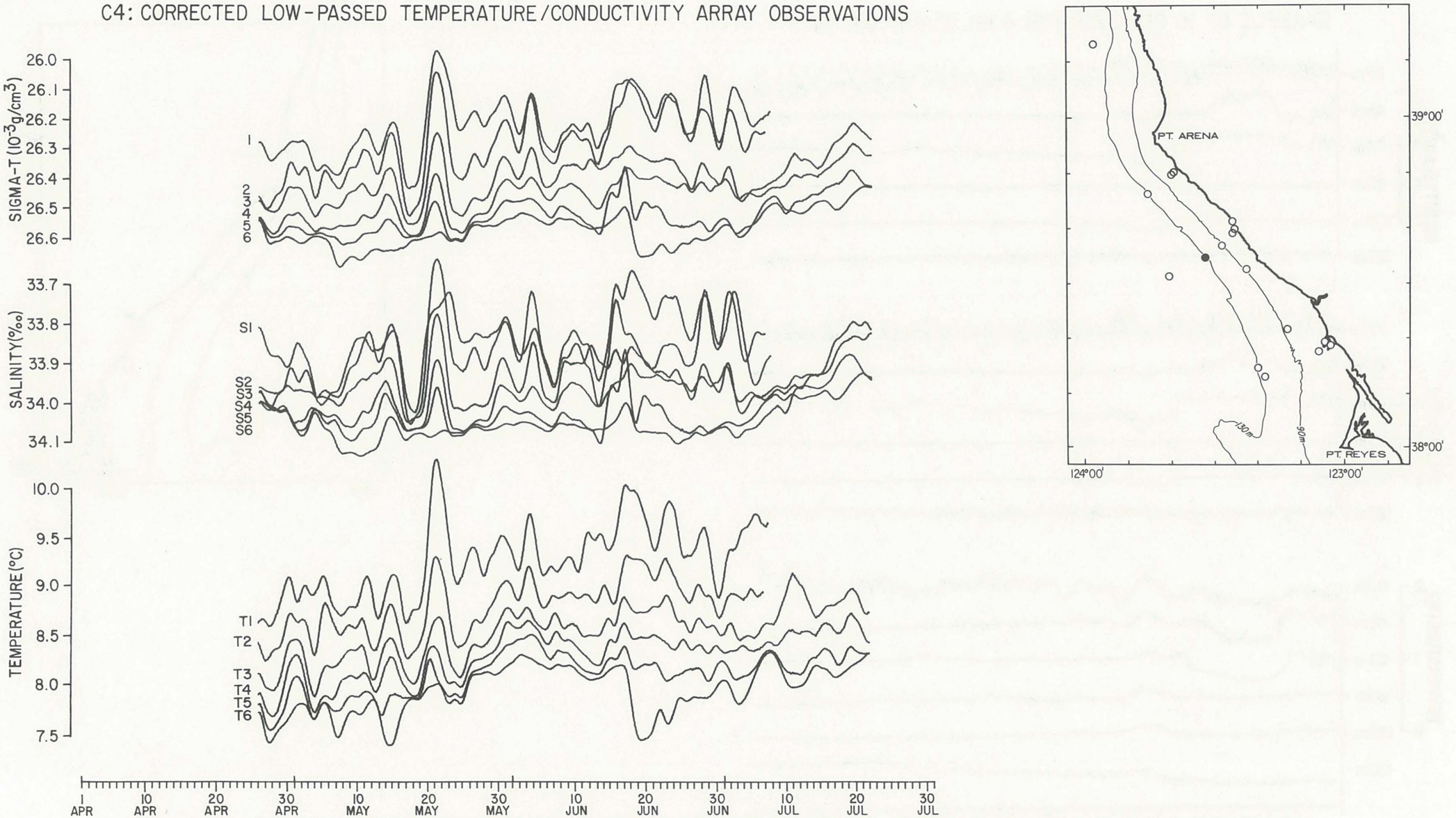

Figure 15. Low-pass filtered corrected temperature, salinity and density results from moored C4 temperature/conductivity array are shown plotted on an absolute scale. The salinities and densities have been computed from the corrected temperatures and conductivities (see text) according to the relationships in Appendix B.

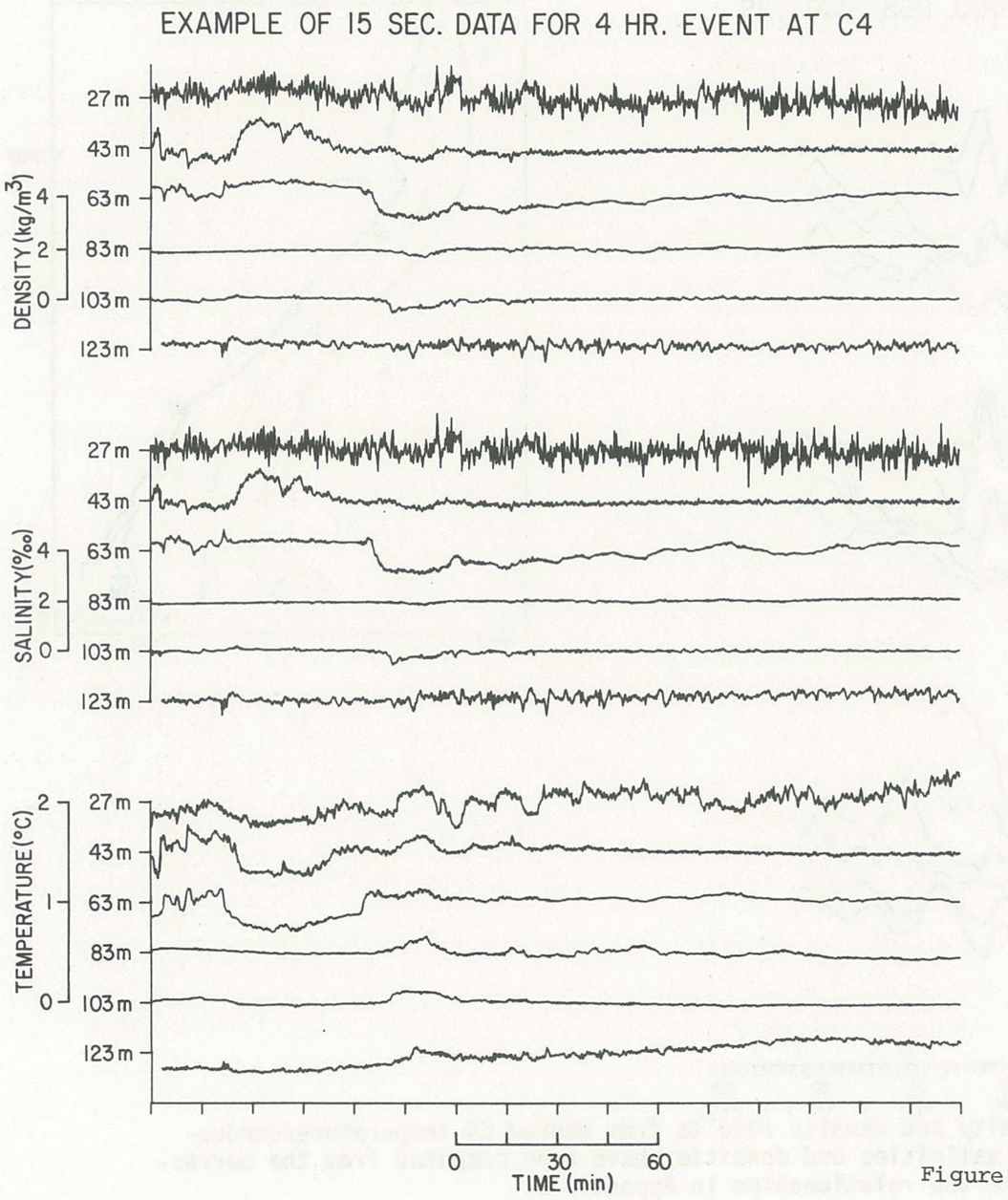
EXAMPLE OF 15 SEC. DATA FOR 4 HR. EVENT AT C4
DENSITY (kg/m3)
SALINITY (‰)
TEMPERATURE (°C)
27 m
43 m
63 m
83 m
103 m
123 m
0
30
60
TIME (min)

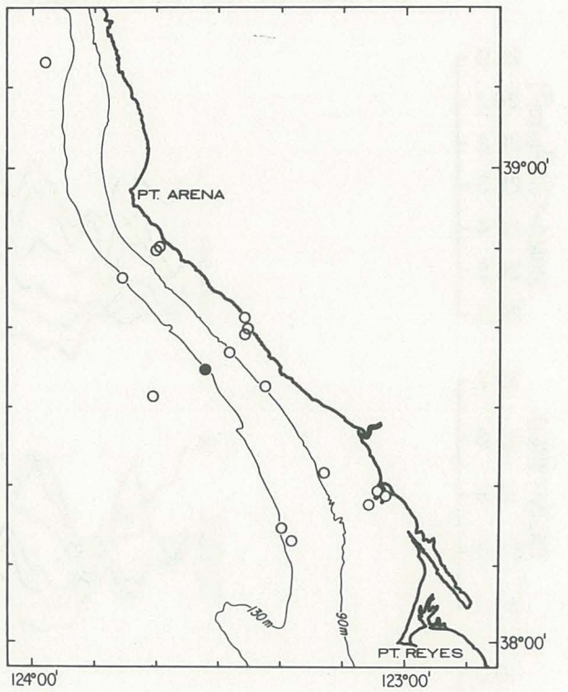
PT. ARENA
PT. REYES
39°00'
38°00'
124°00'
123°00'
130m
90m

Figure 16

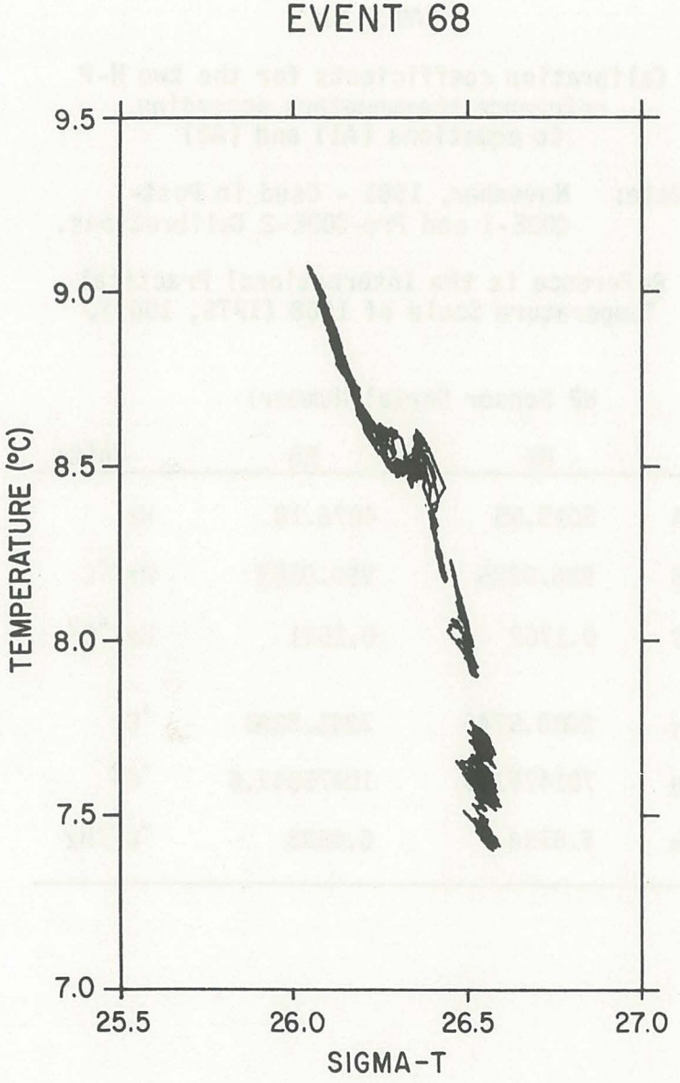

Figure 17. An example of four hours of 15-second T-σ_t results is shown.

APPENDIX A: Laboratory Calibrations

(1) Calibration Tank: All temperature, conductivity and pressure calibrations are done in the UNH temperature-controlled water bath. Figure 18 shows a schematic view of the electrical hook-up (top) and mechanical layout (bottom) of the calibration facility. A 6000 BTU/hour compressor runs continually, cooling the water in a 40-gallon tank which is thoroughly mixed with a stirring motor. A YSI Model 72 proportional temperature controller monitors the temperature of the bath with its own thermistor, and puts the required energy into a heating coil to maintain a constant temperature in the bath. A pump circulates this water through another 40-gallon tank in which the sensors to be calibrated are placed.

Each sensor has a frequency-modulated output which is connected to a distribution box. The frequency of any sensor can be monitored by a Hewlett-Packard Model 5304 counter, and all sensor signals are fed into a UNH microprocessor-controlled counter (a modified version of our seagoing units), which can accept the inputs from up to 18 sensors. The counter takes a 100 second average of the frequency from each sensor

UNH CALIBRATION TANK

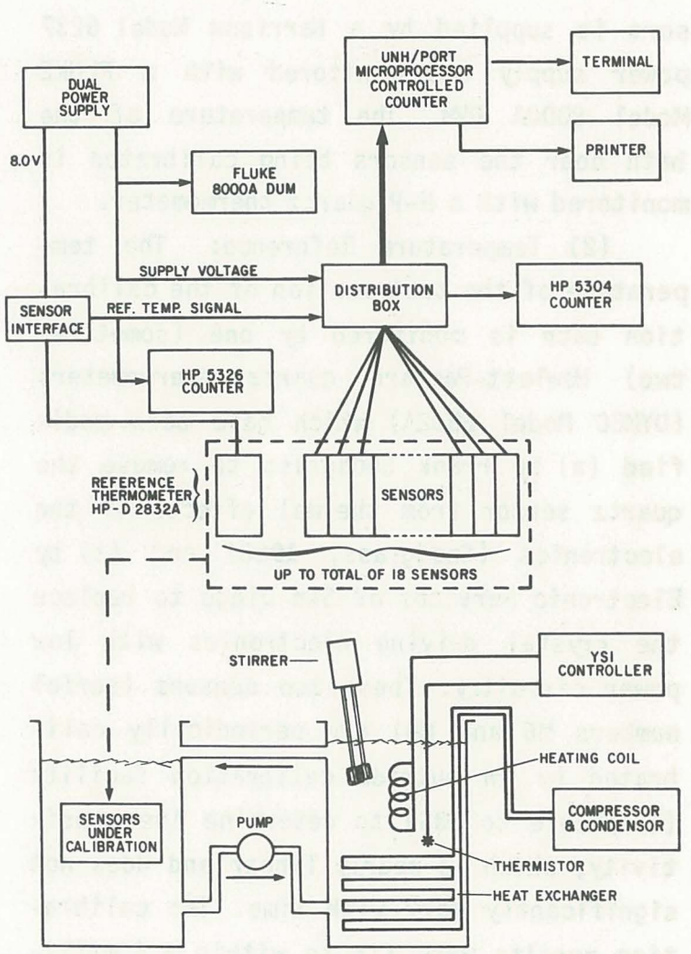

Figure 18

and prints it out. The voltage to the sensors is supplied by a Harrison Model 6237 power supply and monitored with a FLUKE Model 8000A DVM. The temperature of the bath near the sensors being calibrated is monitored with a H-P quartz thermometer.

(2) Temperature Reference: The temperature of the test section of the calibration bath is monitored by one (sometimes two) Hewlett-Packard quartz thermometers (DYMEC Model 2832A) which have been modified (a) by Frank Snodgrass to remove the quartz sensor from thermal effects of the electronics (Snodgrass, 1968) and (b) by Electronic Services of San Diego to replace the crystal driving electronics with low power circuitry. These two sensors (serial numbers M6 and M8) are periodically calibrated by an outside calibration facility (traceable to NBS) to determine the sensitivity, which is nearly linear and does not significantly vary with time. The calibration results were fit to within ± 1 millidegree C by the following quadratic form,

$$F(Hz) = A + BT + CT^2, \qquad (A1)$$

where F is the sensor output frequency in Hz, and T the temperature in degrees Centigrade. We have observed that the sensors exhibit reference temperature shifts if subject to shock. Therefore, the sensors are standardized once a year in a triple-point-of-water cell to adjust the coefficient A. Temperature is then estimated from frequency, F, by

$$T(^\circ C) = -\gamma + \sqrt{\beta + \alpha F}\,. \qquad (A2)$$

The coefficients in equations (A1) and (A2) for our two reference sensors are listed in Table AI. In the calibration facility, the recorded resolution of the reference temperature is 10^{-5}°C.

(3) Conductivity Reference: The salinity of the temperature-controlled bath is measured by running samples in a Guildline Model 8400 salinometer referenced to IAPSO standard sea water P-85. The rated repeatability of this instrument is ± 0.001°/∘∘. (We have not run intercomparisons with other institutions). Salinity is estimated from

$$S = \sum_{n=0}^{5} A_n R^{n/2} + \frac{T-15}{1.0 + 0.0162\,(T-15)} \sum_{n=0}^{5} B_n R^{n/2}\,, \qquad (A3)$$

TABLE AI:

Calibration coefficients for the two H-P reference thermometers according to equations (A1) and (A2)

Date: November, 1981 - Used in Post-CODE-1 and Pre-CODE-2 Calibrations.

Reference is the International Practical Temperature Scale of 1968 (IPTS, 1969).

	HP Sensor Serial Number: M6	M8	Units
A	5015.85	4876.18	Hz
B	986.9225	999.0383	Hz/°C
C	0.1762	0.1541	Hz/°C^2
γ	2800.5746	3241.5260	°C
β	7814751.5	10475847.6	°C^2
α	5.6754	6.4893	°C^2/Hz

where S is the salinity in °/₀₀, R the conductivity ratio at temperature T, and T the temperature in degrees Centigrade. The coefficients A and B are tabulated in Table AII.

The saltwater used in the calibration bath is seawater obtained from the mouth of the Piscataqua River at Portsmouth, N.H. and is assumed to have the ionic contents of standard seawater. The conductivity, C (siemens/meter), is calculated according to

$$C = C_o \times C_p \qquad \text{(A4)}$$

where the conductivity at atmospheric pressure, C_o, is written in terms of a temperature-dependent term, C_t, and a salinity-dependent term, C_s, according to the following formulae of Acerboni and Mosetti (1967),

$$C_o = 0.1\, C_t\, C_s$$

$$\text{where } C_t = A_1 + A_2 \frac{T^{1+a}}{1.0 + T^a} e^{bT} \qquad \text{(A5)}$$

and

$$C_s = \frac{S}{1.0+S^{\alpha}} e^{[\beta S - \gamma(S-35)(T-20)]}.$$

TABLE AII:

Coefficients for the determination of salinity according to Equation (A3).

Referenced to the Practical Salinity Scale of 1978 (Lewis, 1980).

$A_o = 0.0080$	$B_o = 0.0005$
$A_1 = -0.1692$	$B_1 = -0.0056$
$A_2 = 25.3851$	$B_2 = -0.0066$
$A_3 = 14.0941$	$B_3 = -0.0375$
$A_4 = -7.0261$	$B_4 = 0.0636$
$A_5 = 2.7081$	$B_5 = -0.0144$

The pressure correction term, C_p, is calculated according to Bradshaw and Schleicher (1965),

$$C_p = 1.0 + (0.1\, P_1 P_2),$$

$$P_1 = (\Sigma B_i T^i)(\Sigma D_j P^j) + (\Sigma E_k T^k)(\Sigma F_n P^n) \qquad \text{(A6)}$$

where $P_2 = 1.0 + (\Sigma d_i T^i)(35-S)$

and P is the pressure in decibars. The coefficients for equations (A5) and (A6) are tabulated in Table AIII.

(4) Pressure Reference: An Ascroft dead weight tester (borrowed from the UNH mechanical engineering department) is used as the pressure standard. To minimize relative errors, all pressure sensors are connected to a common manifold and mounted at the same depth in the calibration tank. By using a common manifold, any systematic error in absolute pressure will be removed when we estimate pressure gradients. The dead weight applied pressure is converted to absolute pressure by the addition of local atmospheric pressure at the time of the calibration.

TABLE AIII:

Coefficients for the Determination of Conductivity

(1) C_o coefficients; Equation (A5)

$A_1 = 2.1923$	$a = 0.032$
$A_2 = 0.12842$	$b = 2.9 \times 10^{-3}$
$\alpha = 0.1243$	$\gamma = 1.65 \times 10^{-5}$
$\beta = -9.78 \times 10^{-4}$	

(2) C_p coefficients; Equation (A6)

$B_0 = 1.5192$	$D_1 = 1.042 \times 10^{-3}$
$B_1 = -4.5302 \times 10^{-2}$	$D_2 = -3.3913 \times 10^{-8}$
$B_2 = 8.3089 \times 10^{-4}$	$D_3 = 3.3 \times 10^{-13}$
$B_3 = -7.9 \times 10^{-6}$	
$E_0 = 1.0$	$F_0 = 4.0 \times 10^{-4}$
$E_1 = -0.1535$	$F_1 = 2.577 \times 10^{-5}$
$E_2 = 8.276 \times 10^{-3}$	$F_2 = -2.492 \times 10^{-9}$
$E_3 = -1.657 \times 10^{-4}$	
$d_0 = 6.95 \times 10^{-3}$	$d_1 = -7.6 \times 10^{-5}$

APPENDIX B: Computations

For analysis of the moored time series, temperature and conductivity records at a fixed depth (constant pressure) are converted to salinity series by formulae derived by Rohde (1972). It should be noted that the temperature calibrations are referenced to the International Practical Temperature Scale of 1968, T_{68}, and the equations in this section are referenced to the 1948 standard, T_{48}. Mackenzie (1971) gives the difference, T_c, as

$$T_c = T_{68} - T_{48} = -4.88 \times 10^{-4} T_{48} + 5.80 \times 10^{-6} T_{48}^2 \qquad \text{(B1)}$$

over the temperature range -2°C to 35°C. T_{68} can be substituted in the right-hand side of B_1 without significant error. After making the above correction to temperature, the salinity is calculated by

$$S = \Sigma\Sigma\Sigma\, A_{ijk}\, T^k\, C_o^j\, P^i \qquad \text{(B2)}$$

where $T = T_{obs} - T_c$ is the corrected temperature in degrees C, P the pressure in decibars, $C_o = 10\,C - 30$, and C is conductivity in siemens/meter. The coefficients A are tabulated in Table BI.

The density time series are calculated using two empirical formulae. The first is from M. Knudsen and calculates the surface anomaly of density (sigma-t). The second, from V. W. Ekman, calculates the specific volume. Both of these relations were reformulated by Fofonoff and Tabata (1958) to compute density as follows:

$$D = (SIGT + 1000)/SPVOL \qquad \text{(B3a)}$$

where D is in kg/m^3, and

$$SIGT = \Sigma a_i T^i/(T + A_o) + \Sigma\Sigma A_{ij} (SZ)^i T^j$$

for which $$SZ = \Sigma B_j S^j \qquad \text{(B3b)}$$

and $$SPVOL = 1.0 - b_o P/(1.0 + b_1 P) + \Sigma\Sigma\Sigma\, G_{ijk}\, P^i\, SZ^j\, T^k \quad .$$

Here T is the temperature in °C, S the salinity in °/₀₀ and P the pressure in

decibars. The coefficients are tabulated in Table BII.

The velocity of sound in seawater, V, is calculated from the following equations of Wilson (1960)

$$V = 1449.22 + \Delta V_T + \Delta V_S + \Delta V_P + \Delta V_{STP} \quad \text{(B4a)}$$

where V is in meters/second. The deviations from standard velocity are

$$\Delta V_T = \Sigma A_i T^i$$

$$\Delta V_S = \Sigma B_i (S-35)^i \quad \text{(B4b)}$$

$$\Delta V_P = \Sigma D_i P^i$$

and $\Delta V_{STP} = \Sigma\Sigma\Sigma a_{ijk} (S - 35)^i T^j P^k$.

Here P is the absolute pressure in kg-force/cm^2, which is computed from our observed pressure, P_o, from

$$P \text{ (kg-force/cm}^2) = 0.1019716\ P_o \text{ (dbars)} .$$

The coefficients are listed in Table BIII.

The resultant uncertainty in any of the above calculations is estimated from the uncertainty of each of the quantities used in the calculations. Table BIV lists the typical range of values found at C4 during CODE-1. Parts A and B of Table BIV list the sensitivities of the salinity and density determinations at typical CODE-1 values estimated from the appropriate derivatives of equations (B2) and (B3a). Therefore, for the salinity to be within ± 0.01°/oo of its true value, the uncertainty, ε, in each component value must be less than ε_T < ± 0.01°C, ε_C < ± 0.001 s/m, ε_P < ± 25 dbar. Similarly, for the uncertainty in density (or sigma-t) to be less than ± 0.02 kg/m^3 (± 0.02 sigma-t units), the uncertainty, ε, in each component value must be less than ε_T < ± 0.05°C, ε_S < ± 0.01°/oo, ε_C < ± 0.02 s/m (± 0.01 mmhos/cm), ε_P < ± 1.4 dbar. The uncertainty in our measurements in CODE-1 is controlled by the conductivity sensor and our ability to correct for the drift due to fouling.

TABLE BI: Coefficients for calculation of salinity according to eq. (B2)

$A_{000} = 36.2676$	$A_{010} = 1.33711$
$A_{001} = -1.19646$	$A_{011} = -4.47259 \times 10^{-2}$
$A_{002} = 3.38455 \times 10^{-2}$	$A_{012} = 1.33715 \times 10^{-3}$
$A_{003} = -1.11822 \times 10^{-3}$	$A_{013} = -3.58008 \times 10^{-5}$
$A_{004} = 3.28739 \times 10^{-5}$	$A_{014} = 5.0496 \times 10^{-7}$
$A_{005} = -4.4552 \times 10^{-7}$	
$A_{020} = 3.2844 \times 10^{-3}$	$A_{030} = 1.0643 \times 10^{-5}$
$A_{021} = -1.9293 \times 10^{-4}$	
$A_{022} = 6.5837 \times 10^{-6}$	
$A_{023} = -1.1986 \times 10^{-7}$	
$A_{100} = -0.63090$	$A_{110} = -1.769 \times 10^{-2}$
$A_{101} = 3.4267 \times 10^{-2}$	$A_{111} = 7.9932 \times 10^{-4}$
$A_{102} = -1.08718 \times 10^{-3}$	$A_{112} = -1.3712 \times 10^{-5}$
$A_{103} = 2.0785 \times 10^{-5}$	$A_{113} = 4.036 \times 10^{-8}$
$A_{104} = -1.4572 \times 10^{-7}$	
$A_{120} = 5.245 \times 10^{-5}$	$A_{200} = 2.6942 \times 10^{-2}$
$A_{121} = -4.930 \times 10^{-6}$	$A_{201} = -1.3535 \times 10^{-3}$
$A_{122} = 1.0899 \times 10^{-7}$	$A_{202} = 3.9724 \times 10^{-5}$
	$A_{203} = -6.161 \times 10^{-7}$
$A_{210} = 5.336 \times 10^{-4}$	$A_{300} = -4.548 \times 10^{-4}$
$A_{211} = -2.5137 \times 10^{-5}$	$A_{301} = 1.116 \times 10^{-5}$
$A_{212} = 4.065 \times 10^{-7}$	

TABLE BII:

Coefficients for calculation of density according to equations (B3a) and (B3b)

$a_1 = 4.53168$	$A_{10} = 1.0$
$a_2 = -5.45939 \times 10^{-1}$	$A_{11} = -4.7867 \times 10^{-3}$
$a_3 = -1.98248 \times 10^{-3}$	$A_{12} = 9.8185 \times 10^{-5}$
$a_4 = -1.43803 \times 10^{-7}$	$A_{13} = -1.0843 \times 10^{-6}$
$A_0 = 67.26$	$A_{20} = 0.0$
$B_0 = -9.34459 \times 10^{-2}$	$A_{21} = 1.8030 \times 10^{-5}$
$B_1 = 8.14877 \times 10^{-1}$	$A_{22} = -8.1640 \times 10^{-7}$
$B_2 = -4.82496 \times 10^{-4}$	$A_{23} = 1.6670 \times 10^{-8}$
$B_3 = 6.76786 \times 10^{-6}$	
$b_0 = 4.886 \times 10^{-6}$	$b_1 = 1.830 \times 10^{-5}$
$G_{100} = -2.207 \times 10^{-11}$	$G_{200} = -6.680 \times 10^{-22}$
$G_{101} = 3.673 \times 10^{-12}$	$G_{201} = -1.241 \times 10^{-20}$
$G_{102} = -6.630 \times 10^{-14}$	$G_{202} = 2.140 \times 10^{-22}$
$G_{103} = 4.000 \times 10^{-16}$	$G_{210} = -4.248 \times 10^{-21}$
$G_{110} = 1.725 \times 10^{-12}$	$G_{211} = 1.206 \times 10^{-22}$
$G_{111} = -3.280 \times 10^{-14}$	$G_{212} = -2.000 \times 10^{-24}$
$G_{112} = 4.000 \times 10^{-16}$	$G_{220} = 1.800 \times 10^{-23}$
$G_{120} = -4.500 \times 10^{-15}$	$G_{221} = -6.000 \times 10^{-25}$
$G_{121} = 1.000 \times 10^{-16}$	$G_{301} = 1.500 \times 10^{-29}$

TABLE BIII:

Coefficients for calculation of sound in seawater according to equations (B4a) and (B4b)

$A_1 = 4.6233$
$A_2 = -5.4585 \times 10^{-2}$
$A_3 = 2.822 \times 10^{-4}$
$A_4 = -5.07 \times 10^{-7}$

$B_1 = 1.391$
$B_2 = -7.8 \times 10^{-2}$

$D_1 = 1.60518 \times 10^{-1}$
$D_2 = 1.0279 \times 10^{-5}$
$D_3 = 3.451 \times 10^{-9}$
$D_4 = -3.503 \times 10^{-12}$

$A_{011} = -2.796 \times 10^{-4}$
$A_{012} = -2.391 \times 10^{-7}$
$A_{021} = 1.3302 \times 10^{-5}$
$A_{022} = 9.286 \times 10^{-10}$
$A_{031} = -6.644 \times 10^{-8}$
$A_{013} = -1.745 \times 10^{-10}$
$A_{101} = 2.61 \times 10^{-4}$
$A_{102} = -1.96 \times 10^{-7}$
$A_{110} = -1.197 \times 10^{-2}$
$A_{111} = -2.09 \times 10^{-6}$

TABLE BIV:

Salinity and density sensitivities to changes in temperature, conductivity and pressure for ranges of temperature: $7.5^\circ C < T < 13^\circ C$; salinity: $33.1^\circ/\circ\circ < S < 34.1^\circ/\circ\circ$; and sigma-t: $25.0 < \sigma_t < 26.5$.

A. Salinity Sensitivity:

$$\frac{\partial S}{\partial T} \sim -0.9^\circ/\circ\circ/^\circ C$$

$$\frac{\partial S}{\partial c} \sim 10^\circ/\circ\circ/s/m$$

$$\frac{\partial S}{\partial P} \sim -4 \times 10^{-4}\circ/\circ\circ/dbar$$

B. Density Sensitivity:

$$\frac{\partial \rho}{\partial T} \sim -0.2\ kg/m^3/^\circ C$$

$$\frac{\partial \rho}{\partial S} \sim 0.8^\circ\ kg/m^3/^\circ/\circ\circ$$

$$\frac{\partial \rho}{\partial c} = \frac{\partial \rho}{\partial s} \times \frac{\partial s}{\partial c} \sim 8\ kg/m^3/s/m$$

$$\frac{\partial \rho}{\partial P} \sim 0.007\ kg/m^3/dbar$$

Acknowledgments

Collection of the CODE-1 temperature and conductivity data was made possible through the efforts of a great many people. We wish to thank M. Woodbury, E. LaCoursiere, M. Condilis and A. Bugbee of UNH and M. Kirk, P. Dacri, A. Bratkovich and S. Lentz of SIO for their efforts. Members of the WHOI Buoy Group maintained and deployed some instruments and C. Mills helped with the data processing. Without the dedication and versatility of all involved, this level of effort would not have been possible. The skill and cooperation of the officers and crew of the R/V Wecoma (OSU) and the R/V Acania (Monterey Naval Postgraduate School) helped make our seagoing operations possible and productive. The personnel at the U.S. Coast Guard Base at Yerba Buena Island were a key factor in the efficiency and flexibility with which we were able to operate our seagoing operations such long distances from our home base. We make special mention of the assistance of M. Lee (UNH), who arranged much of the logistics and acted as the onshore liaison. The UNH and SIO effort was supported by the National Science Foundation.

References

Acerboni and Mosetti, 1967. Bollettino Di Geofisica Teorica El Appicata, Vol. 9 - N. 34.

Bradshaw, A. L. and K. E. Schleicher, 1965. The effect of pressure on the electrical conductivity of sea water. Deep-Sea Res., 12: 151-162.

Fofonoff, N. P. and S. Tabata. 1958. P.O.G. Manuscript Report Series No. 25.

The International Practical Temperature Scale of 1968 Adopted by the Cmité International des Poids et Mesures, 1969. Intl. J. Scientific Meteorology, 5: 34-44.

Lewis, E. L., 1980. The practical salinity scale 1978 and its antecedents. IEEE, J. Oceanic Engineering, OE-5: 3-8.

Mackenzie, K. V., 1971. A decade of experience with velocimeters. J. Acoust. Soc. Amer., 50: 1321-1333.

Rohde, V. J., 1972. Darstelluug Funktionaler Suzammenhange Swishe Physikalischen Grossen Des Meerwassers Durch Naherungspdynome. Kieler meersforchungen, 20: 130-139.

Snodgrass, F. E., 1968. Deep sea instrument capsule. Science, 162: 78-87.

Wilson, W., 1960. Speed of sound in sea water as a function of temperature, pressure and salinity. J. Acoust. Soc. Amer., 32: 641-644.

CODE-1: BOTTOM PRESSURE OBSERVATIONS

by

W. S. Brown
J. D. Irish

Department of Earth Sciences
University of New Hampshire
Durham, New Hampshire 03824

and

M. R. Erdman

Scripps Institution of Oceanography
University of California, San Diego
La Jolla, California 92093

A. INTRODUCTION

This report describes the moored bottom pressure observations obtained during the first major field phase of the Coastal Ocean Dynamics Experiment (CODE-1), which took place along the northern California coast (shown in Figures 1 and 2) during the months of April through July, 1981. Descriptions of the moored current, temperature, conductivity and meteorological (primarily wind) observations appear in other chapters of this report. In Section B, we describe the array and the instrumentation used in the experiment. In Section C, the bottom pressure results are presented.

B. BOTTOM PRESSURE ARRAY

The CODE-1 bottom pressure array consisted of eight (8) elements deployed by W. Brown and J. Irish from the University of New Hampshire (UNH) and four (4) elements deployed by C. Winant from the Scripps Institution of Oceanography (SIO) at the stations indicated in Table 1 and shown in Figures 1 and 2. Although the deployment configurations differed between the UNH and SIO instruments (see Figure 3), the pressure sensor in each case was manufactured by Paroscientific, Inc. and pressure/temp-

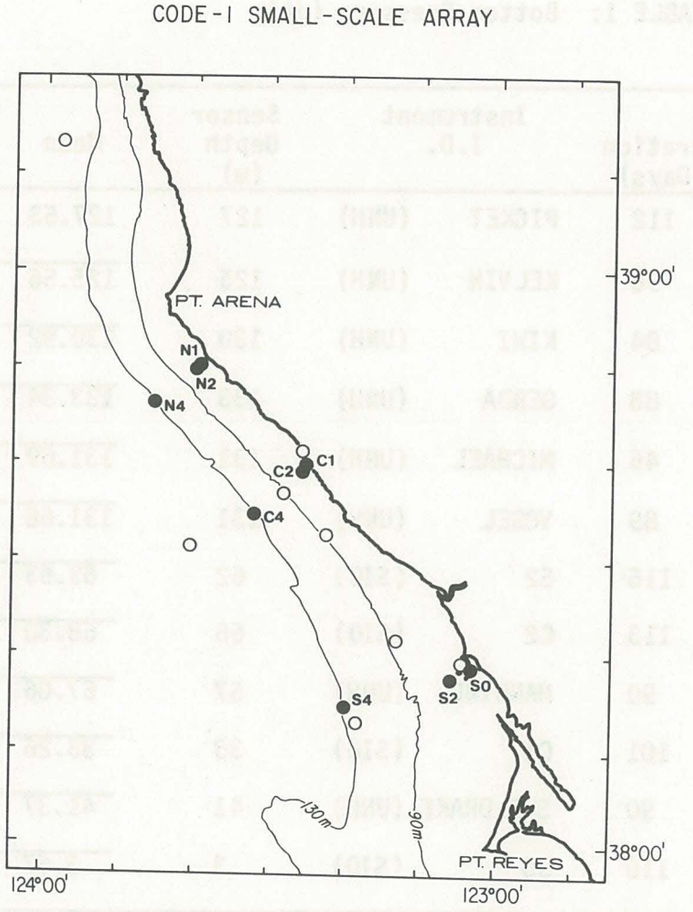

Figure 1. Stations where bottom pressure measurements were made during CODE-1 are shown as darkened circles.

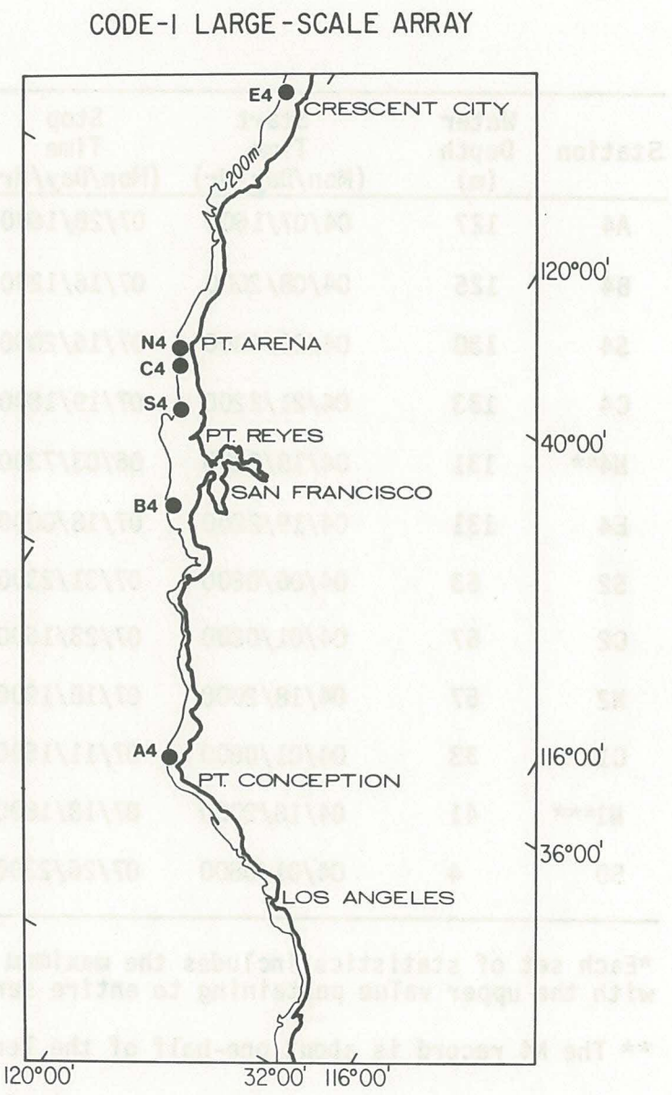

Figure 2. The elements of the large-scale bottom pressure array are shown as darkened circles. N4, C4 and S4 are also part of the small-scale array shown in Figure 1.

TABLE 1: Bottom Pressure (db)

Station	Water Depth (m)	Start Time (Mon/Day/Hr)	Stop Time (Mon/Day/Hr)	Duration (Days)	Instrument I.D.	Sensor Depth (m)	Mean	*Standard Deviation	*Maximum	*Minimum
A4	127	04/07/1600	07/28/1600	112	PICKET (UNH)	127	127.53	0.464	1.147	-1.250
								0.025	0.052	-0.066
B4	125	04/08/2000	07/16/1200	98	KELVIN (UNH)	125	125.56	0.504	1.217	-1.384
								0.027	0.076	-0.076
S4	130	04/23/2000	07/16/2000	84	KIWI (UNH)	130	130.92	0.529	1.248	-1.423
								0.027	0.070	-0.064
C4	133	04/21/2200	07/19/1800	88	GERDA (UNH)	133	133.34	0.532	1.250	-1.437
								0.035	0.090	-0.095
N4**	131	04/18/2200	06/03/7300	46	MICHAEL (UNH)	131	131.69	0.527	1.228	-1.438
								0.021	0.041	-0.046
E4	131	04/19/2200	07/18/0000	89	VOGEL (UNH)	131	131.68	0.652	1.459	-1.773
								0.054	0.127	-0.115
S2	63	04/06/0800	07/31/2300	116	S2 (SIO)	62	63.53	0.528	1.275	-1.462
								0.042	0.093	-0.120
C2	67	04/01/0800	07/23/1500	113	C2 (SIO)	66	68.30	0.522	1.246	-1.418
								0.048	0.086	-0.136
N2	57	04/18/2000	07/18/1900	90	MANNING (UNH)	57	57.06	0.538	1.229	-1.462
								0.047	0.115	-0.134
C1	33	04/01/0800	07/11/1500	101	C1 (SIO)	33	33.26	0.516	1.270	-1.363
								0.046	0.111	-0.118
N1***	41	04/18/2000	07/18/1800	90	SHELDRAKE (UNH)	41	41.37	0.536	1.253	-1.462
								0.044	0.082	-0.126
S0	4	04/01/0800	07/26/2300	116	S0 (SIO)	3	3.67	0.522	1.274	-1.419
								0.048	0.086	-0.134

*Each set of statistics includes the maximum and minimum value relative to the indicated mean value and the standard deviation, with the upper value pertaining to entire series of hourly values and the lower value pertaining to the low-passed series.

** The N4 record is about one-half of the length of the other series.

***The N1 series was very noisy and required a comprehensive editing process which included smoothing of the original 7.5 minute data.

erature calibrations have been performed on all sensors at the UNH calibration facility.

Due to the 100 m depth limitation of the SIO sensors, the shallower sites at C1, C2, and S2 were occupied by SIO instruments, which were mounted on the anchor and deployed and recovered with ground lines. The pressure instrument at SO was mounted on a Coast Guard pier piling in the outer Bodega Bay harbor. At SIO stations S2 and C2, closely-spaced thermistor chains were deployed vertically above the bottom pressure sensor, while at C1 a current meter string was deployed above the anchor on which the bottom pressure sensor was mounted. The UNH bottom pressure/temperature instruments are self-contained bottom instruments consisting of sensors, recording electronics canister, acoustic release frame and anchor. A more detailed description of the "standard" UNH instrument appears in Appendix A. Four of these "standard" instruments were deployed at A4 (PICKET)*, B4 (KELVIN), S4 (KIWI) and E4 (VOGEL) on the 130 m isobath during CODE for purposes of obtaining information about the alongshelf variability in the pressure field. A newer version of the UNH instrument incorporates the use of a microprocessor-based data logging system and thus will be referred to as UNH "micro-instruments". With their greater recording flexibility as described by Irish et al. (1981), the "micro-instruments" are used in connection with the deployment of temperature/conductivity (T/C) chains which are described in the previous chapter. During CODE-1, the C4 pressure instrument (GERDA) was deployed with a T/C chain, while two other micro-instruments were deployed without T/C chains at N4 (MICHAEL) and N2 (MANNING). The eighth UNH instrument (standard type) was mounted on an anchor and deployed with a ground-line at N1 (SHELDRAKE).

The packaging of the UNH and SIO pressure sensors is different. The UNH pressure sensor is mounted in a separate pressure housing, which itself is bolted to the outside of the data logger pressure housing. The SIO sensor is mounted inside the data logger pressure housing and interfaced to the water outside through an oil-filled tube. In both cases, a thermistor temperature of the data logger pressure housing is measured and used during data reduction to account for the temperature sensitivity of the pressure sensor itself.

A pre-CODE pressure calibration has been performed by submerging the array of UNH pressure sensors connected by a manifold into a constant temperature bath. A post-CODE-1 intercalibration of SIO and UNH sensors has been performed also. The expected long-term drift for the 400 psi UNH sensors of about 1 millibar (mb) per month has been confirmed by this calibration sequence. (Wearn, 1980, presents a much more detailed description of the long-term behavior of these sensors.) These long-term drifts are due to several causes including (a) mechanical creep within the sensor itself, (b) settling of the seafloor instrumentation into the sediment and (c) unresolved temperature sensitivity of the pressure sensor. There is nothing one can do about mechanical creep within each sensor except to monitor it with frequent calibrations which we do. Occasionally we observe relatively large (10 to 100 cm) drifts which we attribute to settling of a particular

*( ) indicate UNH instrument identifications which are names of seamounts in the New England Seamount chain.

UNH INSTRUMENT PACKAGE

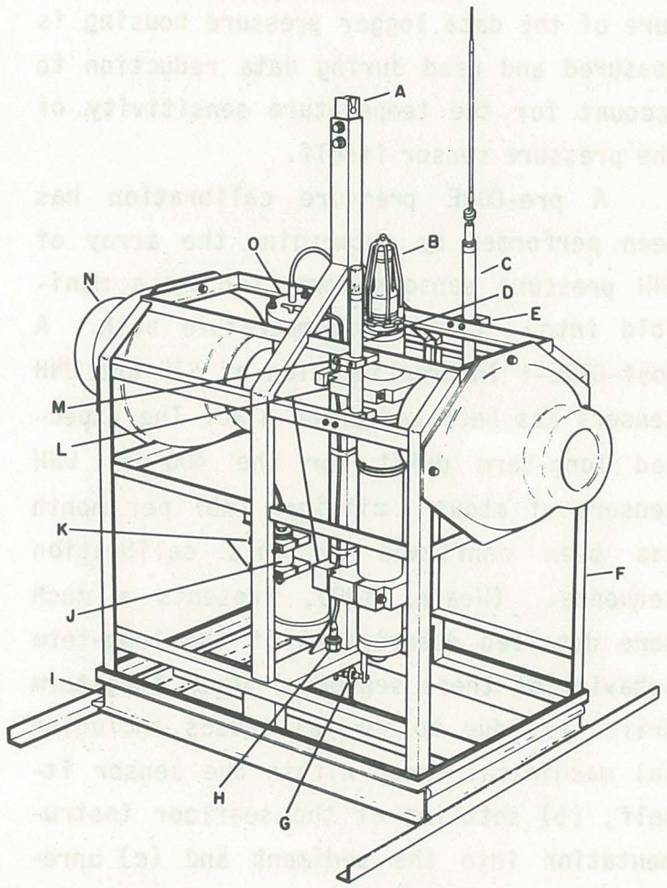

A LIFTING RING
B SONATEK ACOUSTIC RELEASE TRANSPONDER
C OAR RADIO TRANSMITTER
D OAR FLASHING LIGHT
E RADIO LIGHT CLAMP
F INSTRUMENT FRAME
G RELEASE ASSEMBLY
H EXPLODING BOLT
I ANCHOR FRAME
J PRESSURE SENSOR
K PAROS PRESSURE SENSOR CLAMP
L ACOUSTIC RELEASE CLAMPS
M OAR FLASHING LIGHT CLAMP
N BENTHOS GLASS SPHERE BUOYANCY
O DATA LOGGER CANNISTER

SIO INSTRUMENT PACKAGE

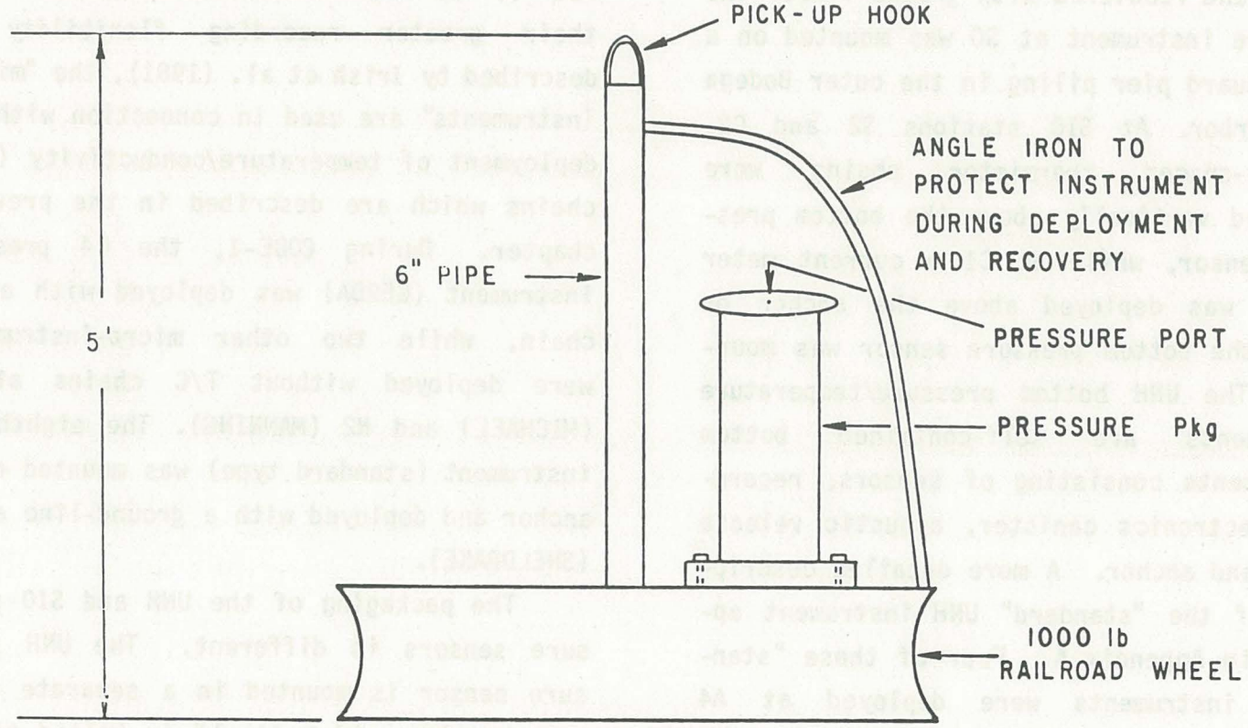

Figure 3

instrument in soft sediment. In both cases (a) and (b) the first-order non-geographical drift can be removed effectively with least squares fitting techniques. The problem of remaining temperature-related uncertainty is less easily resolved and probably represents the limitation in the high frequency precision of bottom pressure measurements. Specifically we find, as discussed in Appendix B, that the typical uncertainty in 400 psi bottom pressure sensors due to temperature effects is about ± 0.1 millibar with a worst case for a 900 psi sensor of about ± 0.5 mb.

C. BOTTOM PRESSURE OBSERVATIONS

Hourly values of the bottom pressure records are shown for along-shelf array stations in 130 m in Figure 4 and the shallower CODE area array stations in Figure 5. (All time series plots are centered on the mean, unless otherwise indicated.) Clearly the tidal signal dominates these bottom pressure records and obscures the lower amplitude wind-forced signal of interest. Our technique for studying the non-tidal signal includes the subtraction of a predicted tide from the raw data records. Thus a preliminary harmonic analysis of the tidal signals was performed and the results of these analyses are summarized in Table 2 in terms of the amplitude and Greenwich phase of the principal semi-diurnal (M2) and diurnal (K1) constituents. In general, the M2 tide is found to increase in amplitude and phase from south to north and numerically is in excellent agreement with observations and predictions regarding California tides by Munk, Snodgrass and Wimbush (1970). These results also indicate a tendency for reduced amplitude and increased phase going from deep stations to shallower stations in the CODE area. The latter results are somewhat tentative because of the relatively smaller signal to noise ratio.

The tidal analysis for a particular station is used to predict a tidal series, which is subtracted from the original series to form a residual series. A low pass filter, with a sharp cutoff at a 36-hour period is applied to the residual series to form the subtidal series. The results of this process for the C4 pressure series is shown in Figure 6. In Figures 7 and 8, the subtidal versions of the pressures are shown for the along-shelf and the CODE area arrays, respectively.

TABLE 2: The harmonic constants for the principal semidiurnal (M2) and diurnal (K1) constituents. The amplitude, A, is expressed in decibars and phase is in Greenwich degrees, G. See Chapter I, Table 2 for mooring positions.

Stn. I.D.	Depth (m)	Days	Tides M2 A	M2 G	K1 A	K1 G
A4	127	112	0.464	165.1	0.337	213.9
B4	125	98	0.518	185.3	0.363	218.7
S4	130	84	0.537	193.0	0.364	223.4
S2	63	116	0.531	195.6	0.369	224.5
S0	Coast	116	0.527	193.1	0.354	222.0
C4	133	88	0.544	194.0	0.385	227.6
C2	67	113	0.538	197.4	0.361	224.6
C1	33	101	0.532	197.8	0.339	223.5
N4	131	46	0.560*	195.5*	0.370*	224.6*
N2	57	90	0.560	194.9	0.383	226.9
N1	41	90	0.557	198.9	0.383	228.8
E4	131	89	0.718	212.7	0.396	228.2

*The N4 constituents were computed for a much shorter series, and thus have greater uncertainty than the others.

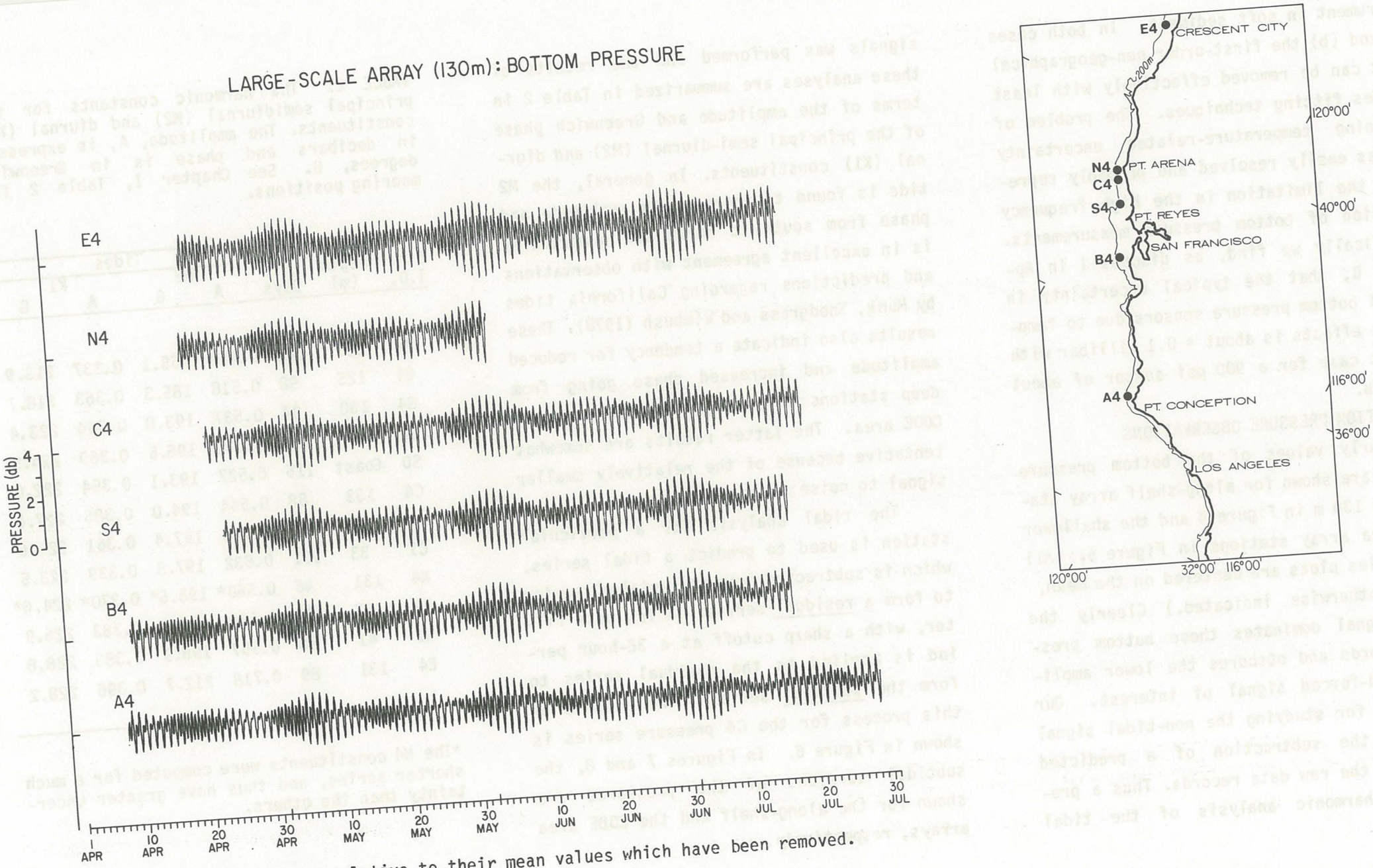

Figure 4. Series are plotted relative to their mean values which have been removed.

SMALL-SCALE ARRAY: BOTTOM PRESSURE

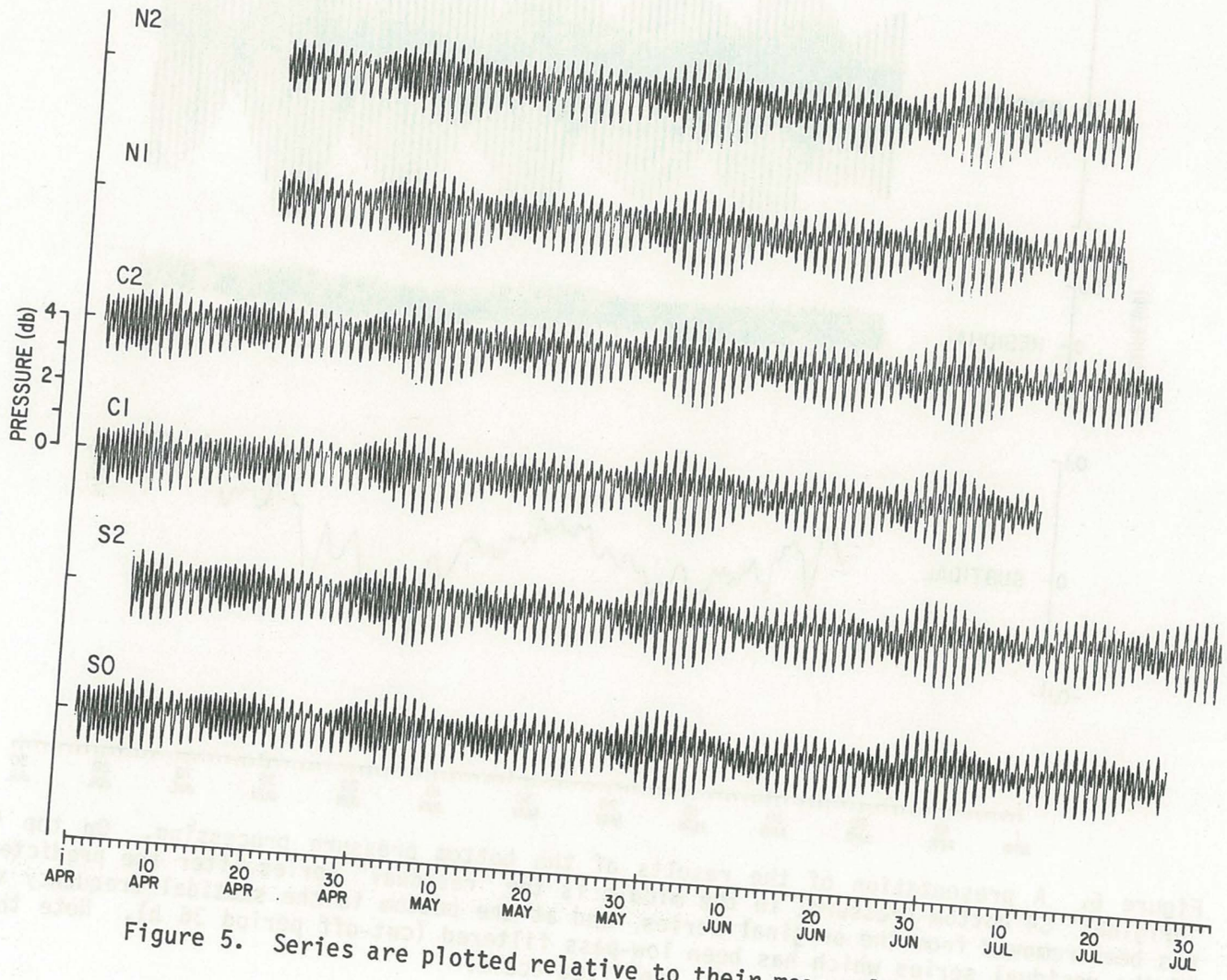

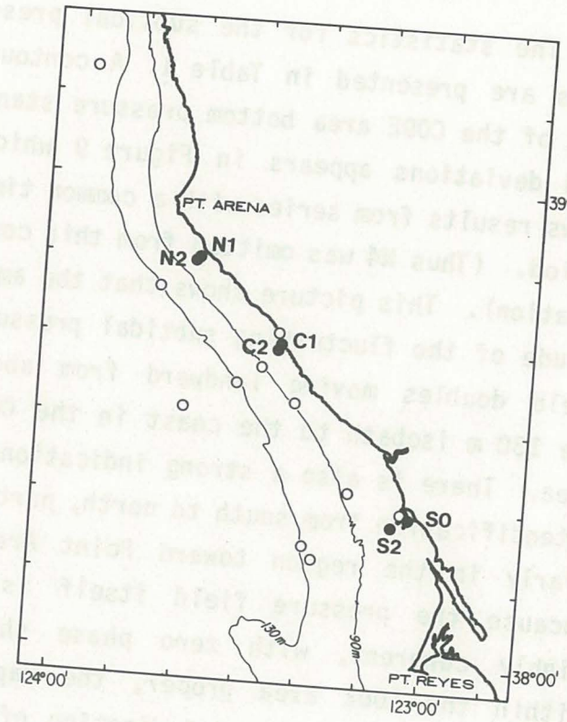

Figure 5. Series are plotted relative to their mean values which have been removed.

The statistics for the subtidal pressures are presented in Table 1. A contour plot of the CODE area bottom pressure standard deviations appears in Figure 9 which shows results from series with a common time period. (Thus N4 was omitted from this computation). This picture shows that the amplitude of the fluctuating subtidal pressure field doubles moving landward from about the 130 m isobath to the coast in the CODE area. There is also a strong indication of intensification from south to north, particularly in the region toward Point Arena. Because the pressure field itself is so highly coherent, with zero phase shifts within the CODE area proper, the map in Figure 9 provides a good indication of the fluctuating subtidal pressure difference field. (These results appear later).

Representative energy density spectra, for the period range from 10.5 days to 2 hours, are shown for the along-shelf and the cross-shelf arrays in Figures 10 and 11, respectively. Clearly, the principal bottom pressure energy resides in the semi-diurnal and diurnal tidal bands, which is separated by a spectral gap from the energy in the 5 to 10-day band. The results of

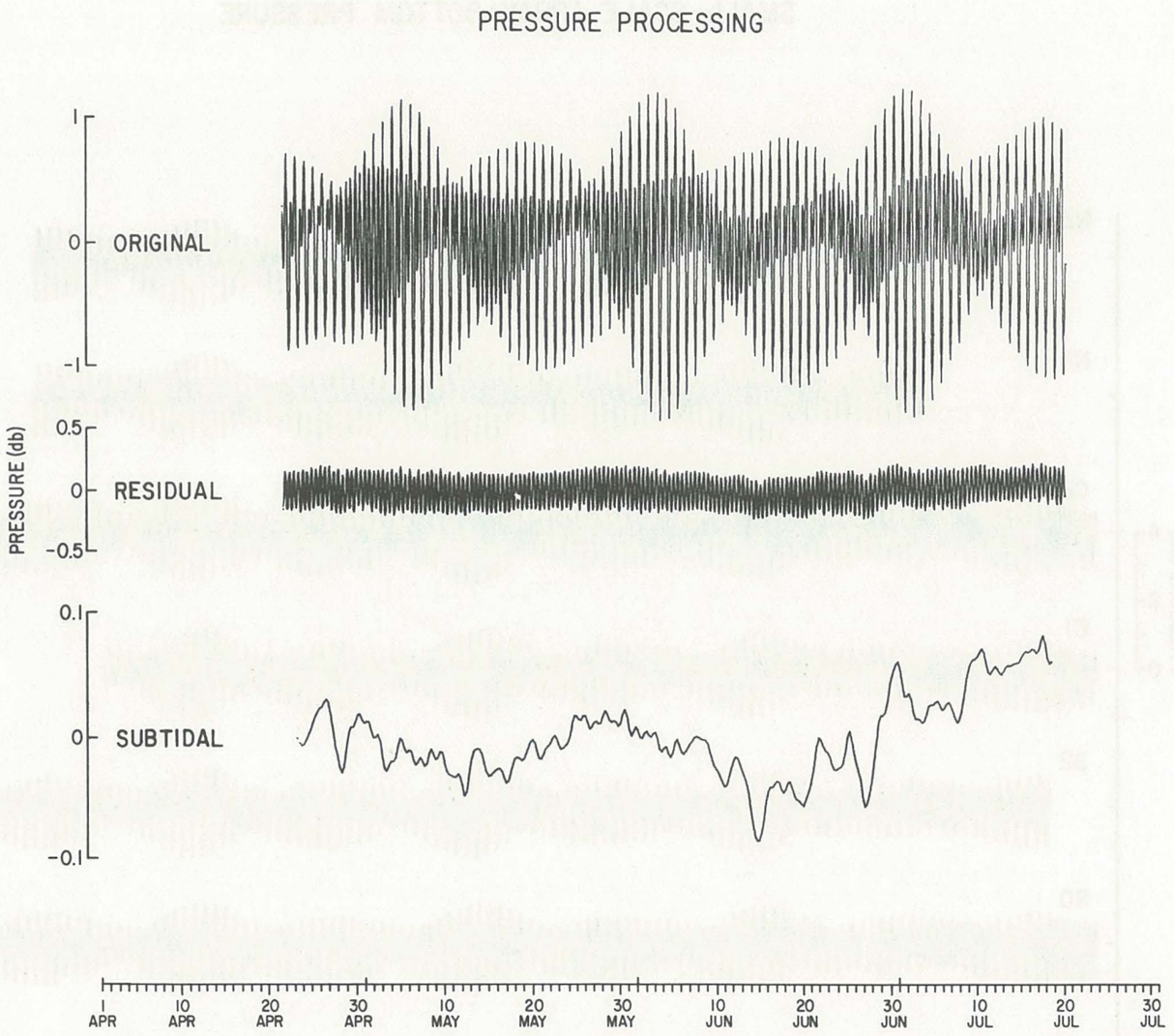

Figure 6. A presentation of the results of the bottom pressure processing. On top is the "original" C4 bottom pressure, in the middle is the "residual" series after the predicted tide has been removed from the original series, and at the bottom is the subtidal frequency version of the residual series which has been low-pass filtered (cut-off period 36 h). Note that the subtidal pressures are shown on a 10x amplified scale.

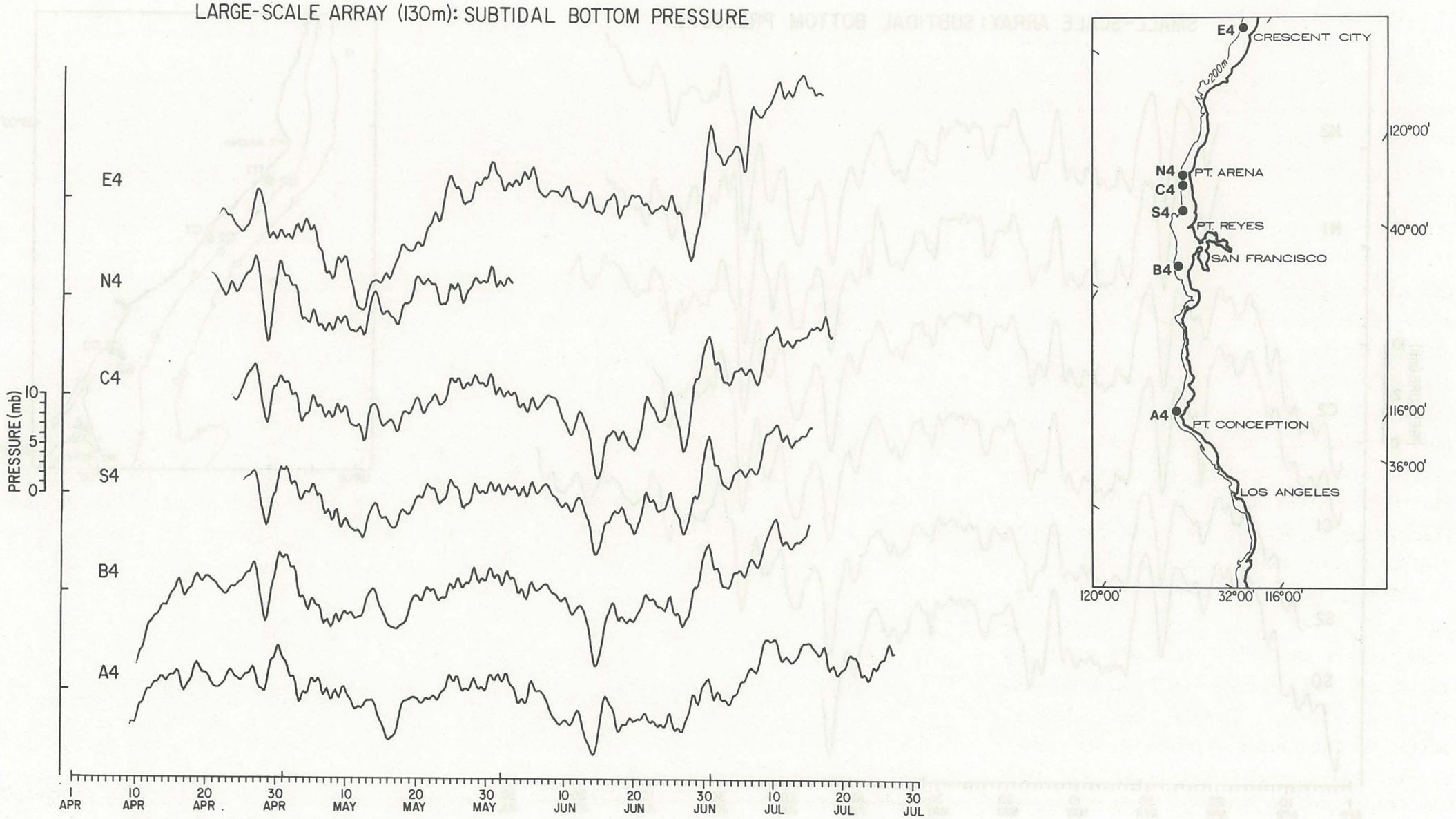

Figure 7. Series are plotted relative to their mean values which have been removed.

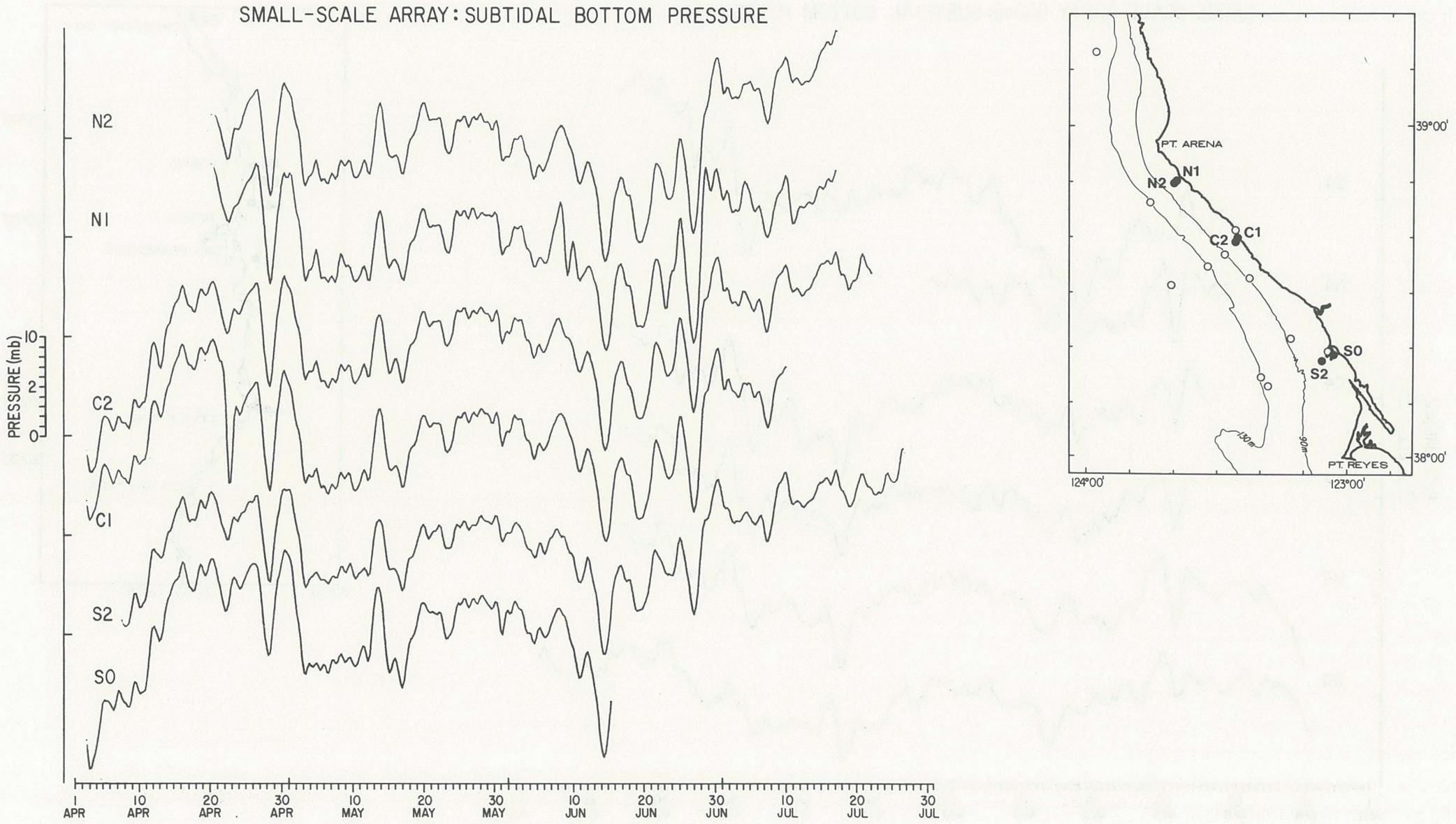

Figure 8. Series are plotted relative to their mean values which have been removed.

Figure 10 show the trend from lower to higher energy at stations from Point Conception (A4) northward to Crescent City (E4). The comparison of results from stations C4 and C1 on the CODE-1 central line in Figure 11 shows the expected shoreward increase in subtidal energy.

D. PRESSURE GRADIENT ESTIMATES

The quantity of dynamical interest, however, is not the bottom pressure per se, but the horizontal pressure gradient. Under certain conditions, the bottom pressure gradient is nearly the same as the overall horizontal pressure gradient, so here we present estimates of the bottom pressure gradient in the CODE area. These estimates are made by first taking the pressure stations (inshore minus offshore and northern minus southern) and then dividing this difference by the station separation distances, which are listed in Table 3. The cross-shelf pressure gradient estimates for the central [CPG = (C2-C4)/(ΔX)] and southern [SPG = (S2-S4)/(ΔX)] are shown in Figure 12. Coherence computations (not presented) show that (a) the subtidal cross-shelf gradients from line to line are highly coherent as we might expect if the along-shelf current is in geo-

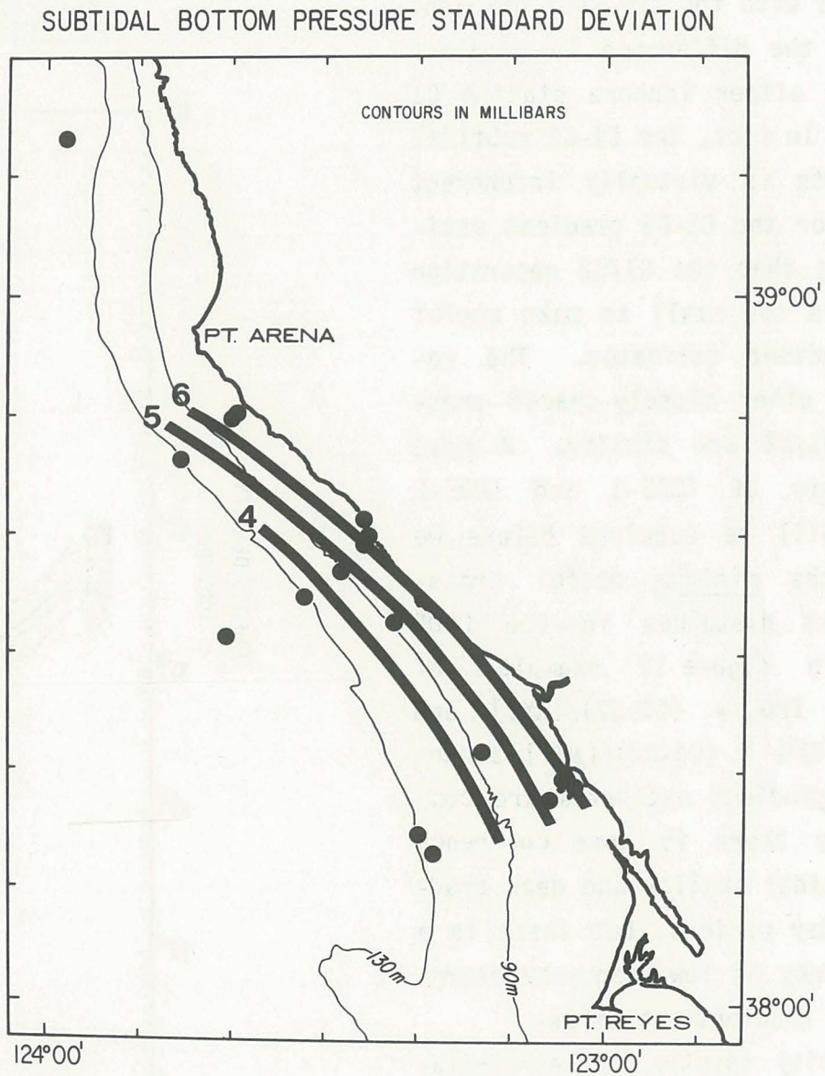

Figure 9. A contour plot of the CODE-1 small-scale array subtidal bottom pressure standard deviations in units of millibars. The results from the short N4 record have not been included in this presentation.

strophic balance with the pressure gradient field, and (b) the difference in gradient estimates using either inshore station C1 or C2 is small. In fact, the C1-C2 subtidal gradient estimate is virtually incoherent with the C2-C4 or the C1-C4 gradient estimates indicating that the C1/C2 separation of about 1 km is too small to make useful cross-shelf gradient estimates. The results from the other closely-spaced pressure pair at N1/N2 are similar. A more detailed analysis of CODE-1 and CODE-2 pressure data will be required before we can estimate the minimum useful cross-shelf separation distances in the CODE area. Also in Figure 12 examples of shallow [65 m, IPG = (C2-S2)/(ΔY)] and deeper [130 m, OPG = (C4-S4)/(ΔY)] along-shelf pressure gradient estimates are compared. Generally there is some coherence between the subtidal shallow and deep gradients for five-day periods, but there is a relative deficiency of low-frequency energy in the shallower gradient estimates.

Energy density spectra of representative pressure gradient estimates are compared in Figure 13. As expected, the subtidal energy in the cross-shelf gradients

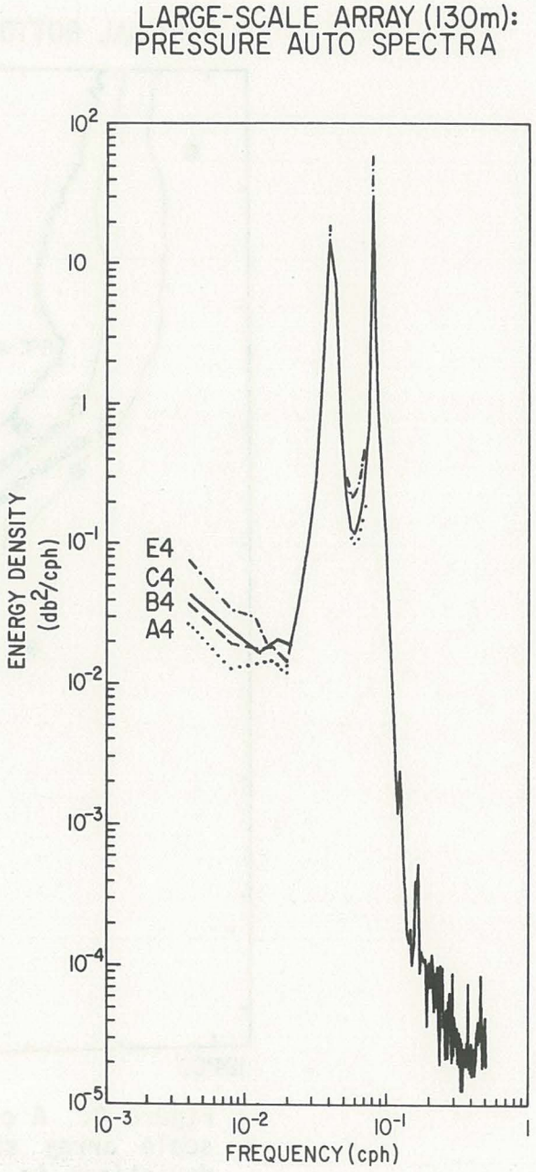

Figure 10

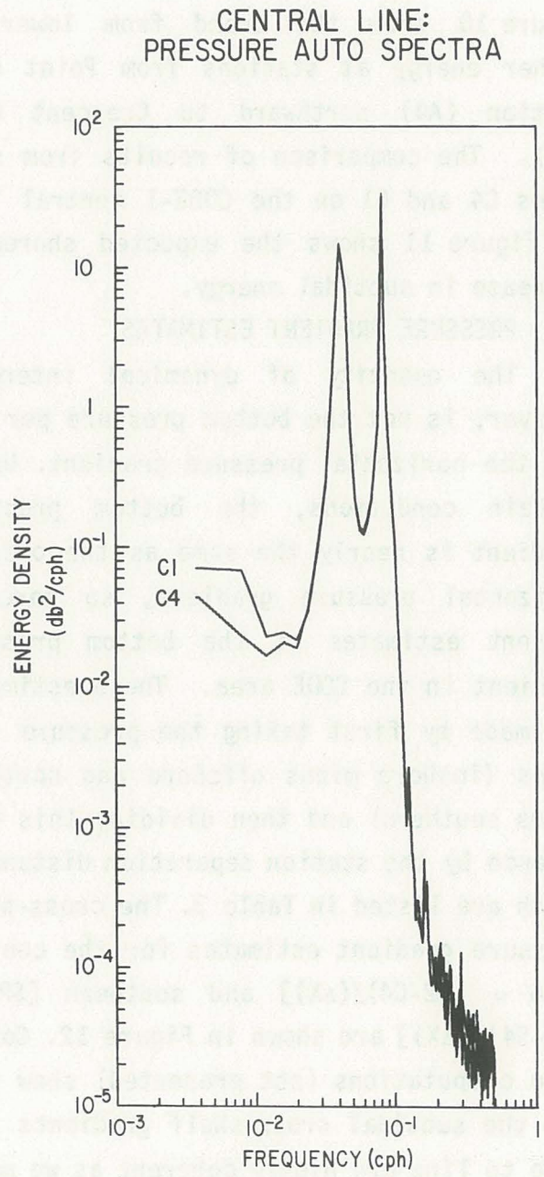

Figure 11

is larger than that in the along-shelf gradients (by about two orders of magnitude). As shown in Figure 13a, the subtidal central line gradient (CPG) is more energetic than the southern line gradient (SPG), which is consistent with earlier observations regarding the pressure field itself. Perhaps unexpectedly as shown in Figure 13b, we find that the subtidal along-shelf gradients in 130 m, OPG, are more energetic than the corresponding gradients along the 65 m isobath, IPG.

TABLE 3: CODE-1 Station Separation Distances in the Along-shelf and Cross-shelf Directions.

Along-shelf Pair	ΔY (km)	Across-shelf Pair	ΔX (km)
E4-N4	372.5	Coast-E4	23.7
E4-C4	400.3	N1B-N2	1.7
E4-S4	442.9	N1B-N4	11.7
E4-B4	555.9	N2-N4	10.2
E4-A4	900.6	C1-C2	1.1
N4-C4	28.5	C1-C4	14.8
N4-S4	70.1	C2-C4	13.9
N4-B4	183.5	S0-S2 (Coast)	3.3
N4-A4	528.2	S0-S4 (Coast)	24.3
C4-S4	41.7	S2-S4	20.9
C4-B4	153.8	Coast-B4	33.7
C4-A4	500.4	Coast-A4	19.3
S4-B4	118.6		
S4-A4	463.3		
B4-A4	339.1		
N2-C2	27.8		
N2-S2	77.2		
C2-S2	49.7		
N1-C1	28.4		
N1-S0	78.8		
C1-S0	50.4		

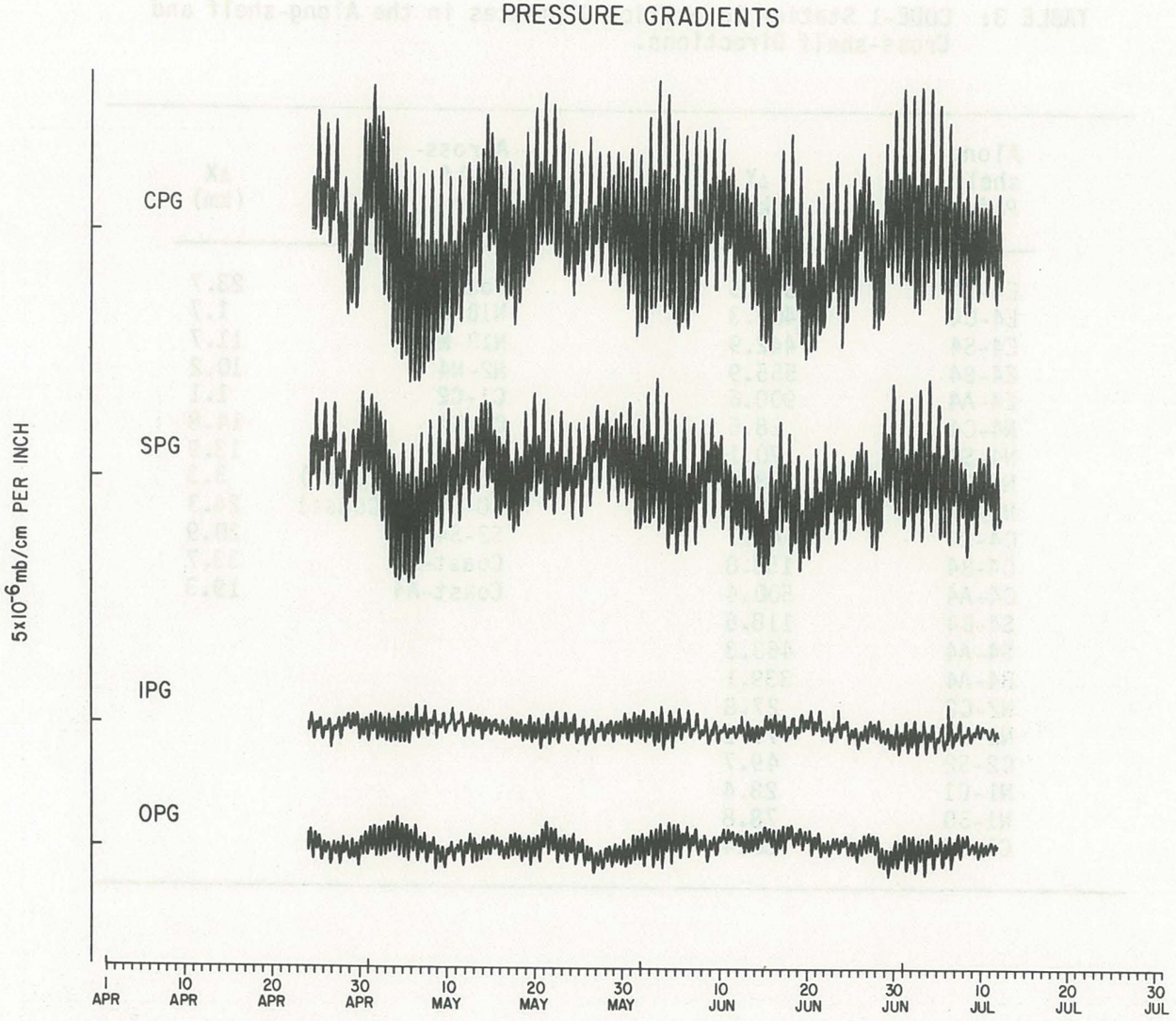

Figure 12. A comparison of representative CODE-1 pressure gradient estimates. The central line (CPG) and southern line (SPG) cross-shelf gradient estimates are clearly more energetic than the 65 m (IPG) and the 130 m (OPG) along-shelf gradient estimates.

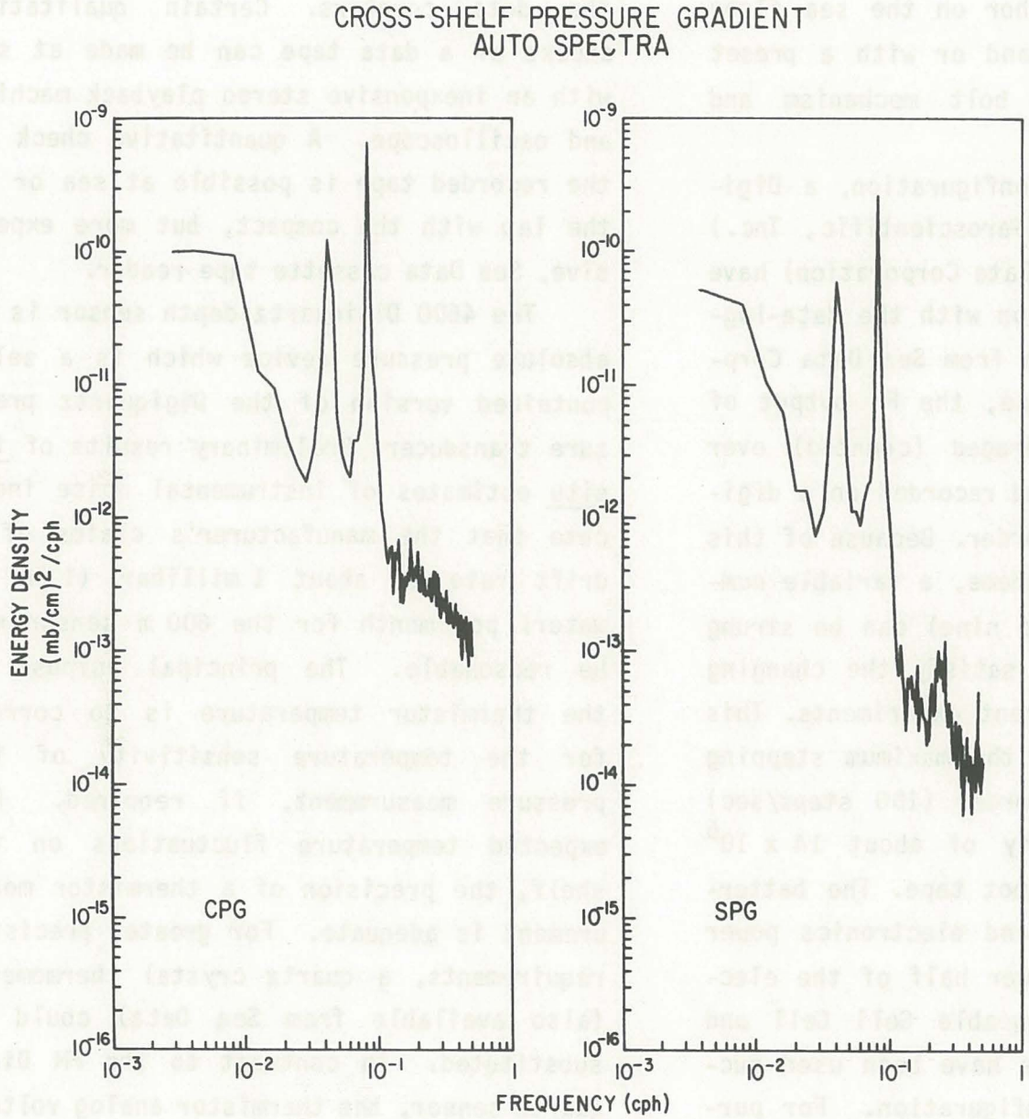

Figure 13a. The energy density spectra are shown for the cross-shelf pressure gradient along the central line (CPG) and southern line (SPG).

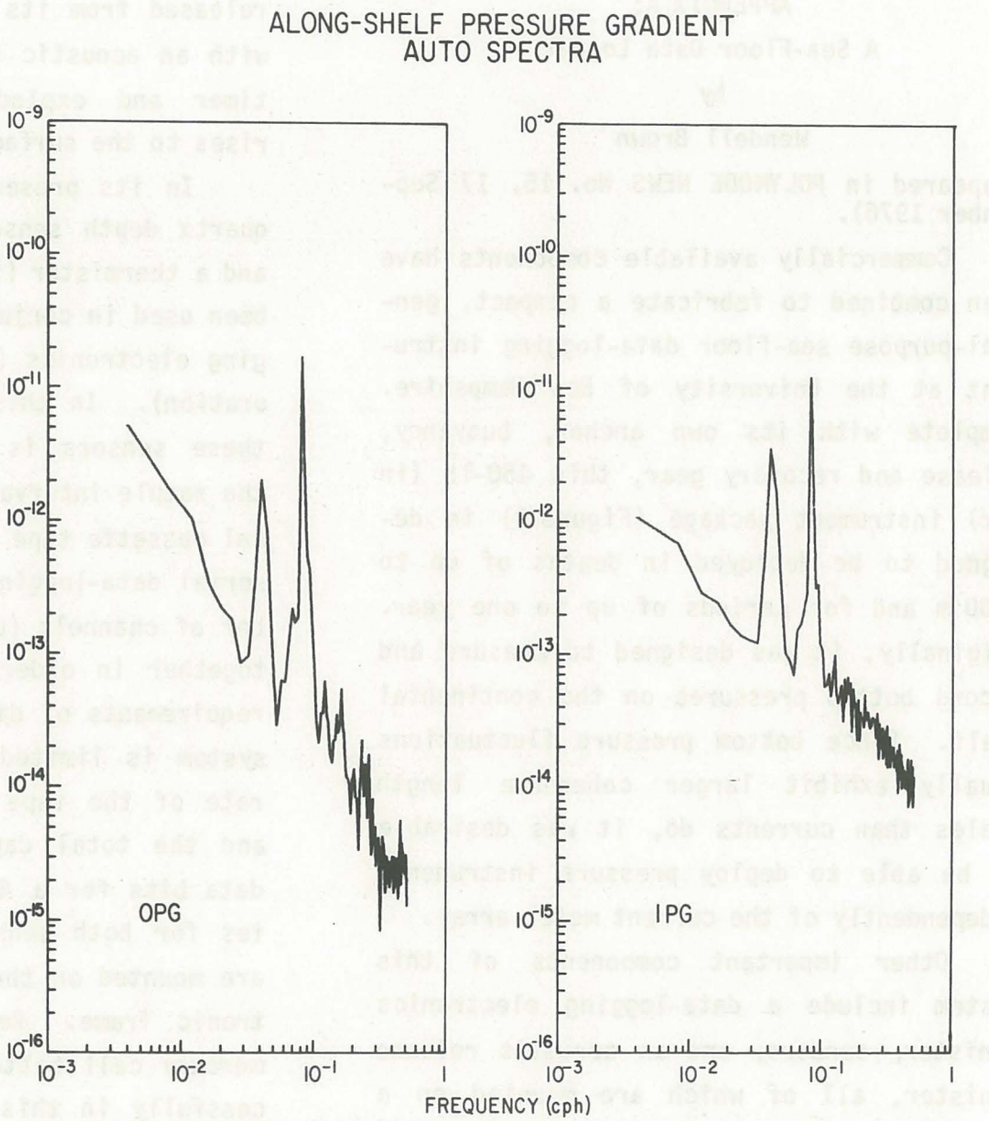

Figure 13b. The energy density spectra are shown for the along-shelf pressure gradient along the 130 m isobath (OPG) and 65 m isobath (IPG).

APPENDIX A:

A Sea-Floor Data Logger

by

Wendell Brown

(Appeared in POLYMODE NEWS No. 15, 17 September 1976).

Commercially available components have been combined to fabricate a compact, general-purpose sea-floor data-logging instrument at the University of New Hampshire. Complete with its own anchor, buoyancy, release and recovery gear, this 450-lb (in air) instrument package (Figure 3) is designed to be deployed in depths of up to 5000 m and for periods of up to one year. Originally, it was designed to measure and record bottom pressures on the continental shelf. Since bottom pressure fluctuations usually exhibit larger coherence length scales than currents do, it was desirable to be able to deploy pressure instruments independently of the current meter array.

Other important components of this system include a data-logging electronics canister, sensors, and an acoustic release canister, all of which are mounted on a lightweight aluminum frame. At the conclusion of an experiment, the main frame is released from its anchor on the sea floor with an acoustic command or with a preset timer and exploding bolt mechanism and rises to the surface.

In its present configuration, a Digiquartz depth sensor (Paroscientific, Inc.) and a thermistor (Sea Data Corporation) have been used in conjunction with the data-logging electronics (also from Sea Data Corporation). In this case, the FM output of these sensors is averaged (counted) over the sample interval and recorded on a digital cassette tape recorder. Because of this serial data-logging scheme, a variable number of channels (up to nine) can be strung together in order to satisfy the changing requirements of different experiments. This system is limited by the maximum stepping rate of the tape recorder (100 steps/sec) and the total capacity of about 14×10^6 data bits for a 450-foot tape. The batteries for both sensor and electronics power are mounted on the lower half of the electronic frame. Rechargeable Gell Cell and mercury cell batteries have been used successfully in this configuration. For purposes of counter checkout, a Sea Data "bit box" is used to scan out the contents of the data counters. Certain qualitative checks of a data tape can be made at sea with an inexpensive stereo playback machine and oscilloscope. A quantitative check of the recorded tape is possible at sea or in the lab with the compact, but more expensive, Sea Data cassette tape reader.

The 4600 Digiquartz depth sensor is an absolute pressure device which is a self-contained version of the Digiquartz pressure transducer. Preliminary results of in-situ estimates of instrumental noise indicate that the manufacturer's claims of a drift rate of about 1 millibar (1 cm of water) per month for the 600 m sensor may be reasonable. The principal purpose of the thermistor temperature is to correct for the temperature sensitivity of the pressure measurement, if required. For expected temperature fluctuations on the shelf, the precision of a thermistor measurement is adequate. For greater precision requirements, a quartz crystal thermometer (also available from Sea Data) could be substituted. In contrast to the FM Digiquartz sensor, the thermistor analog voltage is converted to an FM output before it, too, is counted.

The Sonatek, Inc. acoustic release is a relatively lightweight unit (55 lb in air and 27 lb in water), which employs a burn-wire technique for releasing an anchor load. When the release command is received from the sea surface, a stainless steel wire, which is coupled to the anchor through a mechanical linkage, is caused to electroplate away by the current from the pinger batteries. A confirmation code is transmitted simultaneously to the surface. This unit is also provided with a transposed feature which is used to determine slant range from a surface ship to the instrument. A preset time and exploding bolt mechanism serves as a backup to the acoustics for releasing the anchor.

Two 17-inch glass spheres (Benthos) provide the buoyancy (112 lb net) which is required to float the instrument package to the surface once the anchor has been released. Once on the surface, an Ocean Applied Research citizen band transmitter and flashing light are used to aid in the recovery of the instrument package.

APPENDIX B:
UNH Pressure Sensor Calibration Considerations

Over the past seven years we have calibrated our pressure sensors (up to 15 sensors) before and after each deployment, for a total of five calibrations to date. Our procedure is to calibrate all sensors simultaneously attached to a single pressure manifold, in a temperature-controlled bath. Pressure is applied to all sensors simultaneously with an Ashcroft dead weight tester in 50 PSI increments from 0 to 400 PSIR and then corrected to absolute pressure with the addition of local atmospheric pressure. The calibration data for each sensor is fit to the functional form

$$P(PSIA) = A(1-f/f_o) + B(1-f/f_o)^2 \qquad (1)$$

where A, B, and f_o are temperature sensitive coefficients and f is the measured output frequency. Calibrations are performed at a minimum of five temperatures evenly spaced between 0 and 25°C. The three constants derived from the calibration fit at each temperature are plotted as a function of temperature to determine the temperature sensitivity of each. During the reduction of raw data from an experiment, the measured temperature is used to compute the "instantaneous" values of the calibration coefficients A, B and f_o before computing the pressure itself.

Our history of calibration shows that, over our calibration temperature range ($0 \leq T(°C) \leq 25$) and within the accuracy of the dead weight tester, the coefficients A and f_o are linear functions of temperature and the coefficient B is nearly independent of temperature. Thus, we are justified in expressing the coefficients as

$$f_o = C3 + \gamma T;\ A = C1 + \alpha T;\ \text{and } B = C2 \qquad (2)$$

where T is temperature. For a typical 400 psi sensor (S/N 7512),

$$f_o = 41{,}057.086 + 0.142\ T;\quad A = 4535.9911 - 0.0357\ T;\ \text{and}\ B = 2214.6. \qquad (3)$$

For this sensor at 200 psi and 10°C, f = 39,200 Hz and (3) becomes,

f_o = 41,058.506 Hz; A = 4535.634 psia; (4)

and

B_o = 2216.4 psia

At a specified frequency, the temperature sensitivity of the pressure relationship in (1) is

$$PTS = \left.\frac{\partial P}{\partial T}\right|_f = \frac{\partial A}{\partial T}(1 - \frac{f}{f}) - \frac{\partial B}{\partial T}(1 - \frac{f}{f})^2 \quad (5)$$

$$+ \frac{\partial f_o}{\partial T}(\frac{f}{f_o})^2 [\frac{A}{f} + 2B (\frac{1}{f_o} - \frac{1}{f})].$$

Substituting (2) into (5) results in

$$PTS = \left.\frac{\partial P}{\partial T}\right|_f = \alpha(1 - \frac{f}{f_o}) \quad (6)$$

(a)

$$+ \gamma(\frac{f}{f_o})^2 [\frac{A}{f} + 2 \times C2 (\frac{1}{f_o} - \frac{1}{f})],$$

(b) (c)

Which for the conditions specified in (4) gives

$$PTS = -1.62 \times 10^{-3} + 1.50 \times 10^{-2}$$

$$- 6.62 \times 10^{-4} \text{ psi/°C}$$

$$= 1.27 \times 10^{-2} \text{ psi/°C} = 0.88 \text{ mb/°C}.$$

Note that the principal contribution to PTS is from the term (b) which represents the temperature sensitivity of f_o. Thus there are uncertainties in the pressure determination which are directly related to our uncertainty in determining the temperature sensitivity of the pressure calibration coefficients. The temperature sensitivity uncertainty of the pressure calibration, ε_{PTS}, is related to the uncertainties in estimating the temperature-dependent coefficients as follows

$$\varepsilon_{PTS} = [(\frac{\partial PTS}{\partial f_o} \varepsilon_{f_o})^2 + (\frac{\partial PTS}{\partial A} \varepsilon_A)^2 + (\frac{\partial PTS}{\partial \alpha} \varepsilon_\alpha)^2 \quad (7)$$

$$+ (\frac{\partial PTS}{\partial \gamma} \varepsilon_\gamma)^2 + (\frac{\partial PTS}{\partial C2} \varepsilon_{C2})^2]^{1/2}.$$

Computing the gradient terms in (7) using (6) and then substituting the results of (3) and (4) gives

$$\frac{\partial PTS}{\partial f_o} = \alpha \frac{f}{f_o^2} + 2\gamma(2 \times C2 - A)\frac{f}{f_o^3} - 6 \times C2 \gamma \frac{f^2}{f_o^4}$$

$$= 1.87 \times 10^{-6} \text{ psi/°C/Hz}$$

$$\frac{\partial PTS}{\partial A} = \gamma \frac{f}{f_o^2} = 3.30 \times 10^{-6} \text{ psi/°C/psia}$$

$$\frac{\partial PTS}{\partial \alpha} = 1 - \frac{f}{f_o} = 4.53 \times 10^{-2} \text{ psi/°C/psia/°C} \quad (8)$$

$$\frac{\partial PTS}{\partial \gamma} = (\frac{f}{f_o})^2 [\frac{A}{f} + 2 \times C2(\frac{1}{f_o} - \frac{1}{f})]$$

$$= 1.01 \times 10^{-1} \text{ psi/°C/Hz/°C}$$

$$\frac{\partial PTS}{\partial C2} = 2\gamma(\frac{f}{f_o})^2 [\frac{1}{f_o} - \frac{1}{f}]$$

$$= -2.99 \times 10^{-7} \text{ psi/°C/psia}$$

The uncertainties in computing the temperature sensitivity of the coefficients are estimated from the plots regressing each pressure calibration coefficient against temperature. For a typical sensor (S/N 7512), the uncertainties are

$\varepsilon_{f_o} < \pm 1$ Hz; $\varepsilon_{\gamma} < \pm 0.03$ Hz/°C;

(9)

$\varepsilon_A < \pm 0.1$ psia; $\varepsilon_{\alpha} < \pm 0.03$ psi/°C;

$\varepsilon_{C2} < \pm 8$ psia.

Evaluating (7) for the uncertainties given in (9) and the sensitivities in (8) gives

$$\varepsilon_{PTS} = \pm [(1.8\times10^{-6})^2 + (2.0\times10^{-6})^2 + (1.4\times10^{-3})^2 + (3.0\times10^{-3})^2 + 2.4\times10^{-6})]^{1/2} \quad (10)$$

$$\varepsilon_{PTS} = \cong 3.2 \times 10^{-3} \text{ psi/°C}$$

This means that the standard deviation of the pressure uncertainty, ε_{PTS}, due to temperature variability with a standard deviation of 1°C (typical of the shelf) is $\pm 3.3 \times 10^{-3}$ psi or about ± 2 equivalent mm of sea water elevation. A similar computation for one of our older, more temperature-sensitive Paroscientific 900 psi sensors yields an uncertainty 2.5 times larger, which represents a worst case temperature uncertainty for our sensors. Clearly from (10), the largest terms (and only significant terms) are due to the uncertainties in estimating the slopes of f_o and A. Both of the uncertainties computed above assume the best linear temperature corrections have been made to the data. Additional use of the information from all the calibrations of each sensor helps to reduce the uncertainty due to temperature sensitivity effects on the pressure measurement to less than 1 equivalent cm of water.

Acknowledgments

The execution of the CODE-1 pressure field program was made possible through the efforts of a great many people. At UNH, the extraordinary efforts of M. Woodbury, E. LaCoursiere, M. Condilis and A. Bugbee are noteworthy. The corresponding contributions by Scripps personnel M. Kirk, P. Dacri, A. Bratkovich and S. Lentz are equally noteworthy. Without their dedication and versatility, this level of effort would not have been possible. The skill and cooperation of the officers and crew of the R/V Wecoma (OSU) and the R/V Acania (Monterey Naval Postgraduate School) helped make our seagoing operations possible and productive. The officers and crew of the U.S. Coast Guard Base at Yerba Buena Island were a key factor in the efficiency and flexibility with which we were able to operate our seagoing operations such long distances from our home base. We make special mention of the assistance of M. Lee (UNH), who arranged much of the logistics and acted as the onshore liaison. The UNH and SIO effort was supported by the National Science Foundation.

References

Brown, W. S., 1976. A seafloor data logger. POLYMODE News, 15, 17 September 1976.

Irish, J. D., W. S. Brown and M. P. Woodbury, 1981. Conditional sampling of oceanic variability with microprocessor-controlled instrumentation. Proceedings of Ocean, 81. IEEE Int. Conf. on the Oceans, Boston, MA. September, 1981. pp. 484-488.

Munk, W. H., F. E. Snodgrass and A. M. Wimbush, 1970. Tides offshore: transition from California coastal to deep-sea waters. Geophys. Fluid Dynam., 1: 161-235.

Wearn, R. B., Jr. and N. G. Larson, 1980. The Paroscientific pressure transducer, the measurements of its sensitivities and its drift. APL-UW Technical Report 8011, Applied Physics Laboratory, University of Washington, Seattle, WA, 88 pp.

CODE-1:
LARGE-SCALE WIND AND SEA LEVEL OBSERVATIONS

By

G. R. Halliwell, Jr.
J. S. Allen

School of Oceanography
Oregon State University
Corvallis, Oregon 97331

A. INTRODUCTION

The purpose of the large-scale component of CODE is to study the large-scale response of shelf circulation to atmospheric forcing. Using sea level as an indicator of the response, models of wind-driven shelf circulation can be tested, and currents measured at the CODE site can be related to non-local atmospheric forcing and the propagation of free coastal-trapped waves into the site. This effort requires good wind and sea level data to be collected for a sufficiently large alongshore domain containing the CODE site. Atmospheric pressure must also be collected to barometrically adjust sea level. To properly assess non-local forcing of shelf currents at the CODE site, the large-scale analysis domain extends equatorward to northern Baja California, more than 1000 km from the site. In order to resolve long shelf waves, the domain extends poleward to the Alaskan border, about 1800 km poleward of the CODE site.

Most of the data set will span the period 1 December 1980 through 30 November 1982, but part of the set will extend from 1 April 1980 through March or April 1983 when the final long-term current meters are retrieved. Only data from the four-month subset of 1 April through 31 July 1981 will be presented in this report for comparison to the other CODE-1 data sets.

To properly assess the response of sea level and currents to wind forcing, the best possible sets of winds must be obtained. There are four wind sets which can be used in the present study: measured winds and three analyzed wind fields. These analyzed fields are: (1) Bakun winds from Fleet Numerical Oceanography Center (FNOC), Bakun (1973); (2) Marine winds from FNOC, Caton, et al. (1978); and (3) Six-hour forecast winds from the National Weather Service Limited Fine Mesh II (LFM-II) model, Newell and Deaven (1980) and Gerrity (1977). (Different boundary layer corrections are applied to the Bakun and marine winds at FNOC.) Ideally, measured winds should be used. A large number of wind measurement stations exist along the West Coast of the U.S.; however, topographic influences and data gaps are problems at many of them. It is therefore necessary to consider using analyzed wind fields. These analyzed fields are presently being compared to measured winds to determine if they adequately represent the large-scale atmospheric forcing along the West Coast. Measured winds are emphasized in this report. Some Bakun wind time series are also shown for comparison to the measured winds.

This report is organized as follows: The stations and variables in the data base are described in Section B.1, and the editing and processing are presented in Section B.2, the wind data is in Section C, and adjusted sea level statistics and plots are presented in Section D. Alongshore-time contour plots of Bakun alongshore wind stress and adjusted sea level are presented in Section E to illustrate the sea level response to stress.

B. THE LARGE-SCALE DATA BASE FOR THE CODE-1 EXPERIMENT

B.1 Description of the Data Base

Information on measured wind stations is summarized in Table 1. Only the measurement stations with data available during the CODE-1 experiment are included. The locations of these stations are shown in Figure 1. Information on the CODE analysis grid is presented in Table 2. Time series from the analyzed wind fields were obtained at these points. The locations of these

TABLE 1: Meteorological Station Information

Station	Abbrev-iation	Latitude (Deg Min)	Longitude (Deg Min)	Atmospheric Pressure	Alongshore Position (km)	Elevation (m) (1)	Anemometer Height (m)	Coast Orientation (Deg) (2)	Period of Record (3)
Cape St. James, BC	CSJ	51°57'N	131°05'W	No	1800		6.1	138	12/80-Present
Cape Flattery, WA	CPF	48°23'N	124°44'W	No	1104		6.1	120	12/80-Present
Neah Bay, WA	NBA	48°22'N	124°35'W	No	1101	15	6.1	120	12/80-Present
Quillayute, WA	QUI	47°57'N	124°32'W	Yes	1055	56	6.7	110	12/80-Present
Destruction Island, WA	DST	47°40'N	124°29'W	No	1022	21	6.1	110	12/80-Present
Hoquiam, WA	HOQ	46°58'N	123°56'W	Yes	942	8	6.1	95	12/80-Present
Ocean Shores, WA	OSH	46°57'N	124°06'W	No	939	3	8.8	95	04/80-Present
Grays Harbor, WA	GRH	46°55'N	124°06'W	No	936	5	6.1	95	12/80-Present
Cape Disappointment, WA	CPD	46°17'N	124°03'W	No	865	55	6.1	90	12/80-Present
Columbia River LNB	CLR	46°11'N	124°11'W	Yes	854	0	10.0	90	12/80-Present
Astoria, OR	AST	46°09'N	123°53'W	Yes	850	3	6.1	90	12/80-Present
Tillamook Bay, OR	TIL	45°34'N	123°48'W	No	786	3	6.1	82	04/80-Present
Newport, OR	NEW	44°38'N	124°03'W	Yes	683	55	6.1	90	12/80-Present
Siuslaw River, OR	SIU	44°00'N	124°07'W	No	612	15	6.1	81	12/80-Present
North Bend, OR	NOB	43°25'N	124°15'W	Yes	547	5	6.1	73	12/80-Present
Five Mile Point, OR	FMP	43°14'N	124°23'W	No	525		10.0	73	04/81-Present
Five Mile Point, OR	FMP	43°14'N	124°23'W	No	525		20.0	73	04/81-Present
Five Mile Point, OR	FMP	43°14'N	124°23'W	No	525		40.0	73	04/81-Present
Cape Blanco Tower, OR	CBT	42°50'N	124°32'W	No	480		9.1	90	12/80-10/81
Cape Blanco Tower, OR	CBT	42°50'N	124°32'W	No	480		30.0	90	12/80-10/81
Cape Blanco Tower, OR	CBT	42°50'N	124°32'W	No	480		45.7	90	12/80-10/81
Cape Blanco Tower, OR	CBT	42°50'N	124°34'W	No	480	55	6.1	90	04/80-Present
Crescent City, CA	CCY	42°47'N	124°14'W	Yes	362	17	6.1	103	12/80-Present
Arcata, CA	ARC	40°59'N	124°06'W	Yes	270	70	6.1	75	12/80-Present
Humboldt Bay, CA	HUM	40°46'N	124°14'W	No	246	3	6.1	75	12/80-Present
Point Cabrillo, CA	PCB	39°22'N	123°49'W	No	87		6.1	90	12/80-Present
NDBO 46014	014	39°13'N	123°58'W	Yes	71	0	10.0	100	04/81-Present
Point Arena Light, CA	ARL	38°57'N	123°44'W	No	41	19	6.1	110	12/80-Present
Point Arena Tower, CA	ART	38°55'N	123°43'W	No	37		9.1	110	04/81-07/81
Point Arena Tower, CA	ART	38°55'N	123°43'W	No	37		45.7	110	04/81-07/81

TABLE 1: Meteorological Station Information (Continued)

Station	Abbrev-iation	Latitude (Deg Min)	Longitude (Deg Min)	Atmospheric Pressure	Alongshore Position (km)	Elevation (m)	(1) Anemometer Height (m)	(2) Coast Orientation (Deg)	Period of Record
Sea Ranch, CA (Cent. Line)	CLI	38°41'N	123°26'W	No	0		10.0	133	03/11/81-08/11/81
C3	C3	38°36'N	123°28'W	No	0	0	3.5	133	04/12/81-07/81
C5	C5	38°31'N	123°40'W	No	0	0	3.5	133	04/13/81-08/03/81
R3	R3	38°22'N	123°13'W	No	-35	0	3.5	133	04/13/81-08/03/81
Bodega Marine Lab, CA	BML	38°20'N	123°04'W	No	-46		10.0	133	04/80-Present
NDBO 46013	013	38°14'N	123°18'W	Yes	-61	0	10.0	133	04/81-Present
Pillar Point, CA	PIL	37°30'N	122°30'W	No	-156	40	15.2	105	04/81-Present
NDBO 46012	012	37°22'N	122°39'W	Yes	-171	0	5.0	105	12/80-Present
Pigeon Point, CA	PIG	37°11'N	122°24'W	No	-191	9	6.1	102	12/80-Present
Point Pinos, CA	PIN	36°38'N	121°56'W	No	-271	6	6.1	110	12/80-Present
Monterey, CA	MRY	36°35'N	121°51'W	Yes	-278	50	6.1	110	12/80-Present
Point Sur, CA	SUR	36°18'N	121°53'W	No	-301	15	6.1	115	12/80-Present
Morro Bay, CA	MOR	35°22'N	120°48'W	No	-455	18	4.0	130	04/81-07/81
Diablo Canyon, CA	DIA	35°14'N	120°50'W	No	-464	2	9.1	120	04/80-Present
Diablo Canyon, CA	DIA	35°14'N	120°50'W	No	-464	2	76.2	120	04/80-Present
NDBO 46011	011	34°53'N	120°52'W	Yes	-506	0	10.0	90	12/80-Present
VWT102[4] (Purisma Point)	V102	34°48'N	120°38'W	No	-524		3.7	90	04/81-07/81
VWT102 (Purisma Point)	V102	34°48'N	120°38'W	No	-524		16.5	90	04/81-07/81
VWT102 (Purisma Point)	V102	34°48'N	120°38'W	No	-524		31.1	90	04/81-07/81
VWT301	V301	34°37'N	120°36'W	No	-540		3.7	90	04/81-07/81
VWT301	V301	34°37'N	120°36'W	No	-540		16.5	90	04/81-07/81
VWT301	V301	34°37'N	120°36'W	No	-540		31.1	90	04/81-07/81
VWT302 (Point Arguello)	V302	34°34'N	120°38'W	No	-545		3.7	90	04/81-07/81
VWT302 (Point Arguello)	V302	34°34'N	120°38'W	No	-545		16.5	90	04/81-07/81
VWT302 (Point Arguello)	V302	34°34'N	120°38'W	No	-545		31.1	90	04/81-07/81
VWT103	V103	34°33'N	120°35'W	No	-548		3.7	90	04/81-07/81
VWT103	V103	34°33'N	120°35'W	No	-548		16.5	90	04/81-07/81
VWT103	V103	34°33'N	120°35'W	No	-548		31.1	90	04/81-07/81
Santa Barbara, CA	SBA	34°26'N	119°50'W	Yes	-623	4	6.1	175	12/80-Present
Point Mugu, CA	MUG	34°07'N	119°07'W	Yes	-678	3	4.0	155	12/80-Present

TABLE 1: Meteorological Station Information (Continued)

Station	Abbrev-iation	Latitude (Deg Min)	Longitude (Deg Min)	Atmospheric Pressure	Alongshore Position (km)	Elevation (m)	(1) Anemometer Height (m)	(2) Coast Orientation (Deg)	Period of Record
San Nicholas Island, CA	SNI	33°15'N	119°27'W	Yes	-685	173	3.0	155	12/80-Present
Los Angeles, CA	LOS	33°56'N	118°24'W	Yes	-757	34	9.1	150	12/80-Present
Long Beach, CA	LBC	33°49'N	118°09'W	Yes	-785	21	6.1	150	12/80-Present
San Clemente Island, CA	SCI	33°01'N	118°35'W	Yes	-825	52	7.9	130	12/80-Present
San Diego, CA	SDO	32°44'N	117°10'W	Yes	-936	10	6.1	105	12/80-Present
Imperial Beach, CA	IMP	32°34'N	117°07'W	Yes	-954	6	6.1	105	12/80-Present

Notes:

(1) The elevation is unknown for many stations.

(2) Positive angles are measured counter-clockwise from due east.

(3) "Present" indicates that data will be collected at least through 11/82 unless the station is shut down.

(4) VWT stands for Vandenberg AFB WINDS Tower.

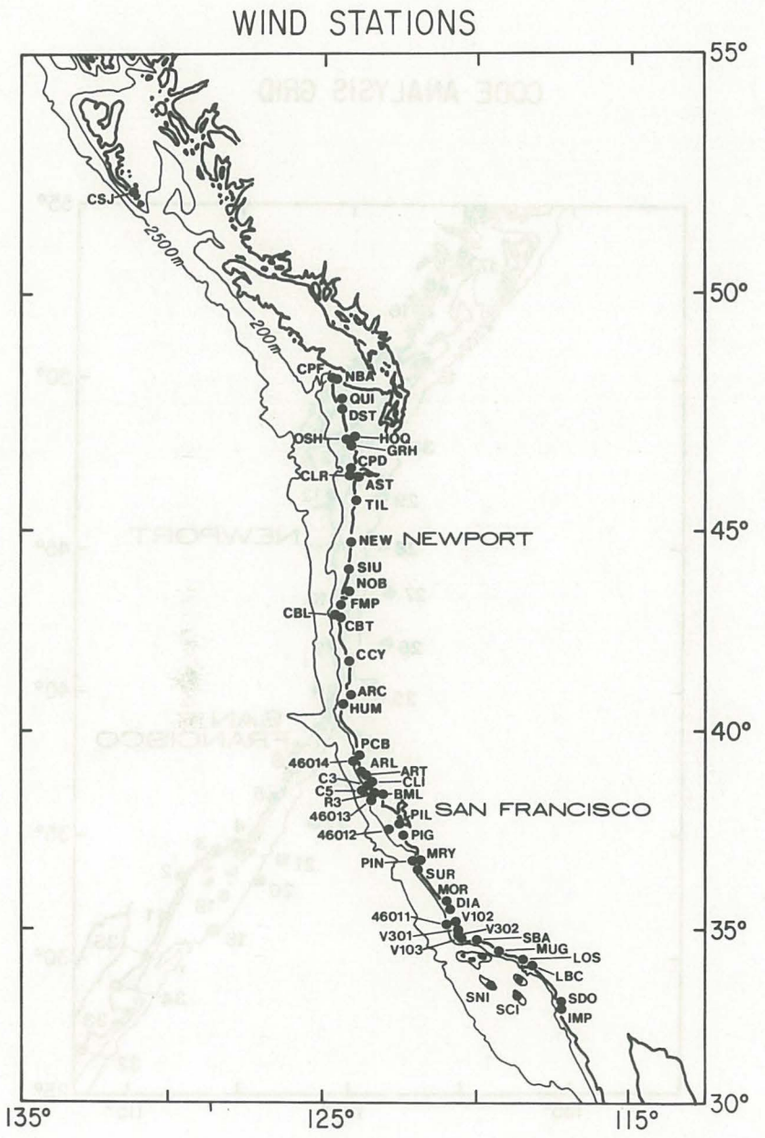

Figure 1

Notes:

(1) Positive angles are measured counter-clockwise from due east.

(2) Coast orientations shown only for coastal grid points.

TABLE 2: CODE Grid for Analyzed Meteorological Fields and Interpolated Sea Level Data

Grid Point	Latitude (Deg Min)	Longitude (Deg Min)	Alongshore Position (km)	Coast Orientation (deg)(1)
1	31°27'N	116°44'W	-1080	110
2	33°00'N	117°21'W	-900	110
3	34°01'N	118°53'W	-720	150
4	34°35'N	120°39'W	-540	90
5	35°39'N	121°31'W	-360	128
6	37°18'N	122°24'W	-180	102
7	38°42'N	123°27'W	0	133
8	40°12'N	124°18'W	180	130
9	41°46'N	124°12'W	360	130
10	43°21'N	124°20'W	540	73
11	44°58'N	124°03'W	720	85
12	46°36'N	124°05'W	900	95
13	48°11'N	124°42'W	1080	120
14	49°23'N	126°06'W	1260	128
15	50°32'N	121°13'W	1440	100
16	52°10'N	128°19'W	1620	115
17	54°09'N	130°20'W	1800	120
18	30°46'N	118°21'W	--	(2) --
19	32°19'N	119°08'W	--	--
20	32°56'N	121°03'W	--	--
21	33°40'N	122°22'W	--	--
22	35°10'N	123°21'W	--	--
23	36°38'N	124°16'W	--	--
24	38°05B	125°23'W	--	--
25	39°52'N	126°17'W	--	--
26	41°46'N	126°29'W	--	--
27	43°21'N	126°36'W	--	--
28	44°58'N	126°22'W	--	--
29	46°36'N	126°24'W	--	--
30	48°07'N	127°00'W	--	--
31	26°07'N	112°40'W	-1800	130
32	27°20'N	113°52'W	-1620	130
33	28°47'N	114°41'W	-1440	130
34	30°00'N	115°54'W	-1260	115

points are shown in Figure 2. The alongshore separation of adjacent coastal grid points is 180 km, sufficient to resolve the smallest spatial scales in the LFM analyzed wind fields. Information on sea level stations is summarized in Table 3, and their locations are shown in Figure 3. Atmospheric pressure stations (Bakun and measured) used to adjust these sea level time series are also listed in Table 3.

Alongshore position is determined as follows: The CODE central line is assigned a position of 0 km, with alongshore distances poleward of this line assigned positive values.

B.2 Data Editing and Processing

Assembling the CODE large-scale data base from many diverse sources requires considerable effort to edit and process the data. Characteristics of source meteorological data and analyzed meteorological fields are summarized in Table 4. (Important abbreviations in this table are listed and explained at the bottom of the table.) Only pressure and winds are routinely processed, except for Bakun wind stress curl plus air and sea surface temperatures at the NDBO buoys.

The basic editorial procedure is as follows:

1. Transcribe manuscript data or teletype output onto computer coding forms, then keypunch.

2. Read source magnetic tapes or computer cards into the computer. For a given time series, if no source data are available at a given time, the value of the cell of the one-dimensional array containing the time series in the core is filled with a missing data spacer (the number 10^{35}).

3. Convert source winds to u and v components, if necessary.

4. Convert all variables to common units (mb for pressure and m/s for wind).

5. Check for physically unrealistic data values for each variable. If any exist, replace these values by a missing data spacer.

6. Search for unusual data jumps or spikes by flagging all points in a time series that differ from either the point before or after it by more than three standard deviations of all first-differences. Determination of whether these data jumps are due to one or more bad data values is made by visual inspection of each flagged point with nearby points in the series. If a point is determined to be bad, it is replaced by a missing data spacer.

CODE ANALYSIS GRID

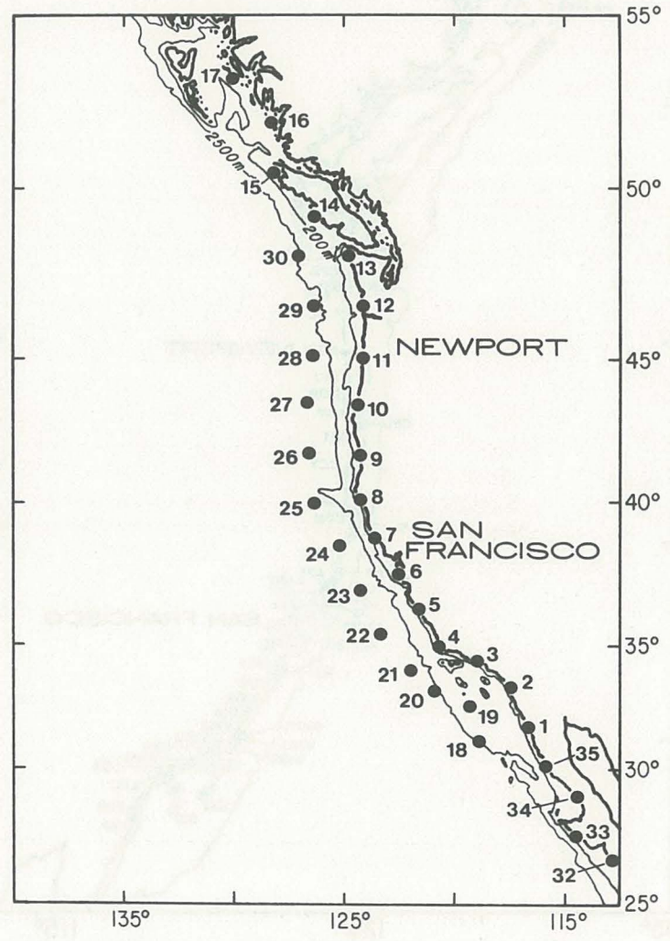

Figure 2

TABLE 3: Coastal Sea Level Station Information

Station	Abbreviation	Latitude (Deg Min)	Longitude (Deg Min)	Alongshore Position (km)	Period of Record	(1) Atmospheric Pressure Station Used to Barometrically Adjust
Prince Rupert, BC	PRR	54°19'N	130°20'W	1883	12/80-Present(2)	CG17
Bella Bella, BC	BBL	52°10'N	128°08'W	1608	12/80-Present	CG16
Zebelos, BC	ZBL	50°01'N	126°47'W	1349	12/80-Present	CG14
Tofino, BC	TOF	49°09'N	125°55'W	1232	12/80-Present	CG14
Bamfield, BC	BAM	48°49'N	125°06'W	1164	12/80-Present	CG14
Port Renfrew, BC	REN	48°33'N	124°24'W	1110	12/80-Present	QUI
Neah Bay, WA	NBA	48°22'N	124°37'W	1100	12/80-Present	QUI
Toke Point, WA	TKP	46°42'N	123°58'W	911	12/80-Present	HOQ
Astoria, OR	AST	46°10'N	123°46'W	852	12/80-Present	AST
South Beach, OR	SBC	44°38'N	124°03'W	683	12/80-Present	NEW
Charleston, OR	CHR	43°20'N	124°19'W	538	12/80-Present	NOB
Crescent City, CA	CCY	41°45'N	124°11'W	359	12/80-Present	CCY
Trinidad Head, CA	TRH	41°03'N	124°09'W	277	12/80-Present	ARC
North Spit, CA	NSP	40°45'N	124°14'W	244	12/80-Present	ARC
Arena Cove, CA	ARC	38°55'N	123°43'W	37	12/80-Present	CG7
Point Reyes, CA	PRY	38°00'N	122°58'W	-76	12/80-Present	46012
San Francisco, CA	SFO	37°48'N	122°28'W	-126	12/80-Present	46012
Monterey, CA	MRY	36°36'N	121°53'W	-276	12/80-Present	MRY
Port San Luis, CA	PSL	35°10'N	120°45'W	-473	12/80-Present	46011
Rincon Island, CA	RIS	34°21'N	119°27'W	-650	12/80-Present	SBA
Santa Monica, CA	SMA	34°01'N	118°27'W	-739	12/80-Present	LOS
Los Angeles, CA	LOS	33°43'N	118°16'W	-780	12/80-Present	LBC
La Jolla, CA	LAJ	32°55'N	117°51'W	-920	12/80-Present	SDO
San Diego, CA	SDO	32°45'N	117°10'W	-938	12/80-Present	SDO

Notes:

(1) Bakun pressure was used at the CODE analysis grid points.
(2) "Present" indicates that data will be collected at least through 11/82 unless the station is shut down.

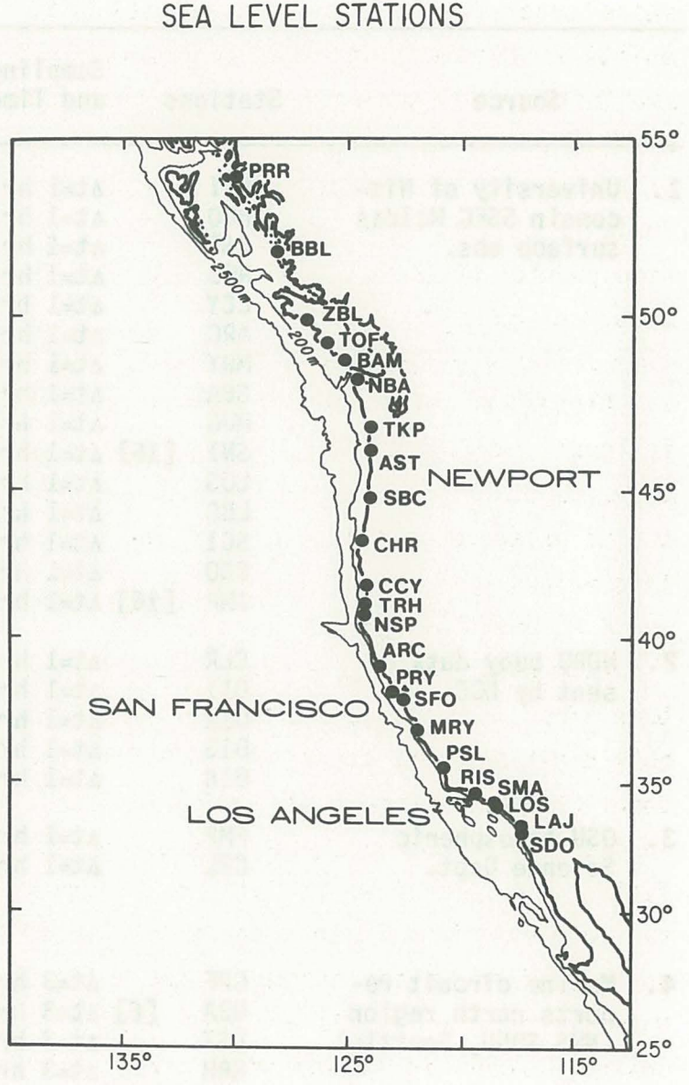

Figure 3

TABLE 4: Meteorological Data Source Information

	Source	Stations	Sampling Times and Time Zone	Source Format	Source Units: Pressure	Source Units: Winds	Other Variables Received
1.	University of Wisconsin SSEC McIdas surface obs.	QUI HOQ AST NOB CCY ARC MRY SBA MUG SNI [16] LOS LBC SCI SDO IMP [16]	Δt=1 hr(1) GMT Δt=1 hr(1) Δt=1 hr(1) Δt=1 hr(1)(2) Δt=1 hr(1) Δt=1 hr(1) Δt=1 hr(1) Δt=1 hr(1) Δt=1 hr(1)(3) Δt=1 hr(1) Δt=1 hr(1) Δt=1 hr(1) Δt=1 hr(1) Δt=1 hr(1)(4)	card-image magnetic tape	altimeter setting	speed - knots direction-degree clockwise from N	air temperature relative humidity precipitation visibility
2.	NDBO buoy data sent by NCC	CLR 011 012 013 014	Δt=1 hr(1)(5) GMT Δt=1 hr(1) Δt=1 hr(1) Δt=1 hr(1) Δt=1 hr(1)	card-image magnetic tape in NDBO format containing data from all buoys worldwide	mb	speed - m/s direction-degree clockwise from N	air temperature dew point, weather visibility, sea surface temperature wave statistics
3.	OSU Atmospheric Science Dept.	FMP CBL	Δt=1 hr(1)(5) PST Δt=1 hr(1)(5)	card image disk file	(none)	speed - knots direction-degree clockwise from N	(none)
4.	Marine circuit reports north region (NWS SOSU, Seattle)	CPF NBA [6] DST GRH CPD [5] SIU [6]	Δt=3 hr(1)(5) Δt=3 hr(1)(3)(5) GMT Δt=3 hr(1)(5) Δt=3 hr(1)(5) Δt=3 hr(1)(3)(5) Δt=3 hr(1)(3)(5)	teletype output (coded and keypunched)	(none)	speed - knots direction - 16 pt.(6)	wave height(7) air temperature

TABLE 4: Meteorological Data Source Information (Continued)

Source	Stations	Sampling Times and Time Zone	Source Format	Source Units: Pressure	Source Units: Winds	Other Variables Received
5. Marine circuit reports-south region (NWS WSFO Redwood City)	ARL PIG SUR	Δt=1 hr(1)(5) GMT Δt=1 hr(1)(5) Δt=1 hr(1)(5)	teletype output (coded and keypunched)	(none)	speed - knots direction - 16 pt(6)	(none)
6. Meteorological data logs from NCC	TIL [5] HUM PCB PIL PIN	Δt=3 hr(1)(3)(5) PST Δt=3 hr 07,10,13,16,19(1) Δt=3 hr(5)(8) Δt=3 hr	marine coastal weather log (coded and keypunched)	(not digitized)	speed - knots direction - 16 pt.(6)	sky condition visibility sea state air temperature
7. Batelle NW Labs wind tower data.	CBT ART	Δt=1 hr(1)(5) PST Δt=1 hr(1)(5)	card-image magnetic tape	(none)	speed - m/s direction-degree clockwise from N	(none)
8. OSU Oceanography	NEW	Δt=1 hr GMT	card-image magnetic tape	mb	u,v - m/s	(none)
9. Pacific Gas and Electric	DIA	Δt=1 hr(1)(5) PST	card-image magnetic tape	(none)	speed - mph direction-degree clockwise from N	dew point air temperature visibility
10. Vandenberg WINDS anemometer tower data	V102 V301 V302 V103	Δt=30 min(5) GMT	card-image magnetic tape containing data from 23 towers	(none)	speed - knots direction-degree clockwise from N	air temperature
11. Scripps Institution of Oceanography	BML	Δt=1 hr PST	card-image magnetic tape	(none)	speed - cm/s direction-degree clockwise from N	(none)

TABLE 4: Meteorological Data Source Information (Continued)

Source	Stations	Sampling Times and Time Zone	Source Format	Source Units: Pressure	Source Units: Winds	Other Variables Received
12. WHOI CODE anemometers	CLI C3 C5 R3	Δt=1 hr GMT	card-image magnetic tape	(none)	speed - m/s direction-degree clockwise from N	(none)
13. University of Washington	OSH	Δt=1 hr GMT	card-image magnetic tape	(none)	speed - m/s direction-degree clockwise from N	(none)
14. University of British Columbia	CSJ	Δt=1 hr PST				(none)
15. San Luis Obispo Air Pollution Control District	MOR	Δt=1 hr PST	hardcopy data forms	(none)	speed - m/s direction-degree clockwise from N	(none)
16. FNOC/Compass Systems, Inc. Bakun Data	35-pt. CODE Grid	Δt=6 hr GMT	card-image magnetic tape	mb	u(m/s) v(m/s)	wind stress divergence, wind stress curl Ekman transport Sverdrup Transport
17. NCAR LFM-II Meteorological Fields	35-pt. CODE Grid	Δt=12 hr GMT	IBM format packed data on magnetic tape	mb	u(m/s) v(m/s) (6 hr. forecast)	(none)

Notes:

(1) Occasional (< 20 percent) missing data reports. For the SSEC University of Wisconsin data set, most missing reports were due to down time of the McIDAS computers at Wisconsin used for real-time data collection.

(2) After mid-July 1981, station did not record data at night.

TABLE 4: Meteorological Data Source Information (Continued)

Notes (Continued):

(3) The station did not record data at night. The number of reports per day are given in brackets.

(4) The station did not record data at night or on weekends. The number of reports per day during the week are given in brackets.

(5) Long data gaps (> 1 day) occurred occasionally.

(6) N, NNE, NE, etc.

(7) Not at all stations.

(8) Frequent (> 20 percent) missing data reports.

(9) The direction toward which wind is blowing.

Important Abbreviations

FNOC = Fleet Numerical Oceanography Center
LFM-II = The Limited Fine Mesh-II numerical weather forecast model.
NCC = National Climatic Center
NDBO = National Data Buoy Office
NWS = National Weather Service
OSU = Oregon State University
SOSU = Seattle Ocean Services Unit
SSEC = Space Science and Engineering Center, University of Wisconsin
WSFO = Weather Service Forecast Office

7. All short data gaps ($\leq$ 24 hrs in length) are filled using linear interpolation. The missing data spacers in these gaps are replaced by interpolated data.

8. The time zone is adjusted to GMT where necessary.

9. Wind speed is adjusted to an anemometer height of 10 m assuming neutral stability. The correction factor is a function of wind speed and anemometer height as contoured in Figure 4.

10. All time series are converted to a common sampling rate of Δt = 6 hr. Data with sampling rates of 12 hr are subsampled and data with sampling rates of < 6 hr are averaged over 6-hr windows.

11. Time series are plotted and checked.

Additionally, measured sea level data gaps longer than 24 hr in length are patched by linear interpolation using the closest stations to the north and south as input, Table 5. Tests indicate that simple linear interpolation works as well as cubic spline interpolation as long as the poleward propagation of sea level fluctuations is taken into account. For each interpolation, the time lag between the two input stations that maximizes the correlation coefficient is determined. These time series are then

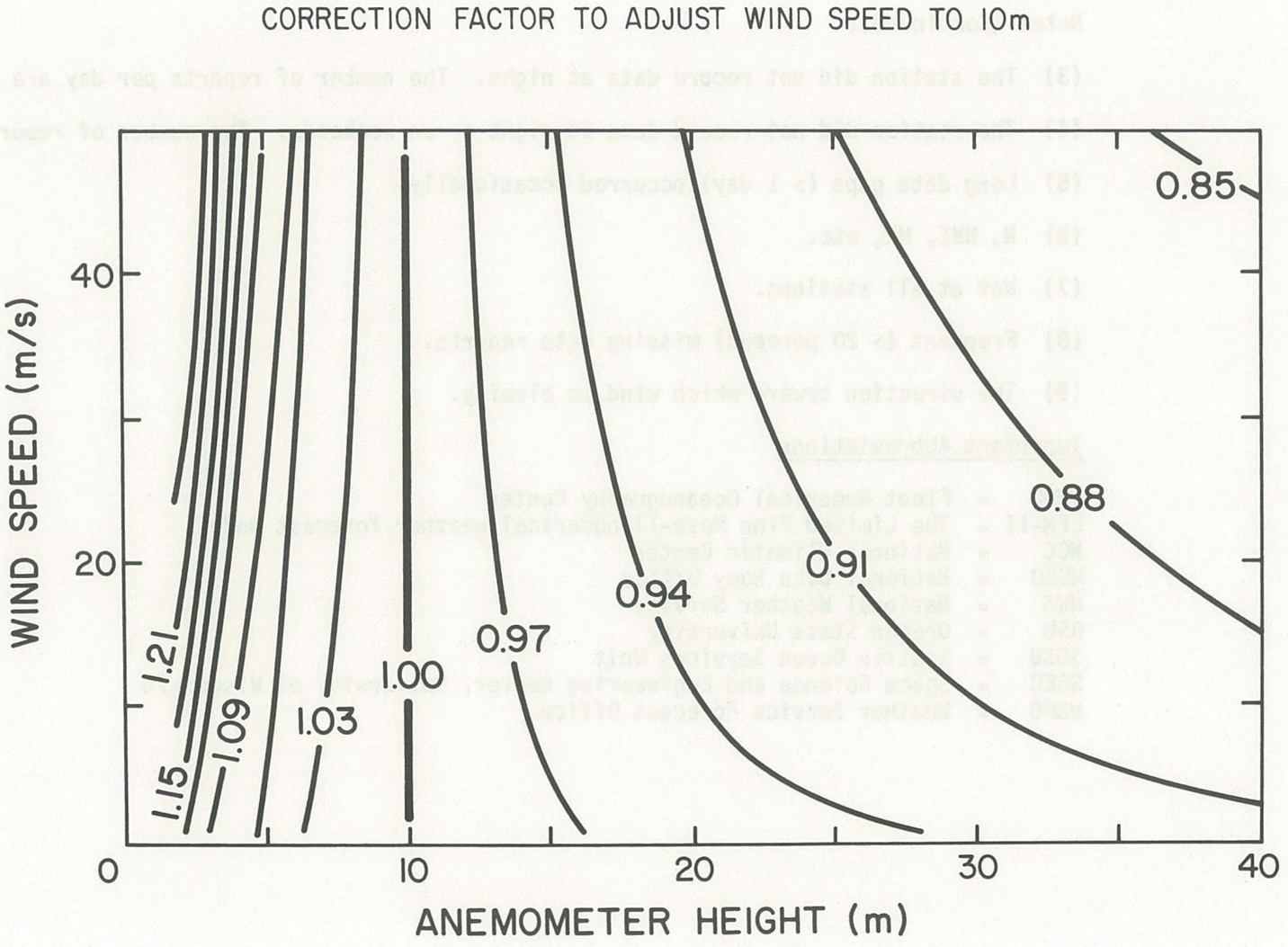

Figure 4

shifted in time relative to the interpolation point based on the relative distances of the interpolation point from the input stations, such that the sum of these two shifts equals the time shift that maximizes the correlation, Table 5. For filling gaps, the interpolation is performed only for the time interval of the gap. The entire time interval is used when time series of sea level are interpolated to the CODE analysis grid, Table 5.

C. WIND DATA

C.1 Statistical Summary of Measured Winds

Measured wind statistics for all available stations between 1 April and 31 July 1981 computed using 6-hr unfiltered data are summarized in Table 6. In addition to the basic statistics of the u and v components, principal axes and coastline orientations, plus standard deviations of the principal axes wind components, are included. A summary of data gaps is also presented.

C.2 Plots of Measured and Bakun Winds

Three sets of 40-hr low-passed wind plots are presented. Data are filtered with a symmetric Cosine-Lanczos filter, Mooers et al. (1968). First, vector plots of meas-

TABLE 5: Interpolation of ASL for Patching Gaps and Creating Time Series of ASL on the CODE Grid.

Station Interpolated to	Input Station 1	Input Station 2	Time Shift (hr)	Time Interval
NSP	ARC	TRH	18	06/26/1800 - 07/31/1800
ZBL	TOF	BBL	6	07/22/0600 - 07/31/1800
CG02	LAJ	LOS	0	12/80-Present(1)
CG03	LOS	RIN	0	12/80-Present
CG04	RIN	PSL	0	12/80-Present
CG05	PSL	MRY	6	12/80-Present
CG06	MRY	SFO	0	12/80-Present
CG07	PRY	ARC	6	12/80-Present
CG08	ARC	NSP	24	12/80-Present
CG09	CCY	CHR	0	12/80-Present
CG10	CHR	SBC	0	12/80-Present
CG11	SBC	AST	6	12/80-Present
CG12	AST	NBA	6	12/80-Present
CG13	AST	NBA	12	12/80-Present
CG14	TOF	ZBL	0	12/80-Present
CG15	ZBL	BBL	6	12/80-Present
CG16	BBL	PRR	6	12/80-Present
CG17	BBL	PRR	6	12/80-Present

Notes:

(1) "Present" indicates that data will be interpolated at least through 11/82.

ured winds at 25 selected stations are presented in Figure 5. Second, major and minor axis plots of measured winds at the same stations are presented in Figure 6. (Refer to Table 6 for principal axis orientations.) Third, vector plots of Bakun winds at selected coastal grid points are presented in Figure 7 for comparison to the measured winds.

The selection of measured wind stations for these plots is based on two criteria: First, enough stations are selected to avoid large gaps in coverage along the shelf as much as possible, and second, in a segment of the shelf where more than one station is available, the better station (i.e., the best exposed, or least influenced by topography) is selected. For Bakun winds, every other coastal grid point is adequate to plot due to high coherence at separation scales less than a few hundred kilometers.

The plotted time series begin at 1200 on 3 April and end at 0600 on 29 July since the low-pass filter requires 2.5 days to be discarded at each end. This also increases the length of each internal data gap by five days, so the gaps in these plots are longer than indicated in Table 6.

TABLE 6: Measured Winds

Station	Alongshore Position (km)	Coast[1] Orientation	Data Gap Summary			Percent Good Data	Principal[1] Axes		Principal Axes Std Dev (m/s)		Wind Components	u,v Basic Statistics (m/s)			
			Number	Start Time	End Time		Major	Minor	Major	Minor		Mean	Std Dev	Max	Min
Cape St. James	1800	138	None			100	136	46	7.48	3.53	u	2.71	5.92	18.1	-17.4
											v	0.34	5.78	18.4	-12.1
Cape Flattery	1104	120	1	05/24/0600	05/27/1800	70	83	-7	3.38	2.31	u	0.94	3.37	14.1	-8.4
			2	06/14/0600	06/16/0000						v	1.89	2.33	8.6	-3.1
			3	07/01/0000	07/31/1800										
Neah Bay	1101	120	None			100	179	89	2.93	1.74	u	2.01	2.93	13.5	-6.0
											v	0.11	1.74	5.3	-6.2
Quillayute	1055	110	None			100	120	30	1.76	1.38	u	0.99	1.49	6.7	-3.0
											v	0.80	1.68	6.0	-3.3
Destruction Island	1022	110	1	05/24/0600	05/27/1800	72	144	54	3.47	2.03	u	0.62	3.05	8.9	-10.4
			2	07/01/0000	07/31/1800						v	0.13	2.62	8.8	-8.2
Hoquiam	942	95	None			100	149	59	3.10	1.98	u	2.36	2.86	9.1	-6.2
											v	-0.51	2.33	6.7	-6.8
Ocean Shores	939	95	1	07/08/1200	07/31/1800	81	155	65	2.79	2.02	u	1.89	2.68	10.6	-4.9
											v	0.34	2.17	8.4	-5.4
Grays Harbor	936	95	None			100	96	6	3.77	2.68	u	2.39	2.70	10.0	-7.9
											v	-0.78	3.76	12.4	-10.1
Cape Disappointment	865	90	None			100	99	9	4.50	2.76	u	2.13	2.82	13.5	-10.6
											v	0.55	4.47	15.3	-8.2
Columbia River LNB	854	90	1	04/01/0000	06/10/1800	31	I.D.	I.D.				(Insufficient Data)			
			2	07/19/0000	07/31/1800										
Astoria	850	90	None			100	141	51	2.78	2.19	u	1.88	2.56	8.8	-4.3
											v	1.02	2.45	9.1	-6.2
Tillamook Bay	786	84	1	07/01/0600	07/31/1800	75	97	7	4.91	2.59	u	0.95	2.64	8.3	-7.0
											v	0.14	4.89	12.6	-15.3
Newport	683	82	None			100	49	-41	3.59	1.71	u	0.70	2.68	10.7	-5.3
											v	-1.18	2.95	7.1	-10.4
Suislaw River	612	81	1	07/01/0600	07/31/1800	75	93	3	5.00	2.20	u	1.44	2.22	8.4	-5.4
											v	-1.06	5.00	15.9	-15.9
North Bend	547	73	None			100	106	16	3.56	1.59	u	1.30	1.87	7.9	-2.9
											v	-1.96	3.83	7.6	-13.0
Five Mile Point	525	73	1	04/01/0000	04/17/0000	73	81	-9	4.74	1.58	u	0.23	1.72	8.5	-4.3
			2	04/23/1800	04/30/1200						v	-3.12	4.70	12.0	-14.3
			3	07/03/0000	07/13/0000										

TABLE 6: Measured Winds (Continued)

Station	Alongshore Position (km)	Coast[1] Orientation	Data Gap Summary			Percent Good Data	Principal[1] Axes		Principal Axes Std Dev (m/s)		Wind Components	u,v Basic Statistics (m/s)			
			Number	Start Time	End Time		Major	Minor	Major	Minor		Mean	Std Dev	Max	Min
Cape Blanco Tower	480	90	1	04/09/1800	04/22/1800	89	89	-1	4.21	1.08	u	-0.34	1.09	3.3	-2.8
											v	-2.94	4.21	12.4	-11.7
Cape Blanco	480	90	1	04/11/1800	04/15/1800	85	82	-8	5.92	1.44	u	-0.73	1.67	6.7	-4.7
			2	07/07/0600	07/20/1800						v	-3.00	5.86	19.4	-11.9
Crescent City	362	103	None			100	103	13	3.97	1.05	u	0.98	1.36	5.9	-2.9
											v	-2.08	3.89	6.9	-15.0
Arcata	270	75	None			100	106	16	2.92	1.29	u	0.80	1.47	5.3	-3.7
											v	-2.00	2.83	4.7	-10.3
Humboldt Bay	246	75	None			100	96	6	3.99	1.84	u	1.16	1.88	6.0	-4.7
											v	-2.81	3.97	7.2	-18.2
Point Cabrillo	87	90	1	06/04/0600	06/07/0000	96	121	31	2.97	1.43	u	1.27	1.96	10.0	-3.3
			2	07/16/0000	07/18/0000						v	-2.19	2.66	6.1	-12.7
NDBO 46014	71	100	None			100	118	28	4.26	1.03	u	3.36	2.20	9.4	-3.0
											v	-6.29	3.79	5.8	-14.1
Point Arena Light	41	110	None			100	95	5	3.53	1.82	u	0.34	1.84	8.6	-6.9
											v	-5.12	3.52	10.2	-12.8
Point Arena Tower	37	110	1	04/01/0000	05/01/0600	46	115	25	3.38	0.82	u	2.54	1.62	6.2	-2.8
			2	05/11/1800	05/15/0000						v	-5.73	3.08	6.8	-10.2
			3	06/16/0000	07/02/0000										
				07/16/0600	07/31/1800										
Sea Ranch	0	133	None			100	127	37	5.37	2.15	u	2.90	3.68	16.9	-2.1
											v	-4.42	4.46	9.1	-14.1
C3	0	133	1	04/01/0000	04/12/0600	91	136	46	4.92	0.95	u	5.59	3.62	12.3	-3.4
											v	-5.40	3.48	5.0	-10.8
C5	0	133	1	04/01/0000	04/12/0600	91	119	29	4.05	0.90	u	4.52	2.10	7.5	-4.0
											v	-7.51	3.59	4.1	-13.2
R3	-35	133	1	04/01/0000	04/13/0600	90	144	54	4.52	0.81	u	5.49	3.68	11.6	-3.8
											v	-3.72	2.76	3.0	-8.3
Bodega Marine Lab	-46	133	None			100	106	16	3.76	1.40	u	1.40	1.68	8.3	-3.3
											v	-3.74	3.64	4.2	-14.5
NDBO 46013	-61	133	None			100	143	53	4.46	1.21	u	7.23	3.59	14.6	-3.2
											v	-4.96	2.92	5.0	-10.6
Pillar Point	-156	105	None			100	142	52	4.48	1.52	u	4.23	3.68	14.9	-7.2
											v	-2.64	3.00	4.5	-15.0

TABLE 6: Measured Winds (Continued)

Station	Alongshore Position (km)	Coast[1] Orientation	Data Gap Summary			Percent Good Data	Principal[1] Axes		Principal Axes Std Dev (m/s)		Wind Components	u,v Basic Statistics (m/s)			
			Number	Start Time	End Time		Major	Minor	Major	Minor		Mean	Std Dev	Max	Min
NDBO 46012	-171	105	None			100	121	31	3.55	1.02	u	3.40	2.04	10.6	-2.6
											v	-3.65	3.09	7.0	-10.9
Pigeon Point	-191	102	None			100	134	44	4.09	1.69	u	4.40	3.10	12.6	-5.9
											v	-3.25	3.17	8.9	-9.9
Point Pinos	-271	110	None			100	135	45	3.10	2.04	u	3.84	2.63	13.4	-3.5
											v	0.20	2.62	7.2	-8.2
Monterey	-278	110	None			100	159	69	1.81	0.97	u	1.97	1.73	8.3	-1.8
											v	-0.59	1.11	2.1	-4.3
Point Sur	-301	115	None			100	112	22	3.60	1.34	u	2.39	1.83	7.6	-3.6
											v	-5.09	3.37	7.1	-12.6
Morro Bay	-455	130	1	04/07/1200	04/09/1800	95	167	77	1.76	1.01	u	1.17	1.73	6.5	-5.5
			2	04/18/0000	04/10/1800						v	-0.25	1.06	1.8	-4.9
Diablo Canyon	-464	120	1	06/09/0600	06/16/1800	94	136	46	3.88	0.85	u	3.12	2.87	10.7	-3.5
											v	-3.05	2.74	4.2	-10.5
NDBO 46011	-506	90	None			100	128	38	3.36	1.01	u	3.65	2.21	9.3	-2.0
											v	-4.49	2.73	3.0	-10.1
VWT102	-524	90	1	04/17/0600	04/10/1800	51	124	34	2.17	1.01	u	1.85	1.48	5.9	-3.3
			2	04/28/1800	04/30/1800						v	-2.16	1.89	9.9	-7.7
			3	05/12/0600	07/02/1200										
			4	07/18/1200	07/10/1200										
VWT301	-540	90	1	04/17/0600	04/20/1800	51	121	31	1.98	1.24	u	0.90	1.48	4.6	-4.5
			2	04/28/1800	04/30/1800						v	-2.38	1.82	10.0	-7.0
			3	05/12/0600	07/02/1200										
			4	07/18/1200	07/20/1200										
VWT302	-545	90	1	04/17/0600	04/20/1800	49	81	-9	2.73	1.70	u	0.51	1.74	8.3	-4.7
			2	04/28/1800	04/30/1800						v	-5.59	2.71	4.7	-11.5
			3	05/12/0600	07/02/1200										
			4	07/18/1200	07/20/1200										
			5	07/25/0000	07/27/1200										
VWT103	-548	90	1	04/17/0600	04/20/1800	51	99	9	3.45	1.05	u	0.96	1.19	4.3	-3.3
			2	04/28/1800	04/30/1800						v	-4.02	3.41	2.8	-12.2
			3	05/12/0600	07/02/1200										
			4	07/18/1200	07/20/1200										

TABLE 6: Measured Winds (Continued)

Station	Alongshore Position (km)	Coast Orientation[1]	Data Gap Summary			Percent Good Data	Principal Axes[1]		Principal Axes Std Dev (m/s)		Wind Components	u,v Basic Statistics (m/s)			
			Number	Start Time	End Time		Major	Minor	Major	Minor		Mean	Std Dev	Max	Min
Santa Barbara	-623	175	None			100	80	-10	2.40	1.78	u	0.19	2.39	8.4	-5.0
											v	1.01	1.80	4.3	-8.9
Point Mugu	-678	155	None			100	161	71	1.96	1.34	u	1.37	1.91	8.2	-6.6
											v	0.01	1.41	6.1	-6.1
San Nicholas Island	-685	155	1	07/04/0600	07/05/1800	99	136	46	3.57	1.12	u	2.81	2.69	12.2	-3.8
											v	-3.02	2.61	4.3	-11.5
Los Angeles	-757	150	None			100	81	-9	2.52	0.85	u	2.29	2.50	7.6	-4.4
											v	0.85	0.93	3.7	-4.5
Long Beach	-785	150	None			100	133	43	2.26	1.55	u	1.00	1.91	8.2	-11.3
											v	1.15	1.96	12.8	-3.1
San Clemente Island	-825	130	None			100	149	59	2.54	1.39	u	2.64	2.29	10.3	-4.9
											v	0.53	1.78	6.9	-5.1
San Diego	-936	105	None			100	117	27	2.43	1.66	u	2.18	1.85	7.1	-3.0
											v	0.30	2.29	6.2	-4.9
Imperial Beach	-954	10	Many[2]			66	149	59	1.79	1.53	u	2.18	1.73	5.8	-2.9
											v	1.02	1.61	8.9	3.1

Notes:

(1) Angles are measured in degrees from due east; positive is counter-clockwise, negative is clockwise.

(2) Imperial Beach has 17 short gaps because it is closed on weekends.

D. COASTAL SEA LEVEL DATA

D.1 Statistical Summary of Adjusted Coastal Sea Level

Adjusted coastal sea level statistics for all available measurement stations are summarized in Table 7. Statistics for interpolated adjusted sea level at the CODE grid points are summarized in Table 8. Grid points CG02 through CG17 are the only coastal grid points within the alongshore domain of sea level stations. A data gap summary is also presented in Table 7. The statistics are computed for stations whose gaps have already been patched by linear interpolation of data from adjacent stations.

D.2 Plots of Adjusted Coastal Sea Level

Plots of 40-hr low-passed adjusted sea level time series are presented for selected stations (Figure 8). Enough stations are plotted to avoid large gaps in coverage along the shelf. As for the winds, the filtering altered the start and end times of the series. All data gaps have been filled with interpolated data prior to plotting.

E. ALONGSHORE-TIME CONTOUR PLOTS

Alongshore-time contour plots of Bakun alongshore windstress (Figure 9) and adjusted coastal sea level (Figure 10) are

TABLE 7: Measured Adjusted Coastal Sea Level (cm)

Station	Along-Shore Position (km)	Data Gap Summary			Percent Good Data	Mean[1]	Std Dev	Max	Min
		Number	Start Time	End Time					
Prince Rupert	1883	none			100	0	5.78	15.2	-14.8
Bella Bella	1608	none			100	0	4.91	12.5	-12.8
Zebelos	1349	1	07/22/0600	07/31/1800	92[2]	0	6.38	16.1	-19.7
Tofino	1232	none			100	0	4.95	10.2	-15.6
Bamfield	1164	none			100	0	4.00	8.5	-9.7
Port Renfrew	1110	none			100	0	4.22	8.7	-11.0
Neah Bay	1100	none			100	0	6.38	12.5	-16.1
Toke Point	911	none			100	0	9.98	25.3	-19.0
Astoria	852	none			100	0	9.15	21.7	-17.6
South Beach	683	none			100	0	5.99	13.3	-15.9
Charleston	538	none			100	0	4.95	9.9	-16.2
Crescent City	359	none			100	0	4.99	10.0	-20.2
Trinidad Head	277	none			100	0	4.63	11.2	-16.2
North Spit	244	1	06/26/1800	07/31/1800	71[2]	0	4.55	11.0	-15.2
Arena Cove	37	none			100	0	5.28	13.1	-13.9
Point Reyes	-76	none			100	0	6.00	13.2	-16.7
San Francisco	-126	none			100	0	4.50	9.2	-13.5
Monterey	-276	none			100	0	4.09	9.3	-9.7
Port San Luis	-473	none			100	0	4.56	10.6	-12.6
Rincon Island	-650	none			100	0	3.93	10.0	-14.0
Santa Monica	-739	none			100	0	3.99	10.2	-11.6
Los Angeles	-780	none			100	0	3.46	8.2	-12.5
La Jolla	-920	none			100	0	3.76	9.5	-11.0
San Diego	-938	none			100	0	3.46	8.4	-10.9

Notes:

(1) Sea level time series were demeaned.

(2) These gaps were filled by linear interpolation before these statistics were computed.

included to illustrate the response of sea level to wind stress fluctuations and the alongshore propagation of some sea level perturbations. Sea level interpolated to the CODE analysis grid are used. All series are 40-hr low-pass filtered, and have been daily averaged prior to contouring.

TABLE 8: Adjusted Coastal Sea Level (cm) Interpolated to the Code Analysis Grid

Station	Alongshore Position (km)	Mean	Standard Deviation	Maximum	Minimum
CG 17	1800	0	5.31	14.3	-13.8
CG 16	1620	0	4.89	12.6	-12.7
CG 15	1440	0	5.64	12.4	-17.0
CG 14	1260	0	5.10	11.4	-14.7
CG 13	1080	0	6.61	13.6	-16.2
CG 12	900	0	9.74	24.5	-18.9
CG 11	720	0	6.44	14.4	-16.4
CG 10	540	0	4.96	10.0	-16.2
CG 09	360	0	4.99	10.0	-20.1
CG 08	180	0	4.61	11.4	-13.2
CG 07	0	0	5.44	13.0	-14.9
CG 06	-180	0	4.32	9.2	-12.0
CG 05	-360	0	4.23	9.2	-10.8
CG 04	-540	0	4.20	10.2	-13.1
CG 03	-720	0	3.58	8.6	-13.2
CG 02	-900	0	3.68	9.2	-11.3

Acknowledgements

The authors wish to thank the following people for their assistance in obtaining or processing data: Dr. Thomas M. Whittaker, University of Wisconsin Space Science and Engineering Center; Dr. Chuck Wash, U.S. Naval Postgraduate School, who served as our initial contact to SSEC; Mr. Andrew Johnson, Mr. Lloyd Ladner, and Mr. Ray Canada of the National Data Buoy Office; Dr. John Wade and Mr. James R. Buckley, Atmospheric Science Department, OSU; Mr. Dave Young, Pacific Power and Light Company, Portland, OR, for obtaining permission to use the data at the OSU Atmospheric Science Department; Mr. Bob Anderson and Mr. Kent Short, National Weather Service, Seattle Ocean Services Unit; Mr. Karl K. Turner, National Weather Service Forecast Office, San Francisco; Dr. William F. Sandersky, Battelle Pacific Northwest Laboratories; Mr. W.E. Gilbert, OSU Oceanography, for processing Newport, OR data; Mr. Henry Pittock, OSU Oceanography, for processing coastal sea level data; Ms. Margaret L. Mooney, Pacific Gas and Electric Company, San Francisco; Major Glenn L. Moody, Vandenberg Air Force Base; Dr. Barbara M. Hickey and Mr. Jack Beck, University of Washington; Dr. Tom Yao, University of British Columbia; Mr. Paul Allen, San Luis Obispo County Air Pollution Control District; Mr. Dennis Joseph, National Center for Atmospheric Research (LFM analyses), and Mr. Arthur D. Stroud, Compass Systems, Inc. (Bakun data and marine winds). Dr. Donald Denbo, OSU, developed the plotting software. Mr. Lawrence C. Breaker is also thanked for helpful discussions on California coastal winds. This work has been supported by the National Science Foundation.

References

Bakun, A., 1973. Coastal Upwelling Indices, West Coast of North America, 1946-1971. NOAA Tech. Rep. NMFS SSRF-671, National Oceanic and Atmospheric Administration, National Marine Fisheries Services, Seattle, WA.

Caton, F. G., M. J. Cuming and B. R. Mendenhall, 1978. A northern hemisphere history of marine wind-based parameters. Tech. Rep. MII Project M-231, Meteorology International Inc., Monterey, CA.

Gerrity, J. F., Jr., 1977. The LFM Model - 1976: a documentation. NOAA Tech. Mem. NWS NMC 60, National Meteorological Center, Washington, D.C.

Mooers, C.N.K., L. M. Bogert, R. L. Smith, and J. G. Patullo, 1968. A compilation of observations from moored current meters and thermographs and of complementary oceanographic and and atmospheric data. OSU Data Rep. No. 30, Ref. 68-5, School of Oceanography, Oregon State University, Corvallis, OR.

Newell, J. E. and D. G. Deaven, 1980. The LFM-II model - 1980. NOAA Tech. Mem. NWS NMC 66, National Meteorological Center, Washington, D.C.

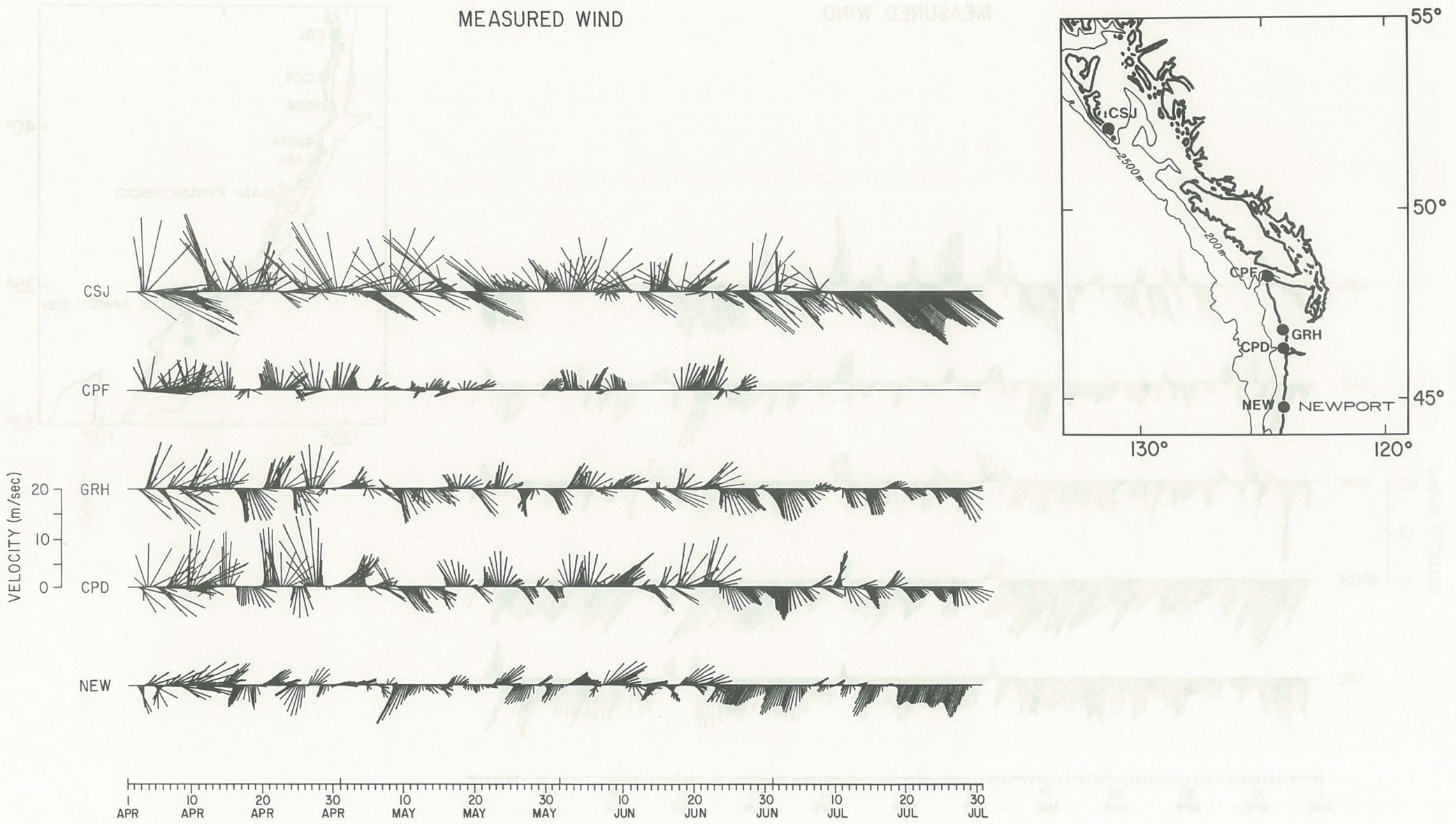
MEASURED WIND
CSJ
CPF
GRH
CPD
NEW
VELOCITY (m/sec)
20
10
0
1 APR
10 APR
20 APR
30 APR
10 MAY
20 MAY
30 MAY
10 JUN
20 JUN
30 JUN
10 JUL
20 JUL
30 JUL
55°
50°
45°
130°
120°
CSJ
2500 m
200 m
CPF
GRH
CPD
NEW
NEWPORT

Figure 5a

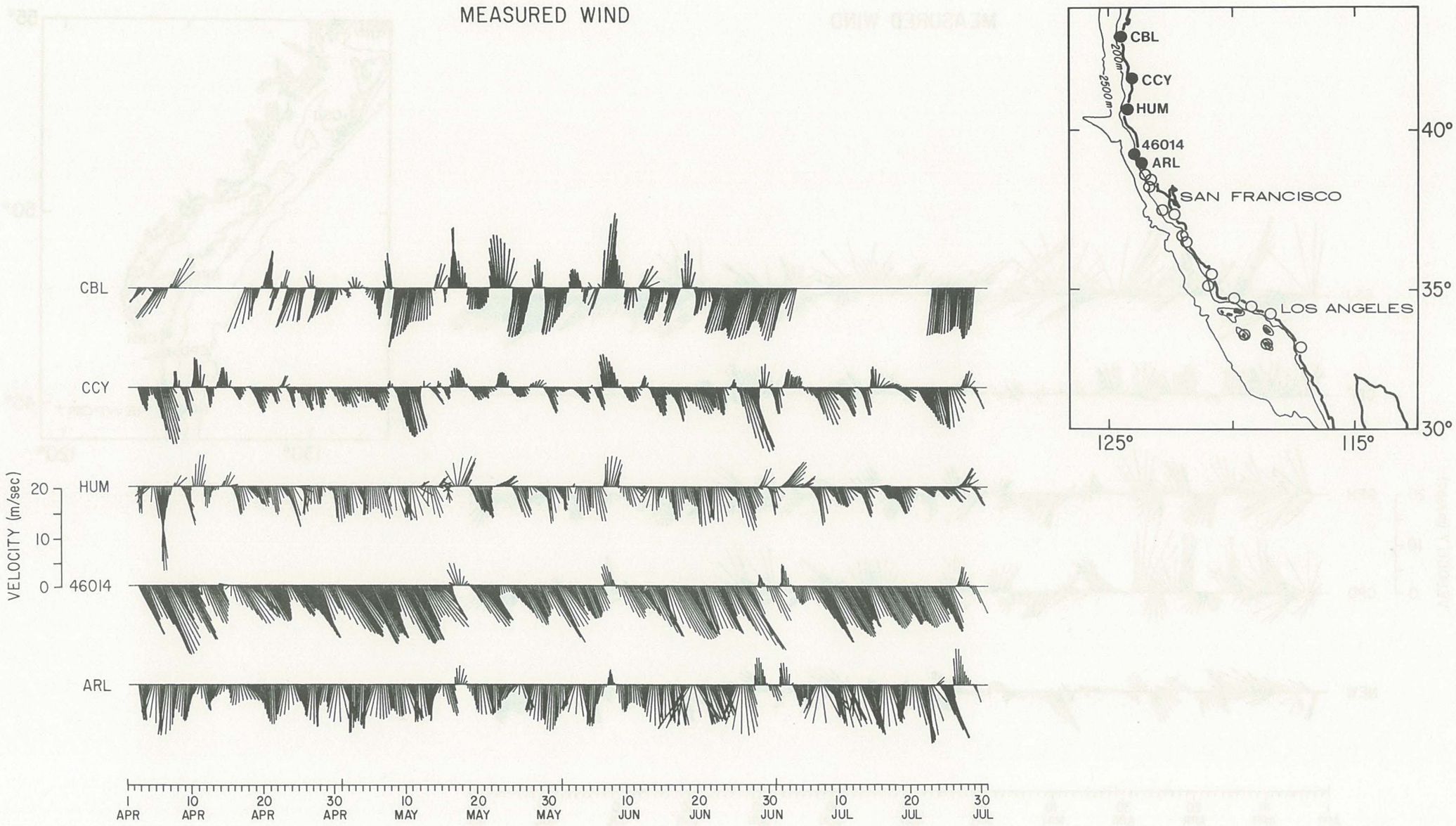
MEASURED WIND
CBL
CCY
HUM
46014
ARL
VELOCITY (m/sec)
20
10
0
1 APR
10 APR
20 APR
30 APR
10 MAY
20 MAY
30 MAY
10 JUN
20 JUN
30 JUN
10 JUL
20 JUL
30 JUL
200m
2500m
SAN FRANCISCO
LOS ANGELES
40°
35°
30°
125°
115°

Figure 5b

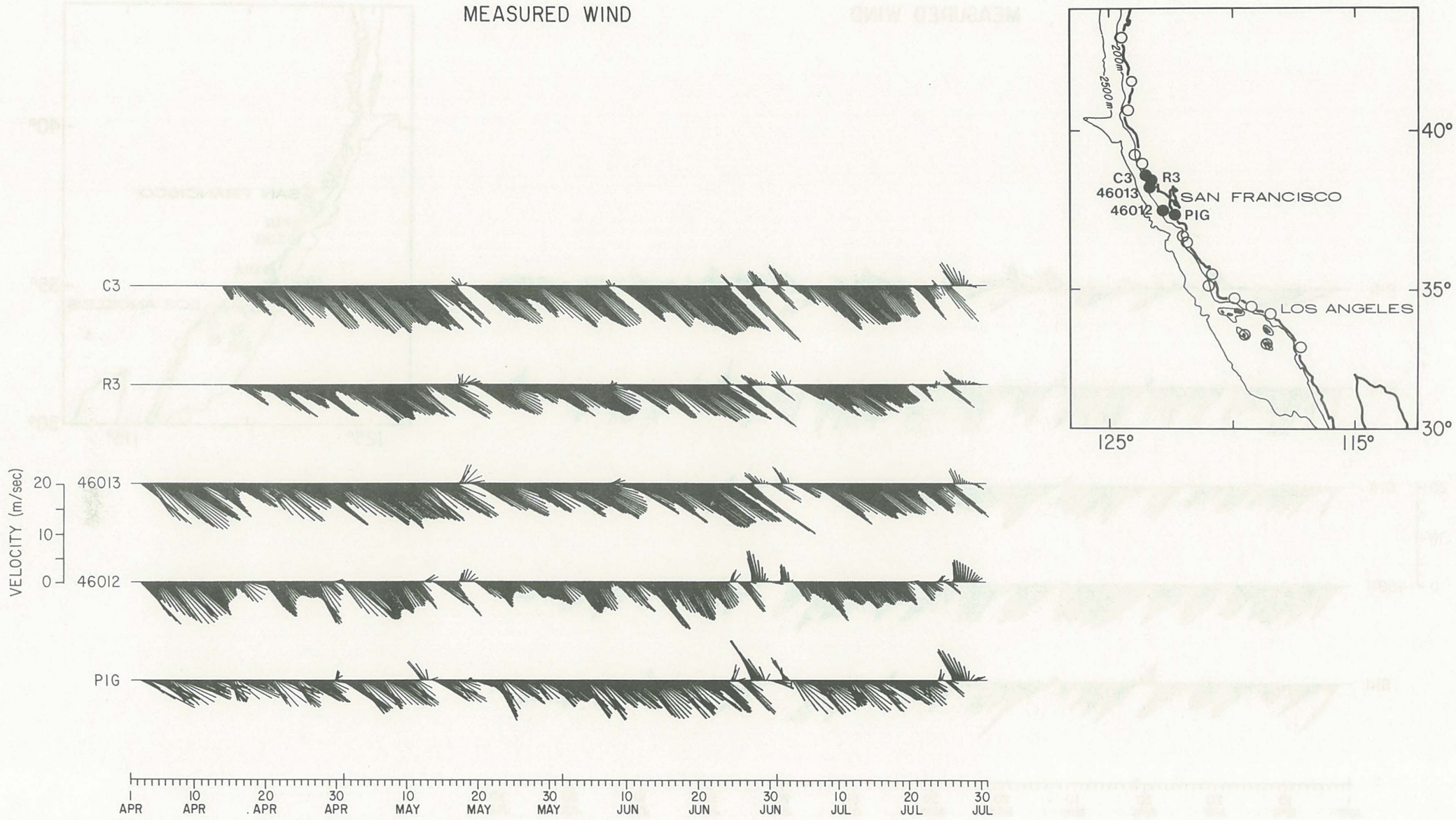
MEASURED WIND
C3
R3
46013
46012
PIG
VELOCITY (m/sec)
20
10
0
1 APR
10 APR
20 APR
30 APR
10 MAY
20 MAY
30 MAY
10 JUN
20 JUN
30 JUN
10 JUL
20 JUL
30 JUL
200m
2500m
C3
R3
46013
46012
PIG
SAN FRANCISCO
LOS ANGELES
40°
35°
30°
125°
115°

Figure 5c

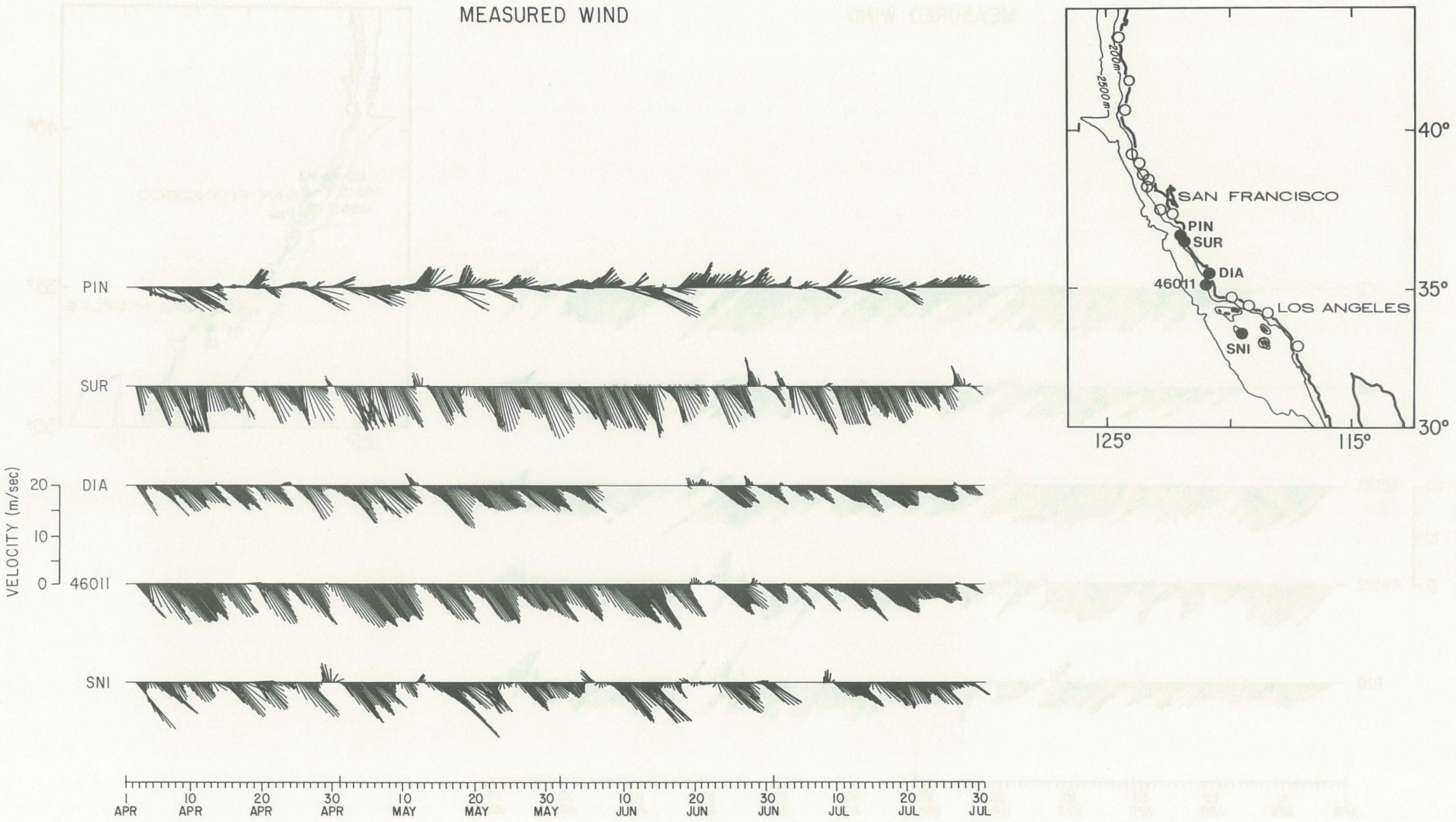
MEASURED WIND
PIN
SUR
DIA
46011
SNI
VELOCITY (m/sec)
20
10
0
1 APR
10 APR
20 APR
30 APR
10 MAY
20 MAY
30 MAY
10 JUN
20 JUN
30 JUN
10 JUL
20 JUL
30 JUL
200m
2500m
SAN FRANCISCO
PIN
SUR
DIA
46011
LOS ANGELES
SNI
40°
35°
30°
125°
115°

Figure 5d

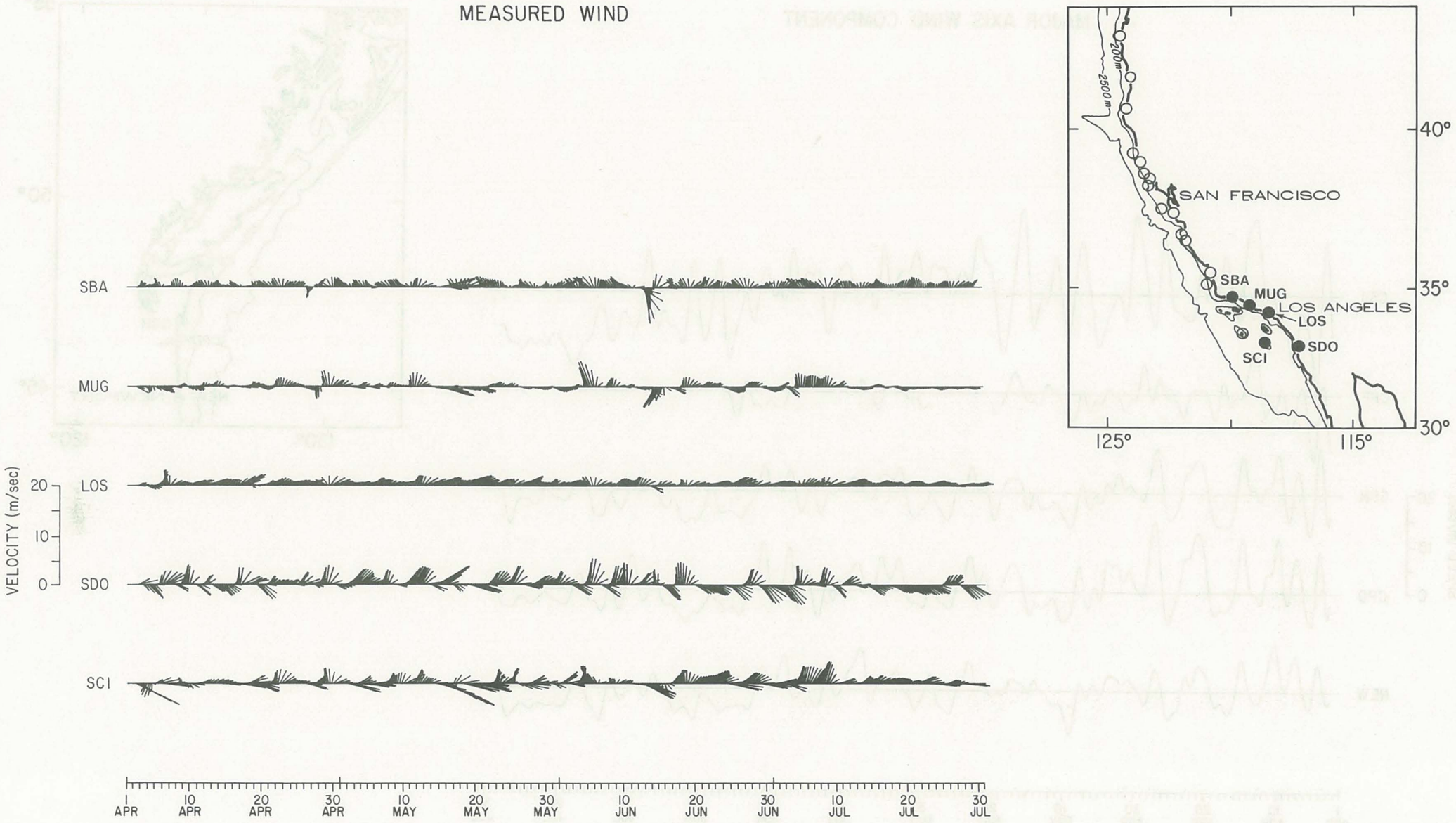
MEASURED WIND
SBA
MUG
LOS
SDO
SCI
VELOCITY (m/sec)
20
10
0
1 APR
10 APR
20 APR
30 APR
10 MAY
20 MAY
30 MAY
10 JUN
20 JUN
30 JUN
10 JUL
20 JUL
30 JUL
200m
2500m
SAN FRANCISCO
SBA
MUG
LOS ANGELES
LOS
SDO
SCI
40°
35°
30°
125°
115°

Figure 5e

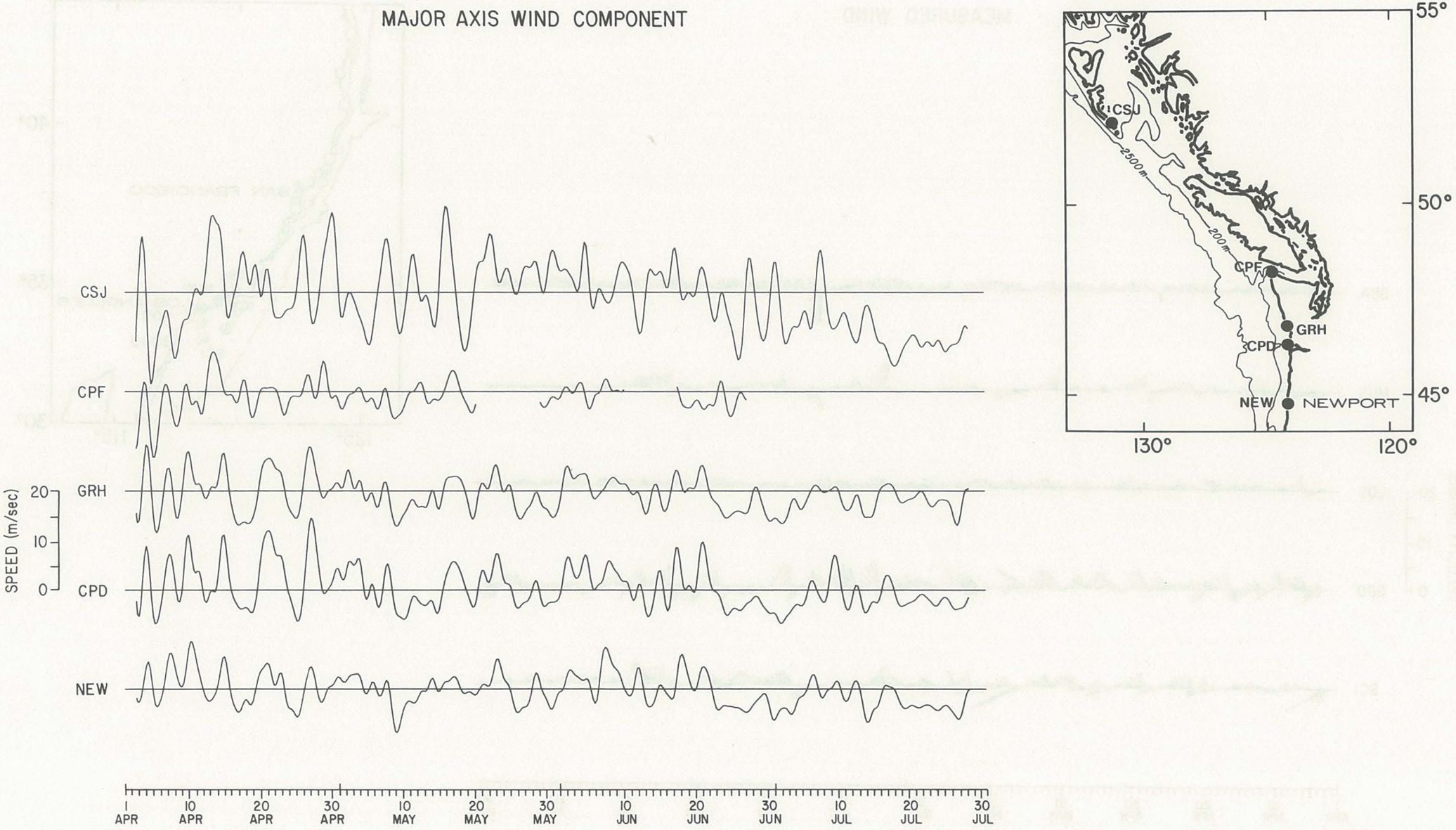
MAJOR AXIS WIND COMPONENT
CSJ
CPF
GRH
CPD
NEW
SPEED (m/sec)
20
10
0
1 APR
10 APR
20 APR
30 APR
10 MAY
20 MAY
30 MAY
10 JUN
20 JUN
30 JUN
10 JUL
20 JUL
30 JUL
55°
50°
45°
130°
120°
CSJ
2500m
200m
CPF
GRH
CPD
NEW
NEWPORT

Figure 6a

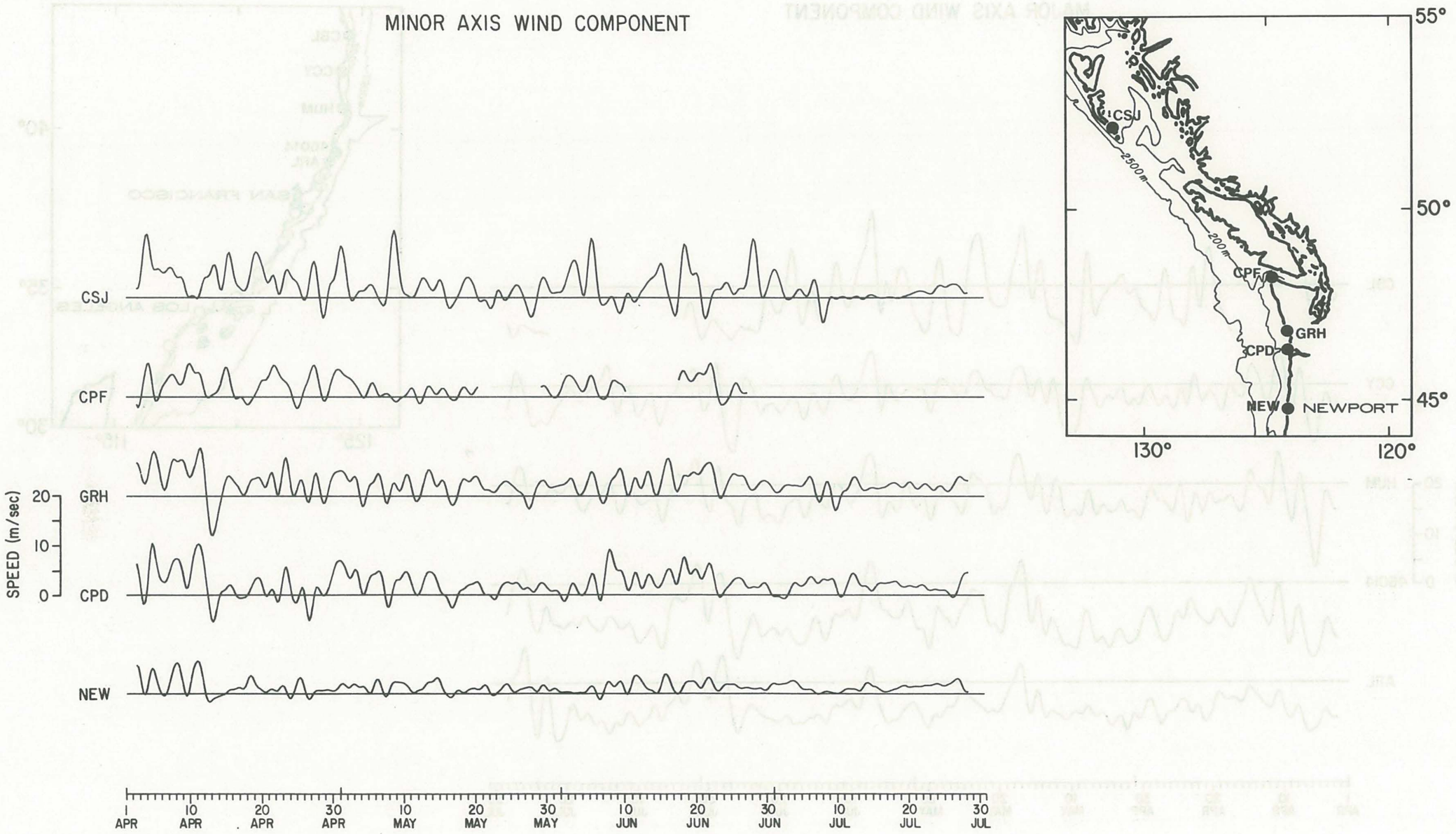
MINOR AXIS WIND COMPONENT
CSJ
CPF
GRH
CPD
NEW
SPEED (m/sec)
20
10
0
1 APR
10 APR
20 APR
30 APR
10 MAY
20 MAY
30 MAY
10 JUN
20 JUN
30 JUN
10 JUL
20 JUL
30 JUL
55°
50°
45°
130°
120°
CSJ
2500m
200m
CPF
GRH
CPD
NEW
NEWPORT

Figure 6b

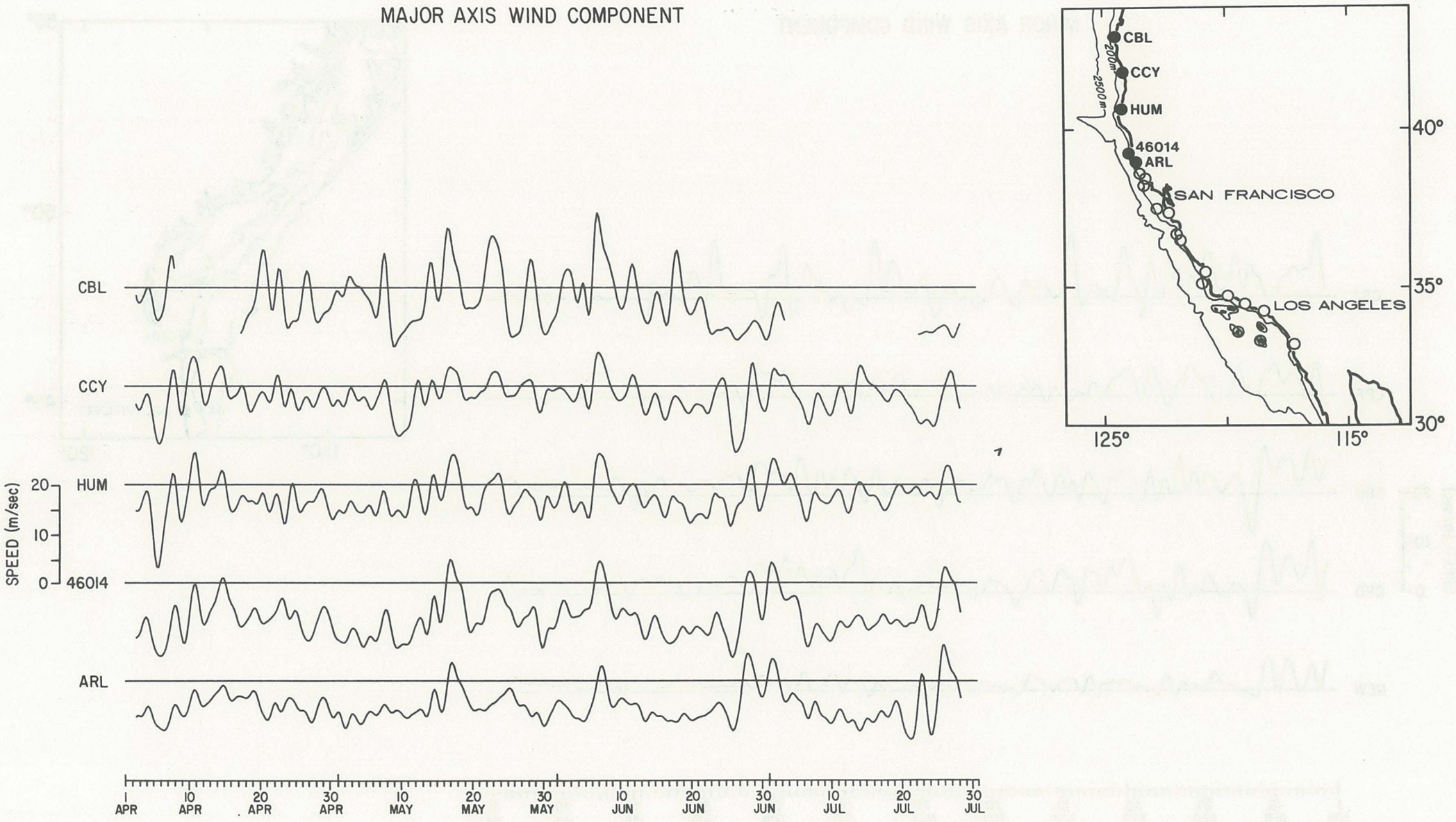
MAJOR AXIS WIND COMPONENT
CBL
CCY
HUM
46014
ARL
SPEED (m/sec)
20
10
0
1 APR
10 APR
20 APR
30 APR
10 MAY
20 MAY
30 MAY
10 JUN
20 JUN
30 JUN
10 JUL
20 JUL
30 JUL
CBL
CCY
HUM
46014
ARL
200m
2500m
SAN FRANCISCO
LOS ANGELES
40°
35°
30°
125°
115°

Figure 6c

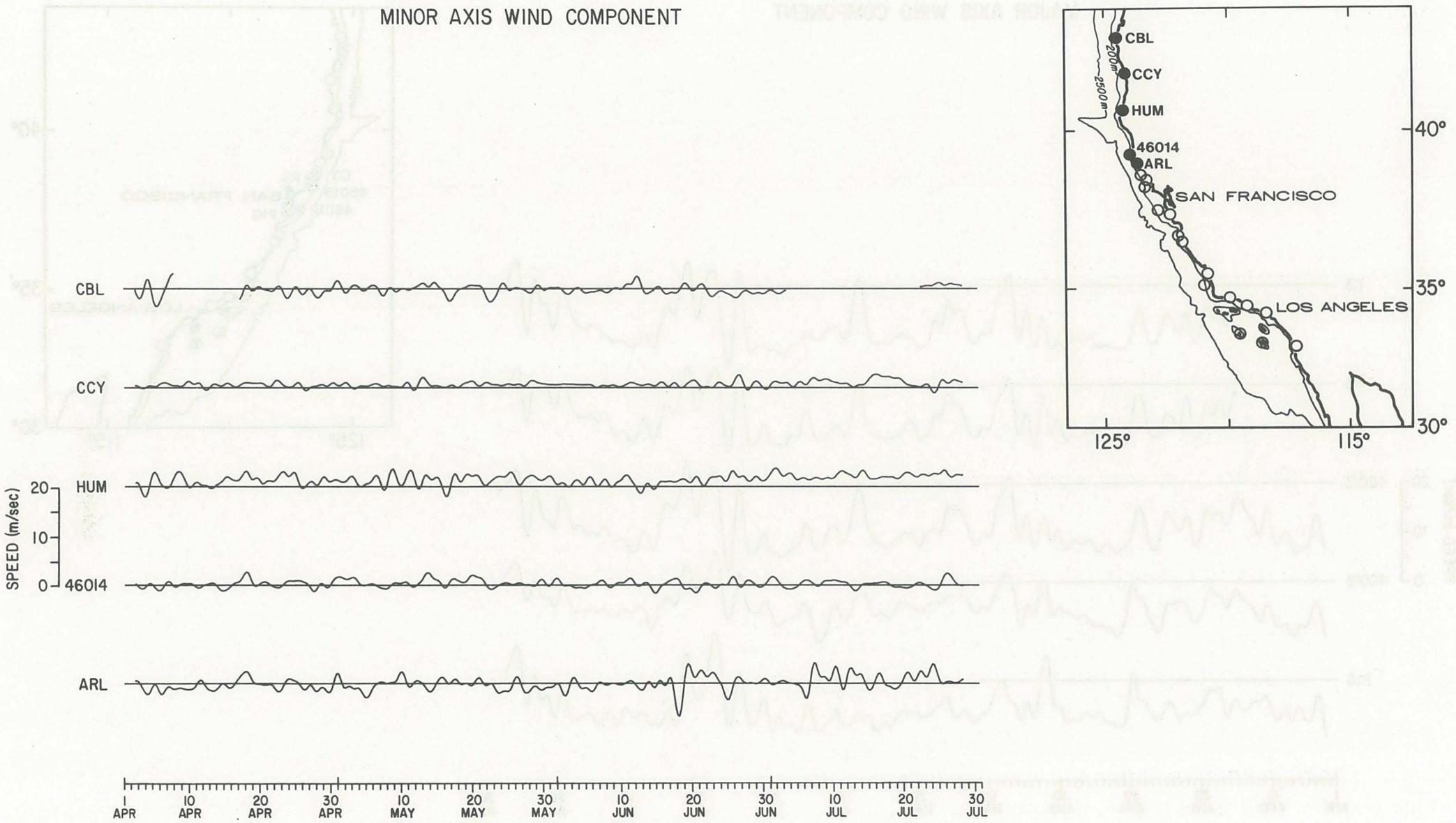
MINOR AXIS WIND COMPONENT
CBL
CCY
HUM
46014
ARL
SPEED (m/sec)
20
10
0
1 APR
10 APR
20 APR
30 APR
10 MAY
20 MAY
30 MAY
10 JUN
20 JUN
30 JUN
10 JUL
20 JUL
30 JUL
200m
2500m
SAN FRANCISCO
LOS ANGELES
40°
35°
30°
125°
115°

Figure 6d

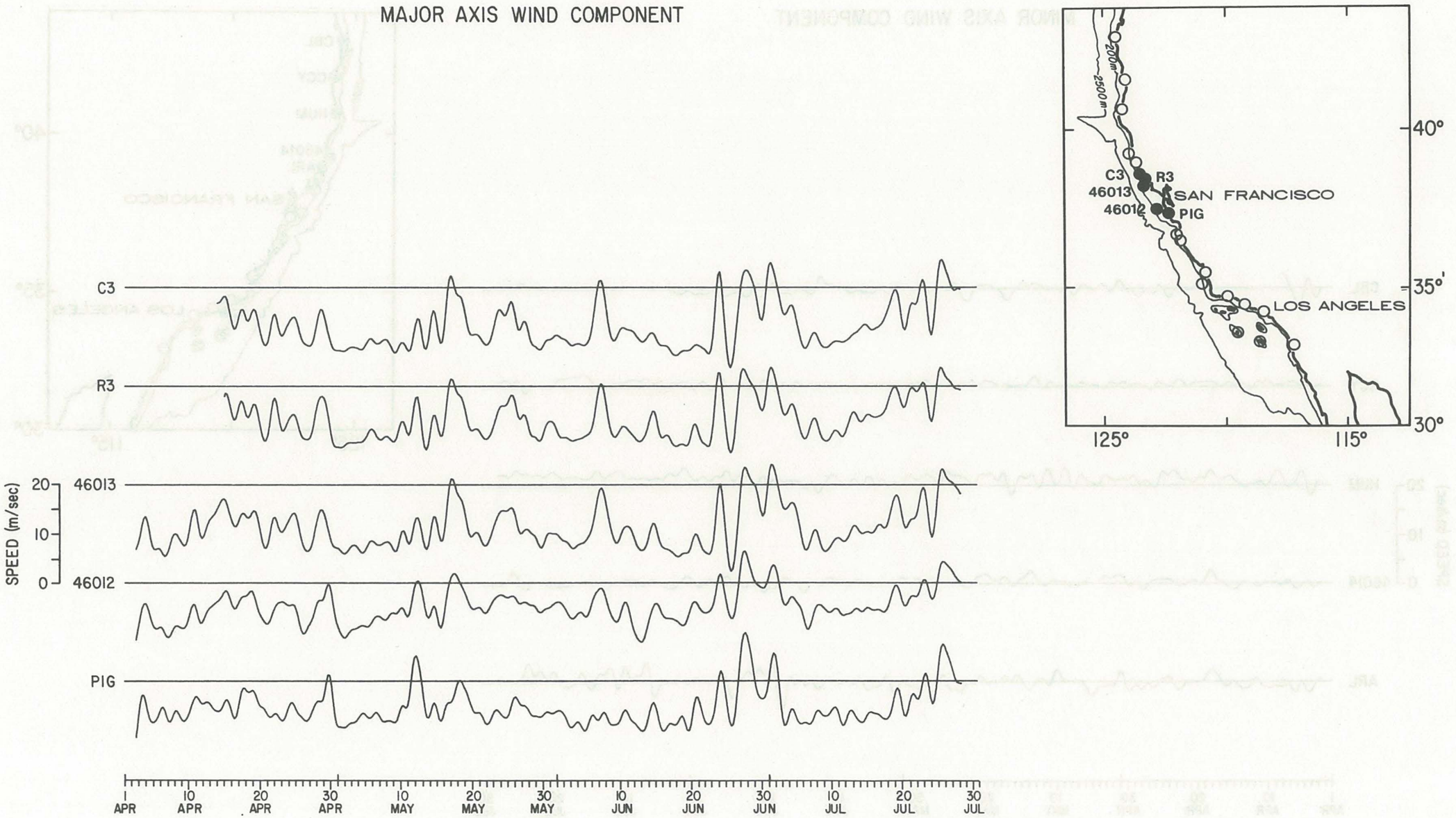
MAJOR AXIS WIND COMPONENT
C3
R3
46013
46012
PIG
SPEED (m/sec)
20
10
0
1 APR
10 APR
20 APR
30 APR
10 MAY
20 MAY
30 MAY
10 JUN
20 JUN
30 JUN
10 JUL
20 JUL
30 JUL
200m
2500m
C3
R3
46013
46012
PIG
SAN FRANCISCO
LOS ANGELES
40°
35°
30°
125°
115°

Figure 6e

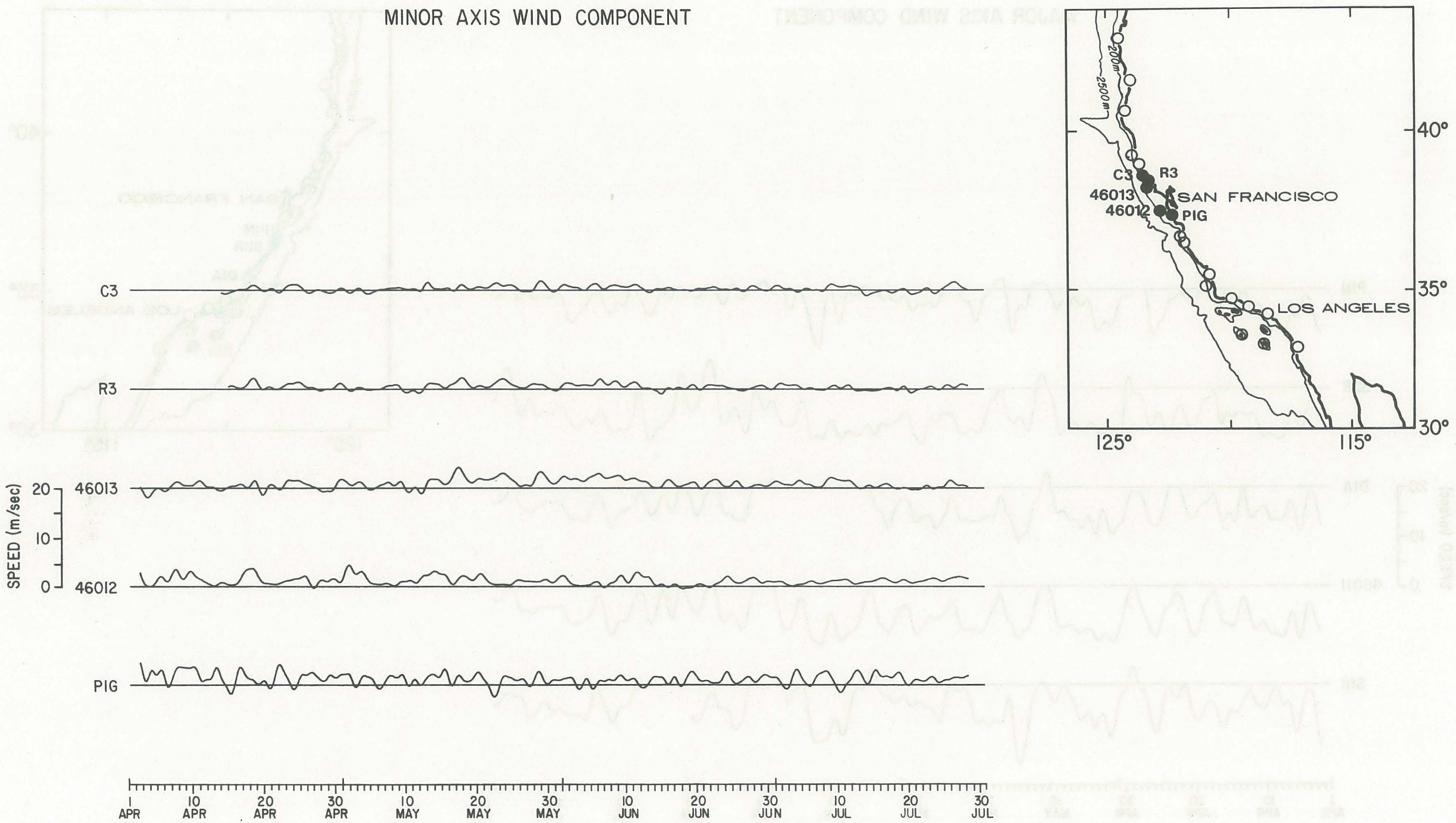
MINOR AXIS WIND COMPONENT
C3
R3
46013
46012
PIG
SPEED (m/sec)
20
10
0
1 APR
10 APR
20 APR
30 APR
10 MAY
20 MAY
30 MAY
10 JUN
20 JUN
30 JUN
10 JUL
20 JUL
30 JUL
200m
2500m
C3
R3
46013
46012
PIG
SAN FRANCISCO
LOS ANGELES
40°
35°
30°
125°
115°

Figure 6f

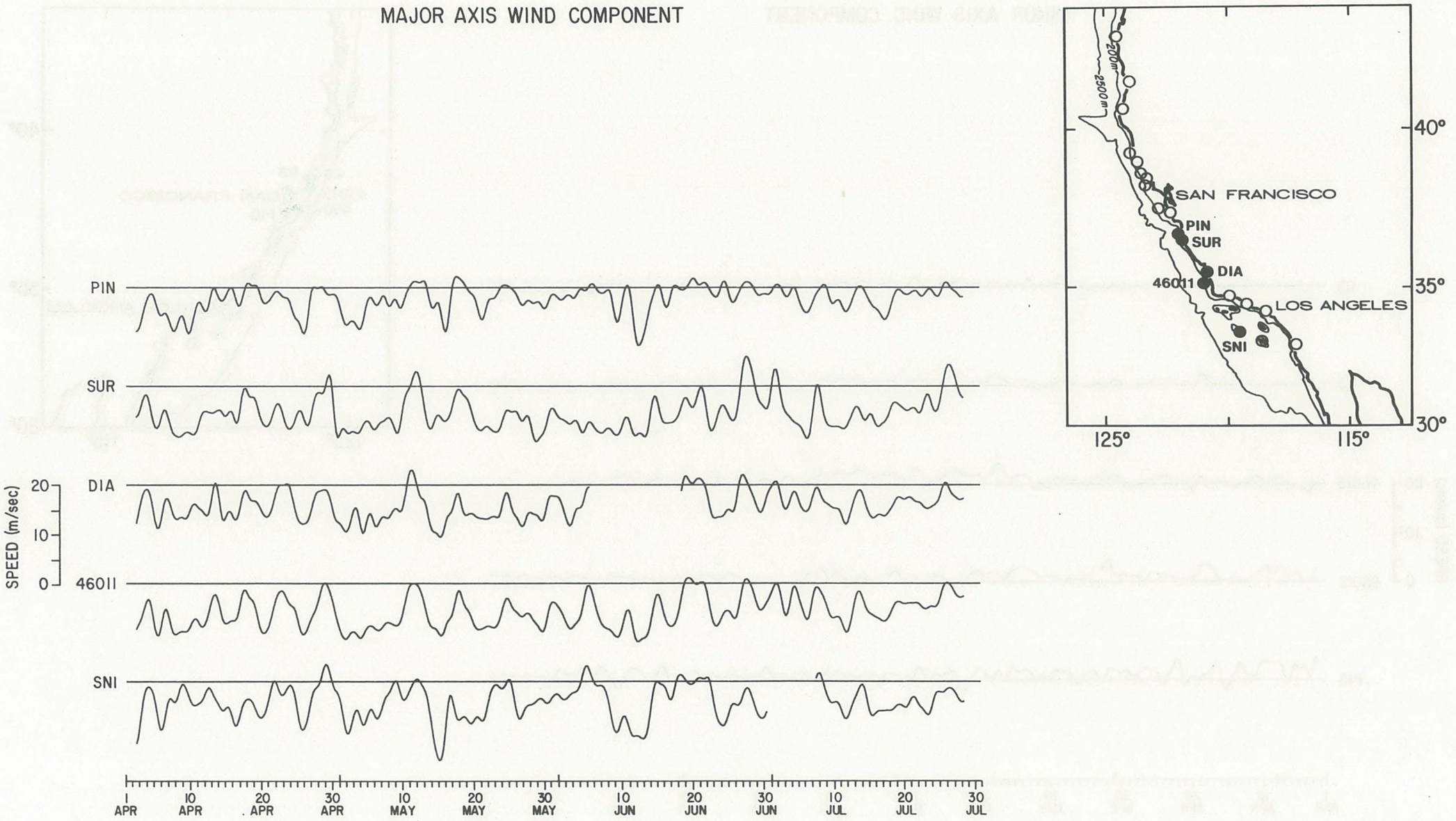
MAJOR AXIS WIND COMPONENT
PIN
SUR
DIA
46011
SNI
SPEED (m/sec)
20
10
0
1 APR
10 APR
20 APR
30 APR
10 MAY
20 MAY
30 MAY
10 JUN
20 JUN
30 JUN
10 JUL
20 JUL
30 JUL
2000m
2500m
SAN FRANCISCO
PIN
SUR
DIA
46011
LOS ANGELES
SNI
40°
35°
30°
125°
115°

Figure 6g

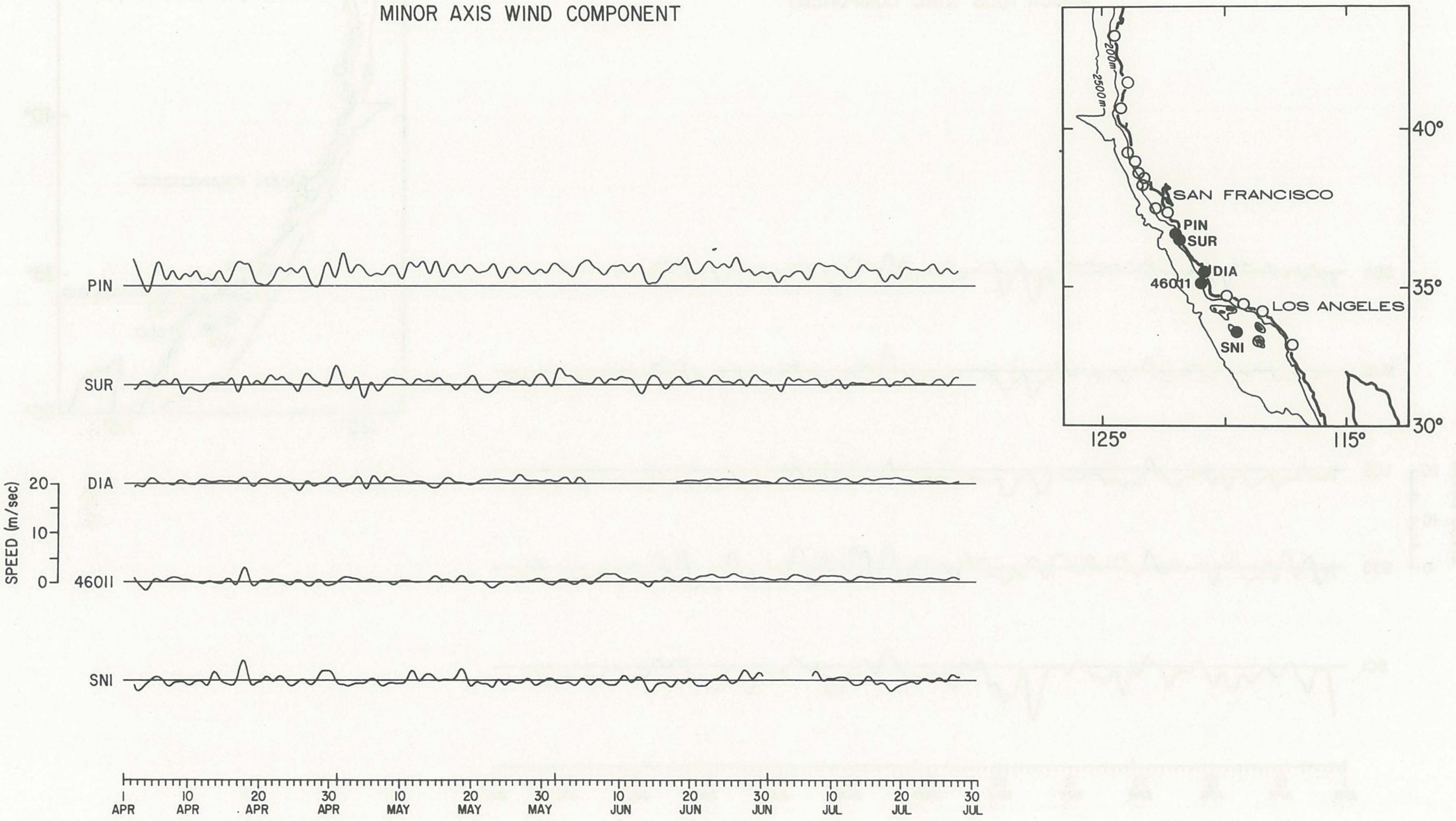
MINOR AXIS WIND COMPONENT
PIN
SUR
DIA
46011
SNI
SPEED (m/sec)
20
10
0
1 APR
10 APR
20 APR
30 APR
10 MAY
20 MAY
30 MAY
10 JUN
20 JUN
30 JUN
10 JUL
20 JUL
30 JUL
200m
2500m
SAN FRANCISCO
PIN
SUR
DIA
46011
LOS ANGELES
SNI
40°
35°
30°
125°
115°

Figure 6h

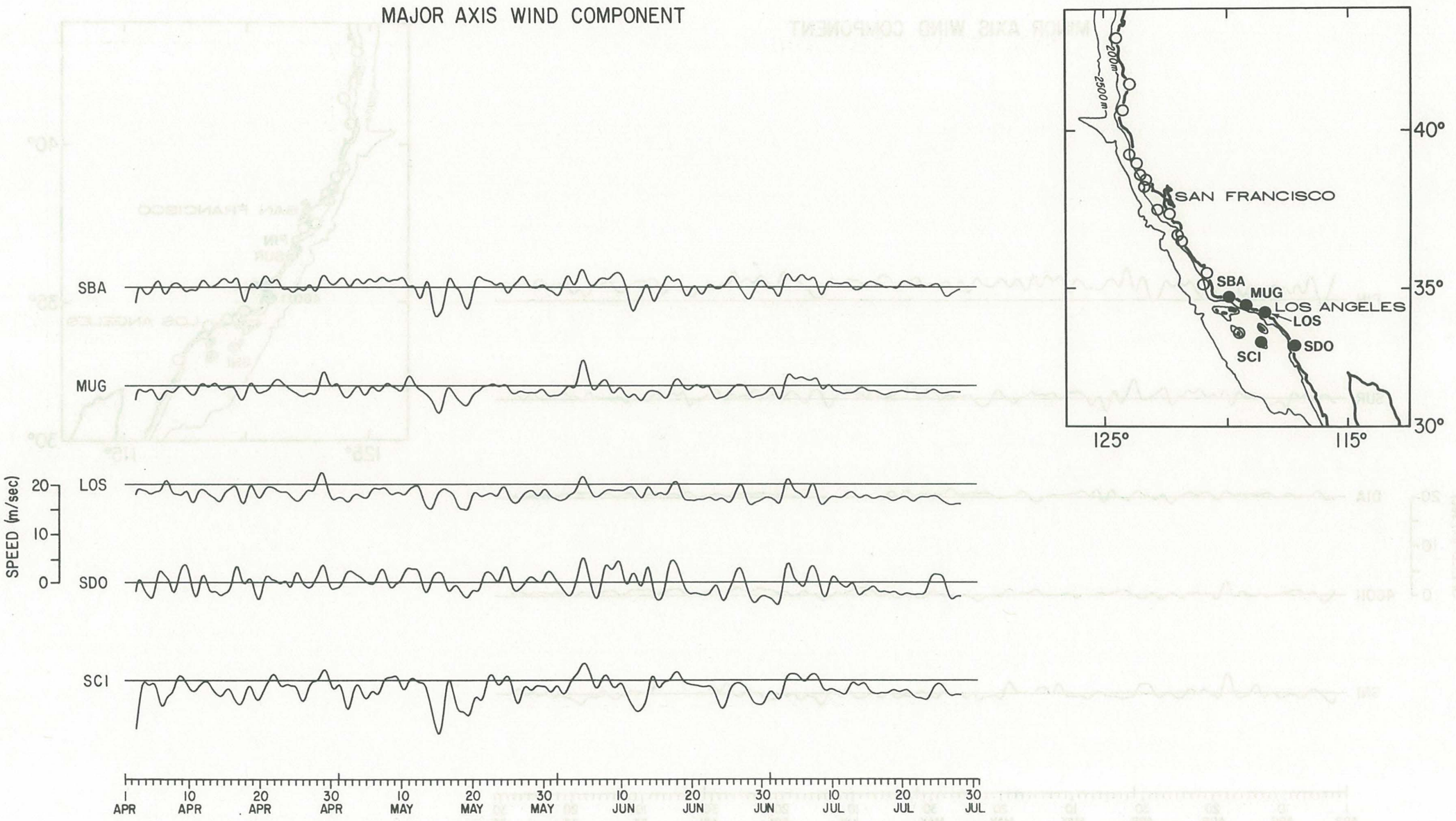
MAJOR AXIS WIND COMPONENT
SBA
MUG
LOS
SDO
SCI
SPEED (m/sec)
20
10
0
1 APR
10 APR
20 APR
30 APR
10 MAY
20 MAY
30 MAY
10 JUN
20 JUN
30 JUN
10 JUL
20 JUL
30 JUL
200m
2500m
SAN FRANCISCO
SBA
MUG
LOS ANGELES
LOS
SDO
SCI
40°
35°
30°
125°
115°

Figure 6i

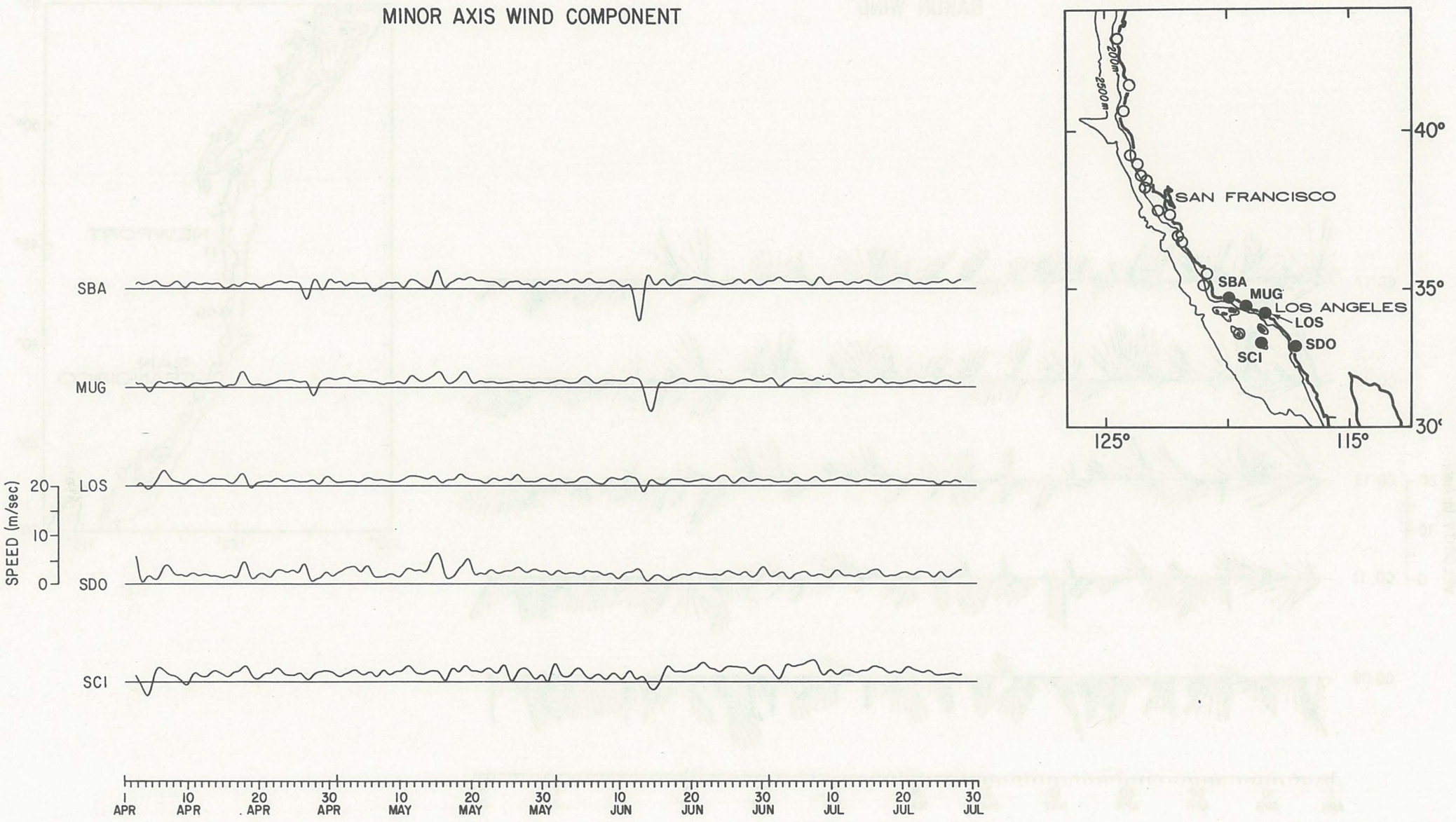
MINOR AXIS WIND COMPONENT
SBA
MUG
LOS
SDO
SCI
SPEED (m/sec)
20
10
0
1 APR
10 APR
20 APR
30 APR
10 MAY
20 MAY
30 MAY
10 JUN
20 JUN
30 JUN
10 JUL
20 JUL
30 JUL
200m
2500m
SAN FRANCISCO
SBA
MUG
LOS ANGELES
LOS
SDO
SCI
40°
35°
30°
125°
115°

Figure 6j

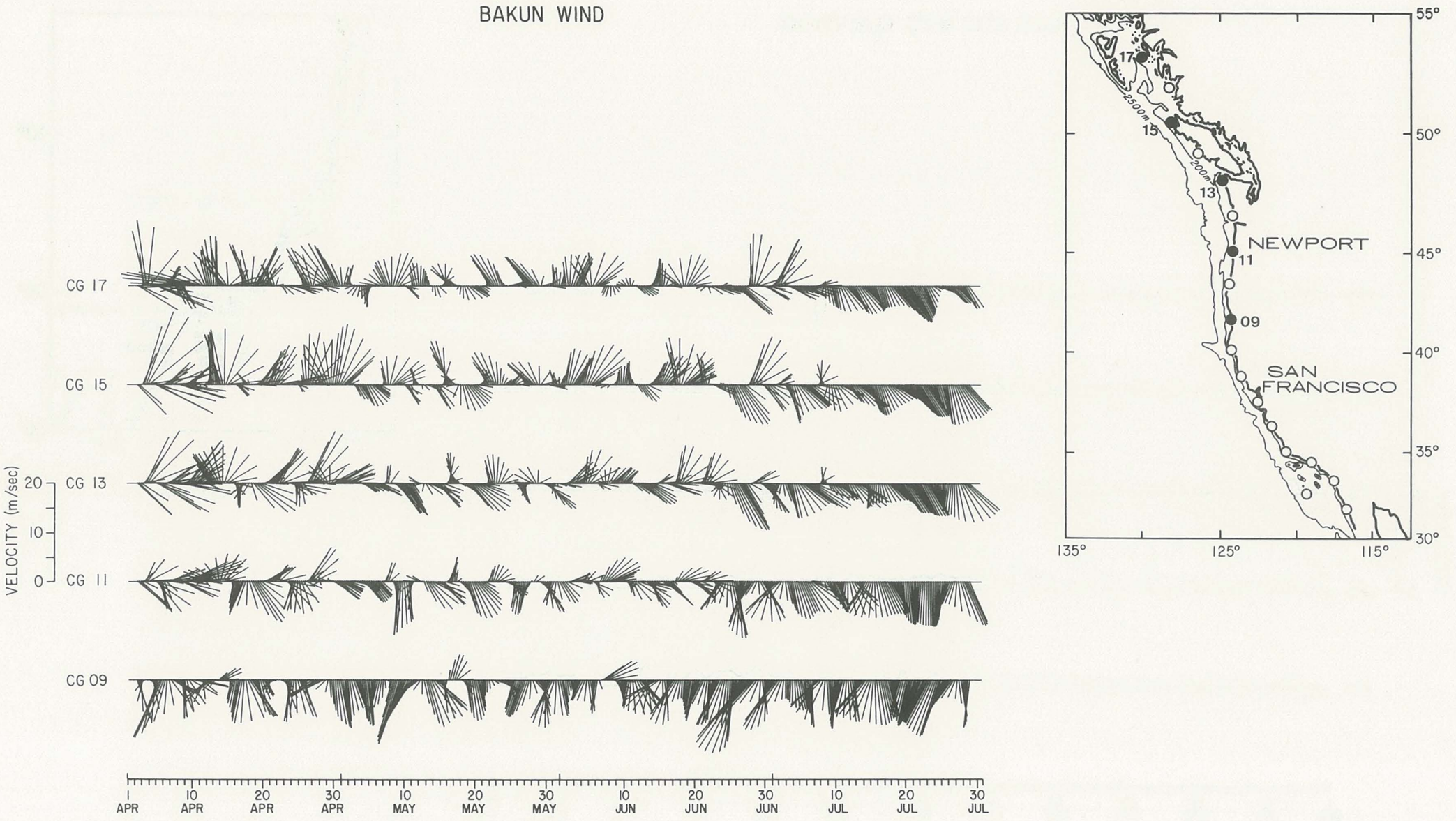
BAKUN WIND
CG 17
CG 15
CG 13
CG 11
CG 09
VELOCITY (m/sec)
20
10
0
1 APR
10 APR
20 APR
30 APR
10 MAY
20 MAY
30 MAY
10 JUN
20 JUN
30 JUN
10 JUL
20 JUL
30 JUL
17
15
13
11
09
2500m
200m
NEWPORT
SAN FRANCISCO
55°
50°
45°
40°
35°
30°
135°
125°
115°

Figure 7a

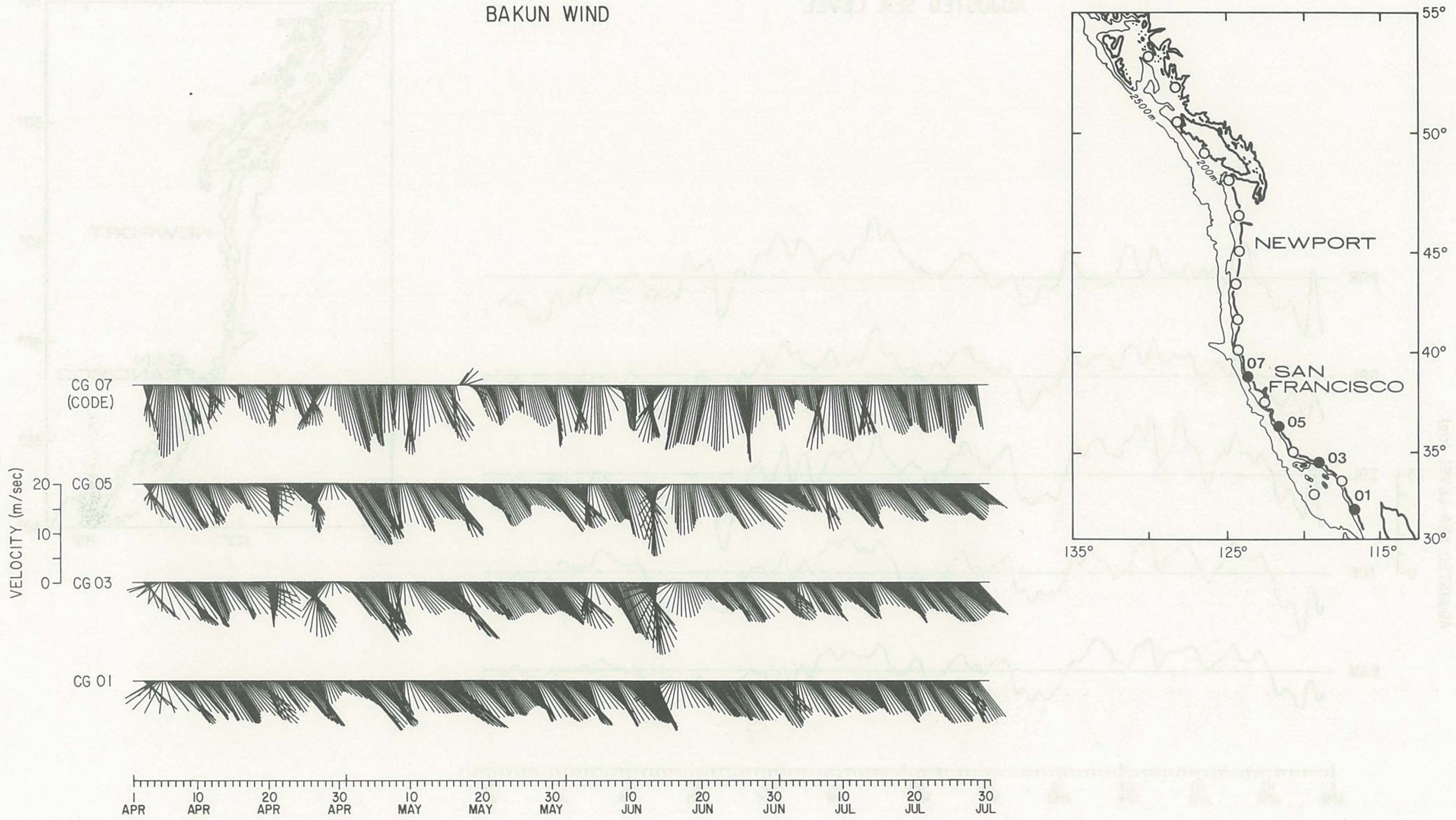
BAKUN WIND
CG 07
(CODE)
CG 05
CG 03
CG 01
VELOCITY (m/sec)
20
10
0
1 APR
10 APR
20 APR
30 APR
10 MAY
20 MAY
30 MAY
10 JUN
20 JUN
30 JUN
10 JUL
20 JUL
30 JUL
2500m
200m
NEWPORT
SAN FRANCISCO
07
05
03
01
55°
50°
45°
40°
35°
30°
135°
125°
115°

Figure 7b

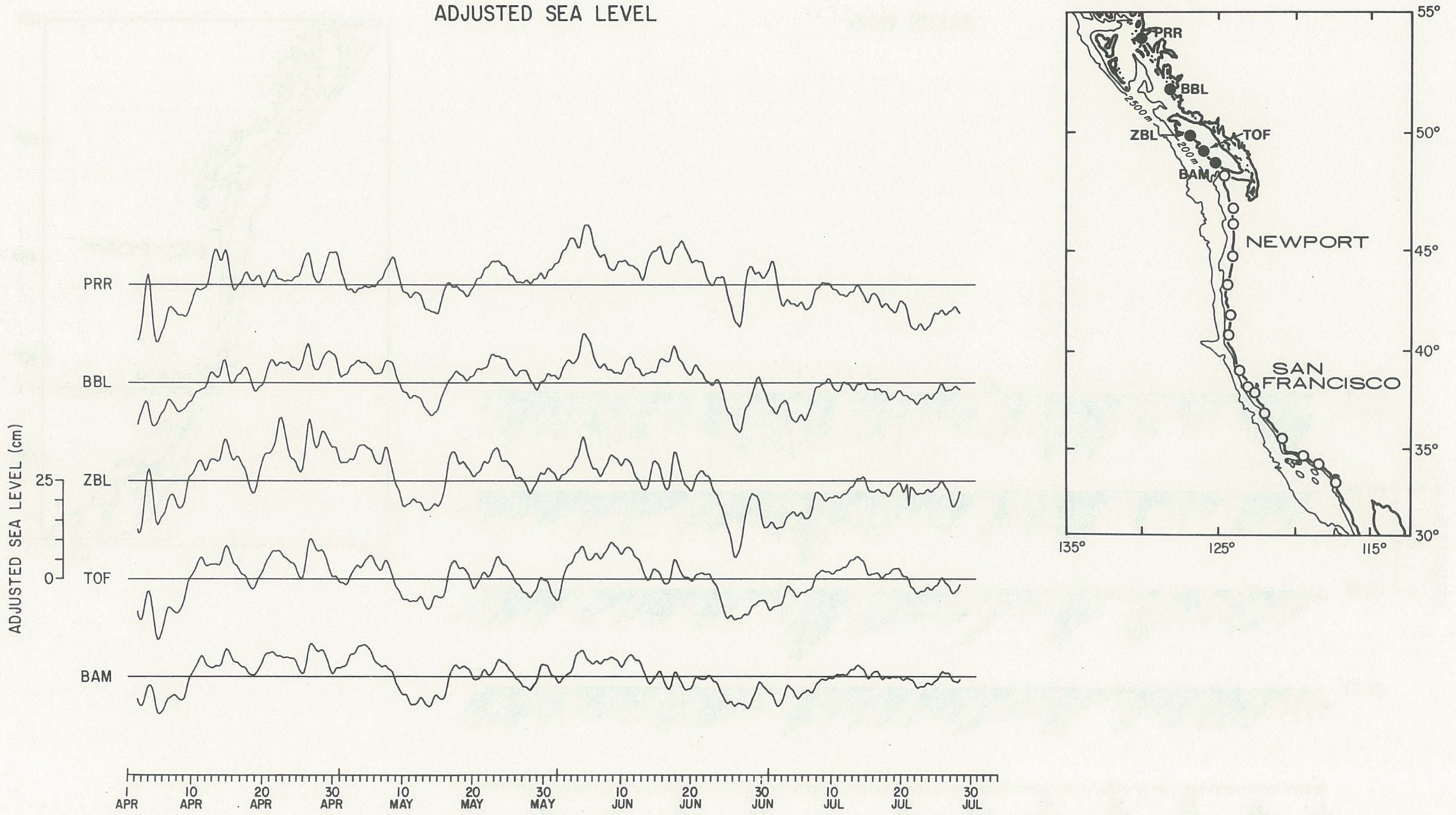
ADJUSTED SEA LEVEL
PRR
BBL
ZBL
TOF
BAM
ADJUSTED SEA LEVEL (cm)
25
0
1 APR
10 APR
20 APR
30 APR
10 MAY
20 MAY
30 MAY
10 JUN
20 JUN
30 JUN
10 JUL
20 JUL
30 JUL
PRR
BBL
ZBL
TOF
BAM
2500 m
200 m
NEWPORT
SAN FRANCISCO
55°
50°
45°
40°
35°
30°
135°
125°
115°

Figure 8a

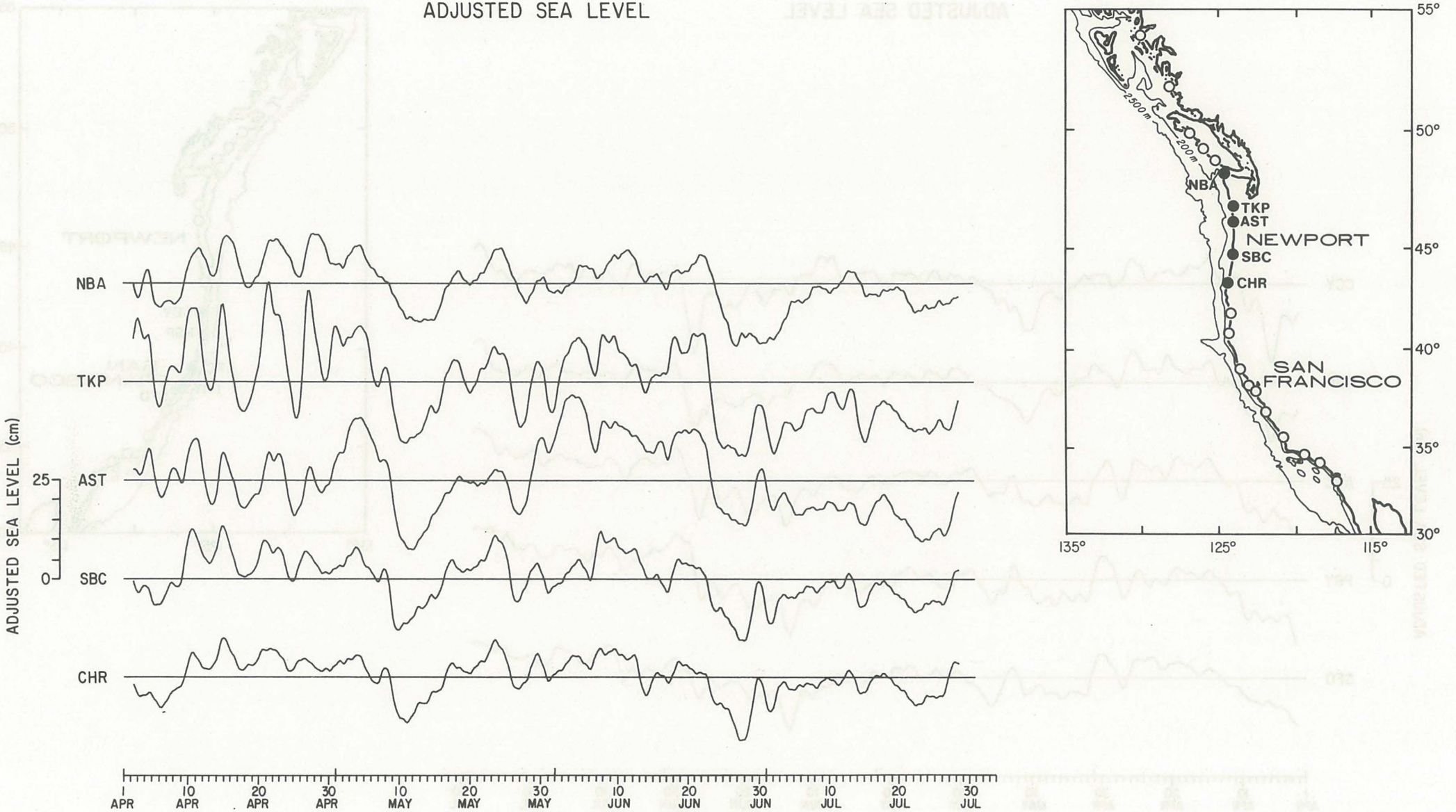
ADJUSTED SEA LEVEL
NBA
TKP
AST
SBC
CHR
ADJUSTED SEA LEVEL (cm)
25
0
1 APR
10 APR
20 APR
30 APR
10 MAY
20 MAY
30 MAY
10 JUN
20 JUN
30 JUN
10 JUL
20 JUL
30 JUL
2500 m
200 m
NBA
TKP
AST
NEWPORT
SBC
CHR
SAN FRANCISCO
55°
50°
45°
40°
35°
30°
135°
125°
115°

Figure 8b

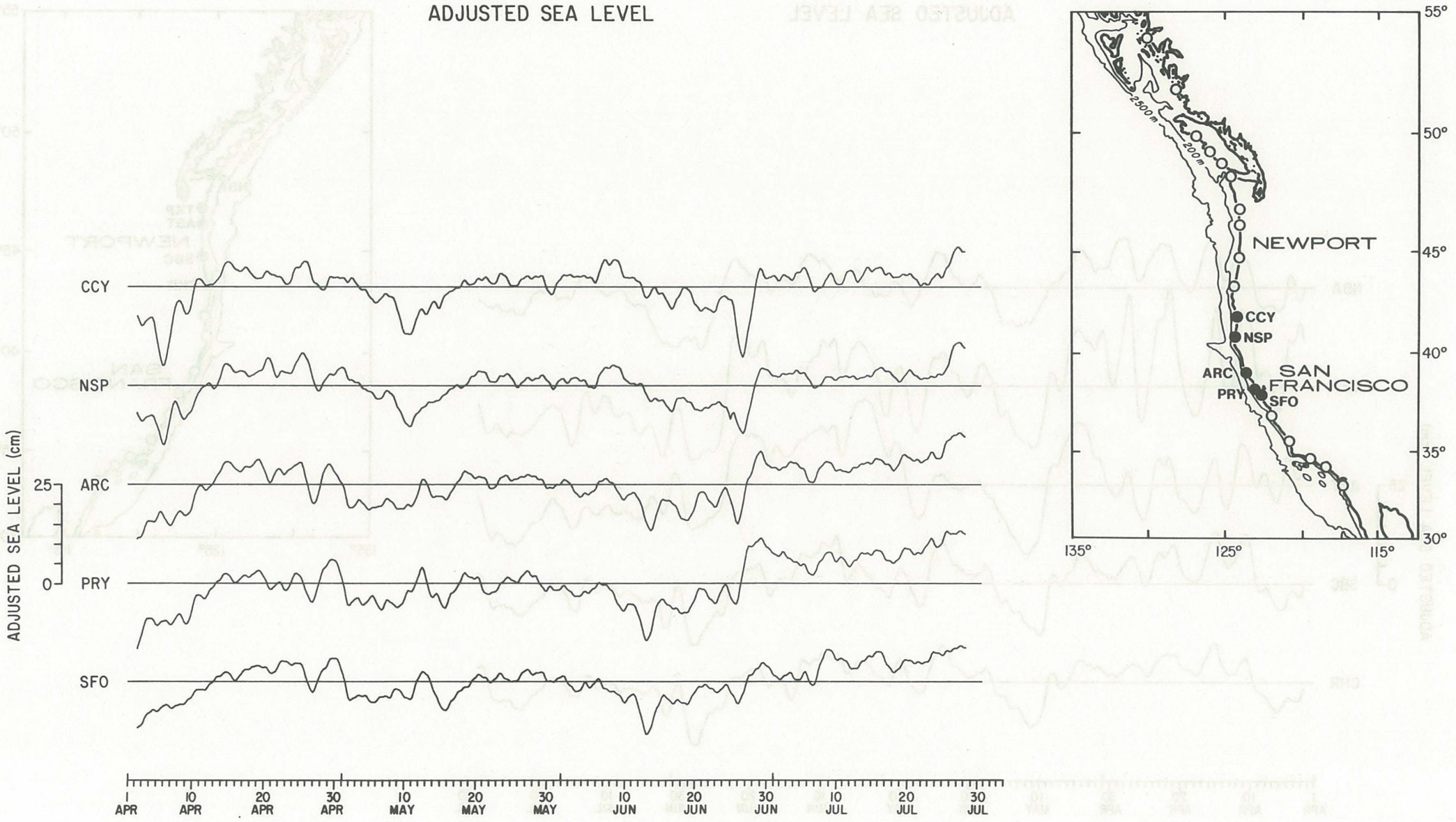
ADJUSTED SEA LEVEL
ADJUSTED SEA LEVEL (cm)
25
0
CCY
NSP
ARC
PRY
SFO
1 APR
10 APR
20 APR
30 APR
10 MAY
20 MAY
30 MAY
10 JUN
20 JUN
30 JUN
10 JUL
20 JUL
30 JUL
2500m
200m
NEWPORT
CCY
NSP
ARC
SAN FRANCISCO
PRY
SFO
55°
50°
45°
40°
35°
30°
135°
125°
115°

Figure 8c

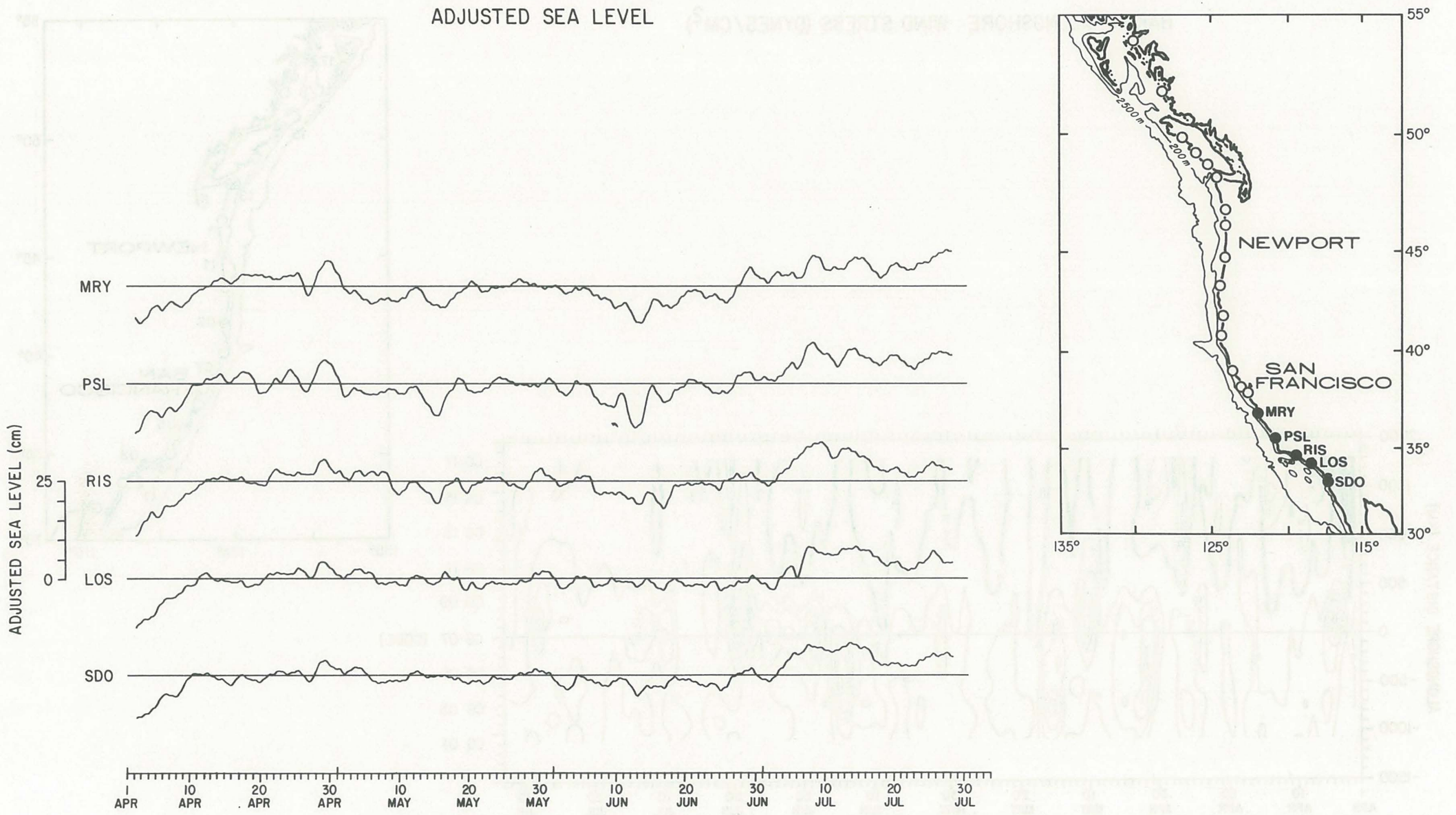
ADJUSTED SEA LEVEL
ADJUSTED SEA LEVEL (cm)
25
0
MRY
PSL
RIS
LOS
SDO
1 APR
10 APR
20 APR
30 APR
10 MAY
20 MAY
30 MAY
10 JUN
20 JUN
30 JUN
10 JUL
20 JUL
30 JUL
2500 m
200 m
NEWPORT
SAN FRANCISCO
MRY
PSL
RIS
LOS
SDO
55°
50°
45°
40°
35°
30°
135°
125°
115°

Figure 8d

BAKUN ALONGSHORE WIND STRESS (DYNES/CM^2)

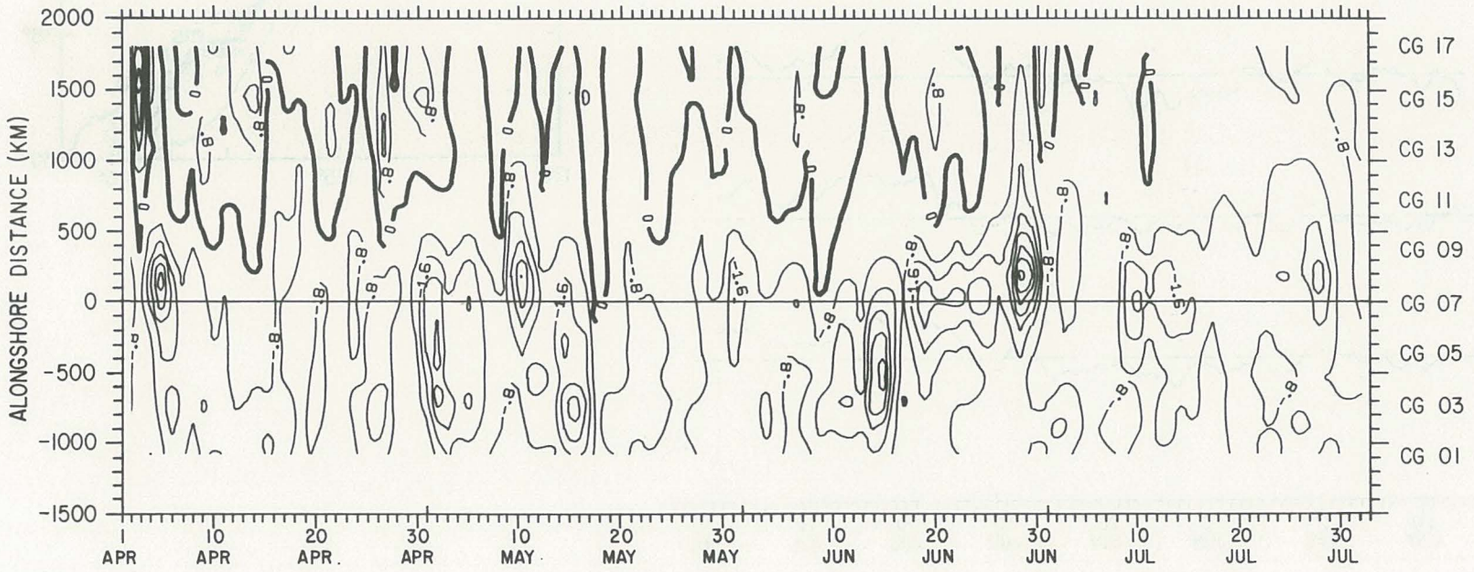

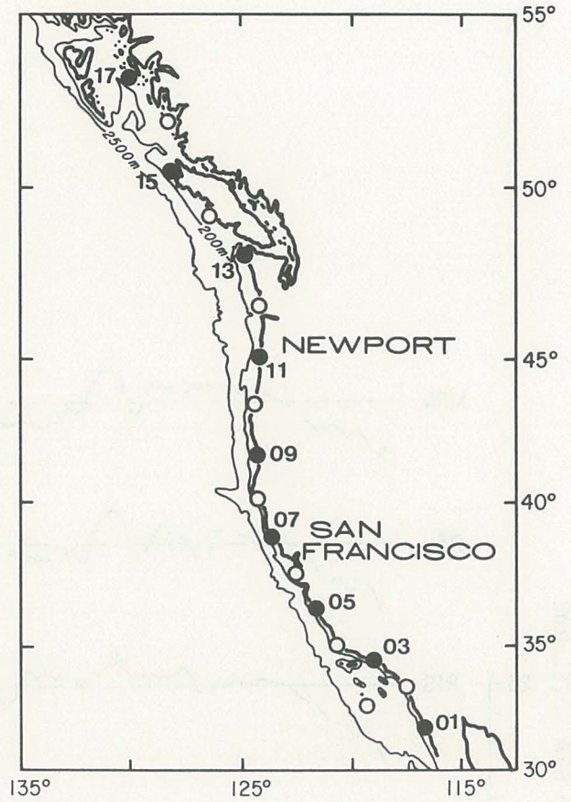

Figure 9

DAILY-AVERAGED ADJUSTED SEA LEVEL (CM)

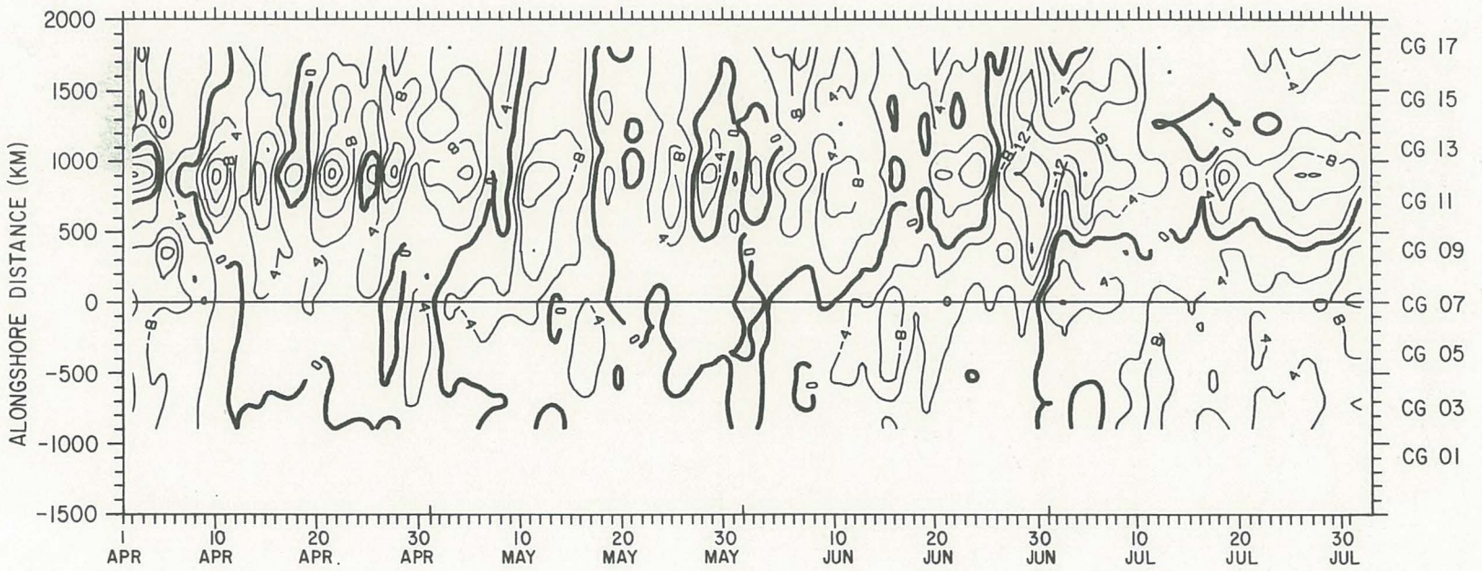

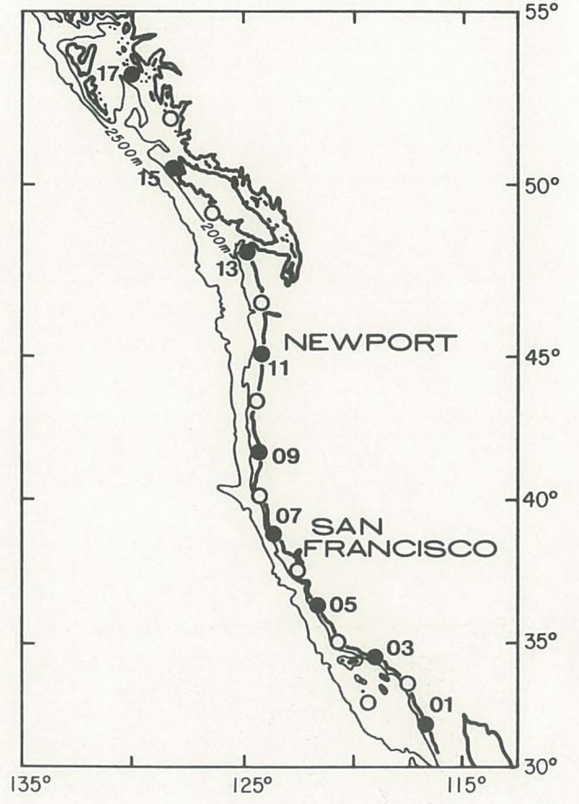

Figure 10